PHOTOCHEMICAL CONVERSION OF COAL TO GASOLINE IN AN ENTRAINED BED REACTOR

By

SUBRAMANIAN SUNDARAM

Bachelor of Science
University of Madras
Alagappa College, Karaikudi, India
1969

Master of Science
Annamalai University
Annamalainagar, India
1971

Submitted to the Faculty of the
Graduate College of the
Oklahoma State University
in partial fulfillment of
the requirements for
the Degree of
DOCTOR OF PHILOSOPHY
July, 1979

DEDICATION

Dedicated to my beloved daughters

SHANTHI and KARPU SUNDARAM

who, together, showed me what life is.

PHOTOCHEMICAL CONVERSION OF COAL TO GASOLINE IN AN ENTRAINED BED REACTOR

Thesis Approved:

Thesis Adviser

Dean of Graduate College

PREFACE

There are no words in the English Language to express my indebtedness to my professional father and Thesis Adviser, Dr. Gilbert J. Mains, for his excellent and enthusiastic guidance throughout this investigation. Without his encouragement, this work may not be in the present form.

My sincere thanks are due to Dr. Joseph A. Solomon of Philadelphia College of Pharmacy and Science, Philadelphia, Pennsylvania, for his helpful suggestions during his sabbatical here.

My thanks are due to my Doctoral Committee members Professors Lionel M. Raff, Edmund J. Eisenbraun and Billy L. Crynes. Their assistance and advisement are appreciated.

I want to take this opportunity to thank the following for their direct or indirect assistance in this work: Mr. Wayne A. Atkins for his commendable glass-blowing; Dr. Fred J. Radd and Dr. Gary W. Keen of Continental Oil Company, Ponca City, Oklahoma, Dr. Gene E. May and especially Mr. Robert K. Isensee of Oral Roberts University, Tulsa, Oklahoma, Dr. Sterling E. Burks and Ms. Elaine of Oklahoma Reservoir Research Center for their generous assistance in the GC-MS analyses; Mr. Tom Hudson of Dow Chemical Company, Freeport, Texas, for XPS analyses; Dr. Alexis A. Vohlborth

of University of California, Irvine, California, for Fast Neutron Activation Analyses; OSU College of Veterinery Medicine for Scanning Electron Microscope Analysis; Continental Oil Company, Ponca City, for Coulter-Counter Analyses; Dr. Donald E. Linder of Continental Oil Company for his valuable suggestions in HPLC analyses; Mr. Ed Obermiller of Consolidation Coal Company, Library, Pennsylvania, for coal samples; Mr. Norman B. Perriera for HRMS; Dr. Darrel K. Berlin and Mr. Stan Sigle for NMR analyses; Mr. Russ Tuebner of the University Computer Center for his assistance in Computer Formating of this Dissertation; and the entire supporting staff of OSU Chemistry Department for their 'sevice with smile'.

Working with people like Mr. Allan Banks, Miss Martha W. Lee and Mr. K. Ramarajan was a great experience. My special thanks are due to Dr. K. Ramalingam of PSG Arts College, Coimbatore, India, for all his helps. The companionship of Mr. G. Prakash during the tiresome hours of writing this Dissertation is highly appreciated.

My thanks are also due to my brother-in-law Mr. KR. KN. Ramanathan Chettiar for his moral support and Dr. and Mrs. A. Ekambaram of Annmalai University, Annmalainagar, India, for their kindness and encouragement. Dr. T. Rangarajan of Annamalai University, Annamalainagar, India, was partly responsible for my higher education in this country and a special 'thank you' is due to him.

The early-days sacrifices of my step-mother Mrs. M. Sp. Valliammai Achi and the present-days sacrifices of my wife Kannathal and children Shanthi and Karpagavalli have no bounds at all and my heart-felt thanks are due to them!

Last, but not least, the financial support of the OSU Chemistry Department in the form of a Graduate Teaching Assistantship and of the United States Department of Energy in the form of a Research Associateship are very highly appreciated.

This manuscript was prepared using a Computer Formating Program called 'SCRIPT' developed at the University of Waterloo, Waterloo, Canada, in 1978 and 'OSUPUB', a special edition of the above, developed at Oklahoma State University in 1979. This required the use of computer notations for mathematical formulations. For example, '10**4' means '10 raised to the power of 4' and '2**0.5' means 'square root of two' etc. Also, the unit numbers for chemical formulas would not be subscripted. For example, CH4 stands for Methane, C10H8 stands for Naphthalene etc.

TABLE OF CONTENTS

LIST OF TABLES

LIST OF FIGURES

CHAPTER I

INTRODUCTION

We are now entering an exciting era of coal chemistry. Coal chemistry has become at least as glamorous as research on outer space or research on atomic energy.

Coal is a heterogeneous solid substance, both physically and chemically, that contains undesirable impurities, some incorporated in the chemical structure and some distributed as discrete minerals throughout the coal structure.

Coal is the most abundant fossil fuel resource which represents about 80 to 85% of the known fossil fuel energy reserves of the United States (4). While the energy content of the whole coal is satisfactory, its mairoscopic and molecular forms are not. Transportation and combustion of the solid coal are both difficult and inconvenient. In view of these facts, it is apparent that the problem in research on coal technology is to develop methods to convert coal into more desirable and environmentally acceptable forms. As Professor Larson (2) recently put it so so aptly:

> To attempt the rational design of catalysts for coal conversion with a reasonable hope of success we need to know much more about its structure and reactivity. The rational design and development for better processes is being hindered enormously by our very poor understanding of coal chemistry.

Coal is a very difficult material to work with, and progress will probably be slow; but our need for and ability to use information about the coal structure and reactivity are enormously greater than the availability of such information..... Because of the past neglect, it is inevitable that we will continue for a while to operate with an inadequate data base (p.8).

CHAPTER II

CLASSIFICATION AND STRUCTURE OF COAL

Of course, the basic problem is with the raw material, coal itself. Formed from the remains of living organisms some 250-400 million years ago and subsequently subjected to biodegradation, it is small wonder that the black carbonaceous material dug from the ground varies macroscopically from the top of the seam to the bottom, from side to side, and microscopically in the form of regions of different properties and atomic compositions (3). Because of this exceedingly complex nature of coal any simple classification in the scientific sense is not possible. Most generally, coal is a microscopically structureless system consisting essentially of a matrix of carbon and hydrogen organic systems. As a consequence, the characterization of coal beyond presenting the geographic source or rank is of little use. Coals, in general, have been classified according to geological age, recognizable coal-forming plant materials, rank, volatile matter and/or fixed carbon content, petrographic consituents etc (1).

The classification developed by American Society for Testing and Materials (ASTM) (5) is in common use. In this

classification system, the higher rank coals are classified according to their fixed carbon content on the dry basis; the lower-rank coals are classified according to their calorific value as shown in Table I. Agglomerating character is used to differentiate between certain adjacent groups. Applying usual methods of elemental analysis, and discounting ash, a typical low-volatile bituminous coal has been found to have an approximate empirical formula of C135H97O9S. Such formulas might range from C75H140O56N2S for a low grade peat to C240H90O4NS for a high grade anthracite (7).

On this basis, several structures have been suggested for bituminous coals. These structures are based on ultimate and functional group analyses, spectrometric and X-ray data and chemical reactions (8). The structures proposed by van Krevelen (9), Given (10) and Sheer (11) are reproduced here in Figures 1, 2 and 3 respectively.

Let us consider Sheer's structure (Figure 3). Of course, it needs to be emphasised that there is no firm basis for choosing this structure over the others. This structure has something of everything. Six membered aromatic rings predominate although significant quantities of five membered configurations exist. The basic ring positions are mostly occupied by carbon atoms although there are many of the rings with a sulfur atom, a nitrogen atom, or an oxygen atom in the ring position. A substantial amount of

hydro-aromatic structures (about 15 to 20%) also exist where a part of the structure is saturated with respect to hydrogen (12). The three hetero-atoms, sulfur, oxygen and nitrogen are present in significant quantities. This structure has almost every type of oxygen, i. e., oxygen in rings, in carbonyls, in ethers and in phenolic hydroxyls; nitrogen in pyrrole and in pyridine and sulfur, predominantly as dibenzothiophene sulfur (13). On an average about one half of sulfur found in bituminous coals is inorganic in nature and the other half exists principally as thiophenes, sulfides, disulfides and mercaptans (14).

The principal types of structures, namely aromatic and hydroaromatic are joined together to yield the fundamental coal structure. It is observed that these ring structures are joined together in various patterns with the basic structure consisting of single rings, condensed double rings, condensed triple rings etc. The current view is based mainly on the X-ray work of Hirsh (15). However, in a recent paper, Given (12) has very strongly criticized and questioned the validity of this work. From the data available at present it could be concluded that the average size of a cluster making up the fundamental coal structure consists of three condensed rings actually ranging from single rings to several condensed rings per cluster. These clusters are connected by various linkages such as ether linkage, sulfide and disulfide linkage and even biphenyl linkage etc.

Given's non-planar structure for a vitrinite of 82% carbon was based on dihydro-anthracene (Figure 2 a). Brown et al., however, soon after the publication of Given's model, demonstrated by NMR studies that it is unlikely that methylene bridges exist in coals (16). Given, in a later paper, agreed and proposed modification to an isometric type of structure based on dihydro-phenanthrene (Figure 2 b) in which no methylene bridges are involved.

The combination of multi-ring aromatic structures and the presence of hetero atoms means that the carbon to hydrogen ratio is too high for the substance to exist as a liquid or gas. Thus as shown in Table II the carbon to hydrogen ratio for a bituminous coal is about 15:1 while for petroleum it is 7:1 (17). Hence, any conversion to gas or liquid perforce requires addition of hydrogen (or removal of carbon as coke or char).

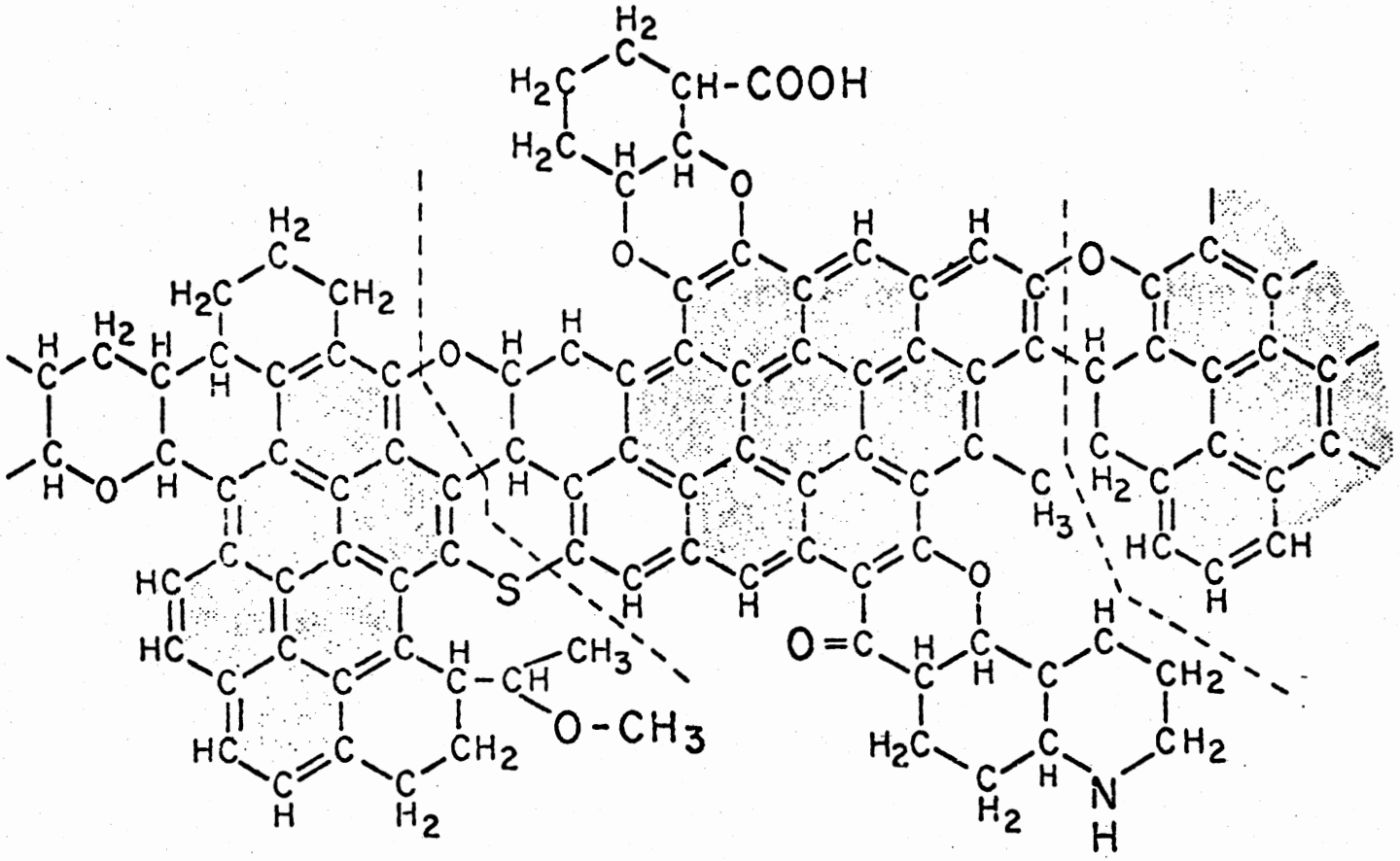

Figure 1. van Krevelen Structure of Coal

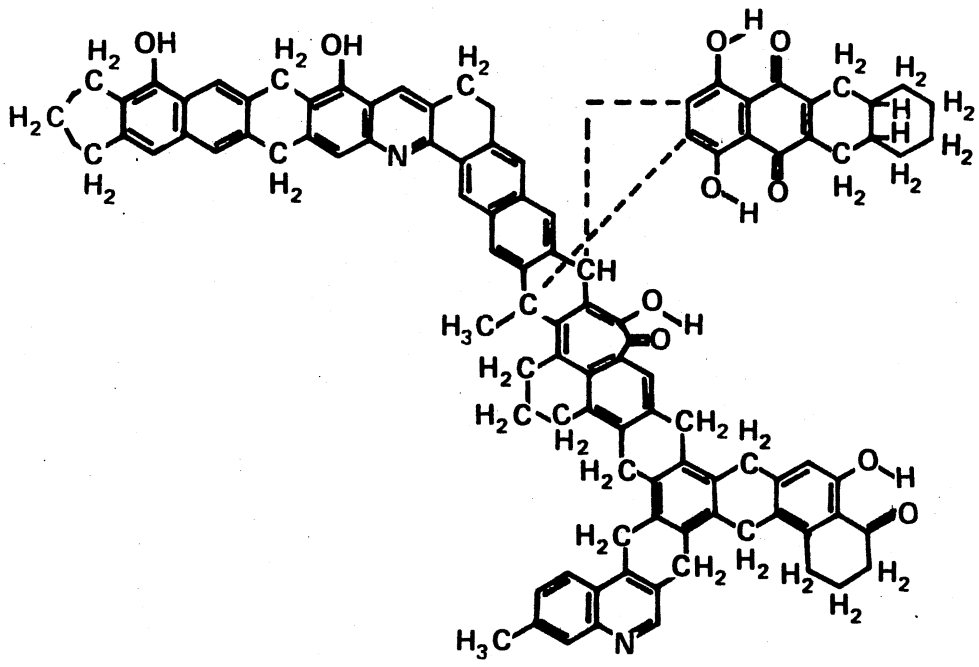

(a) MODEL OF CHEMICAL STRUCTURE OF COAL

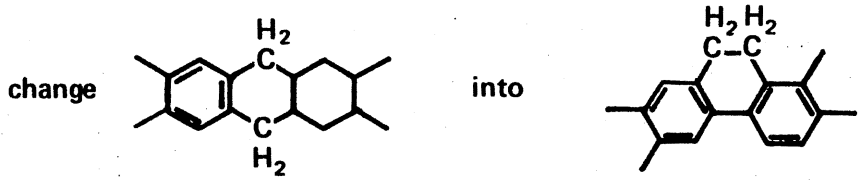

(b) GIVEN'S SUBSEQUENT MODIFICATION TO THE ABOVE

Figure 2. Given Structure of Coal

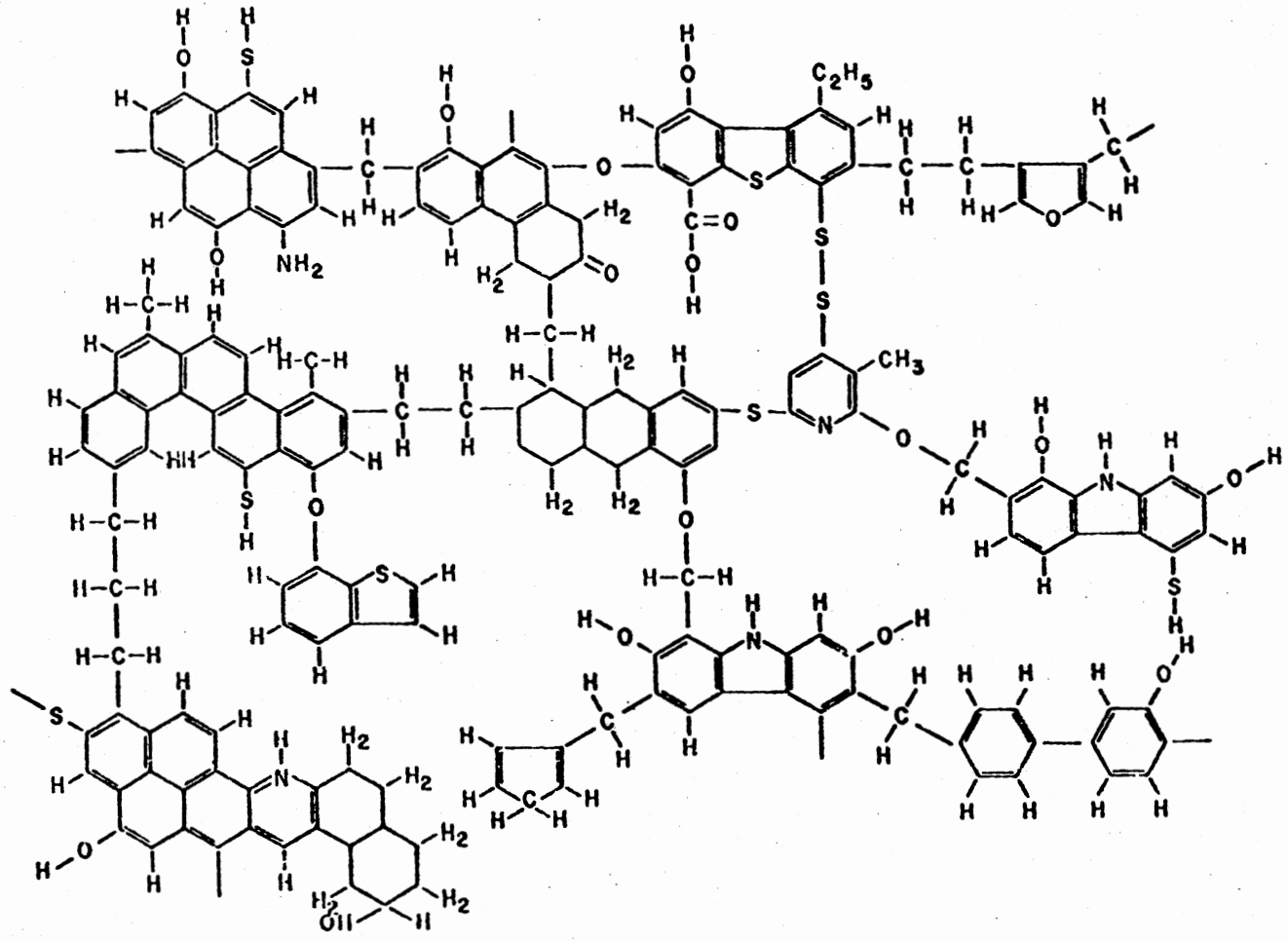

Figure 3. Sheer Structure of Coal

TABLE I

ASTM CLASSIFICATION OF COALS BY RANK

Rank	Btu/Lb
I. Anthracite	
1. Metaanthracite	-
2. Anthracite	-
3. Semianthracite	-
II. Bituminous	
1. Low Volatile	-
2. Medium Volatile	-
3. High Volatile A	-
4. High Volatile B	14,000
5. High Volatile C	13,000
III. Subbituminous	
1. A	11,500
2. B	10,500
3. C	7,500
IV. Lignite	
1. A	9,500
2. B	8,300

Approximate Age ↑ Oxygen Content ↓ Heating Value ↑

TABLE II

CHEMICAL COMPOSITION OF SOME COALS AND PETROLEUM

	Anthracite	Medium Volatile bit.	High Volatile A bit.	High Volatile B bit.	Lignite	Petroleum Crude	Gasoline	Toluene
C	93.7	88.4	84.5	80.3	72.7	83-87	86	91.3
H	2.4	5.0	5.6	5.5	4.2	11-14	14	8.7
O	2.4	4.1	7.0	11.1	21.3			
N	0.9	1.7	1.6	1.9	1.2	0.2		
S	0.6	0.8	1.3	1.2	0.6	1.0		
H/C ratio	0.31	0.67	0.79	0.82	0.69	1.76	1.94	1.14

CHAPTER III

REACTIONS OF HYDROGEN ATOMS WITH CARBON AND COAL

Literature Review

The author's literature search shows only three references to the reaction of atomic hydrogen with coal but many references are available describing the reaction of hydrogen atoms with various forms of carbon.

The direct reaction of hydrogen atoms, produced in a glowing discharge with soot at a temperature of 100 deg C was first reported by the Russian scientist Avramenko (18) in 1946. On the basis of spectral evidence, he suggested that the CH_2 radical was an intermediate in the formation of the products.

Harris and Tickner (19) in 1947 reported additional confirmation of the occurrence of this reaction in an independent work. In 45 minutes runs, soot deposits (made by 'smoking' a glass finger with a gas flame) were treated with hydrogen atoms produced by the standard Wood-Bonhoeffer (20) discharge technique. The walls of the cylindrical reaction chamber were internally 'poisoned' against excessive hydrogen atom recombination by means of a coating of phosphoric

acid and they claimed a 20% concentration of hydrogen atoms at an operating pressure of 0.4 mm. They found methane and C2-C5 hydrocarbons as the products of the reaction.

Blackwood and McTaggart (21) reacted wood chars with hydrogen, oxygen and carbon monoxide, and hydrogen atoms and hydroxyl radicals produced by the action of a radiofrequency field on hydrogen, carbon dioxide and water vapor respectively. The carbon samples used in their study were prepared by carbonizing jarrah wood (Eucaliptus marginta) in a stream of dry, oxygen-free nitrogen to a temperature of 650 deg C. The crushed and sieved samples were divided into several portions and each of these was again heated in a dry, oxygen-free nitrogen atmosphere to various given temperatures ranging from 750-1150 deg C. The chars prepared in this manner contained different amounts of oxygen. One point worth mentioning in their experiment was that the sample was just outside the radiofrequency field (contrary to the later works that follow). The main product of the reaction was methane, although initially a small amount of carbon monoxide was also formed. However, the extent of the reaction is not indicated. They reported no change in the reaction rate with change in the temperature of charring. They postulated that the atomic species reacted on the carbon-surface independent of the number of active sites.

Shahin (22) investigated the reaction of hydrogen atoms, produced by the action of microwave discharge on

hydrogen gas, with carbon and it was found that the total amount of products decreased rapidly when the carbon was moved away from the plasma. On the basis of this experimental evidence, he reported that the reaction occured only when the carbon was in the discharge zone and suggested that the reaction might be wholly due to gaseous carbon. Hydrogen atom concentrations were not measured and the temperature of carbon was 700 deg C. These observations suggested that atomic hydrogen did not react with carbon at room temperature. Methane, acetylene, and to a smaller extent, ethane and ethylene, were the main gaseous hydrocarbon products. Appearance of methane as the major product also suggested that a significant portion of the gaseous carbon was monoatomic. Acetylene could have arisen either from the reaction of a C2- carbon compound with hydrogen or by the attack of atomic carbon on the newly formed methane.

Vastola, Walker and Wightman (23) made a detailed study of room temperature, low pressure reaction of carbon with the products of hydrogen, oxygen and water microwave discharges. The presence of hydrogen atoms was detected qualitatively using a platinum wire. The reaction between atomic hydrogen and carbon occured at an insignificant rate if the carbon was located outside the discharge. When carbon was directly exposed to the discharge, the reaction proceeded at a significant rate, with a series of complex reactions occurring. Ethylene and methane were the major

gaseous products. A yellow hydrocarbon residue was found on the walls within the discharge zone. Minor gaseous reaction products included ethane, propane and n-pentane. The converion efficiency of hydrogen to hydrocarbon products, both gaseous and solid, has been reported to be about 10%. The authors agreed with Shahin's earlier work that the transport of carbon from solid to vapor phase was likely. This was thought to arise from the bombardment of the carbon by energetic ionic species believed to be present in the discharge.

King and Wise (24) studied the reaction kinetics of hydrogen atoms produced by a radiofrequency discharge with evaporated carbon films in the temperature range from 365 to 500 deg K and the total gas pressure from 0.02 to 0.10 mm. The atom densities were measured calorimetrically with a tungsten filament located in the main discharge tube. The principal carbon-containing products were methane and ethane, with ethylene becoming more important at higher temperatures. Other products detected were: alkanes through C7, traces of cyclohexanes, benzene, diacetylene, CS2 and alkyl sulfides, CO, CO2, H2O and traces of oxygenated compounds through C3. The removal of carbon by chemical reaction, as detected by variation of film thickness with time was found to occur at two distinct rates with activation energies of 9.2 and 7.1 kcal/mole. In addition, they studied the formation of hydrogen molecules by atom recombination on the carbon film and concluded that this reaction, with an activa-

tion energy of 2.4 kcal/mole predominated over the hydrocarbon formation in the temperature range they used.

Letort et al. (25) reported the complete gasification of a vitrinite when allowed to react with atomic hydrogen from a Wood's tube (hydrogen flow 3 to 9 l/h). The atomic hydrogen concentration was determined by a Wrede-Harteck gauge, and was usually 30 to 50% at the point where the stream left the Wood's tube. Whether the sample was in the discharge itself is not clear, but vitrinite in fact tumbled through the discharge zone in a special reactor. A pyridine extract of vitrinite, coronene and graphite were also gasified completely. Methane, ethylene and acetylene were the main products. On the other hand, paraffins, phenanthrene and pyrene were attacked but formed in part benzene-insoluble solids which were more resistant than the parent hydrocarbon to attack by hydrogen atoms. The use of dry hydrogen, or hydrogen containing 3% of water, appeared to give similar yields of atoms. Water appeared to increase the gasification rate of vitrinite, with the formation of carbon monoxide and reduction of the hydrocarbon yields.

Gill, Toomy and Moser (26) atomized hydrogen containing tritium at a hot tungsten filament and reacted the atoms with various forms of carbon (graphite, lamp black, and diamond) at 77 deg K. At pressures low enough to allow a collison-free path for the hydrogen atoms between the filament and the surface of the carbon, several saturated hydrocar-

bons, (methane, ethane, propane, n-butane and iso-butane), and unidentified higher molecular weight product(s) were produced. In separate high pressure runs at high temperatures, cis-2-butene was also produced. A very significant aspect of their work is the temperature of the carbon target which was at 77 K. It is hard to imagine that there could have been any gaseous carbon atoms at this low temperature taking part in the reactions. This is totally different from the views held by the previous workers. The authors concluded that methane was the initial product of the reaction of hydrogen atoms with elemental carbon and hot atoms were required to convert methane to higher molecular weight hydrocabons. The data for relative total yield of products presented in the paper suggests that the reactivity of various forms of carbon is in the following order: Graphite > Diamond > Lamp Black.

Wood and Wise (27) studied the kinetics of the reaction between atomic hydrogen produced by radiofrequency discharge and solid graphite in the temperature range 450 to 1200 deg K). Methane was the major product(91%), the rest being unidentified compounds in the range C3 to C8. The rate of the reaction was found to depend on the square root of hydrogen atom concentration and as well as on the hydrogen pressure. On these grounds, they indicated that Rate = k[H2][H] ** 0.5 over the entire temperature range investigated. The authors reported a maximum in the variation of the reaction rate

with temperature and they explained that this was due to the thermodynamic instability of methane, the principal reaction product, at high temperature, the standard free energy of formation of which turns positive for T > 830 deg K. On this basis, they predicted that hydrogen and carbon would become the favored constituents in chemical equlibrium with methane for T > 830 deg K. However, the thermodynamic instability predicted for methane at 850 deg K requires hydrogen and methane to be at unit fugacity and for carbon to be in its standard state, with a state of thermodynamic equilibrium existing between the three species. In the hydrogen atom-carbon reaction, these criteria for the thermodynamic reasoning do not apply; if thermodynamic reasoning in any form could be applied to the reaction, and have any meaning, the system 4H + C = CH4 should bave been considered (30). It is probable that pyrolysis of hydrocarbon reaction products on the high temperature carbon target was responsible for the observed maximum product yield temperature.

Sanda and Berkowitz (28) studied the reaction of discharge generated hydrogen species with coals and carbons. They paid special attention to the effect of the reaction locale on product composition and reaction kinetics. They report a zero-order kinetics for the reaction WITHIN the luminous zone of the discharge and n > 0 for the reactions farther downstream. From this order difference, they sug-

gest that a substantially non-discriminating reaction in the discharge gives way to a selective reaction outside the luminous zone, where most of the surviving hydrogen atom species were believed to react with other than 'active' sites. Reaction with carbon did not yield detectable amounts of anything other than methane whereas that with coal produced ethylene, ethane, propane and n-butane in addition to methane, CO and CO2.

McCarroll and McKee (29) studied the topographical changes resulting from the interaction of hydrogen, nitrogen and oxygen, as well as the corresponding monoatomic species with graphite single crystals with substrate temperatures ranging from 300 - 1000 deg K . Undissociated hydrogen was found to be unreactive (as well as nitrogen) toward heated graphite. However, exposure of graphite crystals to atomic hydrogen (and atomic nitrogen) produced regular hexagonal pits on the cleavage surface. On the basis of this observation they postulated that the reactions depend on direct impingement of atoms from the gas phase at sites of preferred activity and the reaction kinetics, as measured by pit enlargement, would be dependent on the partial pressure of the reactant species.

Snelson (30) made an excellent study on the reaction of thermally produced atomic hydrogen with carbon. At an initial beam temperature of about 2600 deg K, the reaction of a beam of hydrogen atoms with a carbon surface, at approxi-

mately 300 deg C, produced 91% methane, 8.5% ethane and 0.4% propane. Very minor amounts of ethylene, propylene and C4 species were also suspected. Contrary to the earlier report by King and Wise no maximum in the hydrocarbon yield at 720 - 820 deg K was found. However, hydrocarbon formation increased with temperature and the product distribution remained virtually unchanged in the experimental temperature range of 30-950 deg C. He reports a conversion efficiency of (fraction of hydrogen atoms interacting with the carbon target convertd to hydro hydrocarbons) 1.2% at 30 deg C and 3.6% at 950 deg C. The methane yield - temperature dependence was found to have three distinct phases and the following activation energies have been reported: 300 to 500 deg K, E = 0.94 $\pm$ 0.2 kcal/mole 500 to 1000 deg K, E = 0.15 $\pm$ 0.05 kcal/mole and 1000 to 1200 deg K, E =4.5$\pm$1.2 kcal/mole. However, as Snelson himself points out, it should be considered that the temperatures of the hydrogen atoms and the carbon target were considerably different from each other-sometimes by 2000 deg K whereas the simple reaction rate theory assumes equal temperatures for all reactants.

CHAPTER IV

MERCURY PHOTOSENSITIZATION

In order to determine the rate of interaction of hydrogen atoms with fine coal dust, one needs a method of generation of atomic hydrogen from molecular hydrogen which, because of the heterogeneous nature of the reaction, must necessarily be flowing to fluidize the coal dust. In the earlier works reported in the literature, gaseous discharges were used, exclusively, to generate hydrogen atoms. Because of the questionable value of this method, a photochemical method was used to generate hydrogen atoms in the present study.

Certain chemical reactions which will not proceed under the influence of a given wavelength of light in a convenient region in the electromagnetic spectrum can be initiated by addition of a 'sensitizer', which absorbs the radiation and subsequently transfers its energy to the substrate in a collision of the second kind. This kind of inter-molecular transfer of electronic energy is called 'photosensitization' and it is a valuable method in photochemistry.

Although the earliest example of photosensitization was probably the sensitized decomposition of ozone to certain

light frequencies by the addition of chlorine (31), most of the reactions of this type reported have been gas phase photochemical reactions using metal atoms as the sensitizer. The first experimental evidence indicating that mercury atoms, excited by the 253.7 nm resonance line, may transfer their energy to other molecules and cause reactions was shown by Cario and Frank (32) in the mercury-photosensitized decomposition of molecular hydrogen. Since that time, the technique of mercury photosensitization has proven an invaluable means of generating and studying free radicals near room temperature. From the standpoint of photochemistry, mercury photosensitization possesses the following advantages:

1. Mercury has appreciable vapor pressure at room temperature;
2. Mercury has large absorption coefficient for its resonance line and
3. the excitation energy of mercury is sufficient to rupture most chemical bonds.

Thus many molecules which cannot be conveniently studied by direct photolysis can be decomposed by this technique.

Resonance Lines of Mercury

Of the many observed transitions among the energy levels of the mercury atoms, there are only two transitions from the ground state corresponding to lines at 184.9 nm and 253.7 nm (33). Figure (4) shows schematically the low-lying

energy levels of the mercury atom. It will be seen that the two direct transitions from the ground state can be considered as resonance lines, with the 253.7 nm line responsible for the transition 6[1 S 0] --> 6[3 P 1] and the 184.9 nm line responsible for the transition 6[1 S 0] --> 6[1 P 1]. The transition probability for the former is lower than for the latter. The life-time of the 6[1 P 1] state of mercury is approximately 3.01 x 10**-10 second as compared to 1.14 x 10**-7 second for the 6[3 P 1]' state (33), and the absorption coefficient for the 184.9 nm line is so high that effects due to imprisonment of radiation are almost impossible to eliminate. Therefore, relatively little work has been done with the 184.9 nm line because of the many difficulties both in experimental techniques and in theoretical interpretation of results. For mercury photosensitization via absorption of the 253.7 nm line, the unwanted 184.9 nm radiation emitted from a mercury resonance lamp can be easily removed by appropriate filters (34).

By absorption of the 253.7 nm line, mercury atoms are raised to 6[3 P 1] state, corresponding to 112.2 kcal/mole, or 4.86 eV of electronic excitation energy. i. e.,

$$Hg[1\ S\ 0] + h\nu\ (253.7\ nm) \rightarrow Hg^*\ [3\ P\ 1] \qquad (1)$$

the rate of which depends upon the optical cross section for reaction (1) and the incident flux of 253.7 nm radiation.

In addition to the fluorescence, three types of collisional deactivation are possible:

1. Loss of 112 kcal of energy in a collison of the second kind with the production of a normal mercury atom in 6[1 S 0] state;

2. Loss of 5 kcal of energy with production of meta-stable 6[3 P 0] mercury atoms. This transition has been observed to be induced efficiently with molecules such as nitrogen and carbon monoxide (35), having vibrational spacing in the ground state very close to 5 kcal, and

3. Acquisition of 13 kcal of energy through collison with production of 6[3 P 2] mercury atoms. At room temperatures only one collison in about 1.0 x 10** 10 is capable of causing such a transition (33). Hence this transition is neglected in most photochemical studies.

Hydrogen atoms are produced by collisonal deactivation of excited mercury atoms with molecular hydrogen as represented by the reaction (2):

$$Hg^{*}\,[3\ P\ 1] + H2 \longrightarrow Hg\,[1\ S\ 0] + 2H \qquad (2)$$

Several mechanisms have been postulated for reaction (2) (37, 38).

In a classic review, recently Mains (36) discussed the current status of mercury photosensitization and the fundamental mechanisms of energy transfer from Hg [3P1] to the substrates which form its quenching partners. For quenching of Hg [3P1]] by H2, three mechanisms have been postulated. Cario and Frank (32) mechanism involves an elementary collision of Hg [3P1] with H2 to dissociate H2 into 2H atoms. However, this was later rejected by applying the principle of microscopic reversibility. Mitchel (39) postulated that as a result of collision between an excited

mercury atom and a H2 molecule in its ground state, the H2 molecule was excited to a high state of oscillation and rotation as follows:

$$Hg\,[^3P_1] + H_2 \rightarrow H_2^* + Hg[^1S_0]$$

On the basis of spectroscopic evidence, Compton and Turner (40) concluded that the result of collision was a HgH molecule and a H atom.

$$Hg\,[^3P_1] + H_2 \rightarrow [HgH]^* + H$$

Kang Yang et al. (41) projected the formation of HgH on the basis of phase space theory as had Light et al. (42) a little earlier. All these mechanisms are considered to be energetically possible.

Recently, Michael and Yeh (44), proposed the following mechanism for the primary photochemical process in which Hg added to H2:

$$Hg[^1S_0] + h\nu(253.7\ nm) \rightarrow Hg[^3P_1]$$

$$Hg[^3P_1] \rightarrow Hg[^1S_0] + h\nu(253.7\ nm)$$

$$Hg[^3P_1] + H_2 \rightarrow HgH_2^*$$

$$HgH_2^* \rightarrow Hg[^3P_1] + H_2$$

$$\rightarrow Hg[^1S_0] + H_2 + h\nu^*$$

$$\rightarrow Hg[^1S_0] + H_2$$

$$\rightarrow Hg[^3P_0] + H_2$$

$$\rightarrow HgH + H \text{ or } Hg + 2H$$

In spite of the complexity of the processes involved in the quenching of excited mercury atoms, reactions (1) and (2) are considered to be adequate to explain the formation

of H atoms via mercury photosensitization. Hydrogen atoms produced in this manner in the photochemical reactor (to be described later, in situ, were allowed to react with finely divided coal dust. This was the subject matter for this investigation.

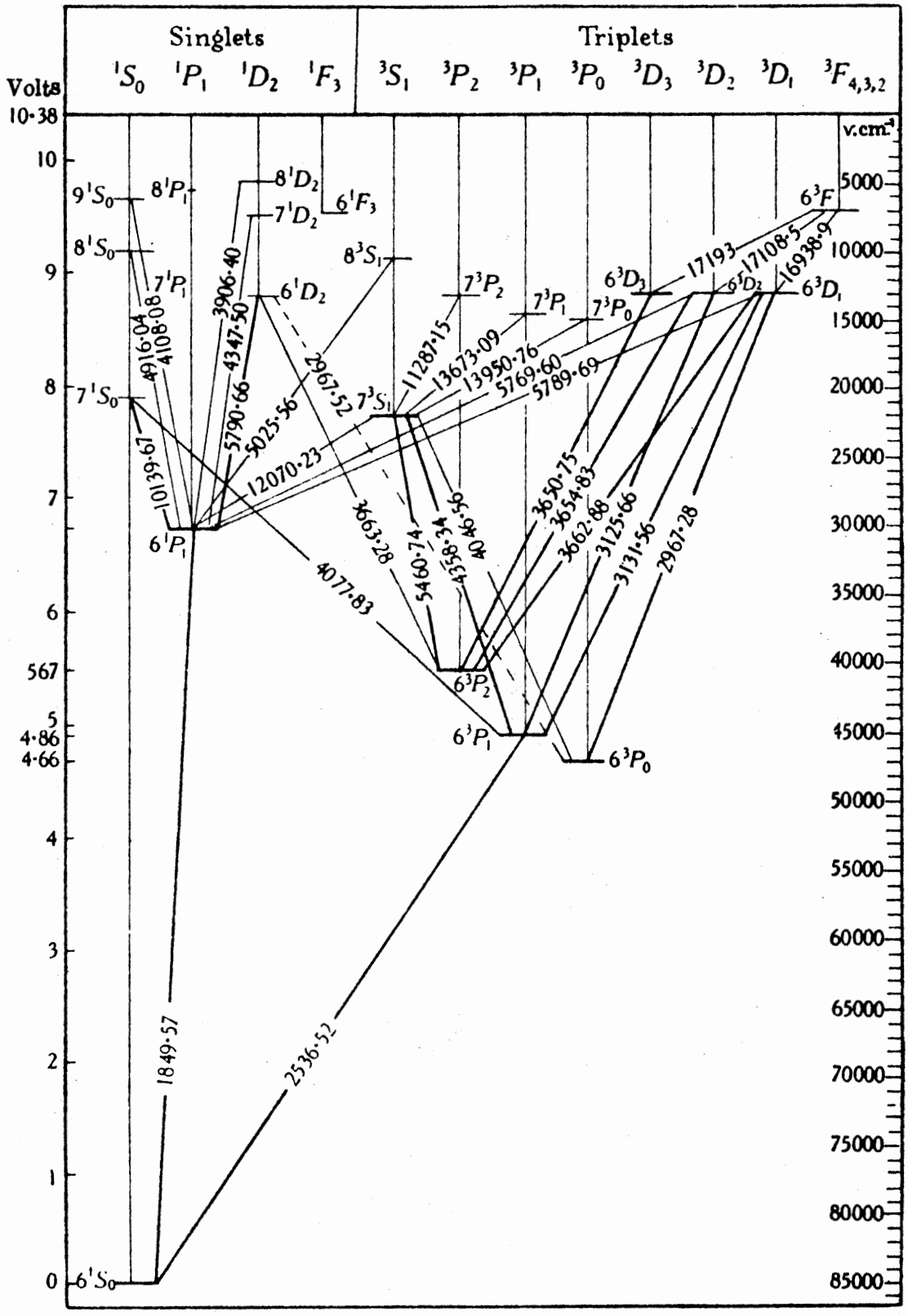

Figure 4. Energy Levels of Mercury Atoms

CHAPTER V

PREPARATION OF COALS

In order to derive meaningful conclusions from the interaction of hydrogen atoms with coal dust, it is important that the changes that occur to the coal samples from the mine to the laboratory be minimized. In addition, the grinding of coal presents a considerable challenge to the experimentalist interested in studying the fundamental properties of coal. Significant quantities of gases are entrained in the micropores of coal (45, 46), mostly air with smaller amounts of carbon dioxide, methane, and other hydrocarbons.

The release of these gases require pore opening and/or widening as is found in solvent extraction of coal with various solvents (47). Contrary to the popular belief, the entrained gases are not totally removed by pumping, even in high vacuum systems (48). Therefore, common grinding process in the presence of air can produce remarkable changes in the coal matrix, including gas evolution, surface oxidation and if, violent enough, even charring.

Indeed, in their study of evolution of gases from coal during grinding in a Bleuler mill, Radd, Carrel and Hamming

(49) have shown that olefinic gases are evolved during the grinding process, apparently as a process of grinding itself. In addition, Melton and Giardini (50) have observed water as the most abundant gas in their study of crushing of West Virginia, Kentucky and Alabama coals; other gases were hydrogen, helium, methane, ammonia, methanol, ethanol, carbon monoxide, nitrogen, ethane, oxygen, hydrogen sulfide, argon and carbon dioxide.

From these evidences it is clear that grinding and storage of coals without necessary precautions can only modify the coal surface and any conclusion from such modified surface will not be relevent. Therefore, it is important that the grinding be mild and that the coal be stored in a protective environment, e.g., nitrogen gas, until ready for use.

Preliminery grinding was done on a mini-ball (Wigglebug Model L960) and further size reduction was accomplished using a mortar and pestle. When fine fractions were needed in quantity, a hammermill was used for grinding coal. The hammermill could grind about 200 grams of coal in about a minute, the product flowing into a forty-quart plastic bag.

Cryocrushing

In order to minimize the modification of the coal surfaces, a new method of grinding was develped during the course of this investigation (51).

Air-dried coal was placed in a Dewar flask containing liquid nitrogen. All but a few milliliters of the liquid nitrogen were decanted and the frozen coal was rapidly transferred to a hammermill (52). The issuing product was below room temperature and was surrounded by an envelope of nitrogen gas rising from the coal. This was in contrast to grinding using a mini-ball mill (Wigglebug) where the issuing ground coal was hot to touch.

Sieving was accomplished using a Fritsch Pulverizette electromagnetic vibrator sieving machine. The sieving was done by pouring the ground coal, enveloped in nitrogen gas, into the sieve system and running the machine for fifteen to thirty minutes. Sieving yield data can be deceptive since one can never be sure if the true size distribution has been achieved on the machine being used. Hence, only the Fritsch Pulverizette was used throughout this study.

While grinding of polymeric materials at reduced temperatures has been reported (53), no such studies have been reported in the literature for coal. That precooling the coal to liquid nitrogen temperature produced dramatic effects on the ground product is evident from Table III.

One hundred-gram samples of Illinois # 6 high-volatile coal were ground under a variety of conitions: in air at ambient temperatures, with dry ice, and in liquid nitrogen. The ground coal was rapidly sieved into three fractions: (i) -500+90 microns, (ii) -90+38 microns and (iii) -38 microns.

TABLE III

PARTICLE SIZE DISTRIBUTION OF COALS GROUND UNDER DIFFERENT CONDITIONS

Sample	Size in Microns								
	+500		−500 +90		−90 +38		−38		Most Probable Size − 38 Fraction (Coulter Counter)
	g	%	g	%	g	%	g	%	
Air (ambient)	----	----	21.5	34.7	35.7	57.6	4.8	7.7*	28 microns
N_2 (ℓ) (air-dried coal)	0.2	0.3	19.4	25.5	32.3	42.4	24.2	31.8**	18 microns
N_2 (ℓ) (wet coal)	----	----	18.9	26.6	27.0	38.0	25.2	35.4	not measured
N_2 (ℓ) (double ground)	----	----	6.3	13.9	22.0	48.3	17.2	37.9	not measured
CO_2 (s)	0.1	0.2	19.9	37.0	23.5	43.5	10.5	19.4	not measured

* After one week, agglomeration reduced this fraction by 40%.

** After one week, agglomeration reduced this fraction by 10%.

Whereas regular grinding in air, resulted in a particle size distribution that averages near the 90 micron size, those grindings at reduced temperature clearly produced an average particle size closer to the 38 micron size. Nearly a third of the coal which was frozen in liquid nitrogen passed the 38 micron sieve compared with 7.7% for the regular grinding. Furthermore, the Coulter Counter study of the particle distributions showed the most probable particle size in the liquid-nitrogen-ground fraction to be 28 microns. The results of Coulter Counter analysis of -38 micron coals ground in liquid nitrogen is shown in Figure 5. The fraction ground at dry ice temperature was not subjected to Coulter Counter analysis but might be expected to be intermediate since the sieve classification is intermediate (55).

The size distribution of a particular grade particles can be determined by using Rosin-Rammler (54) relation,

$$R = 100 \exp[-(x/k)^{**}n]$$

where x = aperture size

k = measure of the finness of a particle

n = measure of the size dispersion and

R = weight of particles greater than size x

When $x = k$, $R = 100/e = 36.79$

Rearranging the former equation,

$$\ln[\ln(100/R)] = n \ln(x) + \text{Constant}$$

Channel	Cum.	Diff.
1	100.3	0.0
2	100.1	1.1
3	99.4	2.0
4	97.6	3.6
5	94.2	5.8
6	88.6	10.2
7	78.6	14.0
8	64.9	18.0
9	47.1	20.9
10	26.5	17.9
11	8.8	7.6
12	1.2	0.9
13	0.4	0.1
14	0.3	0.0
15	0.3	0.3
16	0.0	0.0

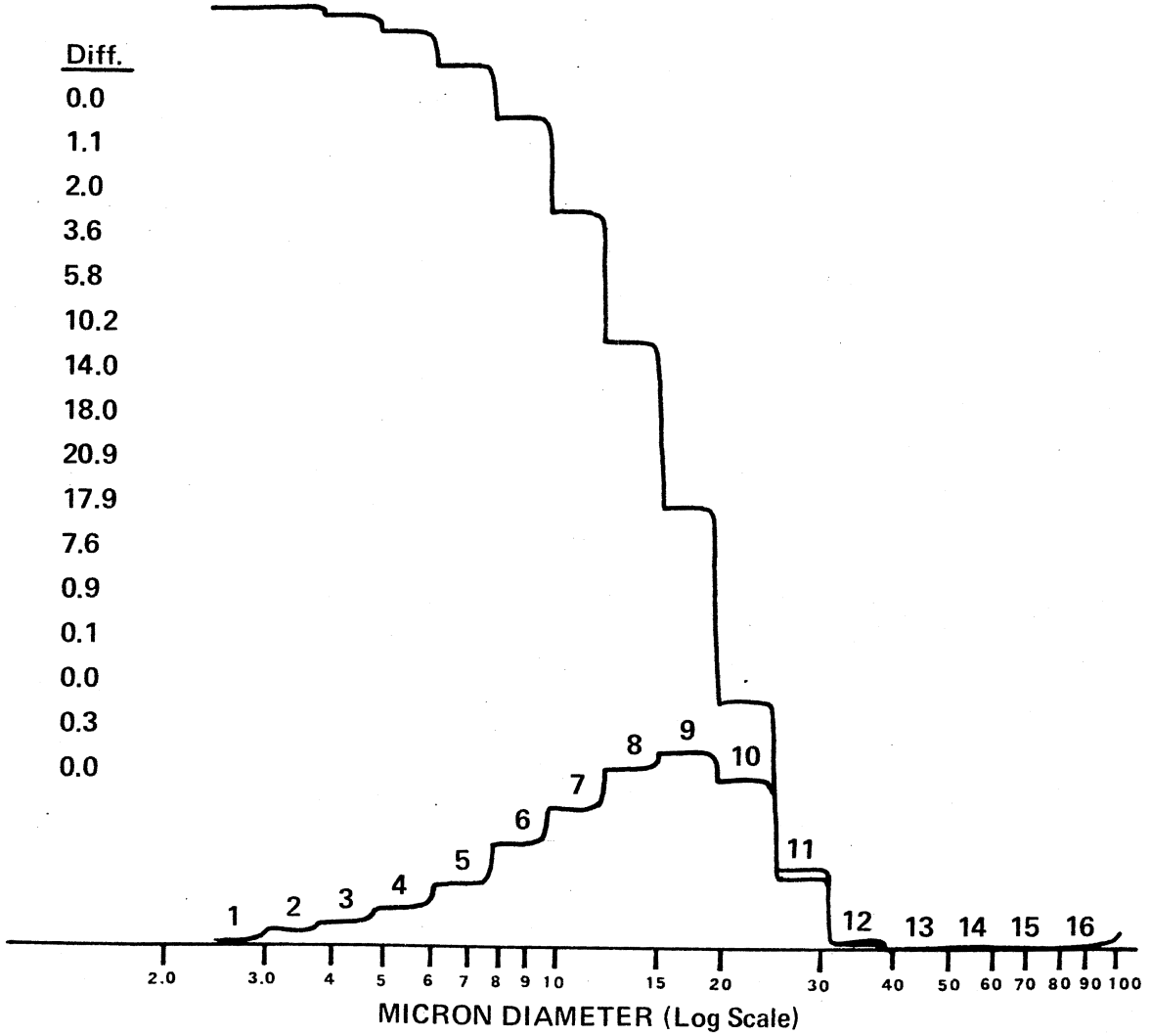

Figure 5. Coulter Counter Analysis of -38 Micron Liquid Nitrogen Ground Coal

Thus, for a size distribution obeying the Rosin-Rammler relation, a plot of ln[ln(100/R)] against ln(x) should give a straight line of slope n.

The friability of coal ground after being cooled in liquid nitrogen is amply illustrated by Rosin-Rammler plot of sieving yields in Figure 6. (Unfortunately, the value of these plots was not appreciated until after the sieving data had been taken. Hence, the limited number of points is regretable.) Despite the fact that the coal samples ground in ambient air, CO 2(s) (and not shown), and liquid nitrogen had almost identical average particle sizes, k = 90 microns, the slopes (n values) decreased in the order cited, suggesting that some 10% of the liquid-nitrogen-ground coal was under 10 microns! Since the Coulter Counter analyses did not find any particles smaller than three microns, it is suspected that these very fine particles were lost in the grinding process and evacuuated through the hood, where the hammermill was located.

That the coal ground under liquid nitrogen tends to undergo less surface oxidation than the coal ground in the presence of air was proved from the ESCA results, the experimental procedure of which is described in Chapter V.

The survey scans of size segregated, air ground and liquid-nitrogen-ground coals are presented in Figures 7 through 10. The relative concentration of all the elements that were present in significant amounts at the coal sur-

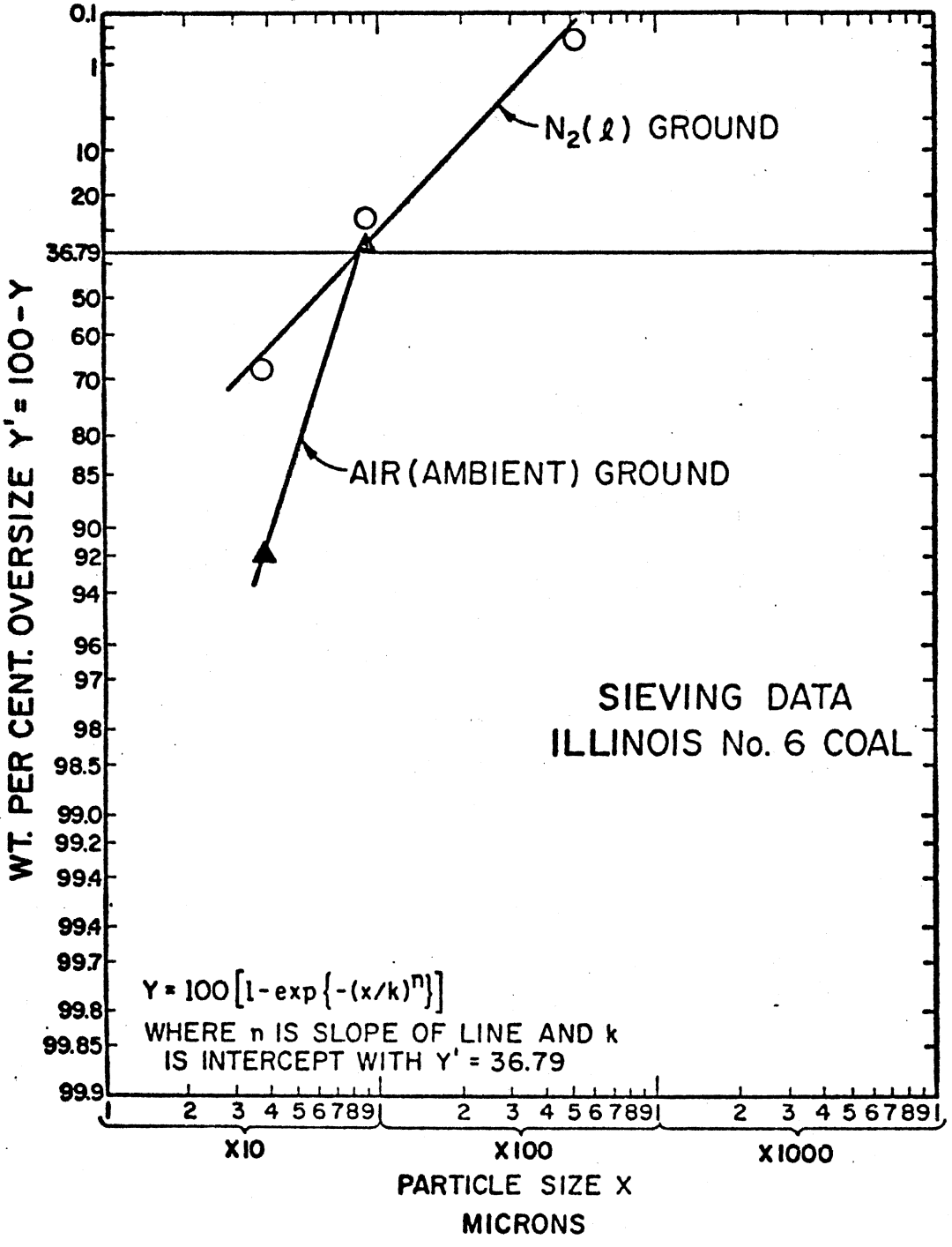

Figure 6. Rosin-Rammler Plot of Sieve Yields of Coals Ground Under Different Conditions

faces and the O/C ratios are shown in Table IV. Because of the low pressures involved and the sample handling techniques (to be described later), the oxygen analysis is believed to represent the chemically bound oxygen and not absorbed oxygen. Further, Table IV shows that there is no significant concentration of Si, Al or S in the liquid-nitrogen-ground coal. It should be observed that nitrogen incorporation onto the coal surface during grinding was negligible. Fast neutron activation analysis of the liquid nitrogen ground coal shows the presence of 19.55 ± 0.16 % oxygen at the coal surface which compares favorably with the results obtained from ESCA. These results suggest that the bulk structure of coals are represented better in the liquid-nitrogen-ground coals than in the air ground coals.

Naphthalene Treatment

A sample of coal, about 15 grams, as received was intimately mixed with an equal amount of naphthalene. A three-day treatment of coal with the sublimable solid, naphthalene displaced large quantities of occluded gases from the coal (56). The coal-naphthalene mixture was frozen in liquid nitrogen and ground in the swinging hammermill. The ground product was heated to 200 deg C to constant weight under flowing nitrogen gas and used in a photohydrogenation experiment. No naphthalene was detected in the hydrogenation products at 200 deg C by either gas chromatography or mass

spectrometry. It is believed that this treatment, followed by storage under nitrogen, represents the ultimate in sample preparation.

Nickel Carbonyl Treatment

At room temperature, nickel reacts with carbon monoxide to produce nickel carbonyl. A sample of coal as received was treated with nickel carbonyl. When the mixture was heated, nickel carbonyl decomposes thereby leaving finely divided Ni on the surface of coal:

$$Ni + 4\,CO \longrightarrow Ni(CO)4 \longrightarrow Ni + 4\,CO$$

The mixture was ground in the same manner as in the case of naphthalene treatment and used in a hydrogenation experiment. The purpose of this pre-treatment was to determine the effect of finely divided Ni catalyst on the photohydrogenation of coal the results of which are shown in Chapter IX.

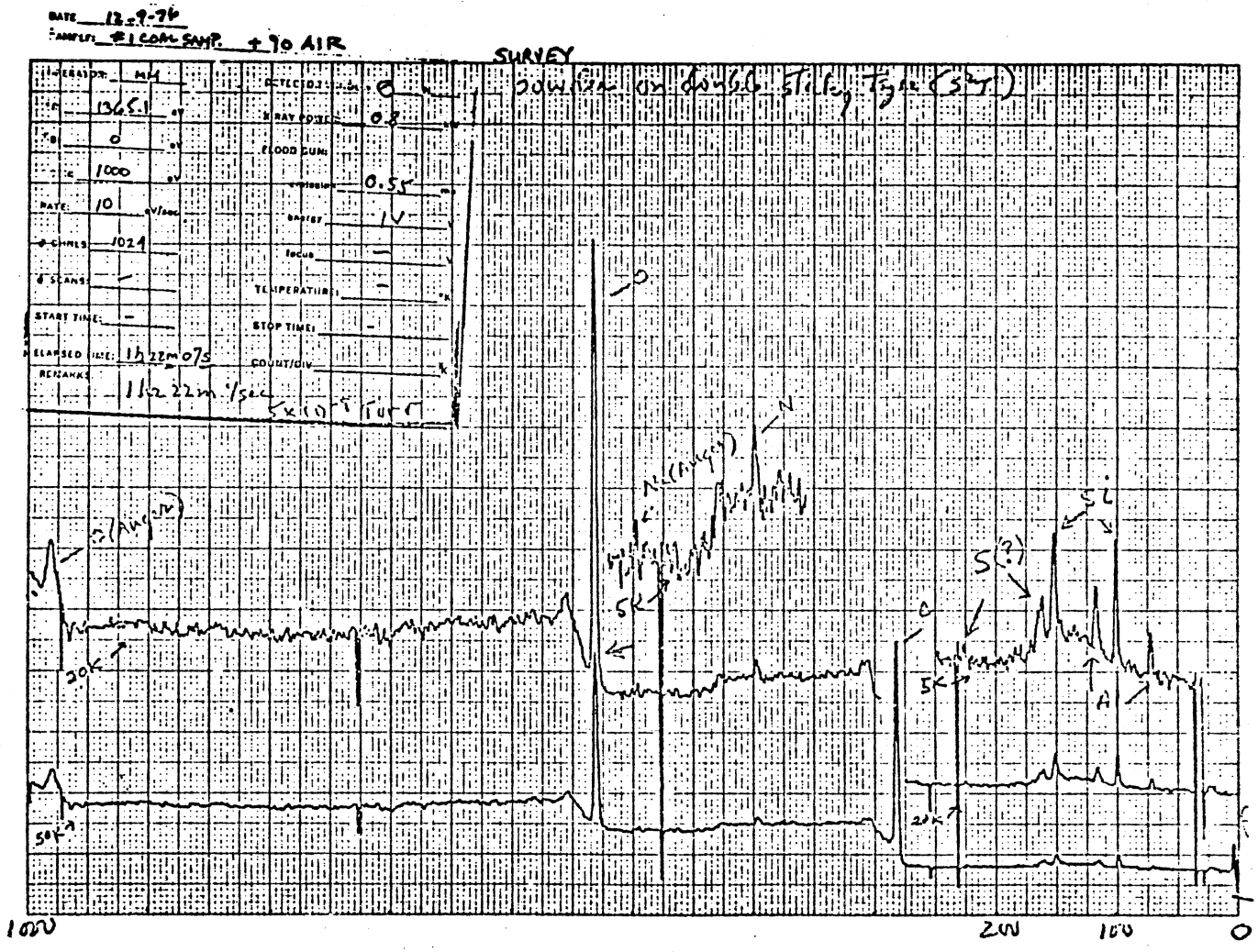

Figure 7. ESCA Survey Scan of +90 Micron Air-Ground Coal

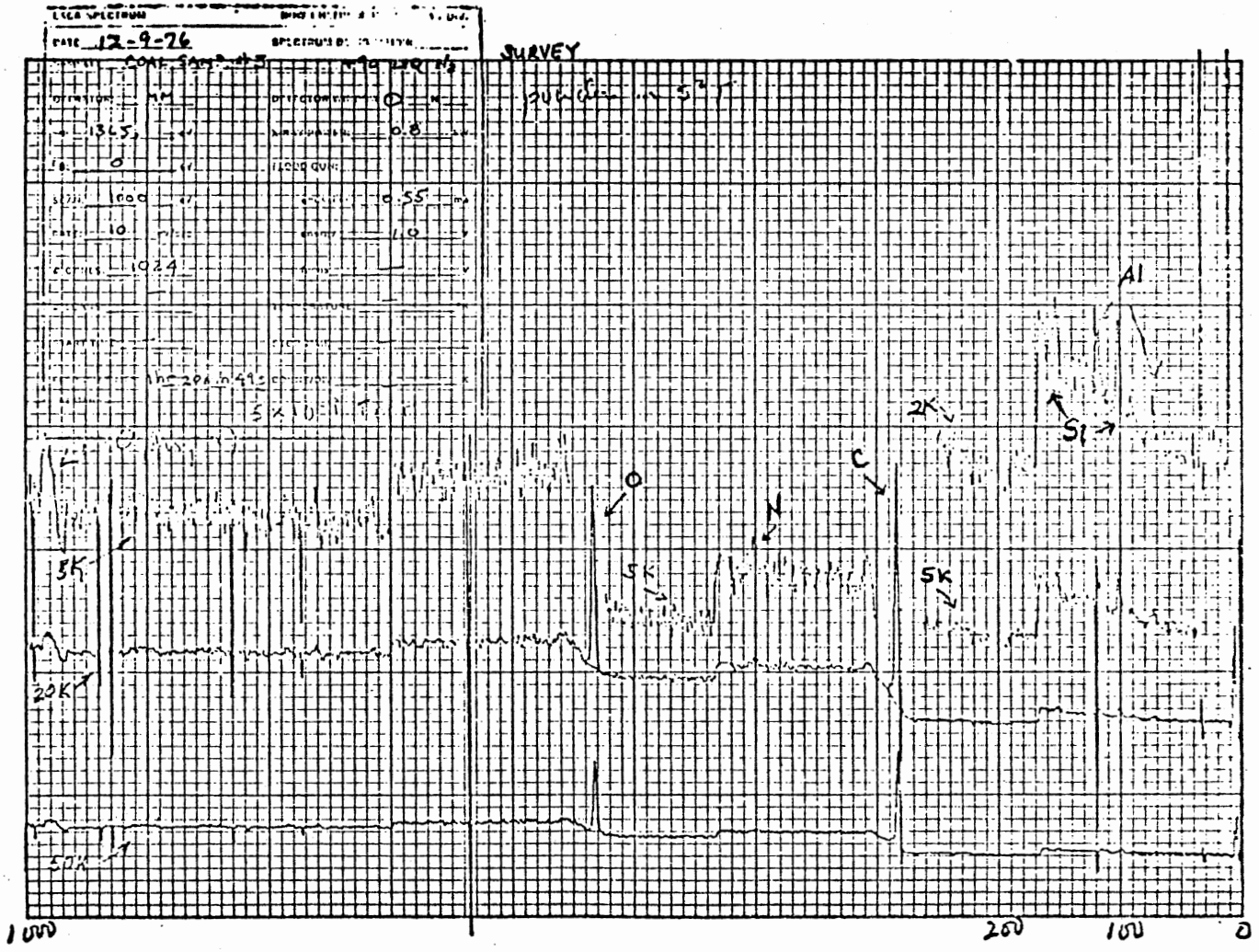

Figure 8. ESCA Survey Scan of +90 Micron Liquid-Nitrogen-Ground Coal

ESCA SPECTRA OF ILLINOIS NO. 6 COAL
(-38 MICRON FRACTION, AIR-GRIND)

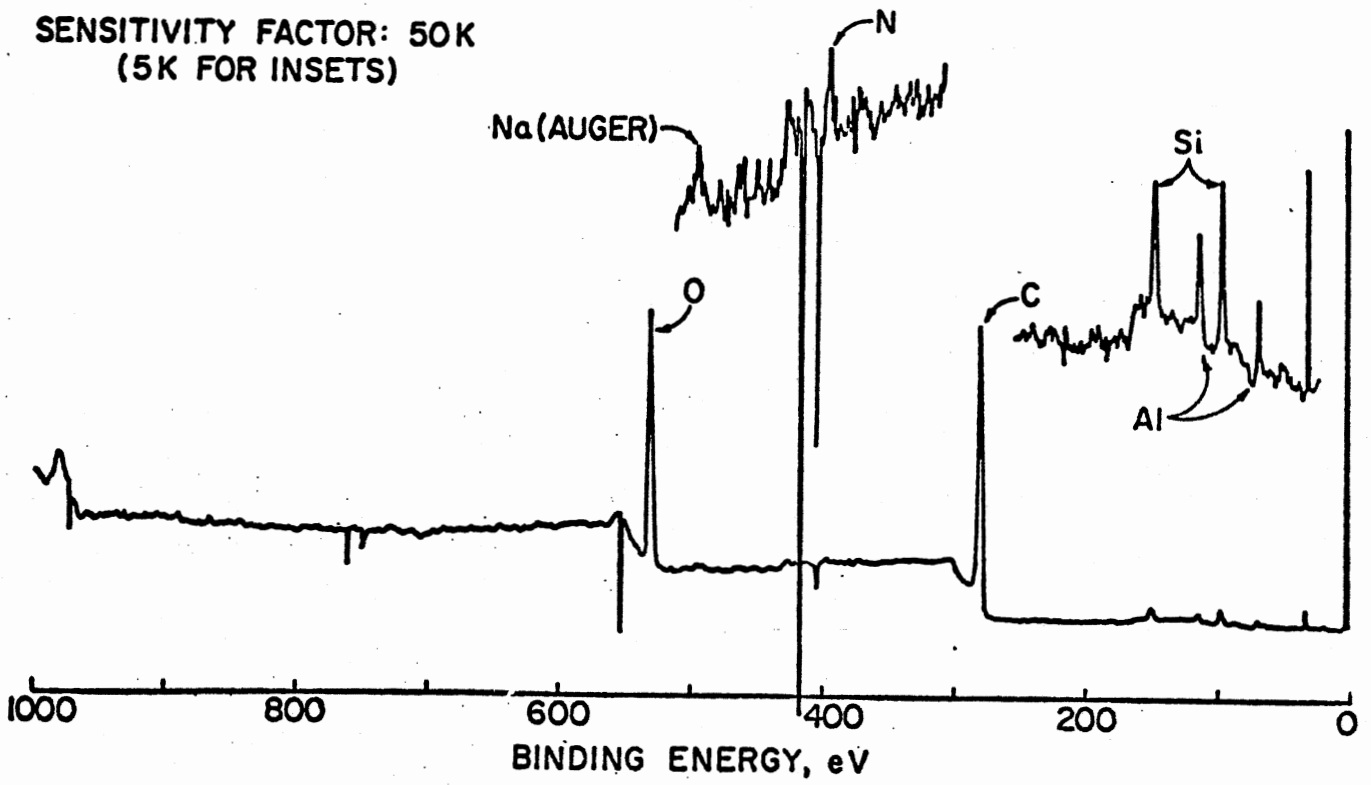

Figure 9. ESCA Survey Scan of -38 Micron Air-Ground Coal

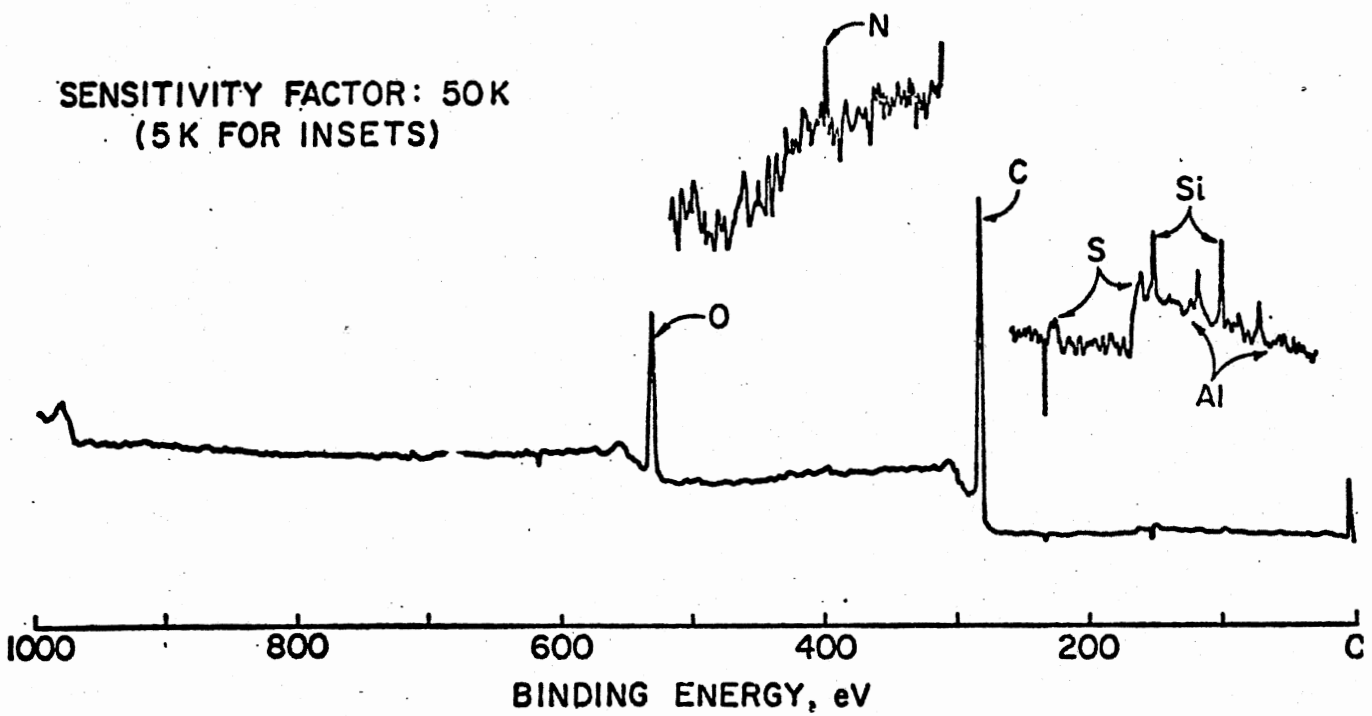

Figure 10. ESCA Survey Scan of -38 Micron Liquid-Nitrogen-Ground Coal

TABLE IV

XPS ANALYSIS OF RELATIVE CONCENTRATION OF ELEMENTS ON THE COAL SURFACES

Element	1	2	3	4
O	27	30	26	20
N	1.4	1.1	0.9	1.3
C	64	63	67	75
S	0.7	0.2	0.3	0.4
Si	4.6	4.8	3.2	2.4
Al	1.8	1.9	1.7	1.0
O/C	0.41	0.48	0.38	0.25

Note:

1. +90 micron fraction air-ground
2. -38 micron fraction air-ground
3. +90 micron fraction liquid-nitrogen-ground
4. -38 micron fraction liquid-nitrogen-ground

CHAPTER VI

GENERATION OF HYDROGEN ATOMS

The method of mercury photosensitization for the generation of hydrogen atoms was ruled out by Pinchin (57) as too inefficient. However, subsequent studies (58, 59) have shown the steady state concentration of hydrogen atoms to be of the order of 10**13 H atoms/cc by this method. The technique requires that the flowing molecular hydrogen be saturated with mercury and irradiated in a quartz reactor (shown in Figure 11) with 253.7 nm resonance radiation.

The reaction sequence in the production of H atoms via mercury photosensitization was discussed in Chapter IV. Hong and Mains (43) have recently employed measurements of Lyman-a absorption by the H atoms produced in the quenching of Hg [3P1] by H2 and HD, and obtained quenching cross-sections of 0.100 ± 0.004 and 0.109 ± 0.012 nm**2 respectively. Hence reaction (2) will occur before the excited mercury atom can diffuse 10**-13 cm or radiate (t=1.14 x 10**7 sec) (61). So the fate of nearly every excited mercury atom is reaction (2) and the rate of H atom production is limited by reaction (1), the rate of photon absorption. Further, since the spectral emission profile of the resonance lamps never

quite matches the absorption spectrum profile of mercury in the reactor, but is, nonetheless, quite high, the absorption is believed to occur within 2-3 mm of the irradiated reactor wall. Thus, the reaction system is not only heterogeneous from a phase point, i.e., "solid" coal dust dispersed in flowing gas, it is also heterogeneous in the generation of atomic hydrogen too.

If the interaction of H atoms with the coal dust is neglected for the moment, the principal back reactions are reactions (3) and (4),

$$2H + H2 \rightarrow 2H2 \qquad (3)$$

$$2H + Wall \rightarrow H2 \qquad (4)$$

the homogeneous and heterogeneous recombination of H atoms.

The three body, homogeneous recombination of H atoms has been studied extensively by several workers for over 50 years. Despite the many studies, there is still considerable uncertainity over the rate data. Applying a resonance theory, Roberts et al. (62) predicted that the rate constant for the reaction (3) reaches a maximum at 80 deg K. However, systematic study of the dependence of the reaction on temperature and inert gases have been less frequent. Bennett (63) obtained a value of 3.7 x 10**-33 cm**6/molecule**2-sec for the rate constant of reaction (3). Trainer et al. (65) reported a value of 8.1 x 10**-33 cm**6/molecule**2/sec for the reaction H + H + H2 and 7.0 x 10**-33 for the reaction H + H + He. Baluch et al. (64)

recommend the value of 8.3 x 10**-33 cm**6/molecule**2/sec, with a suggested error limits of ±50% at 300K.

Numerous measurements of the catalytic effect of various surfaces on the heterogeneous atom recombination, represented by reaction (4) have been carried out in the past. It has been generally accepted that the kinetics of heterogeneous recombination are first order with respect to gaseous atom concentration (66, 67 and 68).

Wood and Wise (69), in a classic paper, discussed the kinetics of H atom recombination on pyrex class and fused quartz and came to the conclusion that at temperatures less than 500 deg K (and greater than 120 deg K), the recombination could be explained by Rideal mechanism, involving a collision between a surface-adsorbed atom (S-H) and a gas atom, i.e., S-H + H --> S + H2, with an activation energy of 2.25 kcal/mole, whereas at temperatures greater than 500 deg K, by Hinshelwood mechanism, involving two surface-bound atoms, i.e., S-H + S-H --> 2S + H2, with an activation energy of 22.5 kcal/mole. Recently, Michael et al. (32) determined the first order rate constant for the reaction (4), k4, on quartz walls and reported a value of 21 per sec at 470 deg K. This was in excellent agreement with earlier findings by Wood and Wise (68) and Gelb and Kim (70).

The differential equation for the concentration of H atoms/cc, n, is given by

$$dn/dt = 2I(a) + D\nabla^2 n - k3(H2)(n^{**}2) - k4Sn \quad (5)$$

where 2I(a) is the rate of production of H atoms at any point in the system, $D\nabla^2 n$ is the diffusion loss, S is the surface area of the reactor, and the last two terms are the back reaction losses at the same point. At the steady state,

$$2I(a) = -D\nabla^2 n + k3(H2)(n^{**}2) + k4Sn \quad (6)$$

The solution for equation (6) is dictated by the assumed functionality of I(a), naively, [dI(a)/dr] or I(o) k exp [-k (R-r)], where I(o) is the incident light flux, R is the reactor radius, and k is the effective absorption coefficient, about 1/8 per cm. Clearly, I(a) and reaction (4) dominate near the wall, R, and the extent to which reaction (3) occurs is determined by the diffusion of H atoms into the center of the reaction vessel, r=0, and the concentration of H2. The extent to which the H atom concentration varies from peaking near the walls or becomes approximately radially uniform in this investigation is not known.

Experimentally, one can meausre the total rate of hydrogen atom production in the system by scavenging them with 1% ethylene and measuring the butane and ethane produced via reactions (8) and (9).

$$H + C2H4 \rightarrow C2H5 \quad (7)$$

$$2C2H5 \rightarrow C2H6 + C2H4 \quad (8)$$

$$\rightarrow C4H10 \quad (9)$$

Values ranging from 1.7 x 10**-13 to 8.5 x 10**-13

cc/molecule-sec have been reported for the rate of reaction (7), k7 by several workers. By an extrapolation method, Oref and Rabinovitch (71) reported a value of 1 x 10**-11 exp (-1.4/RT) for k7. Recent value for k7, for the pressures between 10 and 15 torr, the pressures involved in this reaserch, is 3.9 x 10**-13 cc/molecule-sec reported by Cowfer et al. (73). k8 + k9 is approximately 5.4 x 10**-11 cc/molecule-sec (72). The ratio of products C2H6/C4H10 was believed to be equal to the ratio of rates of disproportionation and combination of ethyl radicals, k8/k9 (74) and it has been reported to be 0.14 (72).

Smith postulated the following alternative reaction scheme for the production of ethane (75):

$$C_2H_5 + H \longrightarrow C_2H_6^* \qquad (10)$$

$$C_2H_6 + M \longrightarrow C_2H_6 + M \qquad (11)$$

$$C_2H_6^* \longrightarrow 2CH_3 \qquad (12)$$

However, this was concluded to be unimportant by Melville and Robb (76). This indicates a negligibly small rate of combination of H atoms with ethyl radicals ().

Thus, the following expressions could be written for the rate of removal of H atoms by (i) homogeneous recombination, (ii) wall recombination and (iii) scavenging by ethylene:

$$-[d(H)/dt]_h = k_3[H]^2[H_2] \qquad (13)$$

$$-[d(H)/dt]_w = k_4[H] \qquad (14)$$

$$-[d(H)/dt]_s = k_7[H][C_2H_4] \qquad (15)$$

For an actinometry gas mixture consisting of 1.28% ethylene and 98.72% hydrogen in it, hydrogn and ethylene concentrations, in moles per cc are given by

$$[H2] = (6.023 \times 10^{**}23/22400)\ (98.72/100) \quad (16)$$

$$[C2H4] = (6.023 \times 10^{**}23/22400)\ (1.28/100) \quad (17)$$

Substitution of these values and the respective rate constants in equations 13 through 15, leads to

$$-[d(H)/dt]h = 2 \times 10^{**}-13\ [H]^{**}2 \quad (16)$$

$$-[d(H)/dt]w = 21 \times [H] \quad (17)$$

$$-[d(H)/dt]s = 1.3 \times 10^{**}5\ [H] \quad (18)$$

From the above expressions, it is evident that in the presence of small amount of ethylene, the removal of H atoms is essentially due to scavenging by ethylene, and hence removal of H atoms by homogeneous recombination and heterogeneous wall recombination could be neglected. Thus, if the rate of production of H atoms, [d(H)/dt], is known, the steady state H atom concentration, [H]s.s. could be calculated.

From the measurement of butane and ethane produced in the actinometry experiment, details of which is given in the next section, it was found that

$$[d(H)/dt] = 5.5 \times 10^{**}14 \text{ atoms/cc/sec} \quad (19)$$

From equations (18) and (19) for [H]s.s., it follows that

$$[H] \text{ s.s.} = 2 \times 10^{**}13 \text{ atoms/cc}$$

Actinometry Experiments

The following experiment was done to determine the appropriate conditions for measuring the butane and ethane produced when the actinometry gas (1.28% C_2H_4 in H_2) was passed through the system. Since an absolute measurement of the gases in the trap was necessary, the experimental reaction time was reduced from one hour (commonly used with coal) to 120 secs. Therefore, a bypass line was used so that the irradiation system had time to equilibrate thermally before products were collected. It was also at this point that analyses of the contents of the traps T2 and T3 in Figure 11 were found to be almost identical, implying low trapping efficiencies and the 6-mm glass beads were added to the traps, raising the collection efficiencies to 47% per trap for n-butane.

The traps were flushed with actinometry gas and precooled, with periodic shaking of the glass beads, for an hour before connecting the traps to the photoreactor and trap bypass. Compressed air was blown through a glass-wool After the experiment, the traps were disconnected from the apparatus and allowed to warm up to room temperature. After several hours, the total gas pressure in each trap was measured by means of an open-ended manometer. Since the trap volume was known from previous calibrations, the total moles of gas in the trap could be calculated.

A 1-cc sample loop, at atmospheric pressure, was used to introduce both the reaction mixture and, separately, a Matheson certified calibration gas (95.05% H_2, 3.95% C_2H_4, and 1.00% n-C_4H_{10}) to the Perkin Elmer Model 990 Gas Chromatograph, equipped with a thermal conductivity detector. Since the PV of the gas sample introduced was known, the exact number of moles of product gas introduced could be calculated. Then, from knowledge of the PVT properties of the trap and collection efficiencies, an absolute number of moles of ethane, butane and ethylene could be calculated for the 120-second actinometry experiment. This leads to an average rate of H atom formation as 5.5 x 10**14 atoms/cc/sec in the effective reactor volume, 5280 cc.

CHAPTER VII

EXPERIMENTAL PROCEDURE

The continuous flow, photochemical reactor that was used for studying the reaction of atomic hydrogen with coal is shown in Figure 11.

A known amount of coal was mixed with an equal amount of ground glass, and placed on a frit, F1, for dispersal in the quartz reator. The traps were evacuated and precooled, with periodic shaking of the glass beads, for an hour before connecting the traps to the photoreactor and trap bypass. A 5 micron size Millipore filter placed at the top of the reactor in the middle of the connector C4 prevents the escape of coal particles from the reactor. The reactor walls were heated by passing current through the Nichrome heaters surrounding the reactor and the temperatures inside the reactor were monitored at seveal locations via a Omega (Stamford, Connecticut) Model 2166A Multipoint Digital Thermometer. The unit was a portable, four digit, manual-scan, thermocouple thermometer capable of measuring any of 10 possible like-type thermocouple inputs and resolving 1 deg C over a range of -200 to +2328 deg C. The unit featured a reference junction compensation (to eliminate the need for

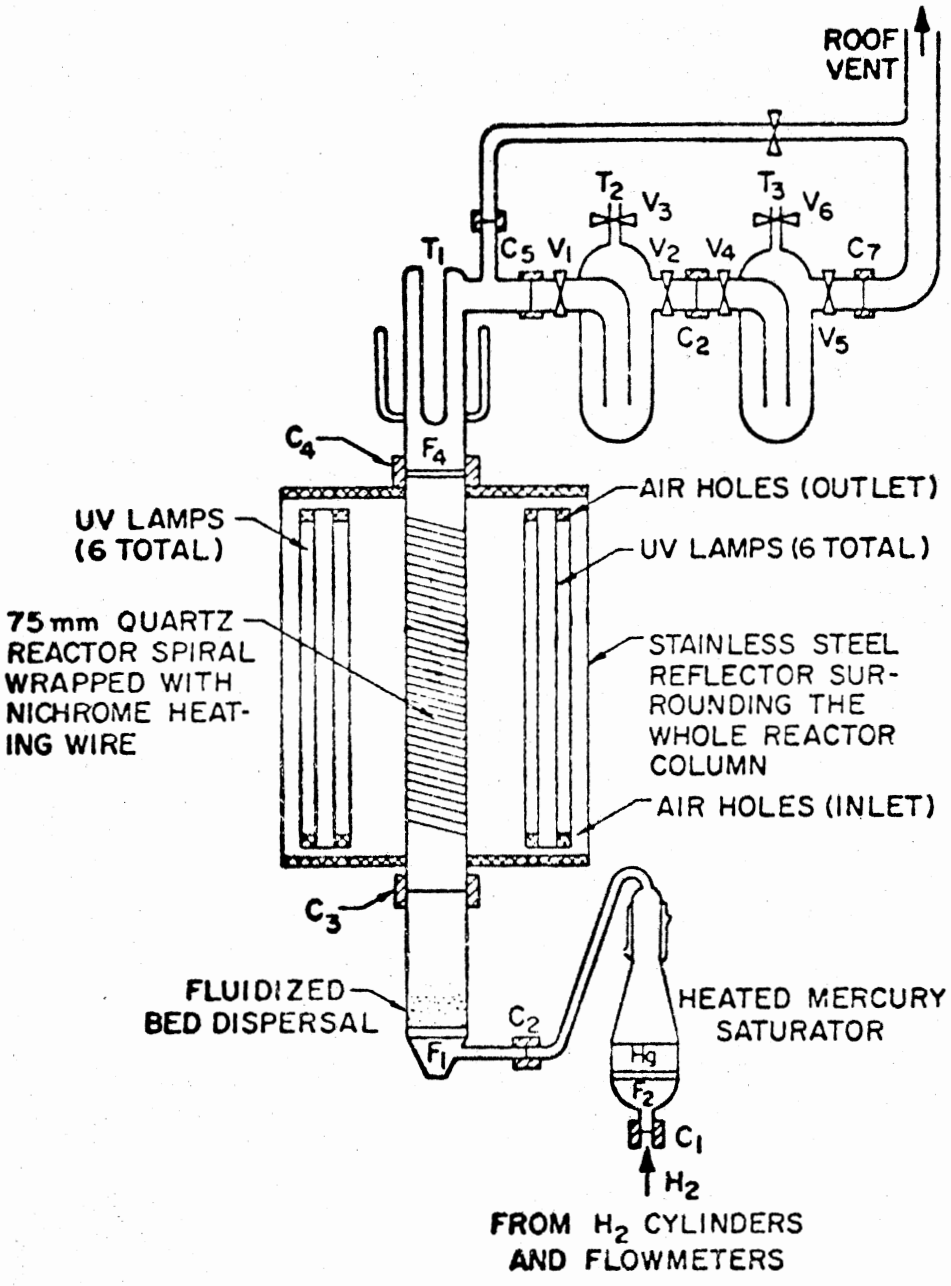

Figure 11. Photohydrogenation Reactor

an ice bath reference junction). The repeatability of the unit was ±1 deg C.

Mercury photosensitization at elevated temperatures is not common because problems are encountered with low pressure mercury lamps if they are heated. Since the lamps are most efficient in the temperature range of 40 - 50 deg C as shown in Figure 12 (60), they must be protected from heat. Actually, if the lamps get too warm, the vapor pressure of mercury becomes sufficient to reverse the resonance line at 253.7 nm, and only broad wings of radiation on either side of the resonance line are emitted (78,79). In order to keep the lamps cool, compressed air was blown through a glass-wool filter, to remove compressor oil, and spiralled around the U.V. lamps.

Next, a stream of hydrogen sufficient to disperse the coal dust (15 liters per minute) was initiated. Traps T2 and T3 were bypassed initially. When the temperature in the quartz reactor reached the desired level, the liquid nitrogen cooled traps were opened, the gas by-pass closed and the U.V. lights were turned on. Throughout the period of the reaction, the finer coal dust, which tended to accumulate on the Millipore filter was recycled using a mechanical vibrator. At the end of the run, the flow was discontinued and tne traps were isolated for analyses.

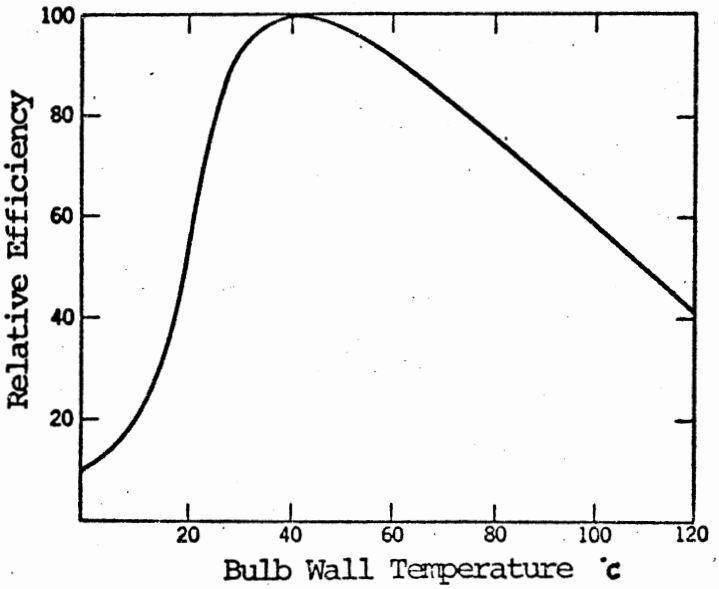

Figure 12. Effect of Temperature on the Relative Efficiency of Production of 253.7 nm Radiation

Temperature Profile in the Reactor

Chromel-Alumel thermocouples were located on the cylindrical axis and on the walls of the reactor at six sites located at the top, half-height, and bottom of the heated and irradiated zones. For a Synthane char run at 200 deg C, the thermocouples read as follows (in deg C):

Position/Cite	Top	Half-height	Bottom
Cylinder Axis	186 ± 5	202 ± 7	94 ± 4
Wall	190 ± 4	200 ± 7	124 ± 4

Thus the nominal temperature is achieved at the wall at the center of the reactor as might be expected for a Nichrome-wire wrapped quartz cylinder being severely cooled at the bottom by the influx of 15 liters per minute of hydrogen, temperature circa 25 deg C, and, undergoing heat losses due to unheated top of the reactor column.

CHAPTER VIII

ANALYTICAL PROCEDURES

PV Measurement

The products from the traps were quantitatively transferred into different gas bulbs by means of a Toepler pump with the traps in succession at i) liquid nitrogen temperature, ii) dry ice temperature and finally at iii) room temperature and the PV product of each fraction was determined from the calibration data. The idea behind this is to increase the recovery of each fraction in the range < C2, C2-C5 and C6-C8 by exploiting the difference in the vapor pressures between them at respective temperatures. However, in the qualitative experiments this procedure was not adopted; the excess hydrogen in the traps were pumped away at liquid nitrogen temperature and the residual gases were subjected to GC or GC-MS analyses after warming the traps to room temperature.

Because of the high vapor pressure of methane and ethane even at the liquid nitrogen temperature (-198 deg C), most of the methane and considerable amounts of ethane too, left the system untrapped and hence their results can not be considered to be quantitative. Furthermore, the yields of

CO_2, H_2S and H_2O produced in the reaction were not taken into consideration for quantitative analyses since the emphasis of this research was on the quantification of hydrocarbon gases alone.

Gas Chromatographic Procedures

The Gas Chromatographs used in the study were: i) an isothermal Perkin-Elmer Model 990 GC equipped with a thermal conductivity detector and ii) a temperature programmable Beckman Model 72-5 GC equipped with a flame ionization detector. The former was used for qualitative analyses while, the latter was used for all quantitative analyses. With the latter, the detection of $10^{**}-11$ moles of a simple hydrocarbon was easily possible.

A 0-400 mm (full scale) Wallace & Tiernan differential pressure gauge was attached to the sample injection loop of the Beckman GC and hence it was possible to inject a gas sample of known PV. From the FID sensitivities, determined from standard mixtures, and the PV data, it is possible to determine the exact number of moles of a particular component in a mixture. The calibration of the chromatograph was periodically checked against injections of known amounts of a calibration mixture.

A 10' long and 0.125" O.D. stainless steel column packed with 80/100 mesh n-Octane on Porasil C was used for all quantitative analyses. The column was used isothermally

at 60 deg C for the analysis of lighter hydrocarbons upto C5 and, for higher hydrocarbons, the column temperature was programmed at the rate of 3 deg C/min for 8 minutes and then kept isothermal at 84 deg C. The other columns that were used in this study, mainly for confirmation purposes, are listed in Table V.

Porapak Q is one of the eight different types of Porapaks available and most widely used for the separation of hydrocarbons. OPN/Porasil C is one of the Durapk packing materials in which a conventional liquid phase coating is pemenantly bonded to a core material. OPN/Porasil C separates components of widely varying polarity. C18 Bondapak GC consists of an octadecyl liquid phase chemically bonded to a silica substrate and features high temperature stability and excellent column efficiencies. This is mainly used for the analysis of polynuclear aromatics and fuel oils. Ultrabonds are packing materials in which an ultrathin film, less than 15 A deep and approximately 0.2% weight, of a liquid phase is tightly bound to a solid support. They produce sharp and symmetrical peaks with little tailing. TCEP shows greatest retention for all organic compounds and used frequently for retention of aromatics over aliphatic compounds. 5% Bentone 34 + 5% Isodecyl Phthalate on Chromosorb W-HP could be used for the separation of xylenes.

TABLE V

CHROMATOGRAPHIC COLUMN SPECIFICATIONS

No.	Length[1,2] (inches)	Packing Material	Mesh Size
1	6	Porapak Q	80/100
2	10	OPN[3] on Poracil C	80/100
3	10	C_{18} Bondapak GC	100/120
4	10	Ultrabond	100/120
5	6	10% Carbowax 20M on Chromosorb W-AW	80/100
6	8	10% TCEP[4] on Chromosorb W-HP	80/100
7	10	5% Bentone 34 + 5% Isodecyl Phthalate on Chromosorb W-HP	80/100

Note 1: All columns had an outside diameter of 0.1250"

Note 2: All columns were made of premium stainless steel

Note 3: OPN = Oxy-dipropionitrile

Note 4: TCEP = Tri-cyanoethoxypropane

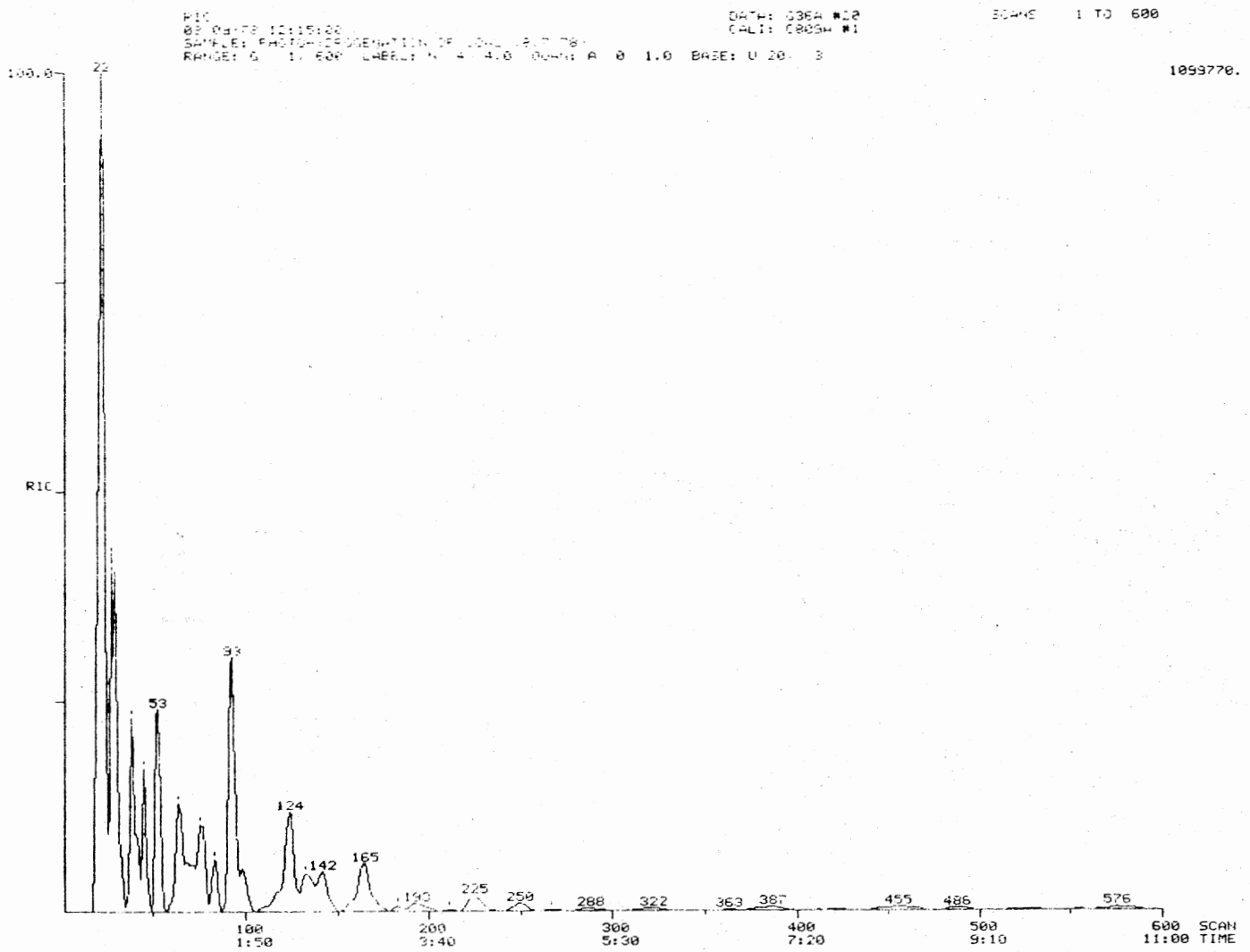

Figure 13. RIC of Products From Illinois # 6 Coal Run

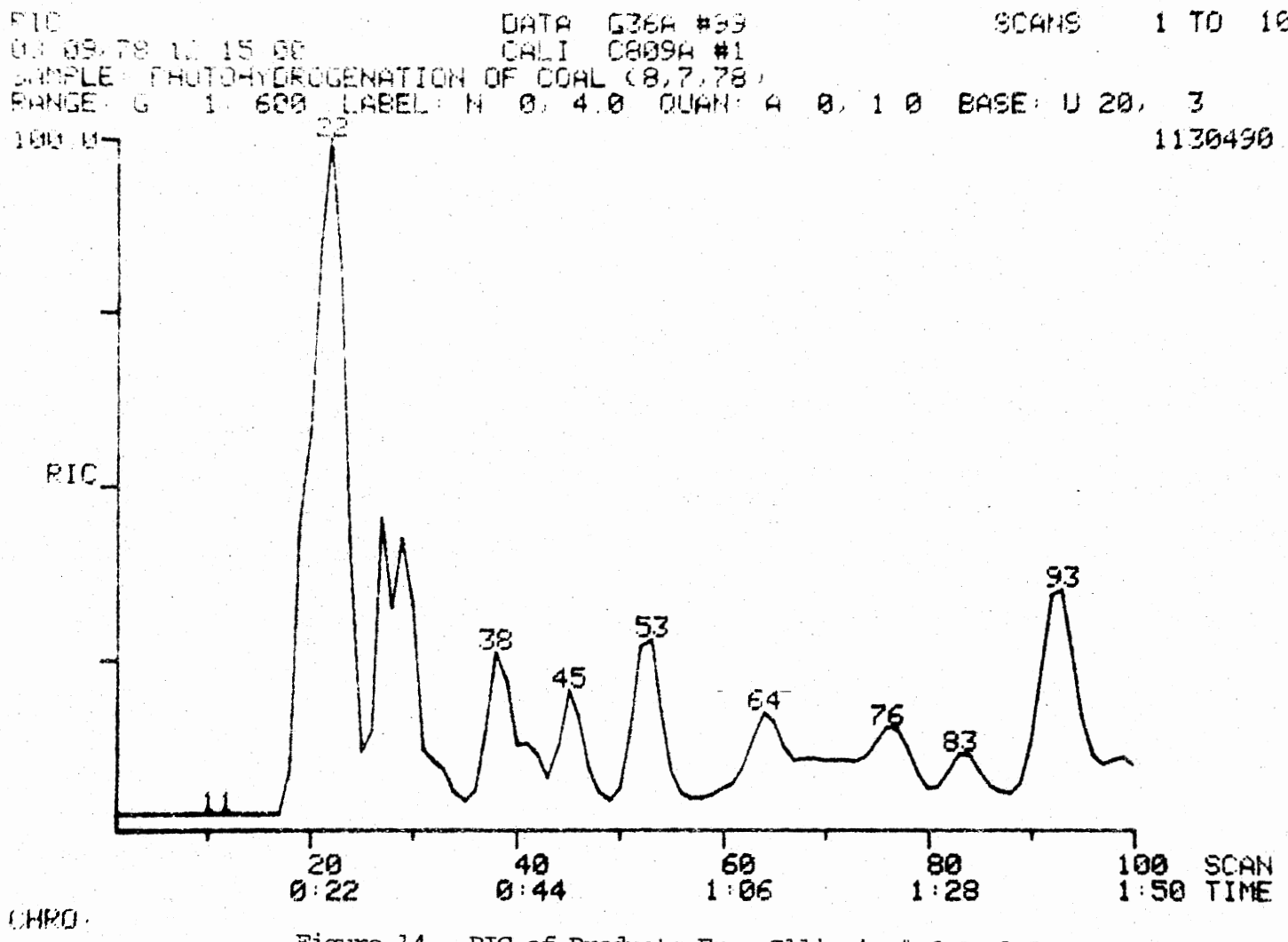

Figure 14. RIC of Products From Illinois # 6 Coal Run-Expanded

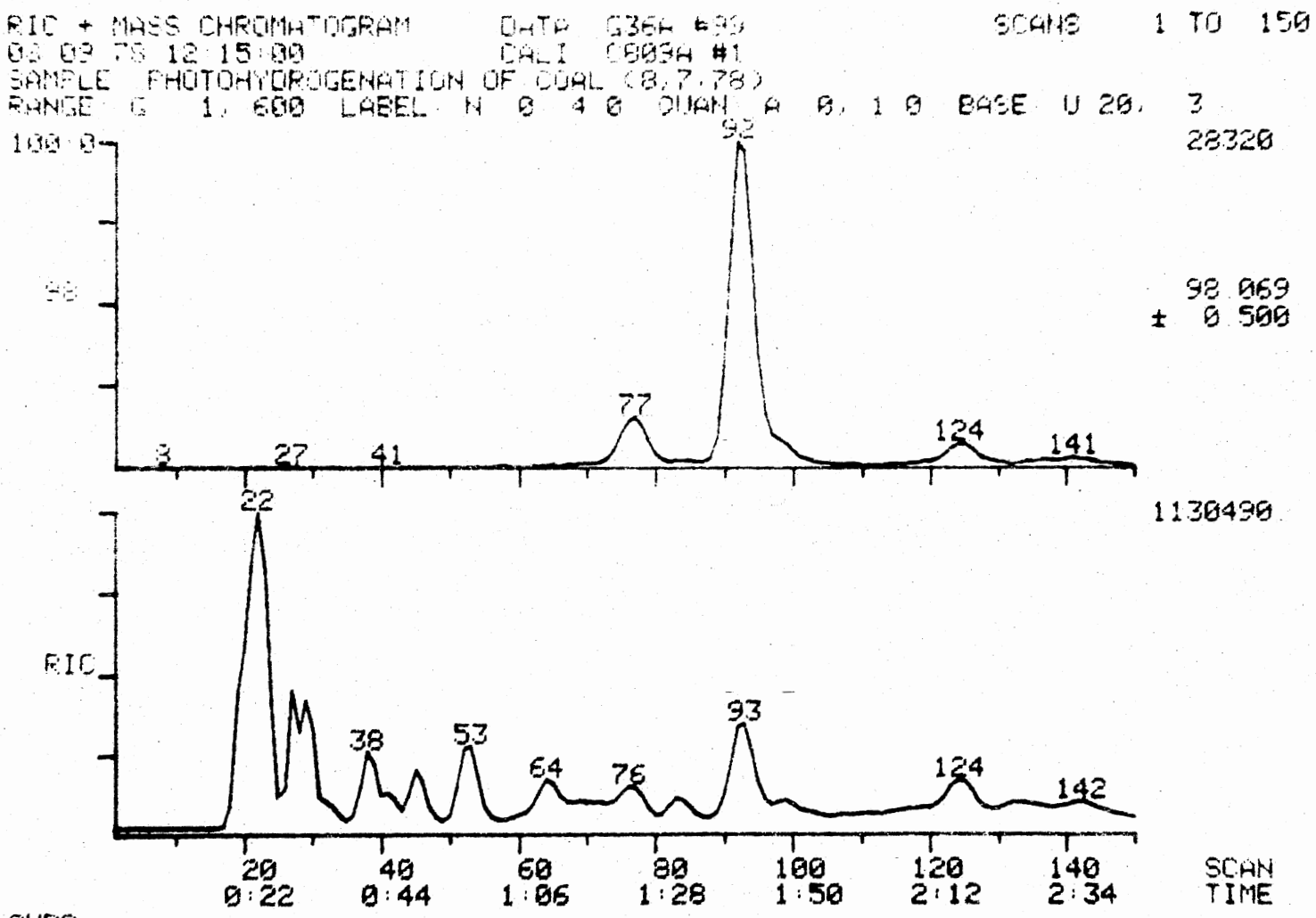

Figure 15. Mass Chromatogram of m/e 98 Ion From Illinois # 6 Coal

Gas Chromatography-Mass Spectrometry (GC-MS)

The GC-MS that was used in this investigation was a Finnigan Series 4000 on-line GC-MS-Computer system equipped with a quadrupole mass analyzer. This system is capable of acquiring and processing large volumes of mass spectral and gas chromatographic data. The GC-MS interactive data system consisted of two separate units: (i) the GC-MS interface module and (ii) the data system console. The data system console consisted of a 16-bit central processor unit, and 8196-word core memory, a 24-million bit disk data storage, pushbutton function panels, and a built-in CRT display. Programs were available for background subtraction and calibration. Further, both the NIH (National Institute of Health) and Battele/EPA (Environmental Protection Agency) mass spectral libraries were available in disks for computerized library search.

A 6' x 0.25" glass OV-1 column and another OV-101 column of same dimensions were used for the analyis of gaseous and liquid products respectively. It was intended to use the same columns under the same conditions as described in the previous section. However, the conditions proved too inadequate for GC-MS operation and new conditions were developed for GC-MS analysis using different columns.

For GC-MS analysis, the product gases were injected as obtained without fractionation on the vacuum lines. A typi-

cal reconstructed ion chromatogram is shown in Figure 13, a portion of which is shown in Figure 14 on an expanded scale. Mass spectra were obtained for each RIC peak and the identification of an individual mass spectrum was not restricted to computer library search alone.

Mass fragmentography, also known as specific ion detection, multiple ion detection, or multiple ion monitoring, technique was very useful in the identification of mass spectra. In this technique, instead of scanning through the entire mass range, the MS is made to look only at specific ions, sequentially and very rapidly. This is a very sensitive and quantitative technique. An example of this technique is given in Figure 15 in which the change in abundance of ion with m/e 98 ± 0.5 during the gas chromatogram (called "mass chromatogram") is shown. This mass chromatogram coupled with the individual mass spectrum taken at the peak of the RIC led to the identification of the peak as methylcyclohexane. If this is true, then the subtraction of the mass spectrum of the pure compound from the sample spectrum should virtually yield no peaks at all. This is shown in Figure 16. This confirms the RIC peak at scan # 93 of Figure 13 or 14 as methylcyclohexane. This procedure was adopted for identification of all peaks. Some of the peaks were not able to be identified unambigously due to the following reasons: (i) unresolved GC peaks, (ii) extremely low concentration of a component - to such an extent that the background could not be subtracted successfully.

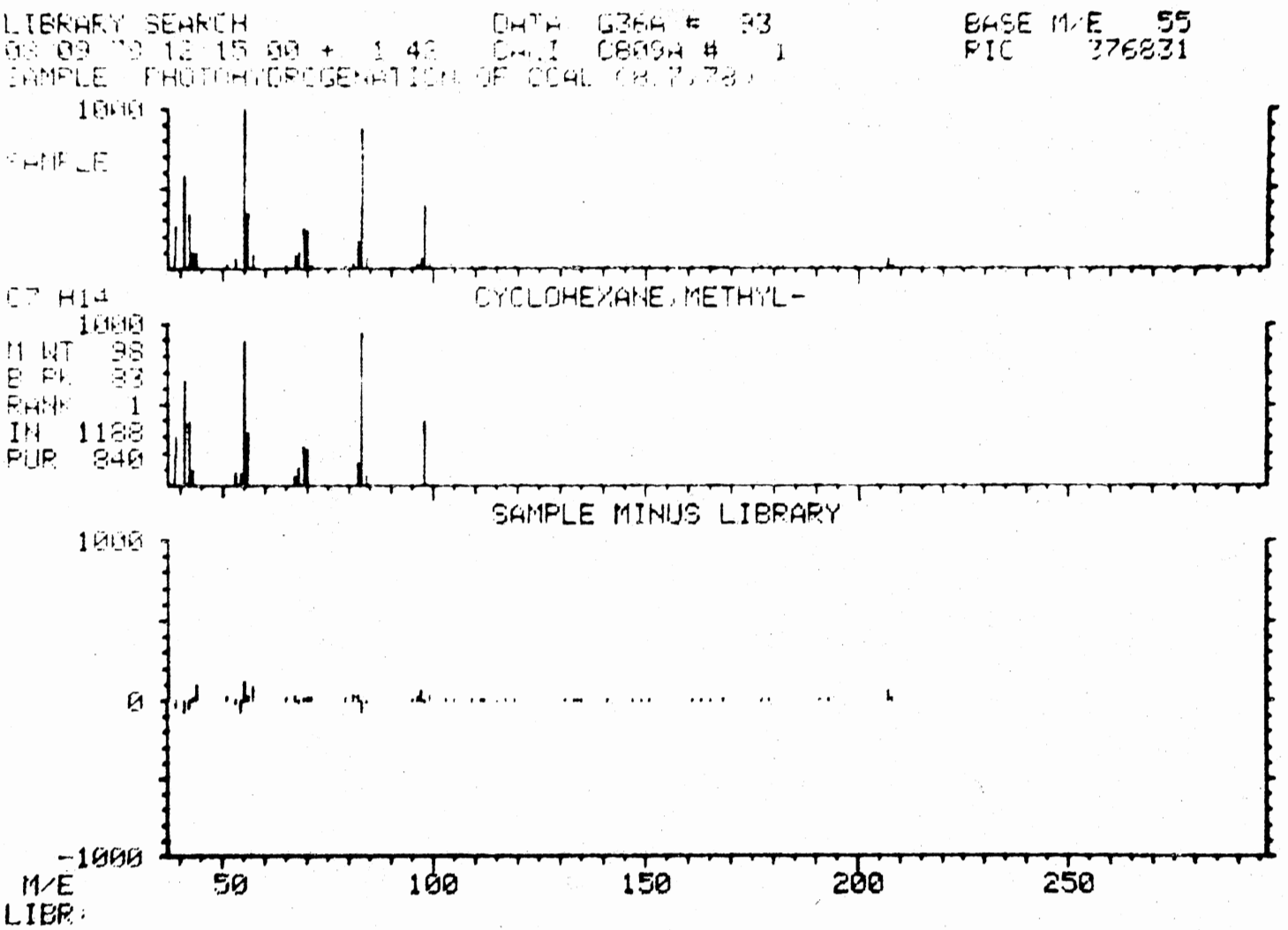

Figure 16. Sample Minus Library Spectrum for Scan # 93

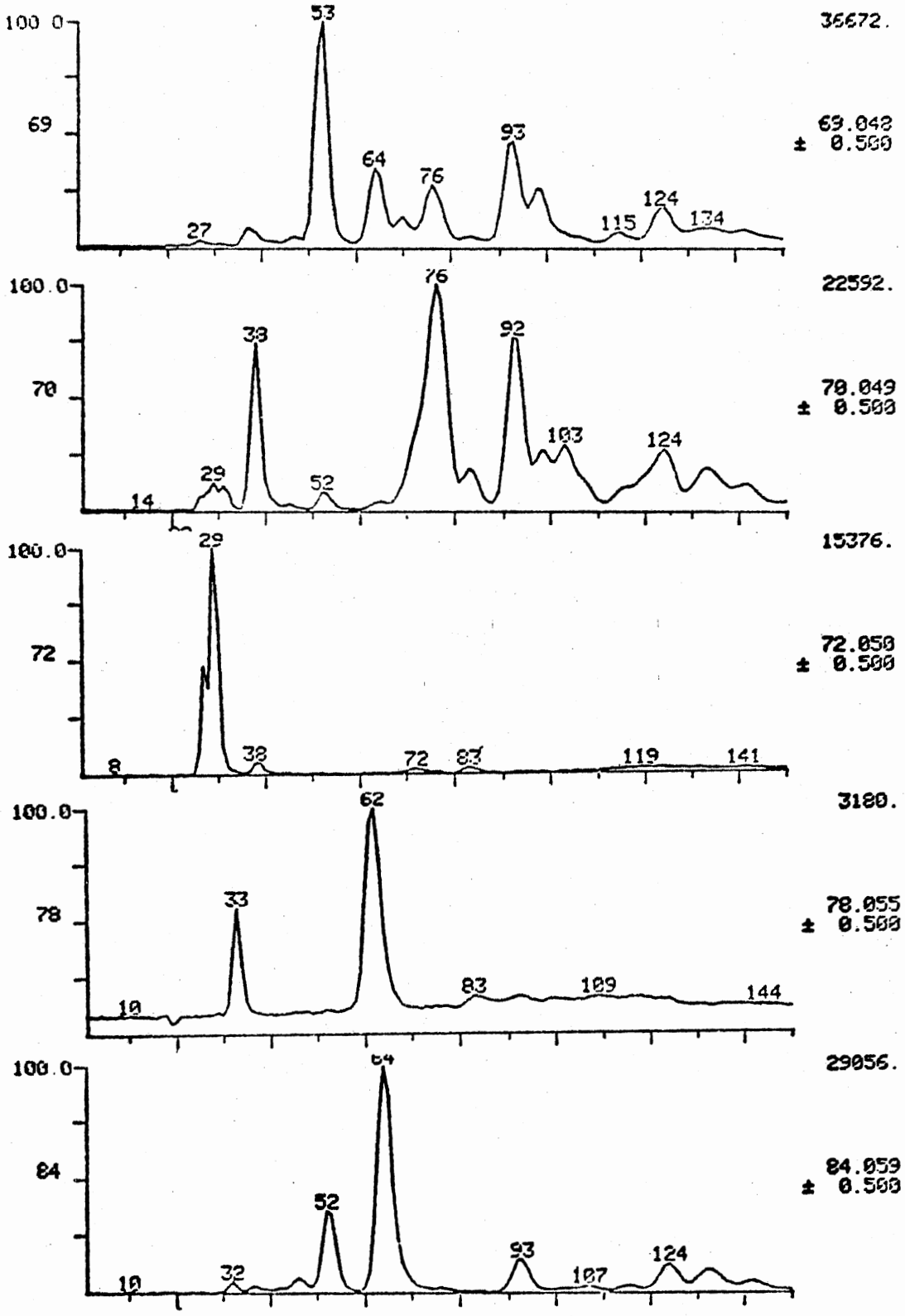

Figure 17. Mass Chromatogram of Selected RIC Peaks From Illinois # 6 Run

Figure 17 Continued ...

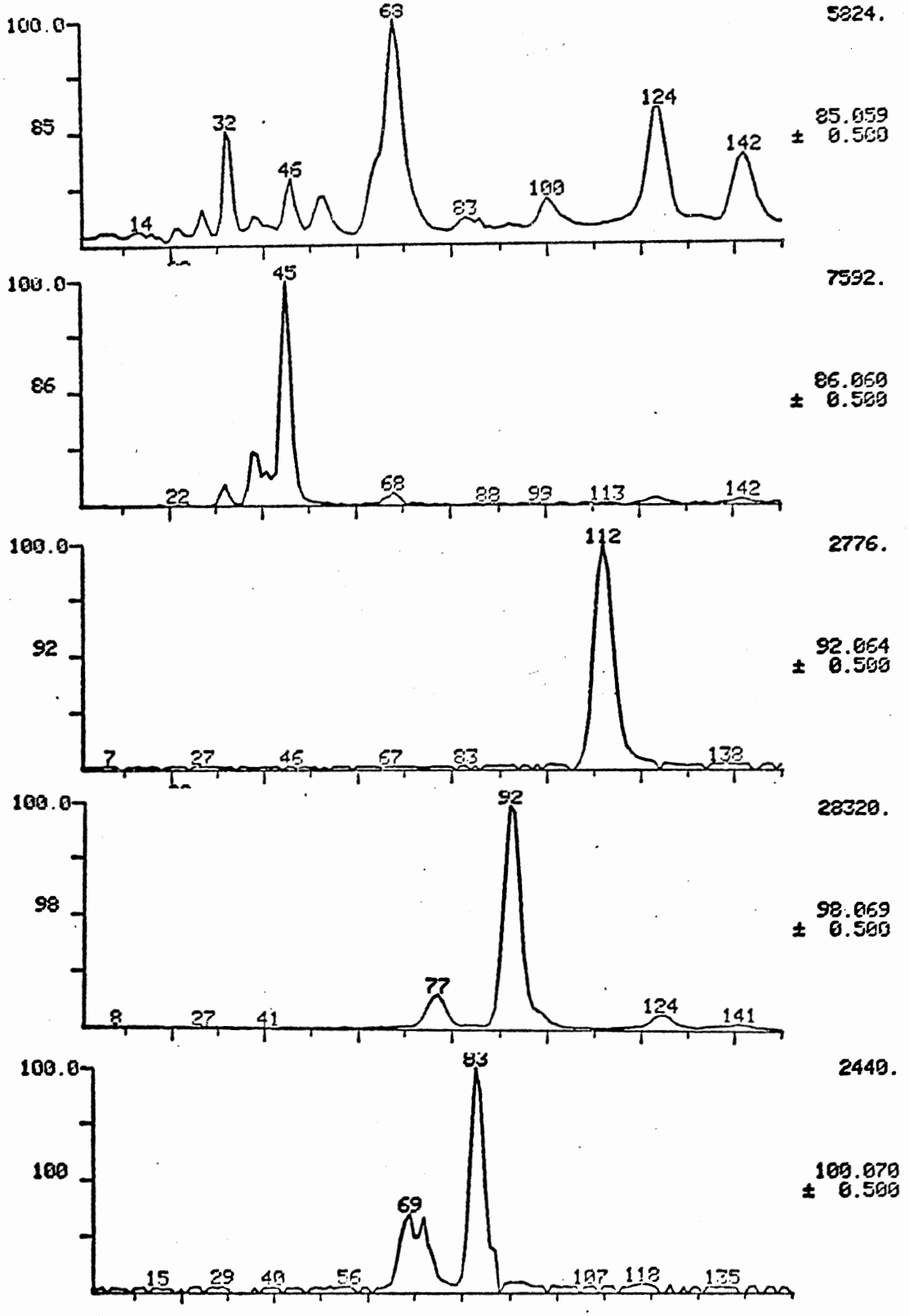

Mass chromatograms of some selected RIC peaks are given in Figure 17 and the individual mass spectra are listed in Appendix B under the heading Mass Spectral Data. Mass spectral assignments to the RIC peaks in Figure 13 are given in Table VI.

In the case of a mixture consisting large numbers of isomers which cannot be easily resolved by GC analysis, identification of individual components would be very difficult. To alleviate this problem, Brown (80) proposed a method in which a group or a compound type is analysed rather than a specific compound. This is based on the fact that for a group of compounds the total ion intensity is distributed over a small number of large peaks which would be characteristic of the compound type. This is shown in Table VII for some class of compounds. An example of this is given in Figure 18 in which the total ion intensities for cycloalkanes in the mixture, (Total Ion Current Map or Isometric Ion Display) which gave the data in Table VI, are shown. Even though the Figure 18 by itself is apparently not very interpretive, nonetheless the importance of this technique cannot be underestimated.

High Pressure Liquid Chromatography

HPLC is a recently developed analytical tool that typically provides a rapid, reproducible analysis of complex mixtures (82). Since HPLC can offer unique identification

TABLE VI

MASS SPECTRAL ASSIGNMENT TO RIC PEAKS
FROM ILLINOIS #6 RUN

Scan #	Assignment
19	Propane, CO_2
22	Butanes
27	neo-Pentane
28	iso-Pentane
29	n-Pentane
38	Cyclopentane
45	n-Hexane
53	Methylcyclopentane
64	Cyclohexane
76	Dimenthylcyclopentane
83	3-Methylhexane
93	Methylcyclohexane
99	Methylcyclohexene
124	1,2-Dimethylcyclohexane
133	Ethylcyclohexane
165	Methylethylcyclopentane
183	1,3,5-trimethylcyclohexane
193	p-Xylene
211	t-Butylcyclopentane
225	1,2-Dieth-lcyclopentane
250	1,1-Diethylcyclopentane
283	i-Propylcyclohexane
488	Decalin
576	Methyldecalin

TABLE VII

CHARACTERISTIC IONS OF COMPOUND GROUPS

Compound Type	Characteristic m/e values
1. Paraffins	43, 57, 71, 85, 99
2. Cycloparaffins	56, 70, 84, 98
3. Cycloolefins, diolefins, acetylenes	67, 78, 81, 82, 95, 96
4. Alkylbenzenes	77, 78, 91, 92, 105, 106, 119, 120, 133, 134

Source: 'Fundamentals of Integrated GC-MS', Ed. Gudzinowitz, B., Marcel Dekker Inc., New York, N.Y., 1973, p. 272.

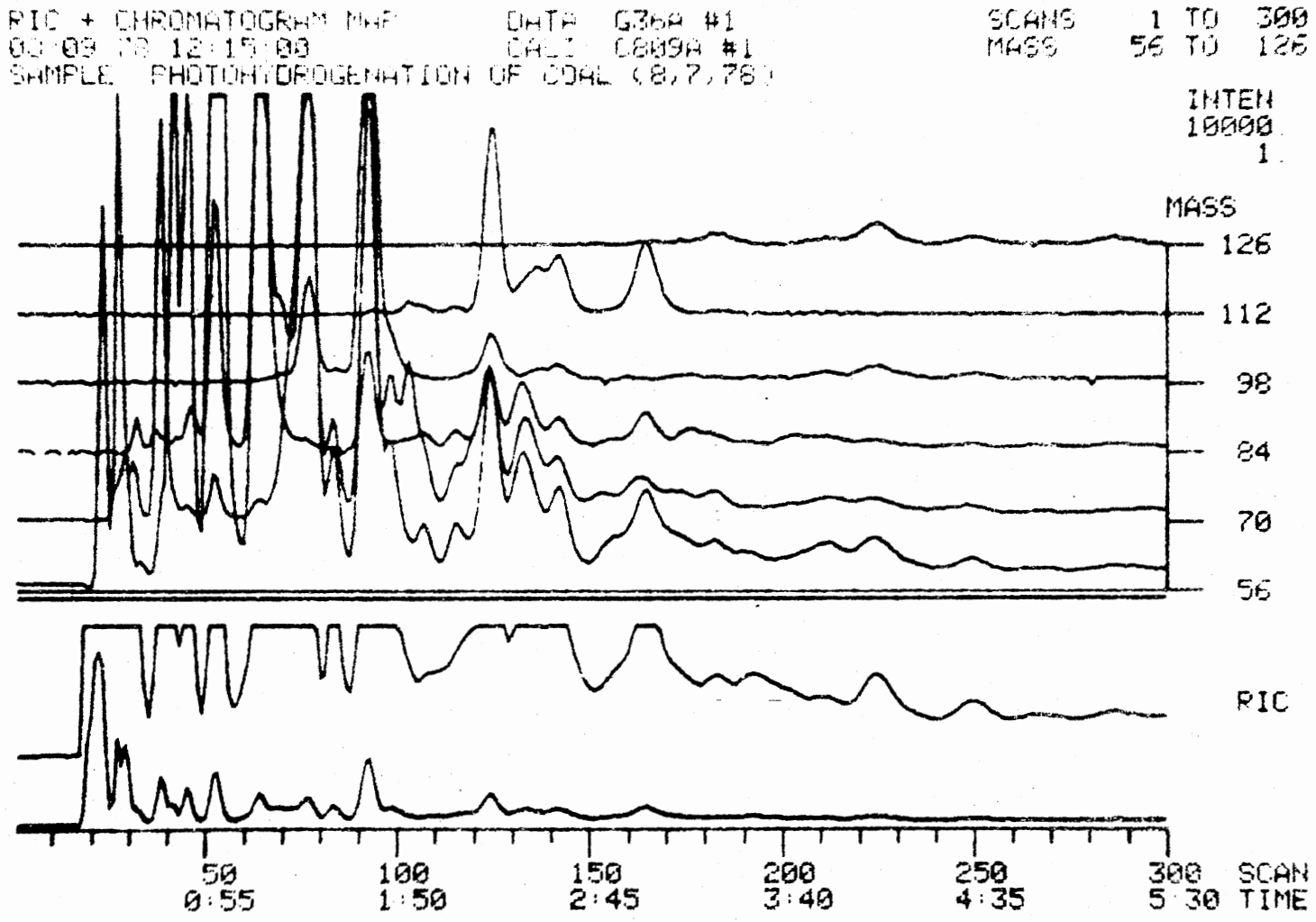

Figure 18. TIC Mapping of Characteristic Ions for Cycloalkanes

of individual components, it is very useful in the characterization and quantification of complex coal derived liquids.

The analytical instrument used throughout this study was a Waters Associates High Pressure Liquid Chromatogrpahic System. The following accessory hardwares (all from Waters Associate, Milford, Massachussetts) were used:

i) Model 6000 Solvent Delivery System

ii) Model 660 Solvent Programmer

iii) Model U6K Septumless Injector

iv) Model 440 UV Absorbance Detector operated at 254 nm (single channel)

v) Model 401 Differential Refractometer

and in addition, a Texas Instrument Model PS02W6A Servo-Riter II 10 mV f.s. two pen recorder.

All solvents used in this study were purchased from Burdick and Jackson, Muskegon, Michigan and they were all of spectroquality.

4 mm i.d. and 30 cm long microparticulate columns packed with 10 micron size micro-porasil particles were used in all quantitative anlyses. The columns, in general, had an efficiency of a minimum of 3000 plates (as determined by 5 σ method).

Better resolution could be achieved by use of a longer column system. This could be done in two ways: Kirkland (83) has reported an efficiency of 25000 theoretical plates

by connecting several columns in series. Even though this improves resolution, it does not always result in linear increase in efficiency with column length. One reason attributed to this phenomenon was inhomogenity in the permeability of the mobile phase across the diameter of the columns (84).

The total number of theoretical plates for a set of columns is given by

$$N(total) = 16\ V(total)^{**}2\ /\ w(i)^{**}2$$

where $w(i)$ = peak width for an individual column in a set

$= 4\ V\ /\ N^{**}0.5$ and

$$w(i)^{**}2 = w(1)^{**}2 + w(2)^{**}2 + \ldots\ldots + w(n)^{**}2$$

This principle is an important consideration in the utilization of connected columns in series where one bad column can destroy the efficiency of several good ones (85).

Another way of improving the resolution is to 'recycle'. In the recycle mode, a closed loop is established between the pump, column bank and detector(s). An example of effect of recycling is shown in Figure (19) from which it could be seen that almost a baseline separation has been achieved between napthalene and biphenyl at the end of the third recycle (86). An empirical estimation of the maximum number of recyles is obtained by dividing the number of theoretical plates of the fused peaks by 40 (86).

A pre-column was always used between the sample injector and the analytical column. The purpose of the precolumn

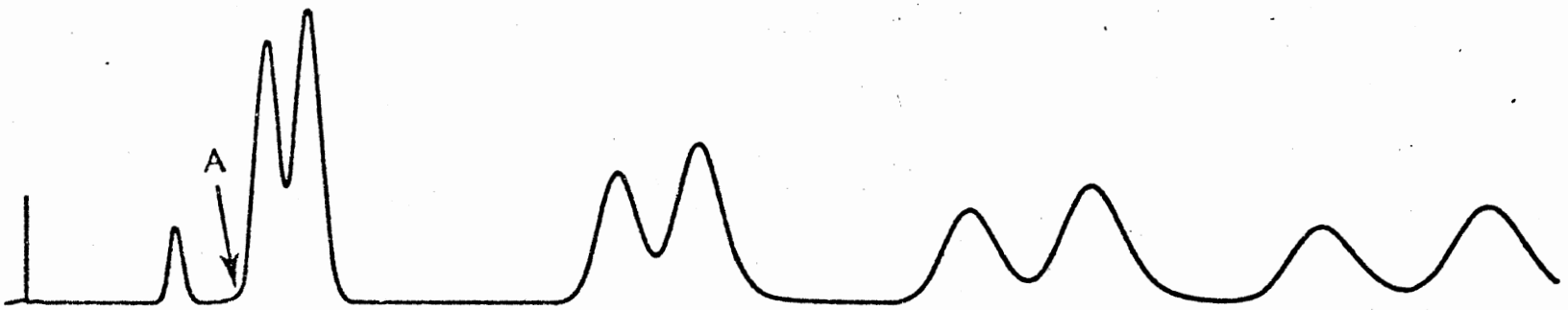

Figure 19. Effect of Recycling on the Separation of Napthalene from Biphenyl

was to serve as a chromatographic filter to retain any materials which would be strongly retained on the analytical column. The pre-column used in this work was a 3' x 0.125" O.D. stainless steel column loaded with less-expensive Corasil II of 37 - 50 micron size which has the same stationary phase functional group as the analytical column. The pre-column was emptied and reloaded at frequent intervals. A disadvantage of the use of the pre-column was that it contributed to band spreading and slightly reduced the efficiency of separation. However, the operating conditions of the system was adjusted in such a way that sufficient resolution of peaks were achieved to allow the use of a pre-column.

The analytical columns were further protected from external contamination by using a Waters Associates sample clarification kit. This kit can be used to remove fine particles of 0.5 microns or greater size from the sample before injection. This prevents the clogging of columns, injection port and syringes thereby prolonging the column life.

The solvents were degassed by means of an Ultrasonicator (Cole-Palmer Chicago, Illinois) in order to remove the dissolved gases which, otherwise, can cause pump malfunctioning and in extreme cases, cavitation in the pumps.

A column containing silica or other high polar surface packings, can become contaminated by the adsorption of water and/or other polar impurities on the packing mate-

rial surface. This will result in the reduced retention time and a loss of resolution in many cases. When these symptoms were noticed, the columns were regenerated by pumping about 40 column volumes of much stronger solvent than was used when impurities were adsorbed.

UV detectors used in HPLC are susceptible to changes in the refractive index of the mobile phase. This causes baseline shifts as seen in the initial portion of liquid chromatogram shown in Figure (20) where all the saturates are being eluted.

Establishing conditions for the separation of an analytical column saves solvent, operation time and sample material. The best operating conditions (column packing, column length, mobile phase and its flow rate etc) were determined by using carefully prepared standards.

For positive identification of the eluted UV peaks through proton NMR, a solvent containing no protons was needed. 1,1,2-trichloro-1,2,2-tri fluoroethane (Freon 113) met all the requirements and it was used for quantification. However, for positive identification through GC-MS, this solvent proved to be inadequate and cyclohexane was used despite its disadvantage of having a relatively high viscosity.

Retention relative to a reference substance under the same chromatographic conditions, is generally more useful than absolute retention values, since this will minimize the

TABLE VIII

RETENTION CHARACTERISTICS OF SELECTED AROMATIC COMPOUNDS

Compound	Relative Retention Volume (Phenanthrene = 1)
Benzene	0.27
Toluene	0.32
Xylenes	0.35
Tetralin	0.41
Napthalene	0.45
2-Methylnaphthalene	0.52
2,6-Dimethylnaphthalene	0.63
Biphenyl	0.80
Anthracene	0.88
Phenanthrene	1.00
Pyrene	1.18
Fluoranthene	1.26
Benzanthracene	1.70
Benzopyrene	2.28

dependence of the retention parameters upon column variables such as dead volume, pressure drop across the column and minor changes in column temperature caused by ambient temperature changes and changes in flow rates caused by pump riddle etc. The relative retention of some selected compounds are given in Table VIII.

Once the desired resolution was achieved, the UV detector sensitivities were determined for the compounds listed in Table VIII. For UV detection, the concentration of a compound can be related to its molar extinction coefficient at a corresponding wavelength (88). The coefficients for a number of aromatic compounds given in Table IX (87). From the table it is evident that a large peak in a chromatogram does not necessarily imply a large concentration of a compound present.

The products derived from the photohydrogenation of coal were analyzed under the same conditions as standards. The separated components were carefully collected and positively identified by GC-MS and in some cases, by micro F.T. proton NMR. As the analytical columns could easily lose resolution by overloading, small amounts of sample materials were injected several times for fraction collection.

A typical liquid chromatogram of products obtained from the photohydrogenation of coal is presented in Figure 20.

TABLE IX

UV ABSORPTION OF SOME AROMATIC COMPOUNDS

Compound	ε -2550 λ	Solvent
Benzene	568	A
Naphthalene	7076	B
Fluorene	39794	B
Anthracene	477120	A
Phenanthrene	77815	A
Pyrene	10000	B
1,2 Benzanthracene	71600	B
1,2 Benzpyrene	50515	B
3,4 Benzpyrene	79934	B

A = Cyclohexane

B = 95% Ethanol

ε = Molar Ext. Coef. (g moles/liter)$^{-1}$

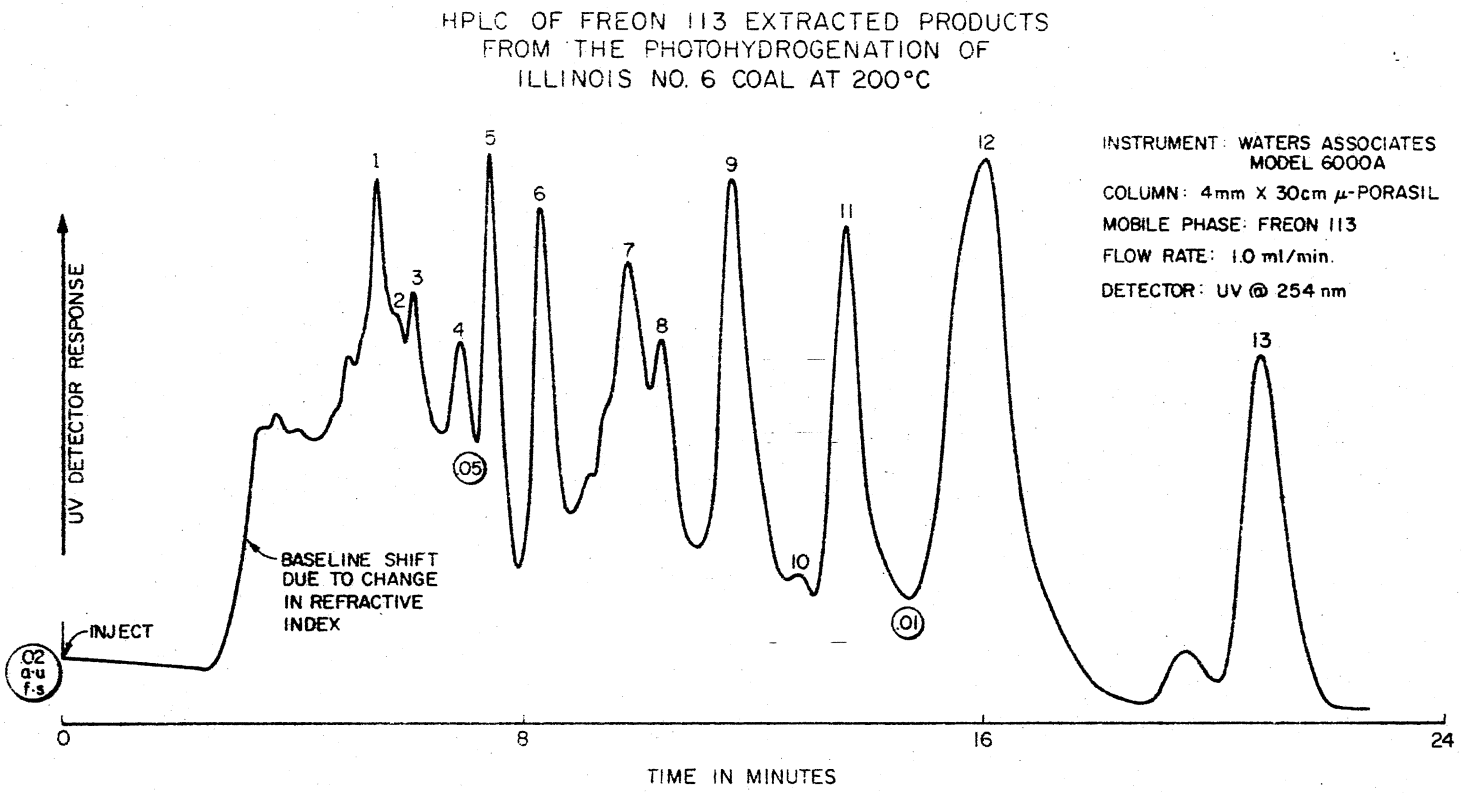

Figure 20. HPLC of Freon 113 Extracted Products From Illinois # 6 Run

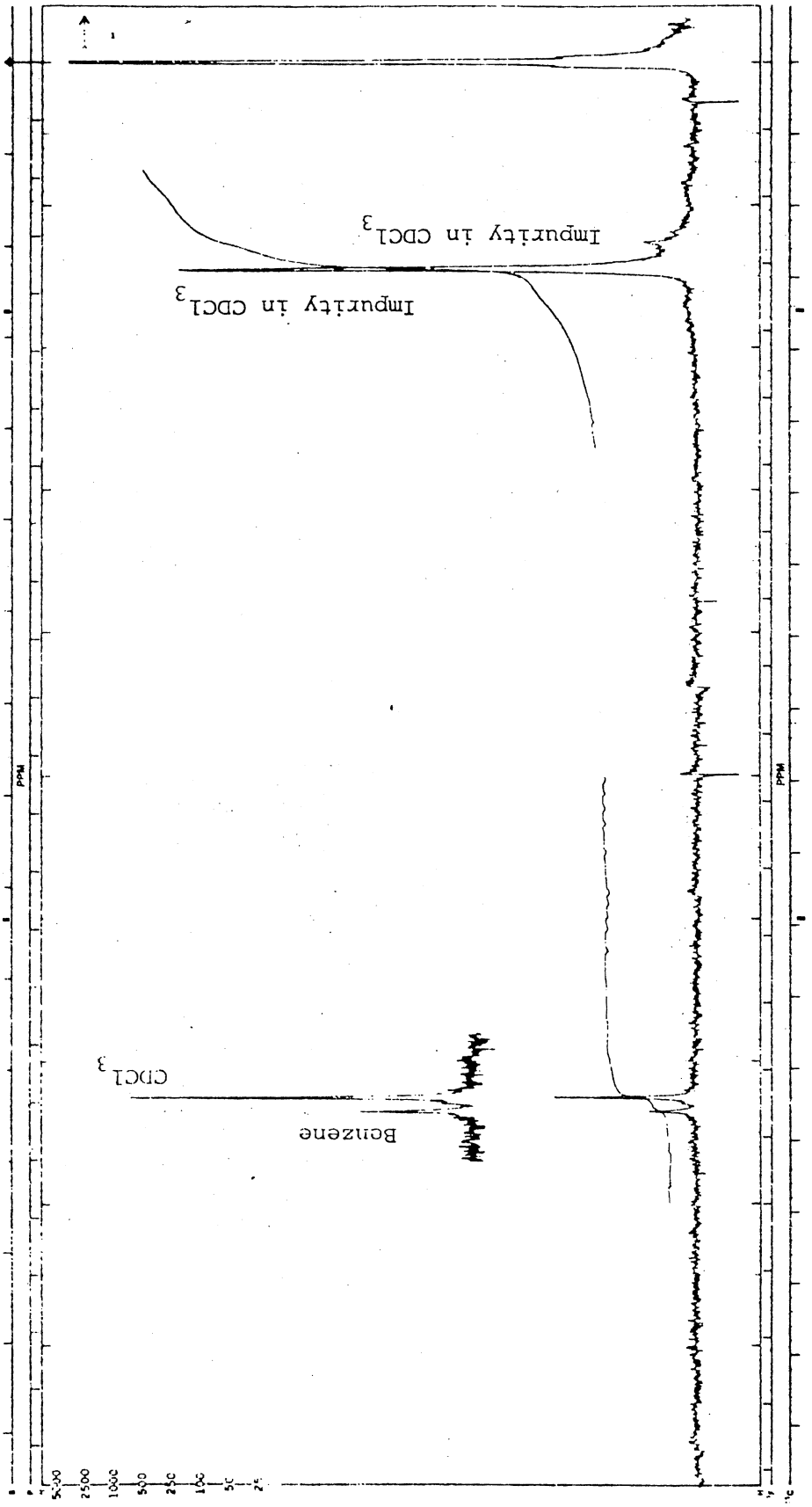

Figure 21. Micro F.T. PMR Spectrum of LC Fraction # 1

Initially attempts were made to colect the UV fractions from the HPLC and positively identify the peaks via proton NMR. Proton NMR under c.w. mode did not reveal any peak at all. Micro F.T. NMR of the concentrated UV fraction labelled as #1 in Figure 20 led to its identification as benzene which is shown in Figure 21 Identification of other fractions via NMR was hindered by very low concentration of the components and hence not ameanable to NMR analyses. Further identification of the liquid sample was done by GC-MS as described before. The GC-MS confirmed the presence of the compounds that were tentatively identified by comparison of their relative retention characteristics in HPLC. The mass spectra of selected peaks are included in Appendix B.

The characteristic ions of some selected polynuclear compounds which were scanned in the GC-MS operation are given in Table XI (81). However, this technique did not detect benzanthracene and benzopyrene in the liquid samples eventhough they were tentatively identified by HPLC. It is believed that the GC conditions were not appropriate for detection of these compounds during the GC-MS run.

TABLE X

IDENTIFICATION OF LC PEAKS FROM
ILLINOIS #6 COAL RUN

Peak Number	Identification
1	Benzene
2	Toluene
3	Xylenes
4	Tetralin
5	Naphthalene
6	Methylnaphthalene
7	Dimethylnaphthalenes
8	Biphenyl
9	Phenanthrene
10	Pyrene
11	Fluoranthene
12	Benzanthracene
13	Benzopyrene

TABLE XI

CHARACTERISTIC IONS FOR SELECTED PNA HYDROCARBONS*

Type	Characteristic ions	z-number
Benzopyrenes	251, 252, 265, 266, 279, 280	-28
Chrysenes	227, 228, 241, 242, 255, 256	-24
Decahydropyrenes	211, 212, 225, 226, 239, 240	-12
Hexahydropyrenes	193, 194, 207, 208, 221, 222, 235, 236	-16
Tetrahydrofluoranthenes	205, 206, 219, 220, 233, 234	-18
Pyrenes/fluoranthenes	201, 202, 215, 216, 229, 230, 243, 244, 257, 258, 271, 272	-22
Dihydropyrenes	189, 190, 203, 204, 217, 218, 231, 232, 245, 246, 259, 260	-20
Octahydrophenanthrenes	185, 186, 199, 200, 213, 214	-10
Hexahydrophenanthrenes	183, 184, 197, 198	-16
Tetrahydrophenanthrenes	181, 182, 195, 196, 209, 210, 223, 224	-14
Phenanthrenes	177, 178, 191, 192	-18
Fluorenes/dihydrophenanthrenes	165, 166, 179, 180	-16
Acenaphthenes/biphenyls/ dibenzofuran	153, 154, 167, 168	-14
Tetralins/benzofuran	103, 104, 117, 118, 131, 132, 145, 146	- 8
Tetrahydroacenaphthenes	129, 130, 157, 158, 171, 172	-10
Naphthalenes	128, 141, 142, 155, 156, 169, 170	-12
Benzenes	77, 78, 79, 91, 92, 105, 106, 119, 120	- 6

Source: 'Fundamentals of Integrated GC-MS', Ed. Gudzinowitz, B., Marcel Dekker, Inc., New York, NY, 1976, p. 273

Nuclear Magnetic Resonance Spectroscopy

NMR spectra were recorded in parts per million downfield from tetramethyl silane on a Varian high resolution XL-100(15) NMR spectrometer with a Nicholet TT-100 Fourier Transform accessory.

X-Ray Photoelectron Spectroscopy (XPS)

XPS is a very sensitive technique capable of determining the elemental composition of the first 20-40 A depth of the surface of a solid (89) which involves the bombardment of the material under study with monoenergetic X-rays of known energy. The characteristic binding energy of the electrons emitted, as a result of absorption of these X-ray photons, are accurately measured and could be used for the identification of an element. It must be noted that the spectrum is only characteristic of the outermost atomic layer of the sample (90) and hence can provide the surface composition of the sample under investigation.

All XPS analyses for this research were done by Mr. Tom Hudson at Dow Chemical Company, Freeport, Texas. Powdered coal samples were loaded onto sample holders covered with a double sticky tape. The tape surface was completely covered with the coal particles in order to eliminate the interference form the underlying tape. Hence, practically all the carbon signal observed in the spectra could be attributed

solely to the sample. All the preparations were carried out in a dry laboratry with a nitrogen atmosphere, in order to prevent the sample from exposure to oxygen and moisture containing atmospheres. After loading on the sticky tape holders, the samples were degassed overnight under a vacuum of 1 X 10**-5 torr. They were then loaded into an HP 5950A ESCA spectrometer equipped with an aluminum anode and analyzed at room temperature under a vacuum of 1 X 10**-9 torr. It is important to note that difficulties are encountered in analyzing for oxygen on coal surfaces at ESCA apparatus pressures above E-8 torr, owing, presumably, to absorption (94).

As a result of escape of photoelectrons, slight positive charge could be created on the surface of a solid. consequently, the energy levels of the sample would be shifted from the normal value. This is called 'charging effect'. In one of the two methods available at present to overcome this charging problem, ultrathin samples are studied on a conducting support; the other method involves a "flood-gun" approach. The latter method was used in this investigation.

In the flood-gun approach (92), an electron gun is used to bathe the sample in an excess of low-energy electrons and thus provide another source to neutralize the surface charge. The electron flood-gun, generally, consists of a tungsten filament, a DC power supply and a current meter. The filament is located near the sample and it is possible

to control the kinetic energy of the released electrons by means of a slit arrangement. However, there is no way of assuring neutralization of the surface positive charge by this method. This places a slight negative bias on the sample and causes a 1 to 2 eV downfield shift of C(1s) photoline from its normal value of 284.3 eV. This requires correction for oxygen and sulfur photolines. A quantitative measure of the elemental composition of the solid surface could be made if the sensitivities of the peak heights (or peak areas) are known (91, 93).

CHAPTER IX

SCREENING EXPERIMENTS

Several experiments were conducted to determine the optimum conditions for the photohydrogenation of coal. The Utah-Emery coal seemed to be the most desirable because of its low coke button value; however, the coal proved too hard to grind with available laboratory facilities and Illinois # 6 coal was selected as the next most desirable 'noncaking' coal. Pittsburgh Hi-Seam, Utah Emery, Montana Rosebud and Reading Anthracite coals were also used for comparison purposes. Analysis of the coals used in this study are listed in Table XII.

Photohydrogenation experiments with air-ground, -53+38 micron Illinois # 6 coal at ambient temperature yielded virtually no volatile products at all. However, the ESR analysis of the irradiated coal collected at the Millipore filter on the top of the reactor showed enhancement in the peak width and peak intensity (Figure 22), strongly suggesting an increase in the free radical content of the coal by H atom treatment. The electron microscope analysis revealed considerable agglomeration suggesting a 'sticky' surface on the irradiated coal which is consistent with the enhanced ESR absorption.

TABLE XII

ANALYSIS OF COALS

Coal	%ash	%sulfur	%volatile matter	coke button
Utah-Emery	9.36	0.93	39.38	1.5
Illinois #6	6.75	1.21	38.15	3.5
Pittsburgh Hi-Seam	7.89	1.58	39.90	8.5
Montana Rosebud	10.1	0.8	35.2	---
Rosebud Synthane Char	31.9	0.2	6.1	---

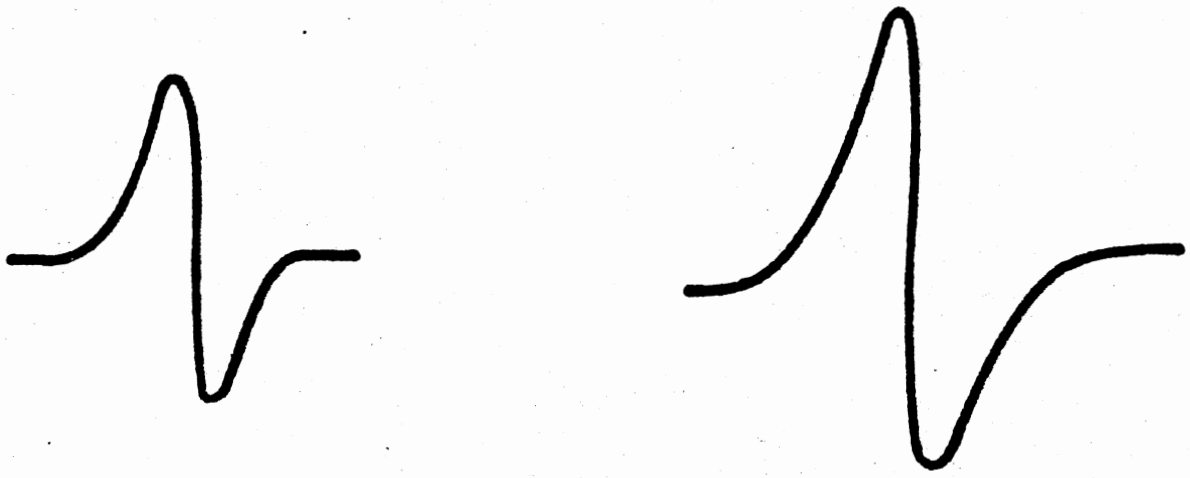

Figure 22. ESR Spectra of Coal Before and After Irradiation

ESCA analysis of the irradiated coal at ambient temperature revealed some interesting facts. The survey scans of the blank coal and top and bottom fractions of the irradiated coals are shown in Figures 23, 26, and 29 respectively. The H atom treated coal shows significantly less oxygen relative to carbon; this is believed to be due to the H atom reduction of the oxygen containing groups on the coal surface. The slow oxygen scans, Figures 24, 27 and 30, show the lower concentration of oxygen on the surface of the H atom treated coal dust clearly. Figure 30, run at higher sensitivity, suggests the presence of two kinds of oxygen on the coal surface (91,93) which has not been reported in the literature so far.

The ESCA spectra also suggest two different kinds of sulfur in the H atom treated coal, Figures 25 and 28 compared with Figure 31. The presence of two different kinds of sulfur in weathered coal has been reported by Frost et al., (94) but the data in Figures 25 and 28 indicate that two different kinds of sulfur are also found in coal subjected to a reducing environment. It is possible that there may have been some fractionation of the mineral impurity during the fluidization. The Si peaks on the insets of the survey scans, Figures 23, 26 and 29 tend to support this explanation.

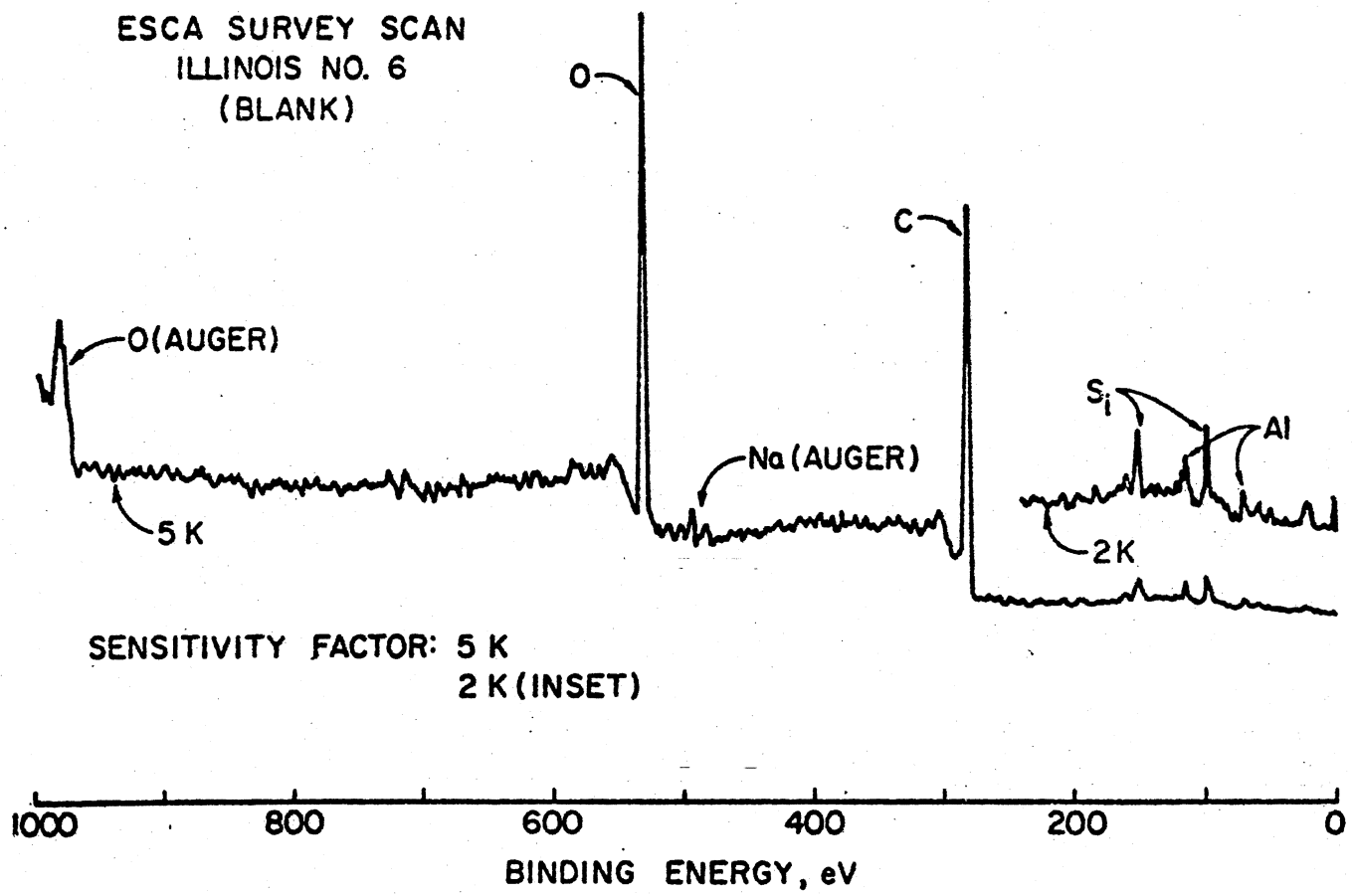

Figure 23. ESCA Survey Scan of Coal Before Irradiation

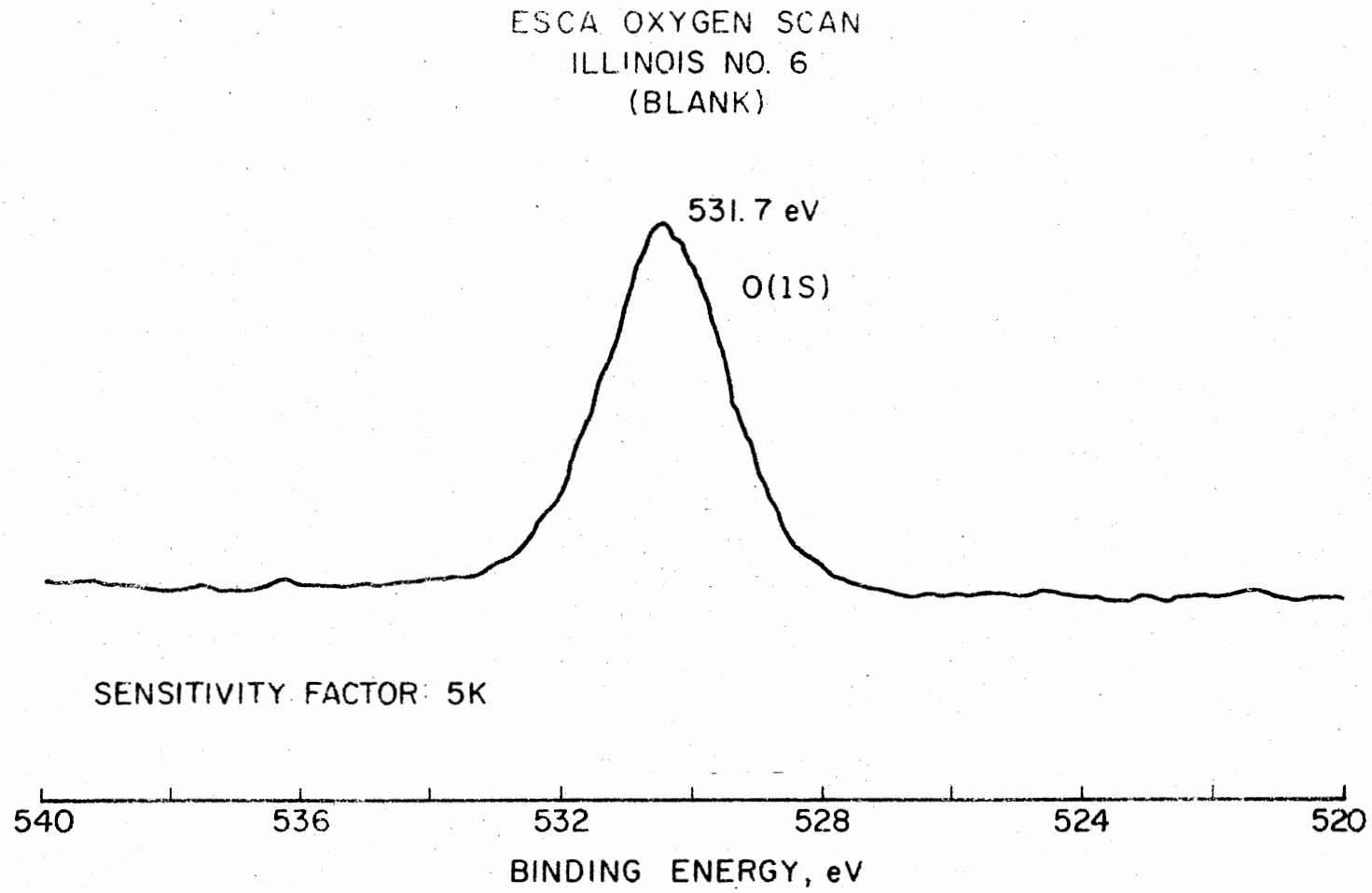

Figure 24. ESCA Oxygen Scan of Coal Before Irradiation

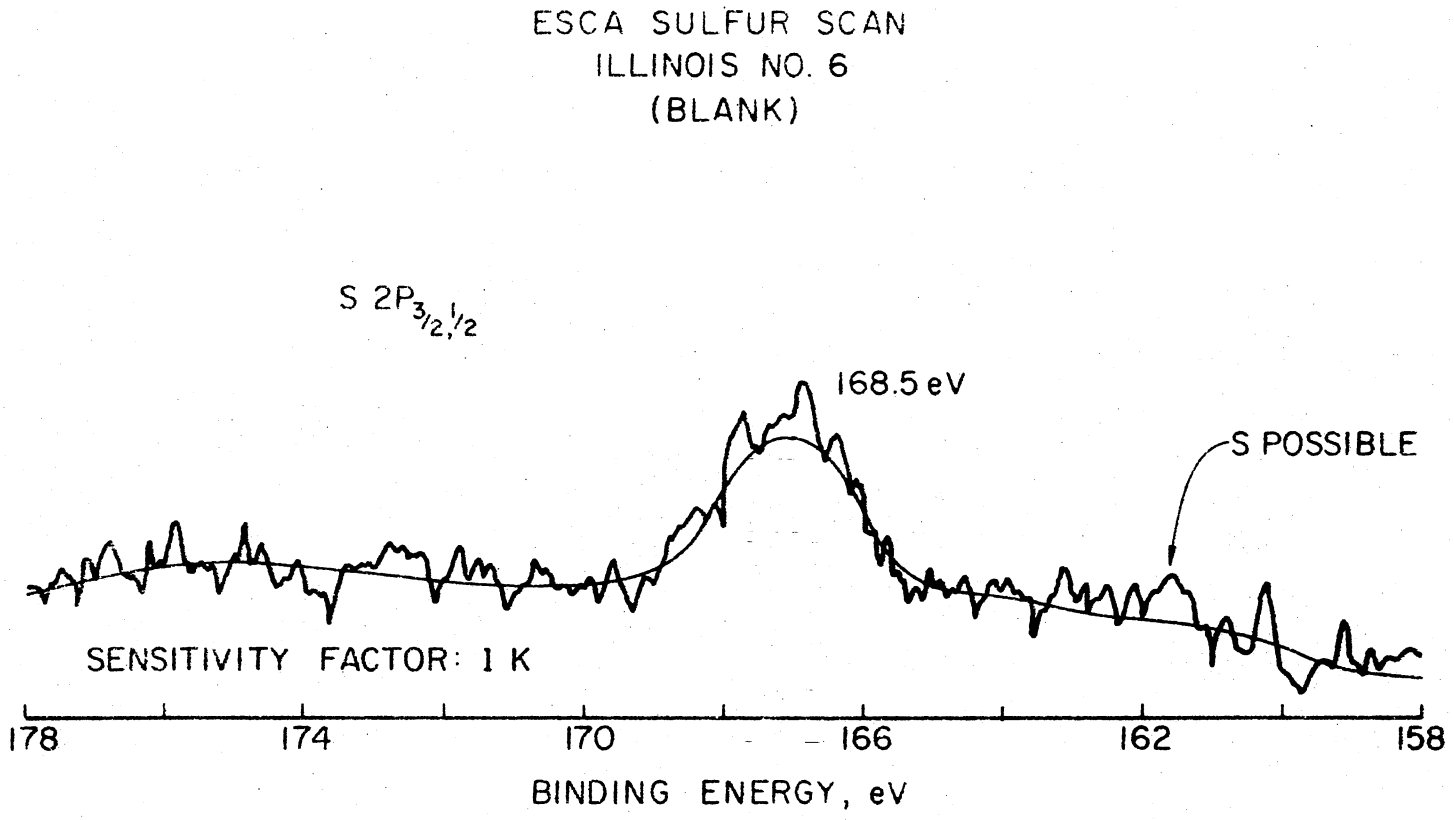

Figure 25. ESCA Sulfur Scan of Coal Before Irradiation

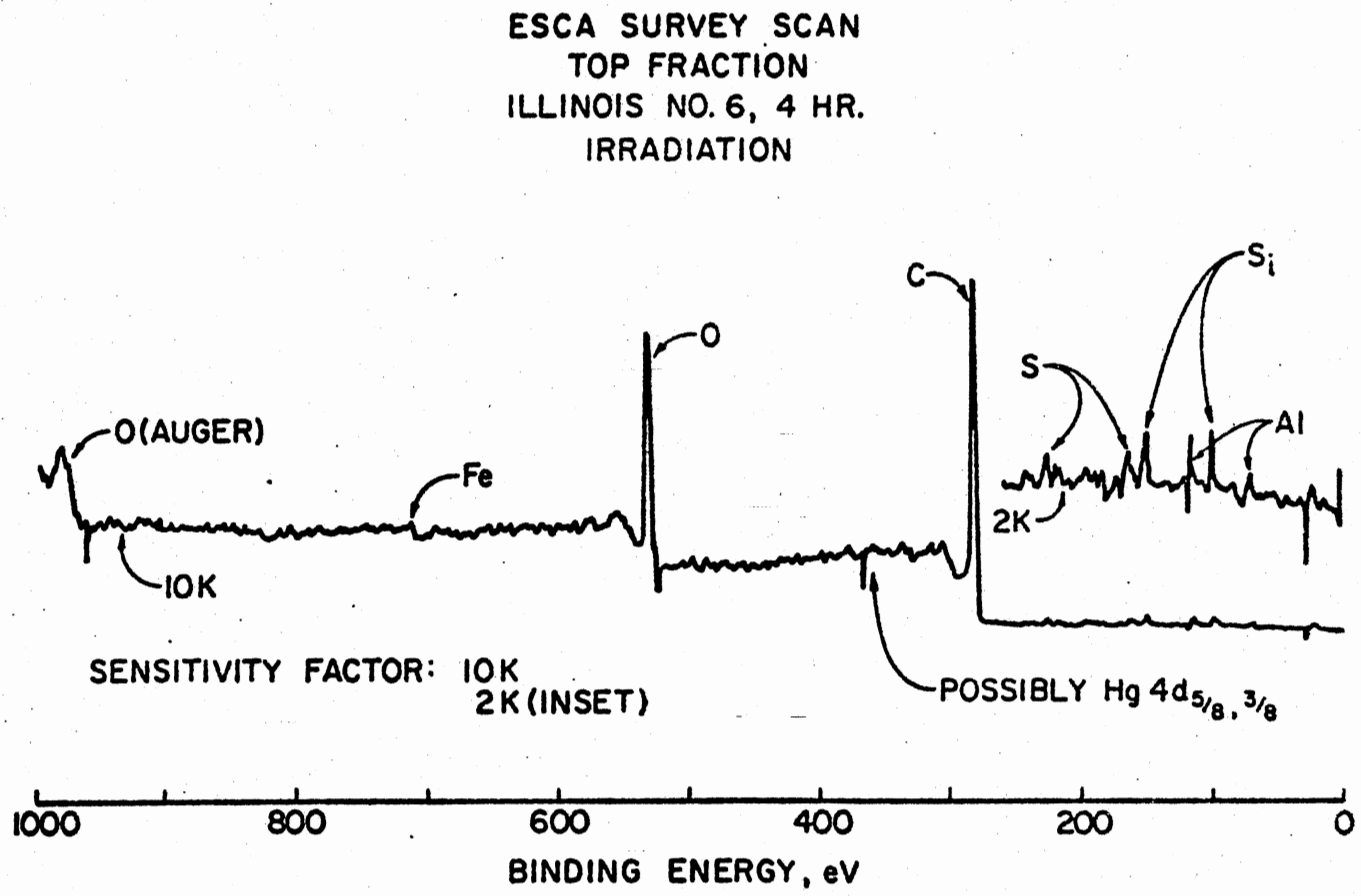

Figure 26. ESCA Survey Scan of Coal After Irradiation: Top Fraction

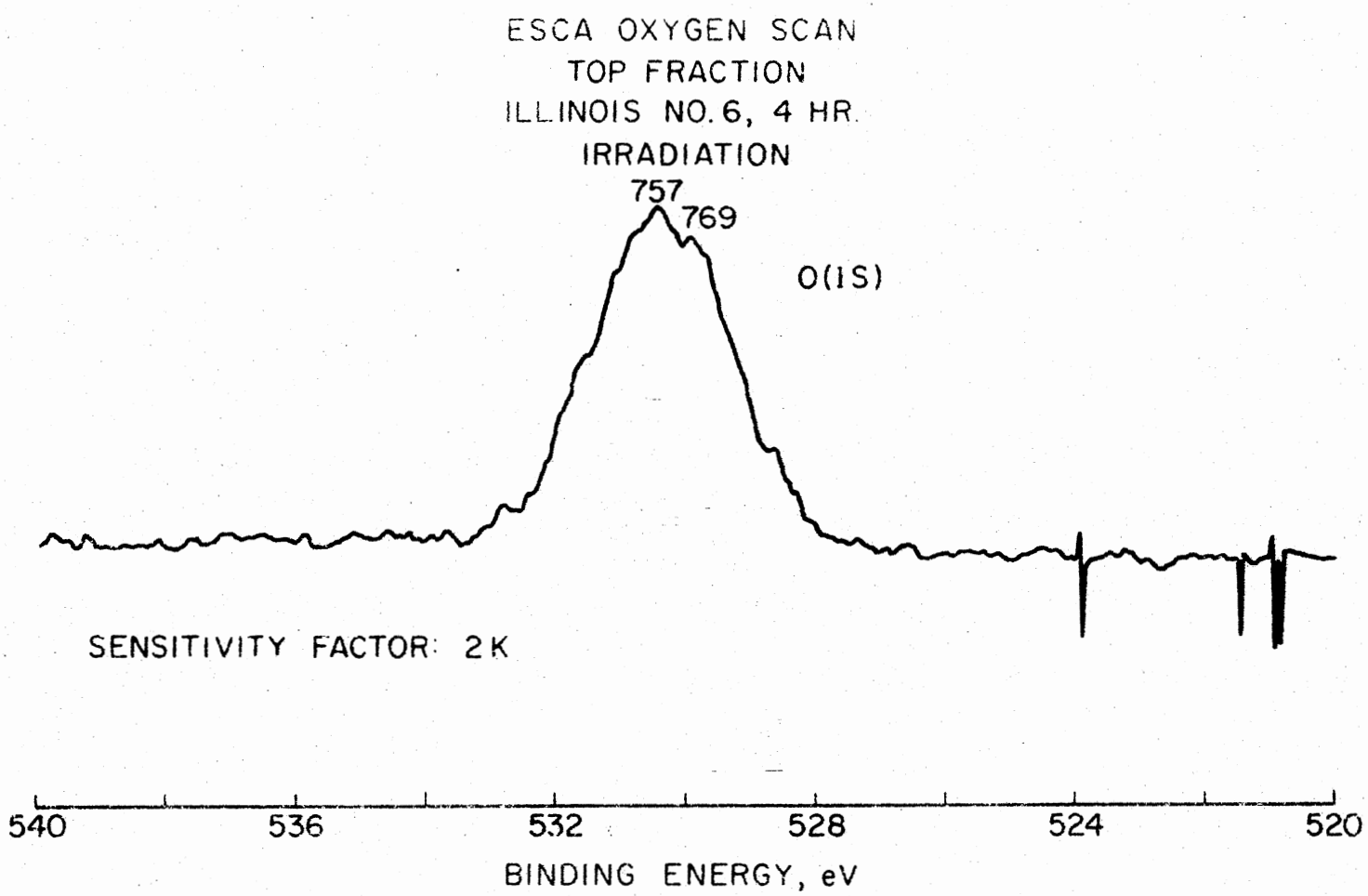

Figure 27: ESCA Oxygen Scan of Irradiated Coal: Top Fraction

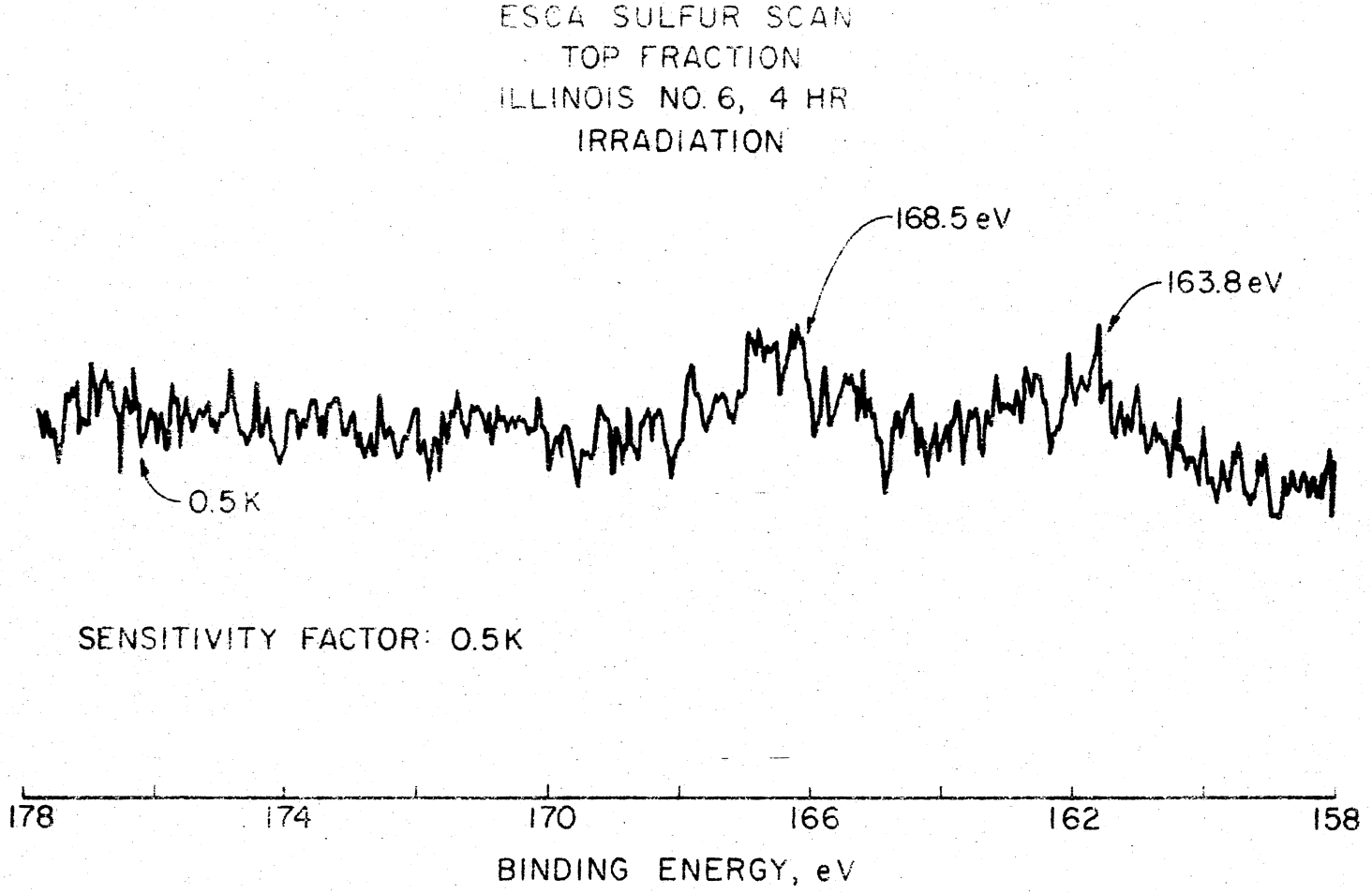

Figure 28. ESCA Sulfur Scan of Irradiated Coal: Top Fraction

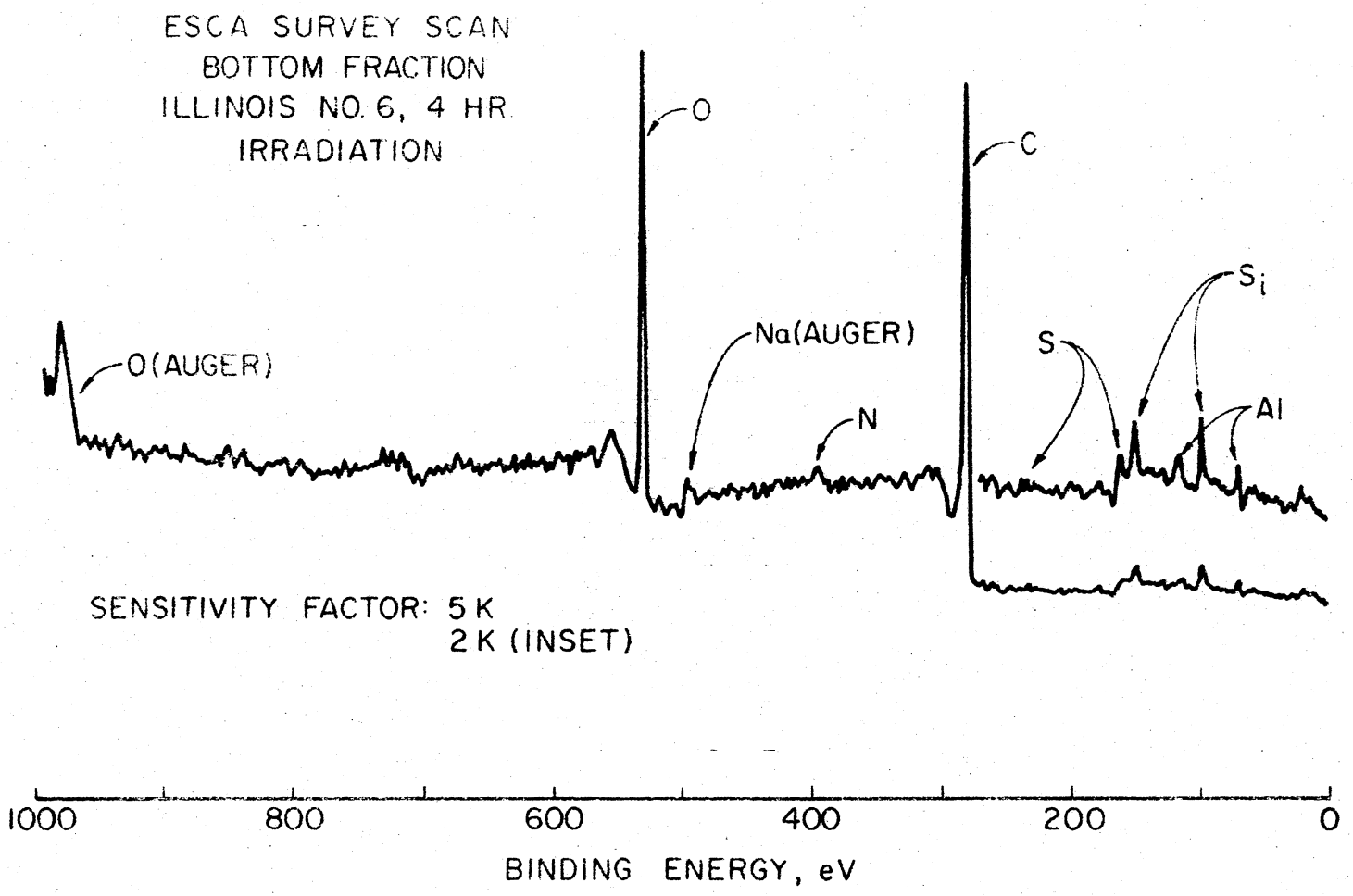

Figure 29. ESCA Survey Scan of Irradiated Coal: Bottom Fraction

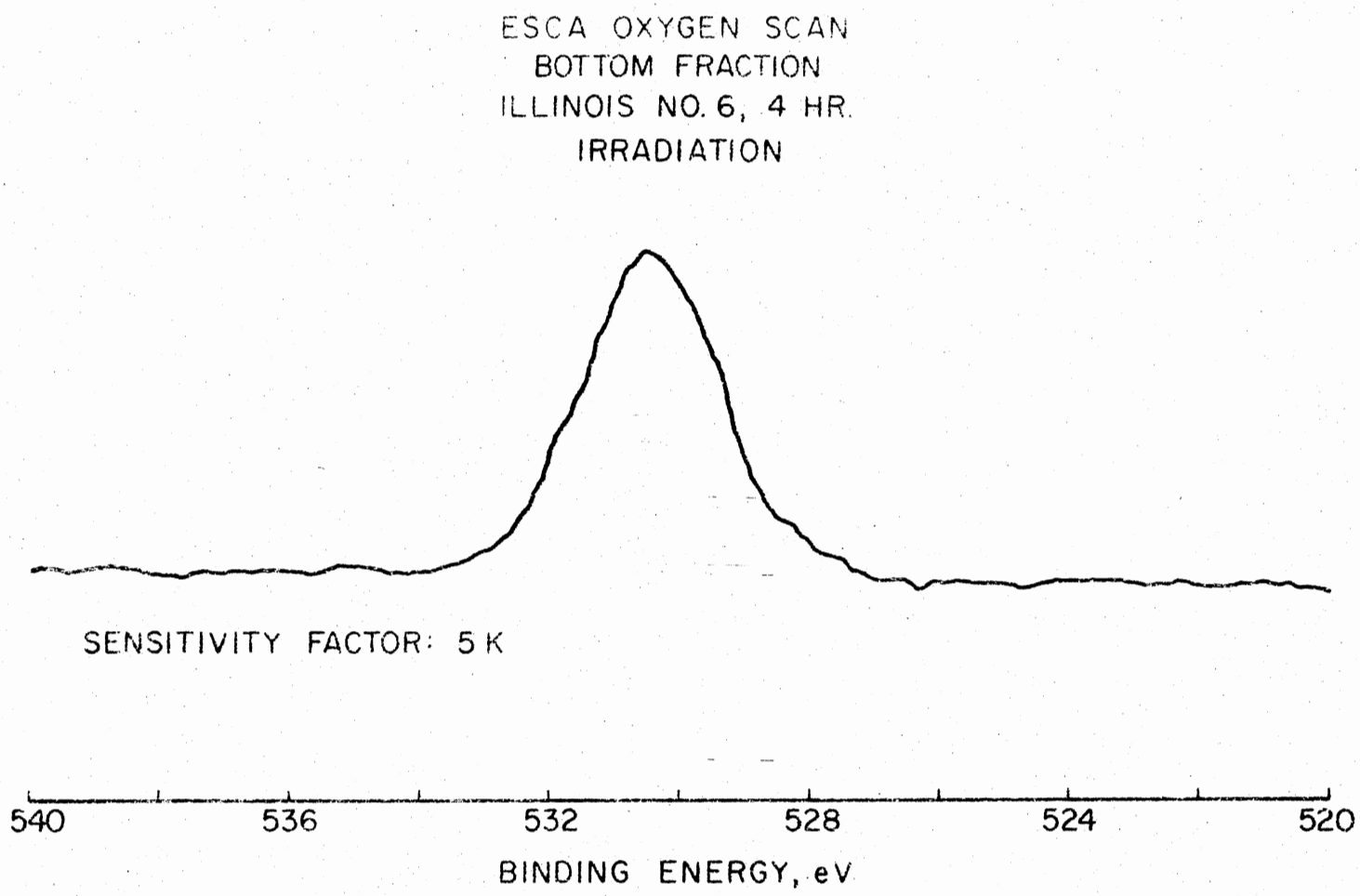

Figure 30. ESCA Oxygen Scan of Irradiated Coal: Bottom Fraction

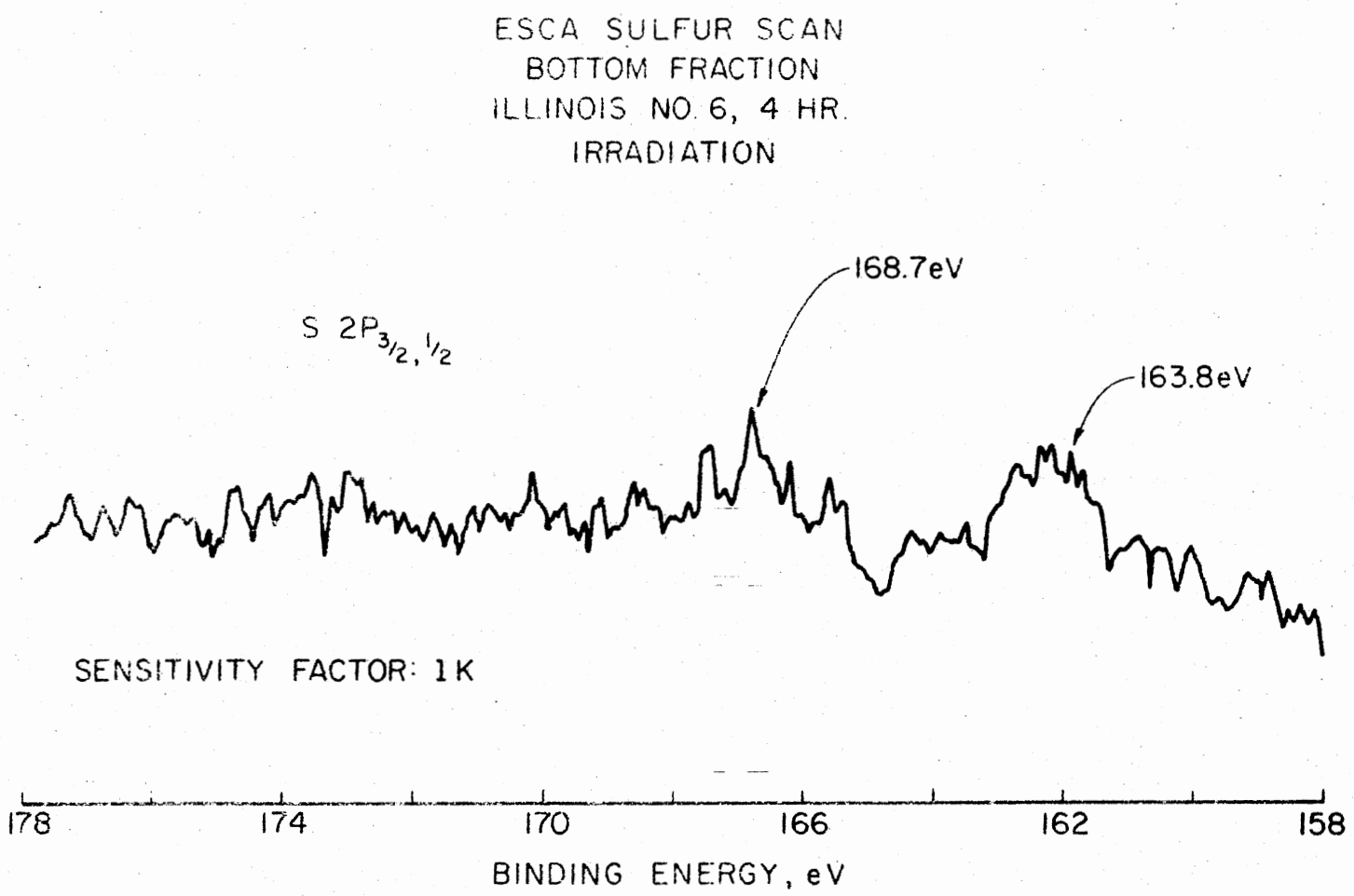

Figure 31. ESCA Sulfur Scan of Irradiated Coal: Bottom Fraction

An important observation in the ESCA spectra of irradiated coal dust is the inability to detect Hg unequivocably on the coal surface. This ruled out the possibility of adsorption of mercury on the coal surface being the cause for the nonreactivity of coal at ambient temperature.

In their study of interaction of H atoms with toluene, Amano et al. (96,95) reported no appreciable cracking at temperatures less than 200 deg C. Their data are reproduced in Figure 32. Similar results were reported by Mulcahay et al (97) earlier. They found that the conversion of toluene to gaseous products was much greater at 390 deg C than at 27 deg C. The number of free radicals that could be induced in solid organic substances when exposed to H atoms were found to be strongly dependant upon the sample temperature by Harrisson (98).

Supported by these findings, the temperature of the reaction of vacuum pumped coal with H atoms was increased to 200 deg C and large amounts of diverse hydrogenation products were observed as shown in Figure 33. Striking similarities between Figure 33, the identification of peaks in which are given in Table XIII, and an actual chromatogram obtained for a natural gasoline shown in Figure 34 (99) reveals the fact that the gaseous products obtained by photohydrogenation atom cracking of coal really correspond to a gasoline range of products.

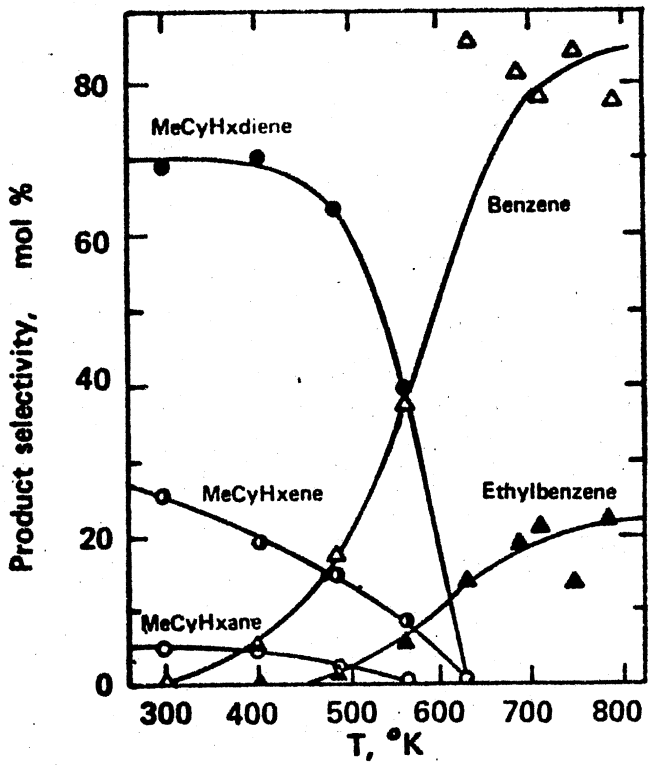

Figure 32. Reaction of H Atoms With Toluene

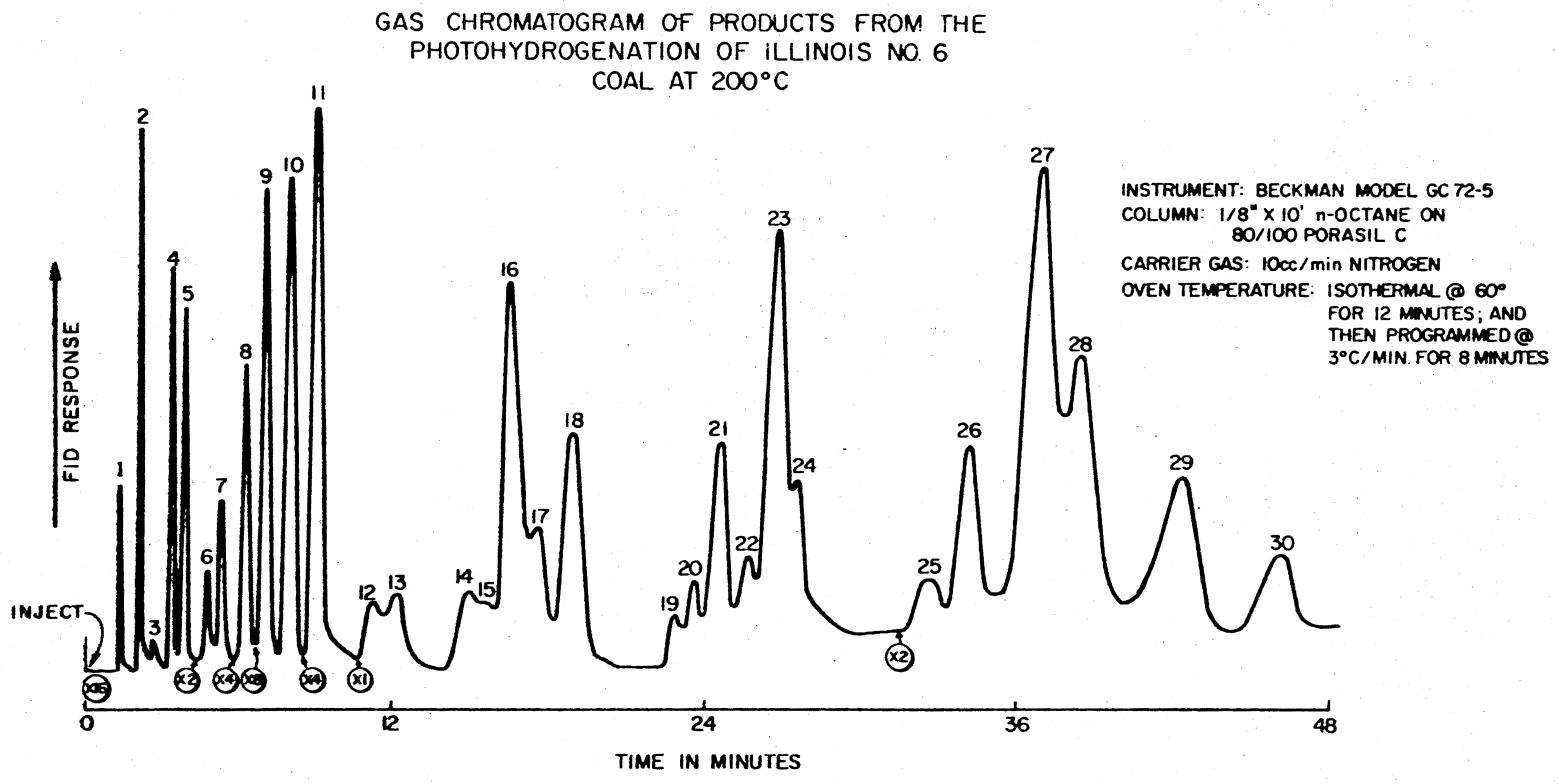

Figure 33. GC Trace of Photohydrogenation of Illinois # 6 Coal

TABLE XIII

IDENTIFICATION OF PRODUCTS FROM
ILLINOIS #6 COAL RUN

Peak Number	Identification
1	Ethane
2	Propane
3	Propylene
4	iso-Butane
5	n-Butane
6	But-1-ene
7	But-2-ene
8	neo-Pentane
9	iso-Pentane
10	n-Pentane
11	Cyclopentane
12	Pent-1-ene
13	Pent-2-ene
14	2-Methylpentane
15	3-Methylpentane
16	Methylcyclopentane
17	n-Hexane
18	Cyclohexane
19	2-Methylhexane
20	3-Methylhexane
21	Dimethylcyclopentane
22	n-Heptane
23	Methylcyclohexane
24	Methylcyclohexene
25	C8
26	C8
27	1,2-Dimethylcyclohexane
28	1,4-Dimethylcyclohexane
29	C8
30	C8+

Subsequent blank runs under the same conditions, but without u.v. irradiation yielded only unremoved hydrogen carrier gas and a trace of ethylene. Another blank run with u.v. irradiation, but with helium as the carrier gas, also revealed no observable products. From this it was concluded that the hydrogenation products were not due to the release of hydrocarbons trapped and/or adsorbed in the micropores of coal but due to the cracking of the coal surface itself.

This was confirmed further by the results obtained from the photohydrogenation of Synthane char of Montana rosebud coal. The analysis of Synthane feed coal and the char are shown in Table XII. In the Synthane process, coal is subjected to a temperature of 1500-1800 deg F and a pressure of 600-1000 psig and gasified using steam and oxygen (6). In order to avoid the possible contamination, the Synthane char recieved was not sieved. However, the particle size of the char received is believed to be less than 60 microns and used after drying at 200 dec C. The sample was exposed to H atoms bombardment under usual conditions and the GC 'fingerprint' is shown in Figure 35. When we consider the severe process conditions to which a feed coal is subjected to in the Synthane process, it is amazing that the H atoms are capable of cracking and hydrogenating the very unreactive carbon residues from Synthane process.

The products obtained from the photohydrogenation of Illinois # 6 coal were found to be independent of the pre-

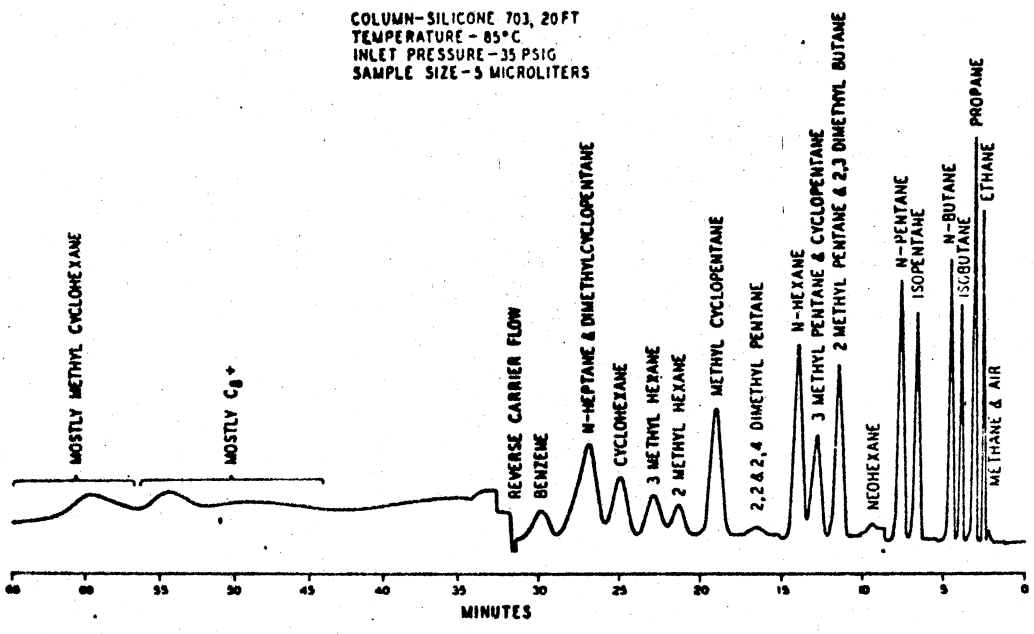

Figure 34. GC Trace of Natural Gasoline

treatment of coal with napthalene or nickel carbonyl. The GC trace of products from napthalene treated coal is shown in Figure 36. Comparison of this with Figure 34 provides additional confirmation to the fact that the observed products were not due to the interaction of H atoms with the gases occluded in the micropores of coal. On the other hand, the GC trace of products from the nickel carbonyl treated coal, shown in Figure 37, indicates that the presence of finely divided Ni catalyst did not change the product distribution. However, the effect of finely divided Ni catalyst on the rate and/or the yield of products formed is not known as the experiment was carried out for qualitative purposes only.

Pittsburgh Hi-Seam and Utah Emery coals, which are also bituminous in nature, gave similar results (Figures 38 and 39). This prompted experiments with coals of different ranks. Sub-bituminous Montanna Rosebud and Reading Anthracite coals were allowed to interact with photoproduced H atoms in separate experiments and the difference was found only with respect to the yield of products than to the kind (Figures 40 and 41). Under the given conditions, the yield of gases decrease in the order sub-bituminous<bituminous<anthracite.

Even though the basic pattern of gas chromatograms of gaseous products from various coals virtually remained unchanged, this was not so in the case of the liquid prod-

ucts as could be seen from the HPLCs presented in Figures 20, 42, 43 and 44. Evidently, Illinois # 6 coal produced a large number of aromatic compounds. Because of the lack of details in the other chromatograms, no much information could be obtained from them except one that they all reflect larger yield of saturated compounds.

The production of large polynuclear aromatic hydrocarbons like phenanthrene, pyrene, fluoranthene, benzanthracene, benzopyrene etc from Illinois # 6 coal is most startling. In fact, Vahrman et al. had to heat their coal for 245 hours in the temperature range of 250 - 300 deg C to release the aromatic compounds upto phenanthrene, trapped and/or adsorbed in the coal matrix (100).

Eventhough the yield of PNA hydrocarbons in this investigation is low, the mere fact that these large hydrocarbons are produced under mild conditions (200 deg C and one atmosphere pressure) adds considerable weight to the argument that these hydrocarbons, and as well as others, must have arisen as a result of the cracking of the coal surface itself rather than by the release of them from the coal matrix.

In an effort to ascertain the nature of precursors, if any, released from the coal surfaces by H atoms, model compounds were studied under the same conditions. Benzene, toluene, p-xylene and napthalene were interacted with photoproduced H atoms in separate experiments. Care was taken to

quench the excited mercury atoms by hydrogen rather than by model compounds under study. This was achieved by controlling the vapor pressure of the model compounds using appropriate slush baths. Corrections were allowed for the differencd in the quenching cross sections between the model compounds and hydrogen. them are shown in Figures 45 through 51.

From the results of the model compounds, it is safe to assume that the H atoms liberate product precursors, at least in part, from the surface of coal, if they are available and these precursors undergo secondary hydrogen atom reactions involving ring saturation, ring opening, isomerization etc to produce smaller hydrocarbons. If no precursors are available, the hydrogen atoms seem to 'crack' the carbon structures rather indiscriminantly as demonstrated by results from Synthane char runs. However, the exact precursors are not known and this subject is discussed in detail in a later section.

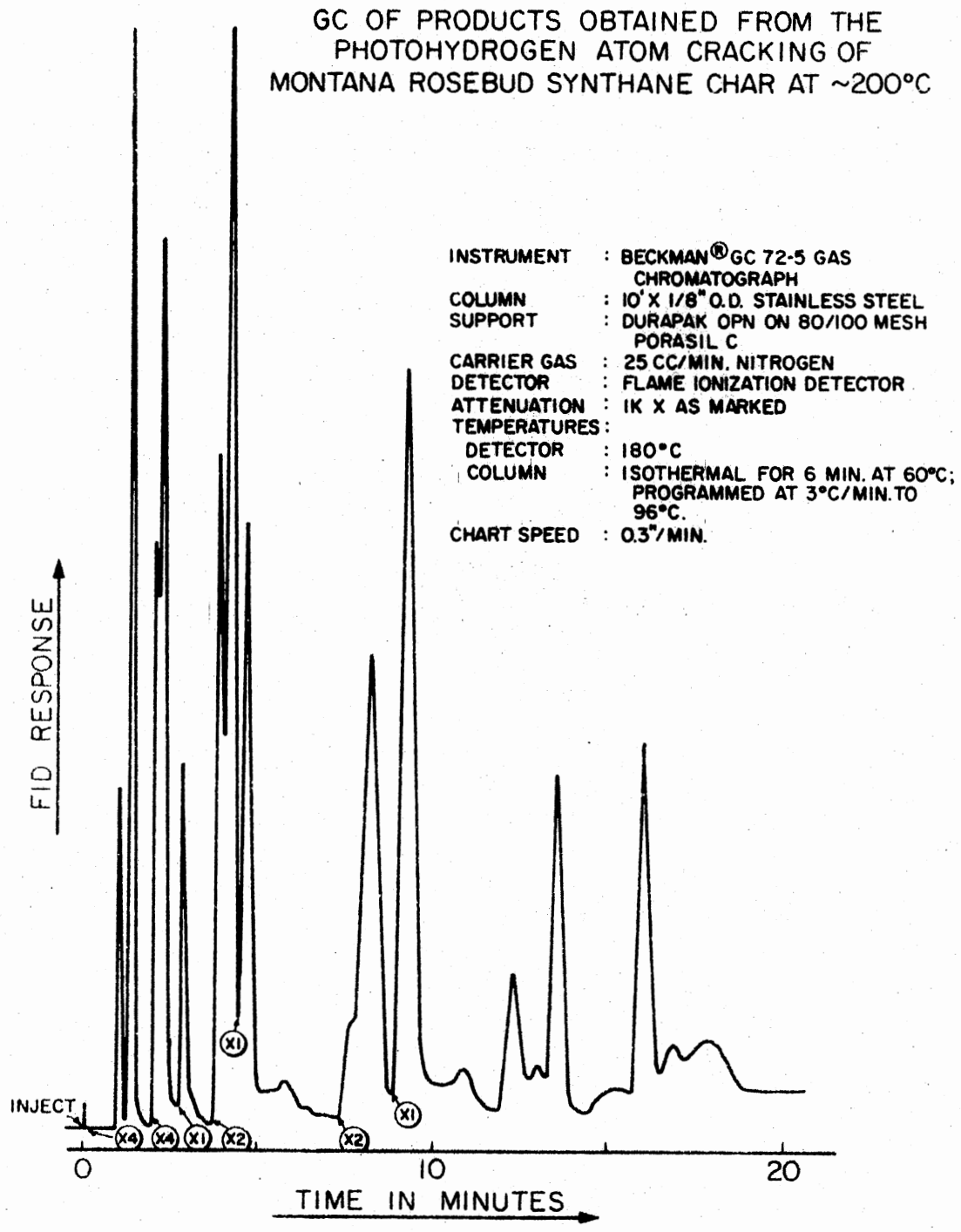

Figure 35. GC Trace of Products From Synthane Char

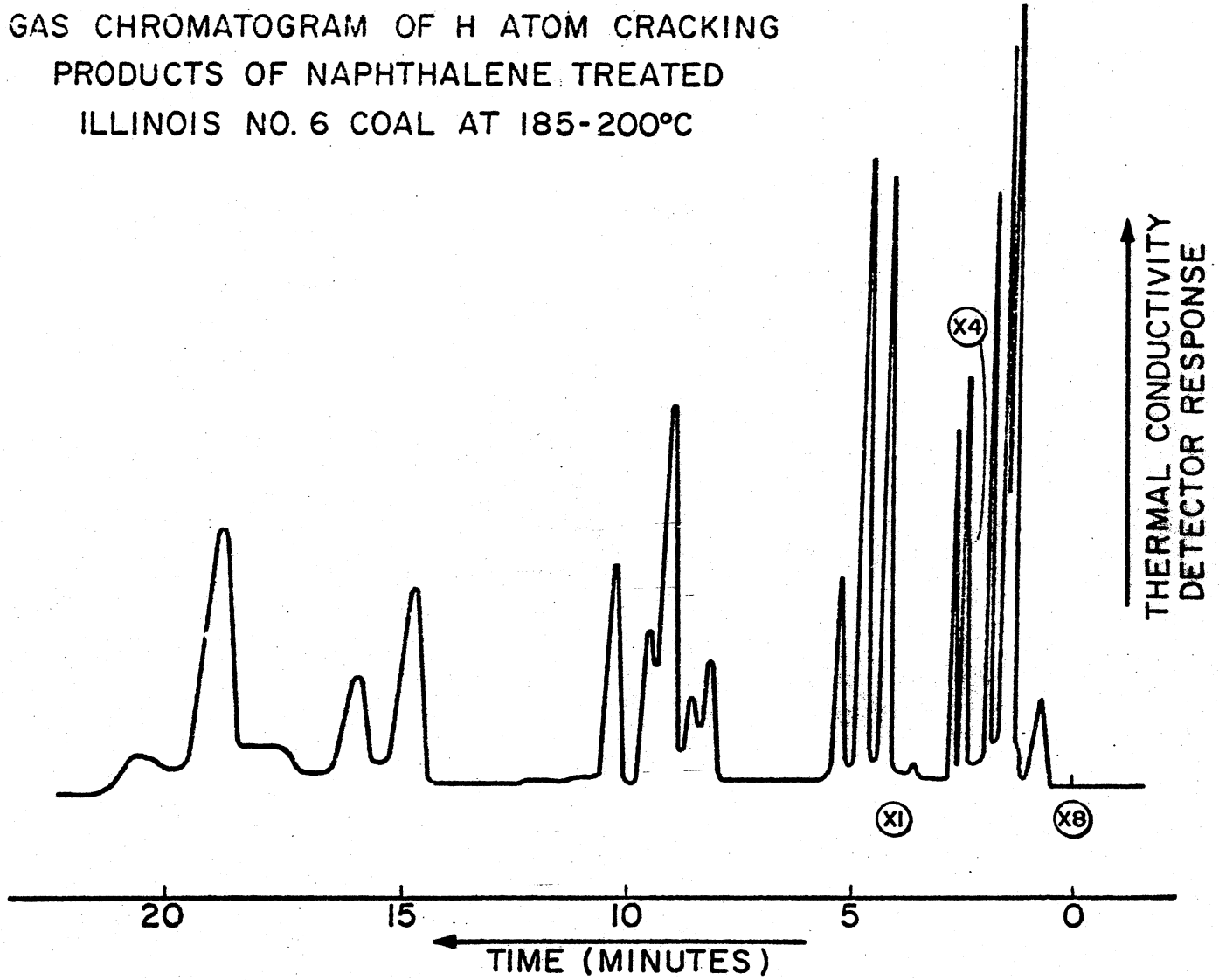

Figure 36. GC Trace of Products From Naphthalene Treated Coal

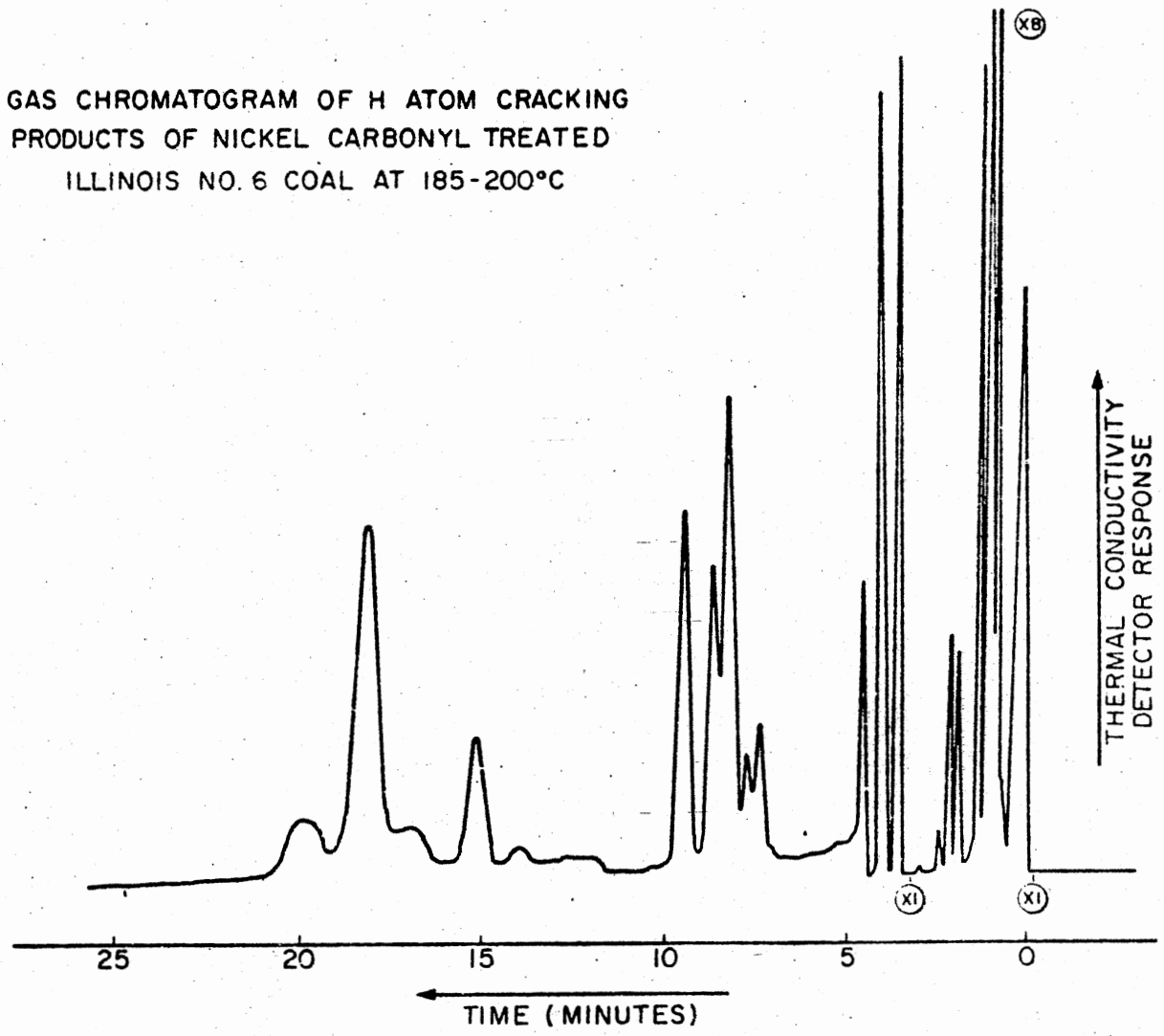

Figure 37. **GC Trace of Products From Nickel Carbonyl Treated Coal**

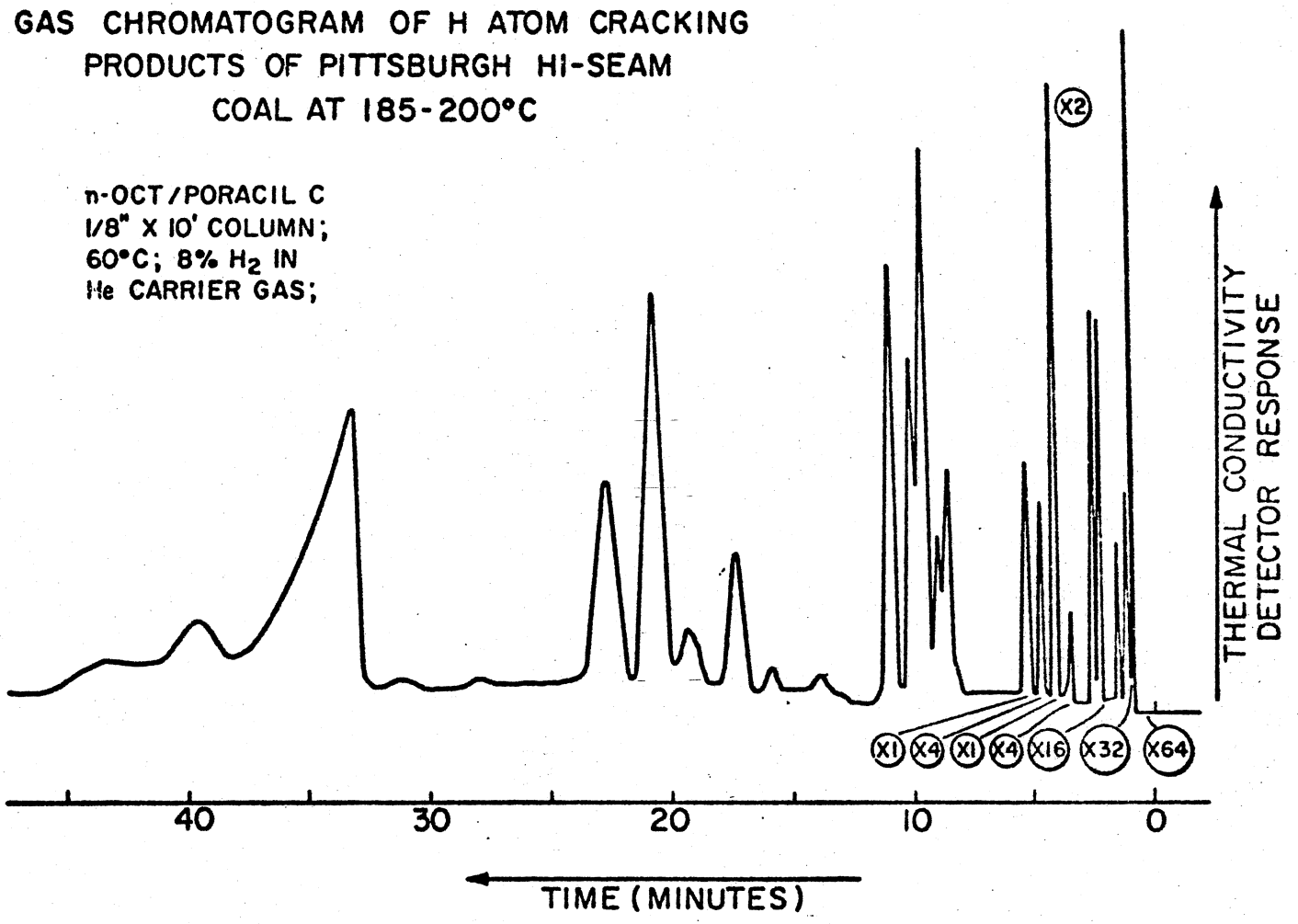

Figure 38. GC Trace of Products From Pittsburgh Hi-Seam Coal

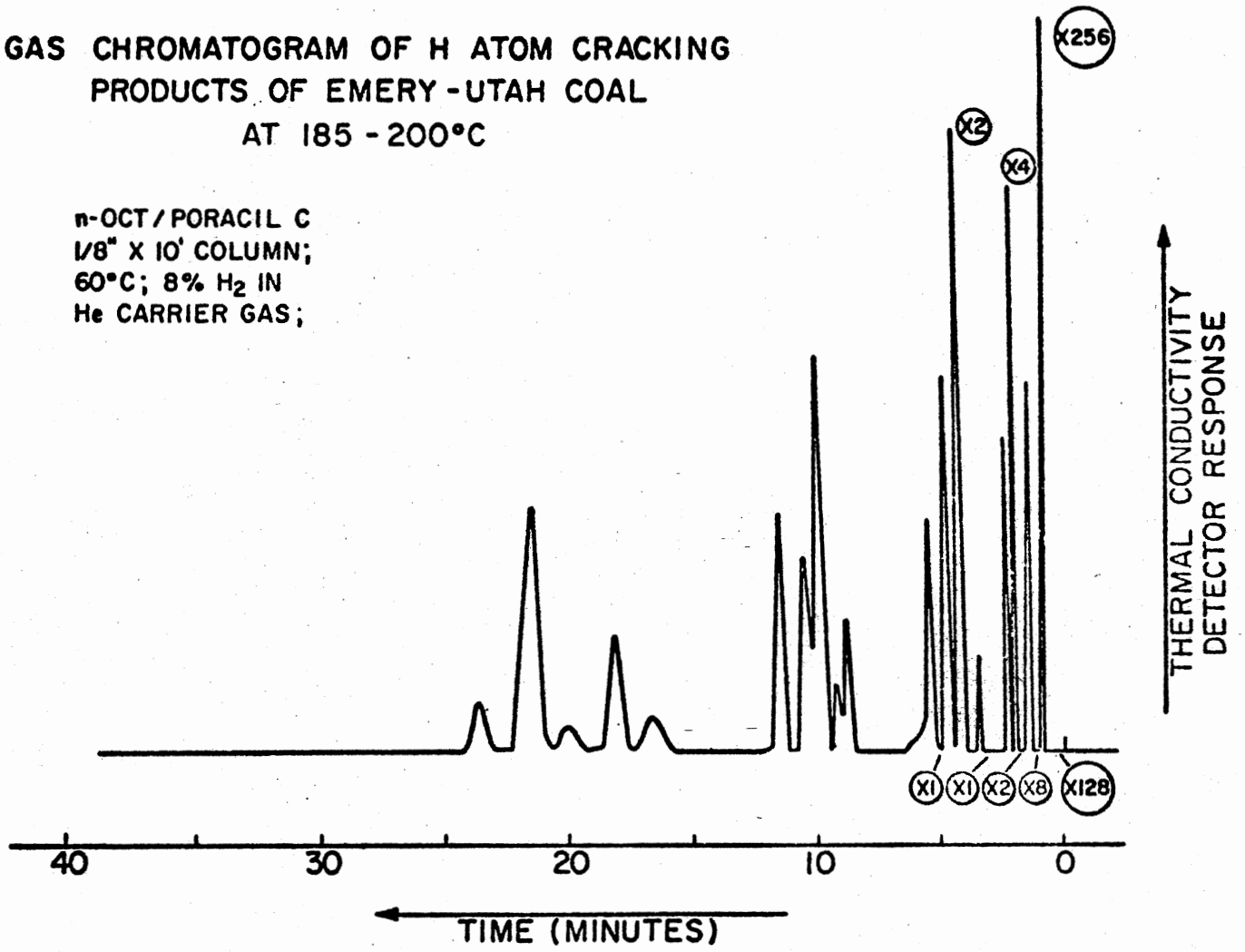

Figure 39. GC Trace of Products From Utah Emery Coal

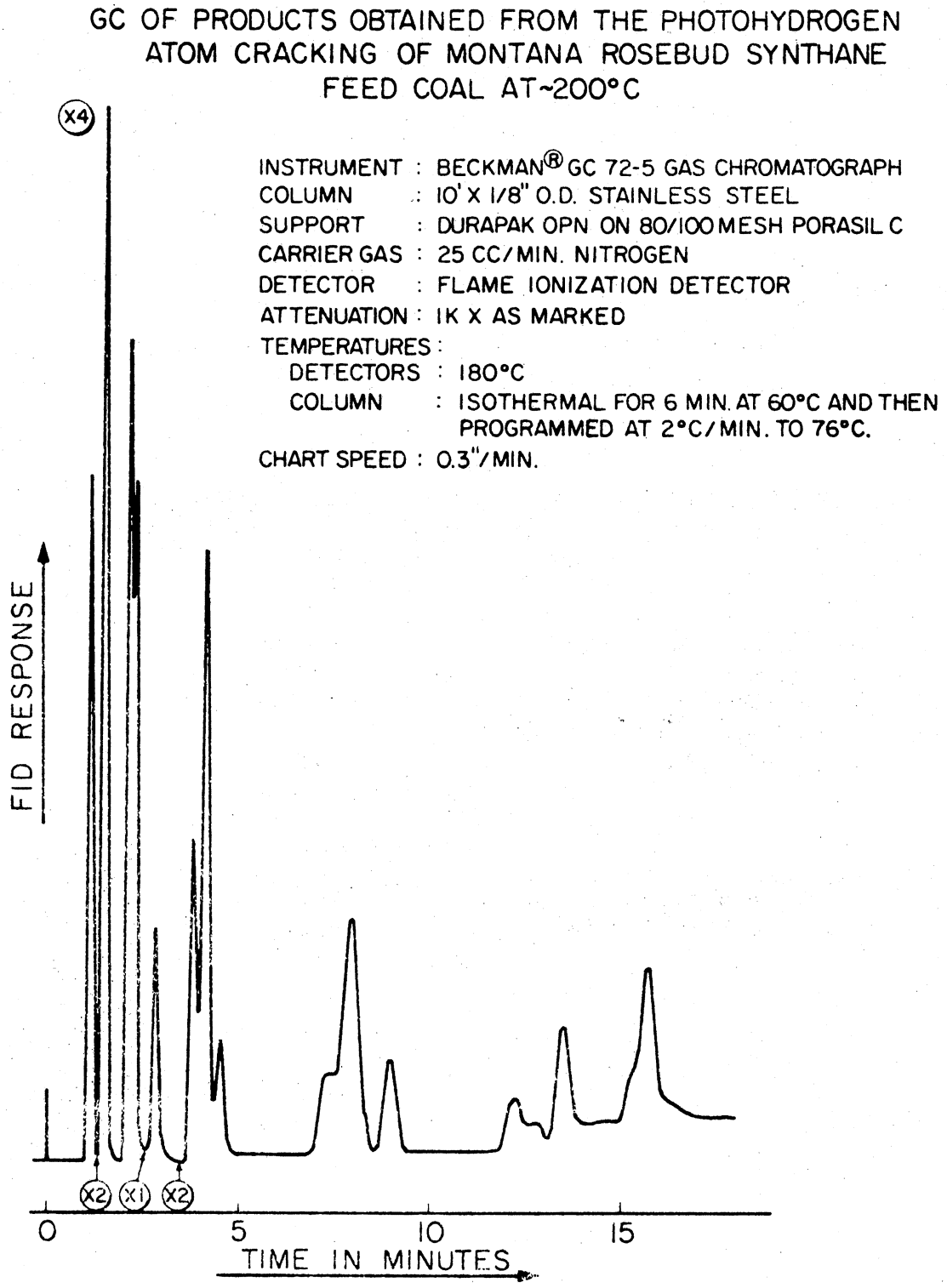

Figure 40. GC Trace of Products From Montana Rosebud Coal

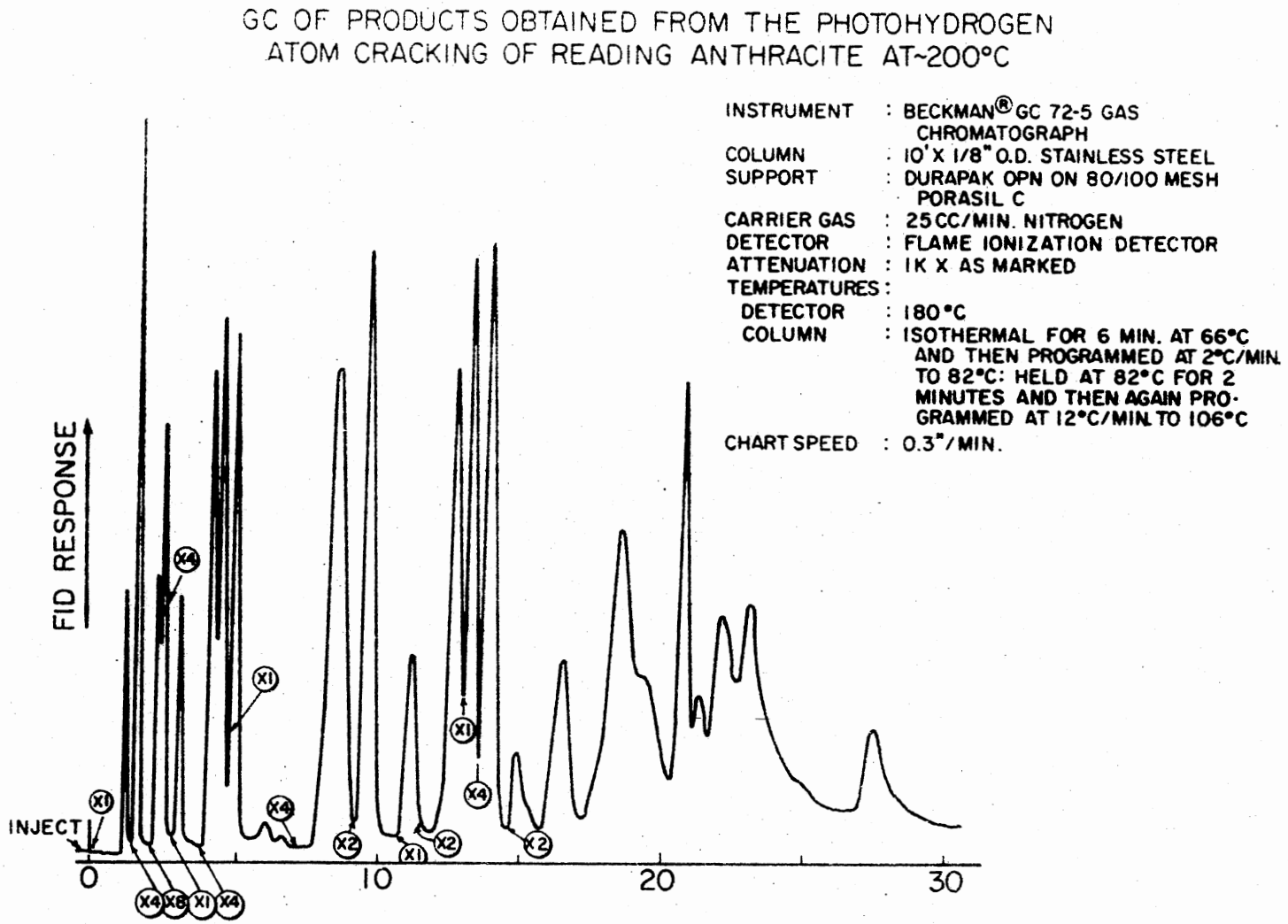

Figure 41. GC Trace of Products From Anthracite Coal

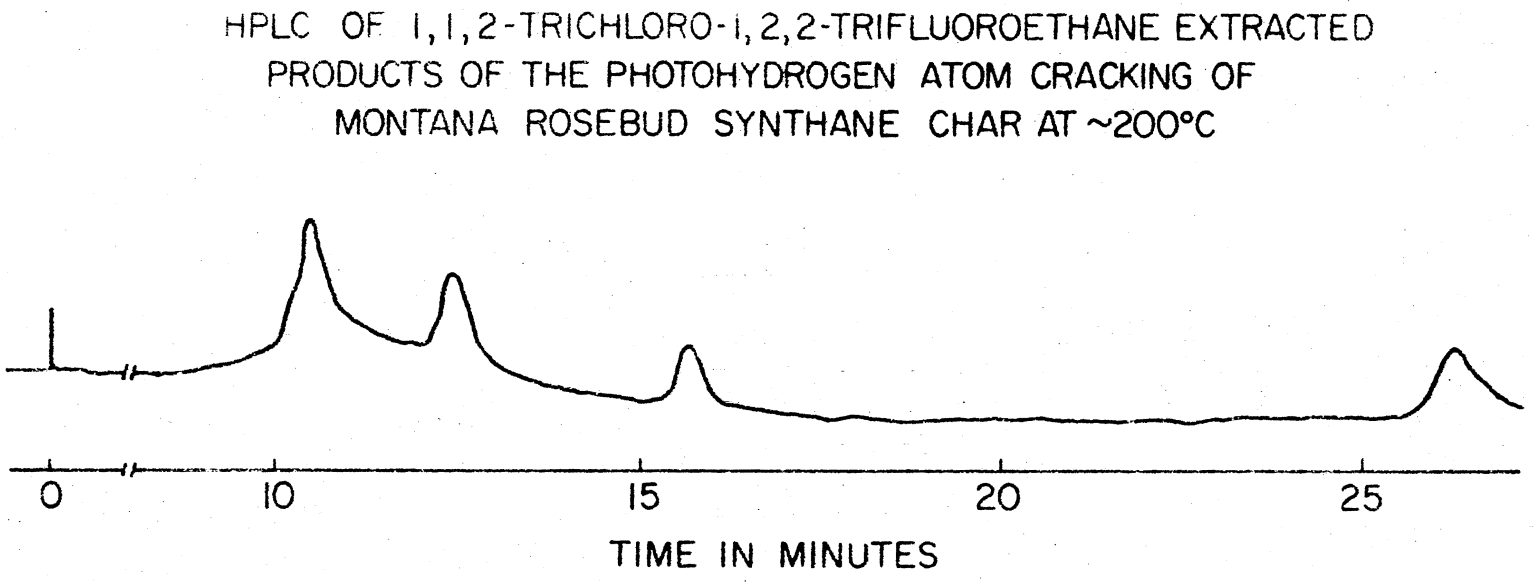

Figure 42. HPLC of Products From Synthane Char

HPLC OF 1,1,2-TRICHLORO-1,2,2-TRIFLUOROETHANE EXTRACTED PRODUCTS OF THE PHOTOHYDROGEN ATOM CRACKING OF MONTANA ROSEBUD SYNTHANE FEED COAL AT ~200°C

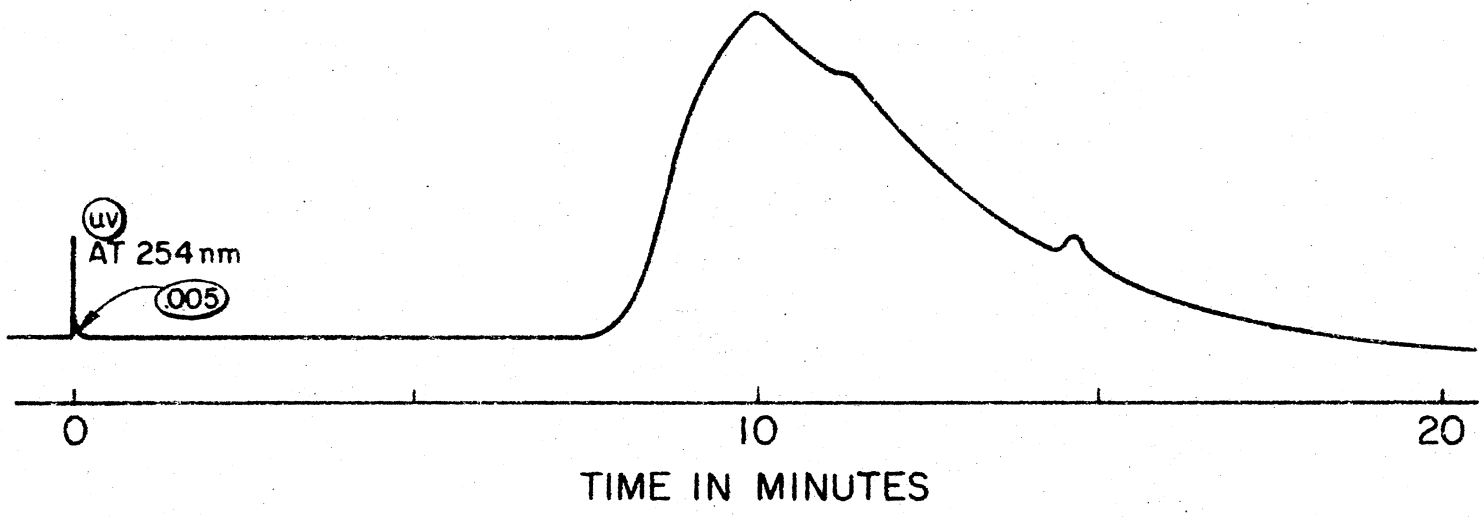

INSTRUMENT	: WATERS ASSOCIATES MODEL 6000A L.C.
COLUMN	: 3.9mm I.D. X 90cm
SUPPORT	: μ-PORASIL
MOBILE PHASE	: 1.0 ml/min. 1,1,2-TRICHLORO-1,2,2-TRIFLUOROETHANE
DETECTORS	: UV AT 254 nm
ATTENUATION	: 0.005 AUFS
PRESSURE DROP	: 1400 PSI
CHART SPEED	: 0.75"/ min.

Figure 43. HPLC of Products From Montana Rosebud Coal

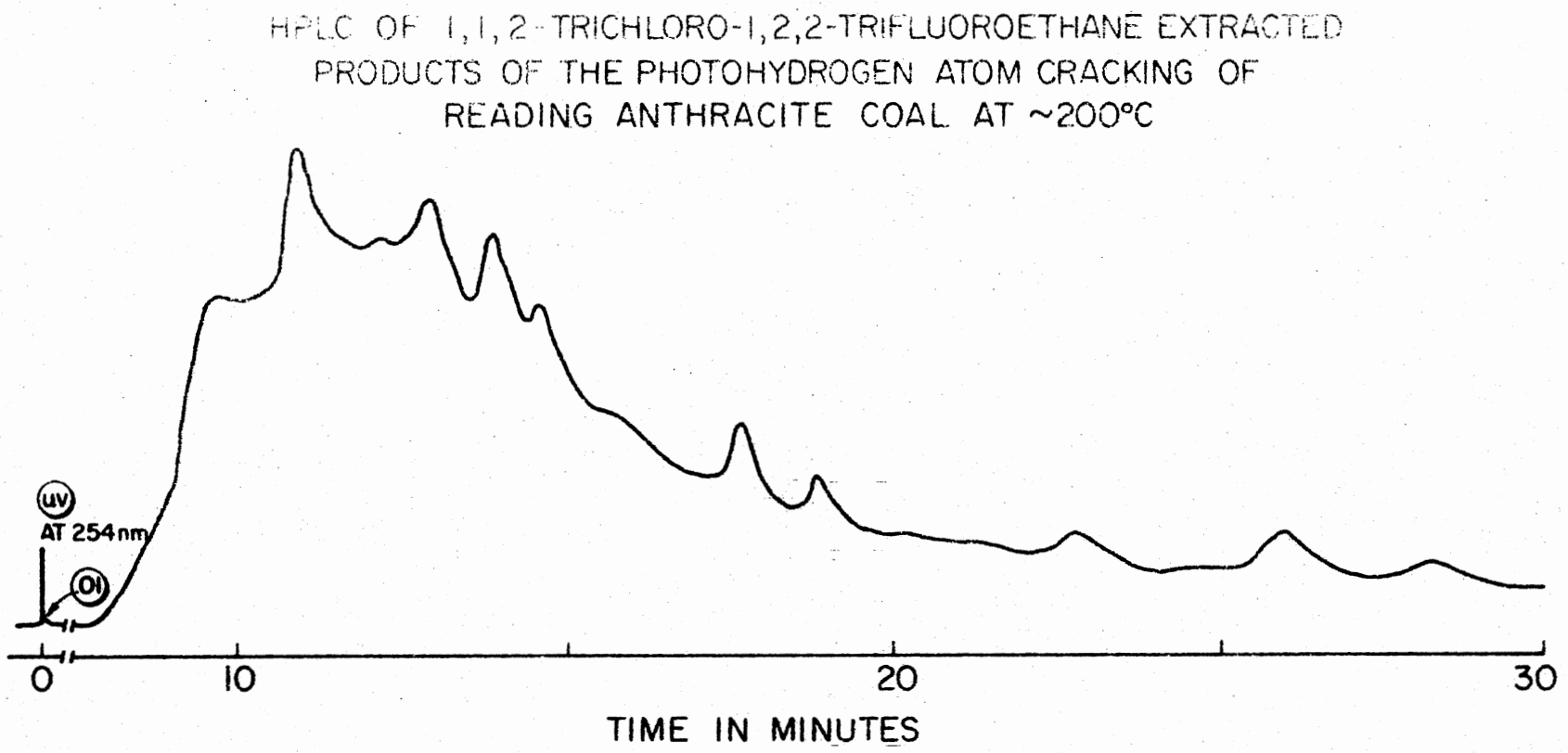

INSTRUMENT	: WATERS ASSOCIATES MODEL 6000A L.C.
COLUMN	: 3.9mm I.D. X 90cm
SUPPORT	: μ-PORASIL
MOBILE PHASE	: 1.0 ml/min. 1,1,2-TRICHLORO-1,2,2-TRIFLUOROETHANE
DETECTORS	: UV AT 254 nm
ATTENUATION	: 0.01 AUFS
PRESSURE DROP	: 1400 PSI
CHART SPEED	: 0.75"/min.

Figure 44. HPLC of Products From Anthracite Coal

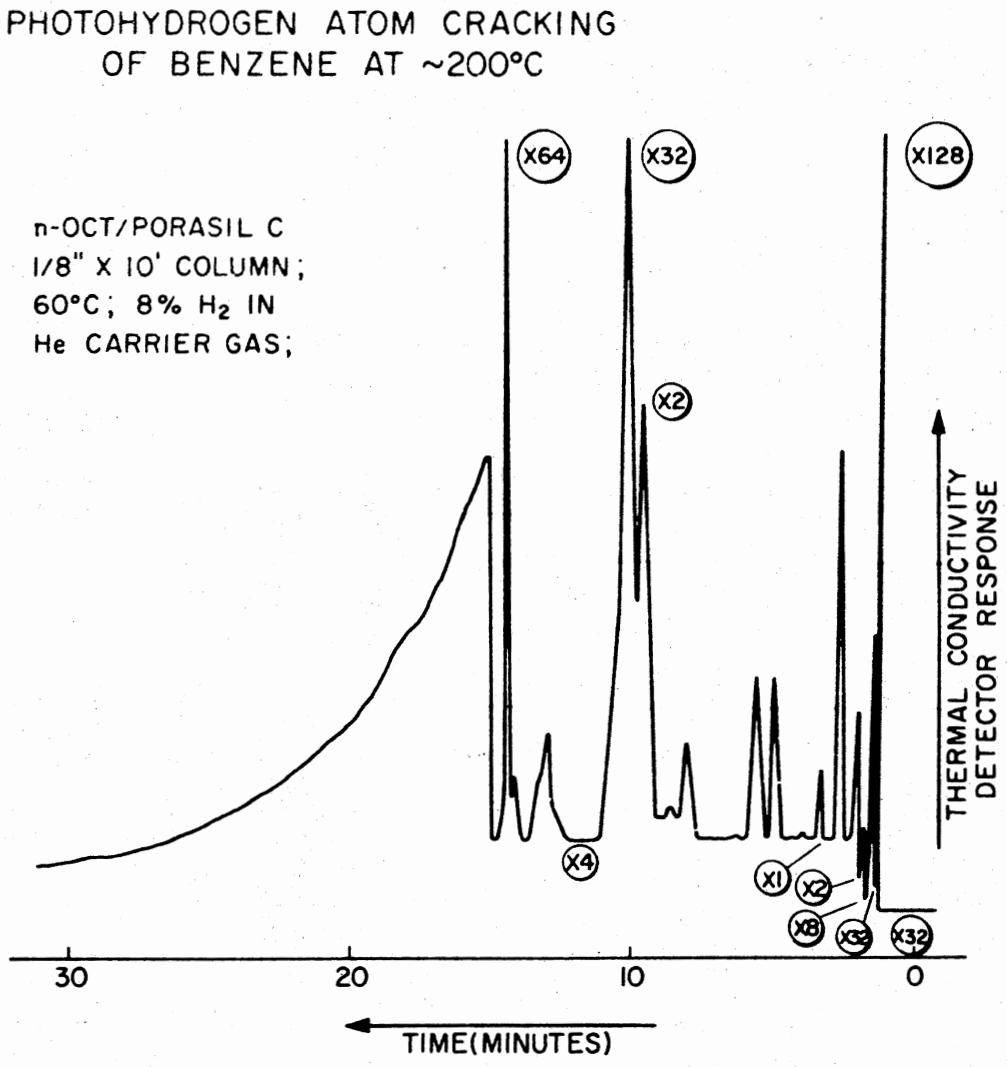

Figure 45. GC Trace of Products From Benzene

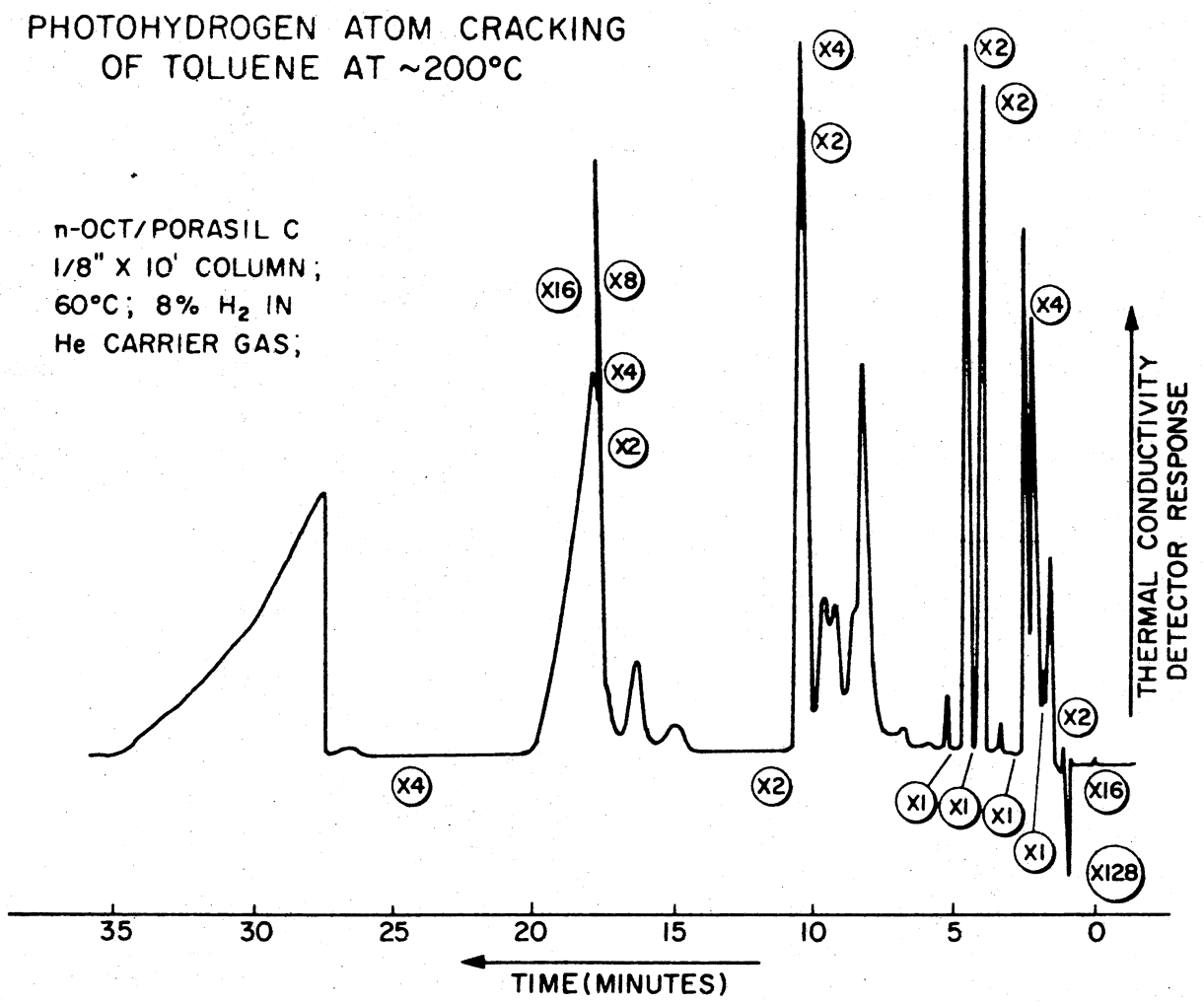

Figure 46. GC Trace of Products From Toluene

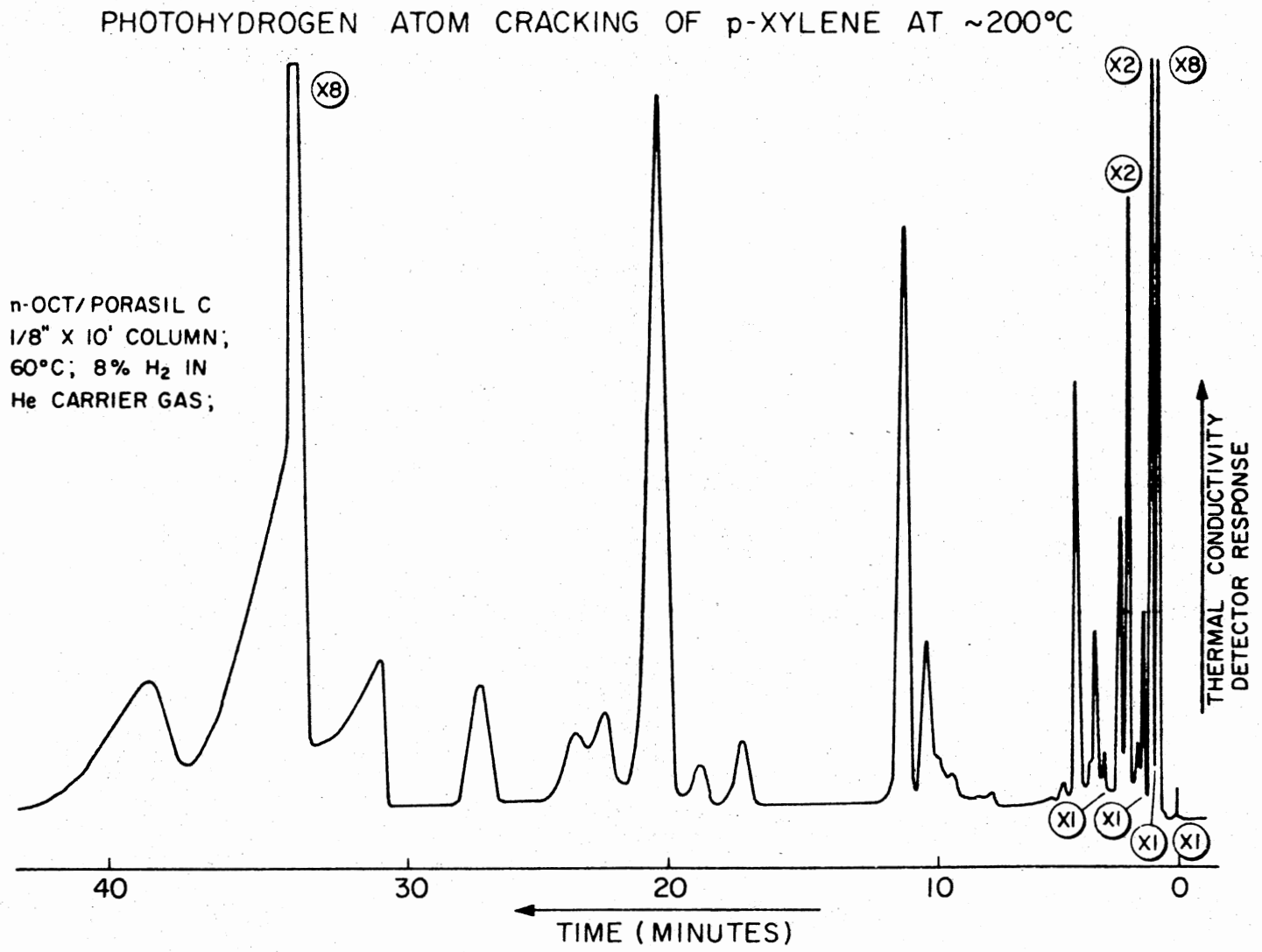

Figure 47. GC Trace of Products From p-Xylene

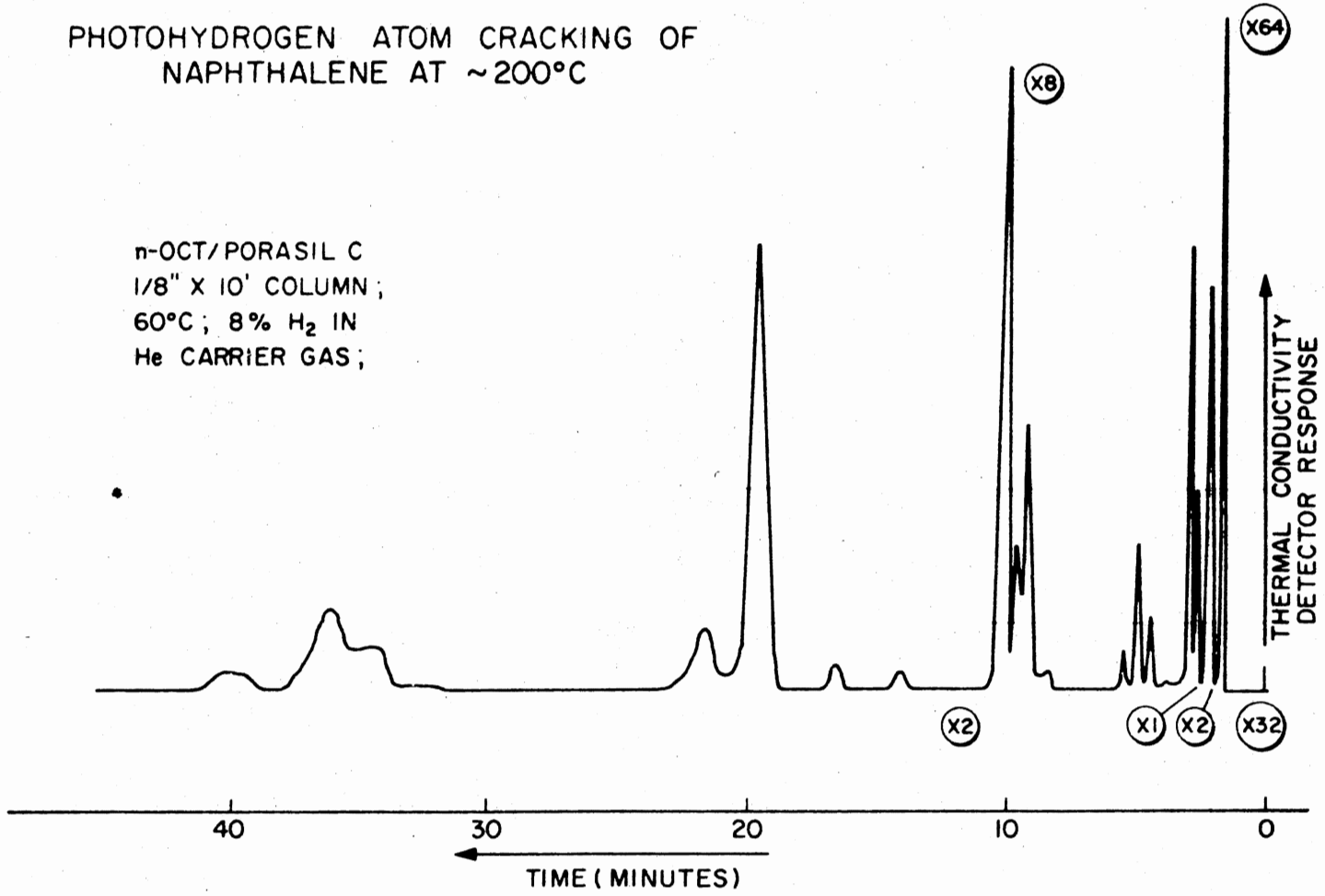

Figure 48. GC Trace of Products From Napthalene

HPLC OF HEXANE EXTRACTED PRODUCTS OF THE PHOTOHYDROGEN ATOM CRACKING OF BENZENE AT ~200°C

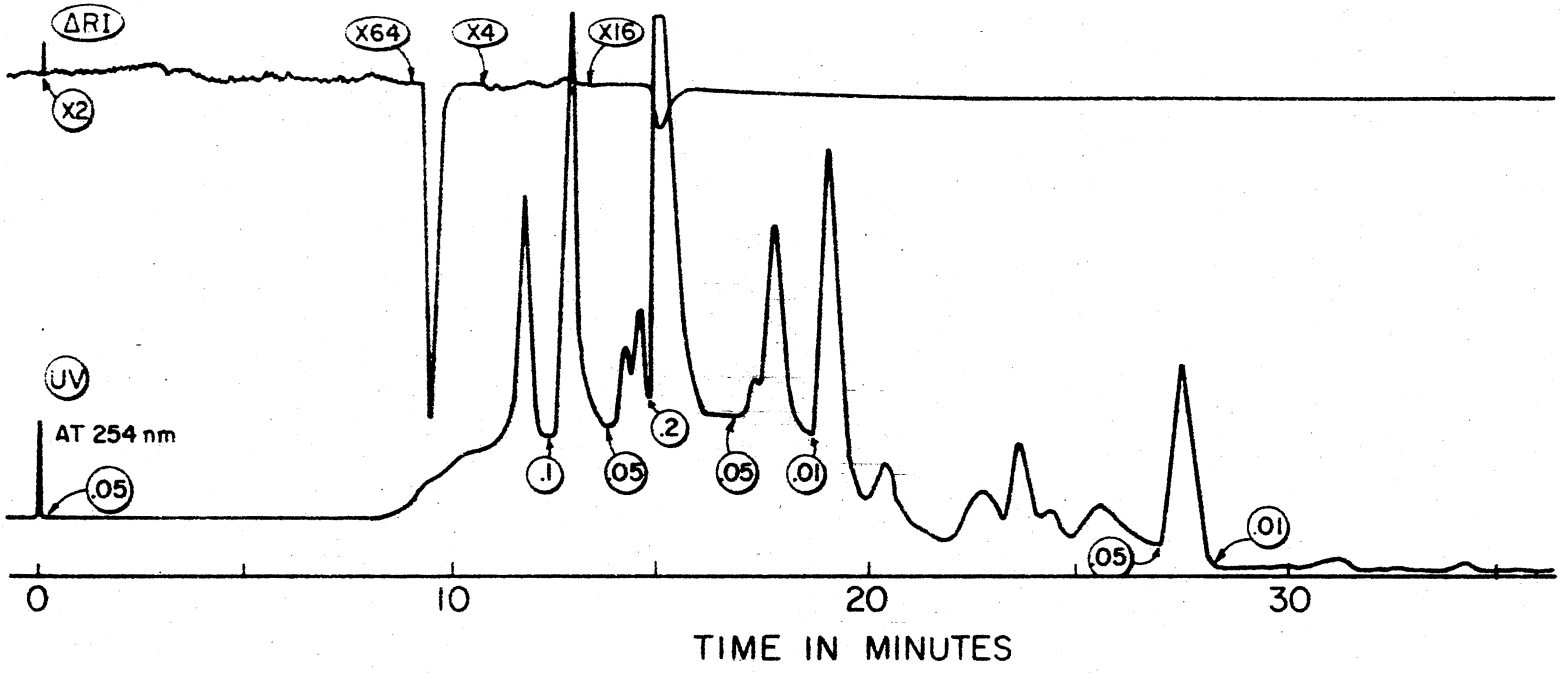

INSTRUMENT	: WATERS ASSOCIATES MODEL 6000A L.C.
COLUMN	: 3.9 mm I.D. X 90 cm
SUPPORT	: u-PORASIL
MOBILE PHASE	: 1.0 ml/min. 1,1,2-TRICHLORO-1,2,2-TRIFLUOROETHANE
DETECTORS	: UV AT 254 nm AND RI
ATTENUATION	: AS MARKED
PRESSURE DROP	: 1800 PSI
CHART SPEED	: 0.75"/min.

Figure 49. HPLC of Products From Benzene

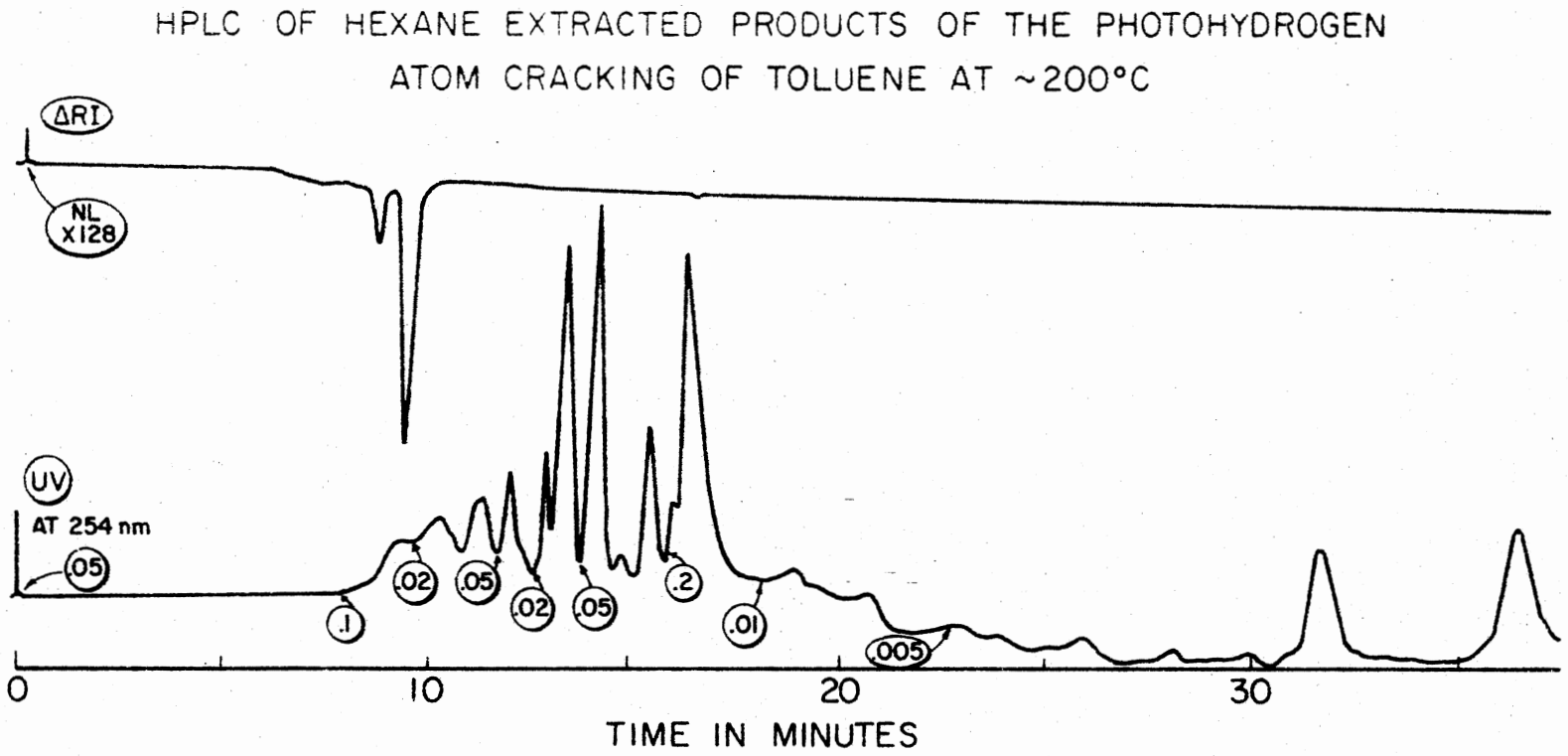

INSTRUMENT	: WATERS ASSOCIATES MODEL 6000A L.C.
COLUMN	: 3.9 mm I.D. X 90 cm
SUPPORT	: u-PORASIL
MOBILE PHASE	: 1.0 ml/min. 1,1,2-TRICHLORO-1,2,2-TRIFLUOROETHANE
DETECTORS	: UV AT 254 nm AND RI
ATTENUATION	: AS MARKED
PRESSURE DROP	: 1800 PSI
CHART SPEED	: 0.75"/min.

Figure 50. HPLC of Products From Toluene

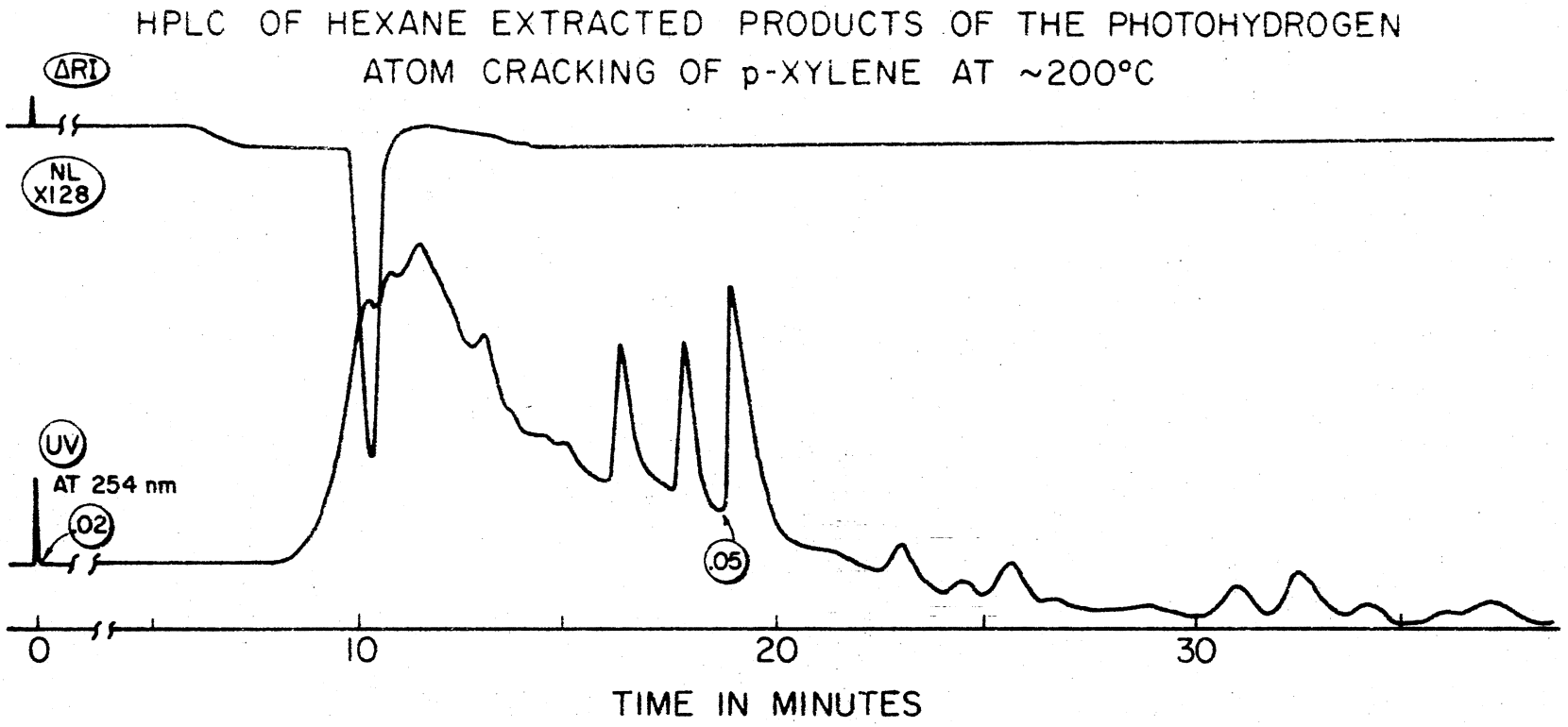

INSTRUMENT	: WATERS ASSOCIATES MODEL 6000A L.C.
COLUMN	: 3.9mm I.D. X 90 cm
SUPPORT	: u-PORASIL
MOBILE PHASE	: 1.0 ml/min. 1,1,2-TRICHLORO-1,2,2-TRIFLUOROETHANE
DETECTORS	: UV AT 254 nm AND RI
ATTENUATION	: AS MARKED
PRESSURE DROP	: 1800 PSI
CHART SPEED	: 0.75"/min.

Figure 51. HPLC of Products From p-Xylene

CHAPTER X

EFFECT OF PARAMETRIC VARIABLES

Once the feasibility of the process was established, attempts were made to quantitatively define the effects of pertinent variables on the photohydrogenation atom cracking of coal. The variables studied were: i) Temperature, ii) Inlet Gas Composition and iii) Particle Size. Because of the experimental difficulties, the effect of particle concentration on conversion could not be studied, as was originally intended.

The data reduction was done by a Computer Program specially written for this investigation. A listing of the program is given in Appendix A. The program is capable of computing molar yields, mole percent, weight percent, rate per unit time, rate per H atom, percent conversion of coal and product efficiencies per H atom. In addition, group yields such as yields (molar and percent) of C2-C4, C5, C6, C7, C8, BTX hydrocarbons, 2-ring aromatics, 3-ring aromatics could also be computed. Computation of yields (molar and percent) of normal, branched, olefinic and aromatic hydrocarbons is also possible. The program was made versatile by including a plot-routine using which **all** the computed data

could be plotted in a line printer. The scales for the plots are selected by the computer; of course, an user may choose his/her own scales. One limitation of the plot-routine is that no connecting lines or curves are drawn between the points. All plots in the following pages were generated by the above program. The input data for the program are: (i) detector sensitivities, (ii) total signal output, (iii) molecular weight of individual compounds, (iv) reaction time, (v) H atom concentration and (vi) percent carbon in the coal used. The program, without any modification, can handle 40 compounds. However, this could be extended to include more compounds, if desired.

The -53+38 micron coal 'dust' was used in all experiments (except the ones which involved particle size as the parametric variable) because of its ready availability in large amounts and also being intermediate in size.

Effect of Temperature

It was pointed out earlier that the experiments at ambient temperatures yielded virtually no products at all. However, the main thrust of this research was to 'crack' coal surface at a temperature as low as possible. A series of experiments was made in the temperature range from 100 deg C to 200 deg C. The products were collected in definite intervals selected at random. An interval of at least an hour was allowed between any two runs. Before the discus-

sion of effects of temperature on the reaction, one source of error must be mentioned here.

Because of the large heat 'leaks' on the top and at the bottom of the reactor due to convection, temperature could not be maintained constant in the reactor. The higher the reactor temperature, the higher was the axial temperature gradient too. The Nichrome wire surrounding the quartz reactor was wound densely at the top and at the bottom of the reactor to minimize the heat leaks. No attempt was made to do this in the UV light portion of the reactor because of the potential danger of attenuation of UV photons entering the reactor. However, the 'desired' temperature prevailed at least in 2/3 portion of the reactor. Nonetheless, the temperature quoted is the temperature inside the reactor and is not the temperature of the coal particles themselves. So the temperatures quoted are nominal temperatures only.

Listed in Table XIV are the effects of temperature on the total yields of products and percent carbon conversion. The same table shows the product efficiency per H atom and number of H atoms utilized for production of one product molecule (reciprocal of the former) for runs at 200 deg C.

The percentage conversion of coal into gaseous and liquid products was dependent on temperature. Higher conversion was achieved at higher reactor temperatures. Percentage carbon conversions for various temperatures have been plotted as a function of time in Figure 52. The runs at

TABLE XIV

EFFECT OF TEMPERATURE ON THE TOTAL YIELD AND PERCENT CONVERSION

PARTICLE SIZE : -53+38 MICRONS
REACTOR TEMP. : 100 - 106
INLET GAS COMPOSITION: 100.% HYDROGEN + 0.% HELIUM

TIME	YIELD	CONVERSION
1	0.4994E-07	0.4574E-03
2	0.1184E-06	0.1050E-02
3	0.2227E-06	0.1941E-02
4	0.3611E-06	0.3152E-02
5	0.6156E-06	0.4992E-02

PARTICLE SIZE : -53+38 MICRONS
REACTOR TEMP. : 150 - 155
INLET GAS COMPOSITION: 100.% HYDROGEN + 0.% HELIUM

TIME	YIELD	CONVERSION
1	0.3009E-06	0.2831E-02
2	0.6961E-06	0.6516E-02
3	0.1303E-05	0.1224E-01
4	0.2162E-05	0.2009E-01
5	0.4522E-05	0.4208E-01

PARTICLE SIZE : -53+38 MICRONS
REACTOR TEMP. : 200 - 206
INLET GAS COMPOSITION: 100.% HYDROGEN + 0.% HELIUM

TIME	YIELD	CONVERSION	EFFICIENCY	H ATOMS
1	0.1581E-05	0.1392E-01	0.2939E-02	341.
3	0.9137E-05	0.7802E-01	0.5662E-02	177.
4	0.1234E-04	0.9869E-01	0.5734E-02	176.
7	0.1655E-04	0.1337E+00	0.4394E-02	228.
20	0.2710E-04	0.2161E+00	0.2518E-02	397.

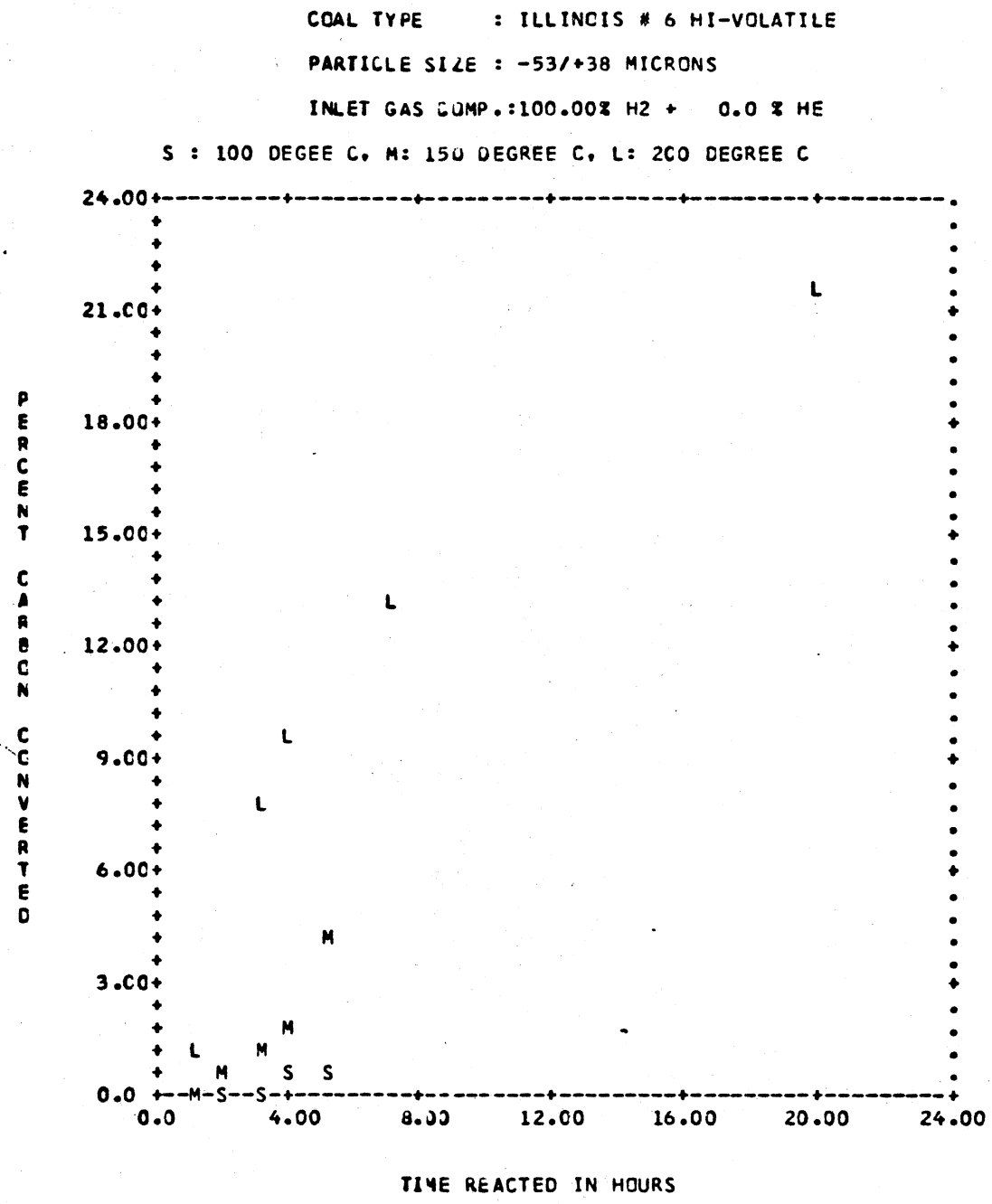

Figure 52. Effect of Temperature on Percent Conversion

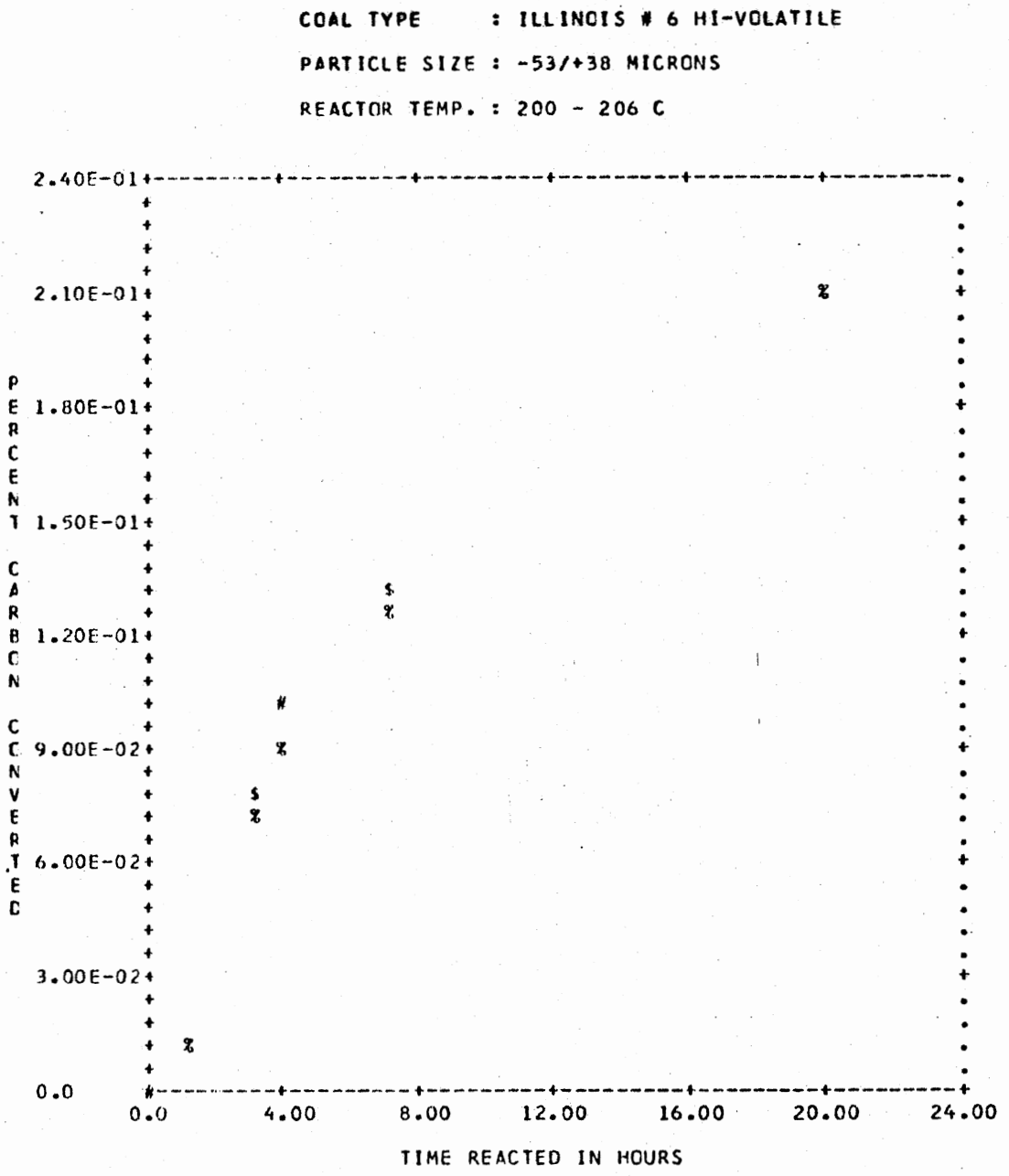

Figure 53. Experimental Reproducibility of Percent Conversion to Gaseous Products

200 deg C (except 20 hour run) were repeated 3 times to check the experimental reproducibility. Except for ethane, molar yields of products were reproducible within ±9%. For ethane, the error was considerably high, ±22%. The large error in the case of ethane is attributed to the poor trapping efficiency of this compound due to its high vapor pressure even at liquid nitrogen temperature. The calculations for percentage carbon conversion show that the results are reproducible within ±7%. An example of this is shown in Figure 53. (The computer generated representation of numbers having four significant figures may be disregarded.)

The number of moles of products formed per H atom is an indication of the change that occurs in the coal surface as the reaction progresses. Table XIV shows that the differential product efficiency goes through a maximum. This means that the cracking of the coal surface becomes increasingly difficult after a certain stage. This could be explained by assuming that the photoproduced H atoms attack some selected sites - active sites on the surface of coal.

The observed maximum in the product efficiency needs some coments. It was mentioned before that the coals used in the experiments were liquid-nitrogen-ground and protected from atmospheric oxygen by an envelope of nitrogen gas during storage. However, the exposure of coal to atmospheric oxygen during loading into the reactor could not be avoided. Hydrogen atoms, thus, actually react, at least initially,

with a coal adsorbed with oxygen on its surface. The implication of this is that the surface area of coal available for hydrogen atom attack depends on the rate of removal of adsorbed oxygen from the surface. With increased removal of oxygen from the surface, more and more reactive coal surfaces are exposed to H atom attack. This will explain the increase in the rate of formation of hydrocarbons with time. The fact that this rate does not level off after certain time, but, indeed, decreases after reaching a maximum makes one to susppect that the hydrogen atoms encounter, partly, with a non-reactive, possibly inorganic lithotype, layer after attack with a reactivee surface. However, in view of the low conversions achieved in the present work, this does not seem to be very likely. It is believed that the H atoms, after the removal of oxygen from the surface, react with a surface which was made 'active' by breaking of chemical bonds, generation of free radicals etc as a result of grinding. Once these active sites are consumed, the rate of conversion starts falling down rapidly. The implication of this is that the bulk coal is not believed to undergo H atom cracking as easily as the grinding-induced reactive surface.

Listed in Table XV through XVII are the yields of each product for different temperatures. Significantly smaller amounts of products were observed in the low temperature runs and higher molecular weight products such as pyrene,

TABLE XV

MOLAR YIELDS OF PRODUCTS AT 100 DEG C

PARTICLE SIZE : -53+38 MICRONS
REACTOR TEMP. : 100 - 106
INLET GAS COMPOSITION: 100.% HYDROGEN + 0.% HELIUM

REACTED HOURS->		1	2	3	4	5
COMPONENTS↓						
1	ETHANE	0.2990E-09	0.9326E-09	0.2965E-08	0.5150E-08	0.1215E-07
2	PROPANE	0.8950E-08	0.2416E-07	0.4764E-07	0.7569E-07	0.1578E-06
3	ISO-BUTANE	0.5805E-09	0.1226E-08	0.3107E-08	0.5022E-08	0.1075E-07
4	N-BUTANE	0.1727E-08	0.3907E-08	0.8195E-08	0.1586E-07	0.3763E-07
5	NEO-PENTANE	0.0	0.0	0.0	0.0	0.0
6	ISO-PENTANE	0.7373E-09	0.1541E-08	0.2968E-08	0.5124E-08	0.1321E-07
7	N-PENTANE	0.1289E-08	0.2798E-08	0.4354E-08	0.5956E-08	0.1161E-07
8	CYCLOPENTANE	0.0	0.0	0.3229E-09	0.9129E-09	0.2991E-08
9	2-METHYLPENTANE	0.0	0.0	0.6792E-10	0.4689E-09	0.9653E-09
10	3-METHYLPENTANE	0.0	0.0	0.0	0.6792E-10	0.5653E-09
11	N-HEXANE	0.2122E-08	0.4590E-08	0.7804E-08	0.1137E-07	0.2321E-07
12	METHYLCYCLOPENTANE	0.0	0.0	0.1671E-09	0.1078E-08	0.3762E-08
13	CYCLOHEXANE	0.2835E-09	0.1376E-08	0.2713E-08	0.5280E-08	0.1477E-07
14	2-METHYLHEXANE	0.0	0.0	0.0	0.0	0.0
15	3-METHYLHEXANE	0.0	0.0	0.0	0.0	0.0
16	N-HEPTANE	0.1298E-08	0.3123E-08	0.5570E-08	0.8109E-08	0.1528E-07
17	DIMETHYLCYCLOPENTANE	0.8419E-09	0.1874E-08	0.3052E-08	0.4306E-08	0.7658E-08
18	METHYLCYCLOHEXANE	0.8890E-08	0.1942E-07	0.3999E-07	0.6274E-07	0.1136E-06
19	CYCLICOLEFINS	0.9078E-09	0.3132E-08	0.8772E-08	0.1471E-07	0.3290E-07
20	DIMETHYLCYCLOHEXANE	0.1806E-07	0.3958E-07	0.6811E-07	0.1161E-06	0.1277E-06
21	C8+	0.0	0.0	0.0	0.0	0.0
22	PROPYLENE	0.1232E-09	0.1885E-08	0.2706E-08	0.3006E-08	0.0
23	BUTENES	0.0	0.2038E-09	0.3476E-09	0.4922E-09	0.0
24	PENTENES	0.2662E-09	0.9910E-09	0.1635E-08	0.2284E-08	0.0
25	BENZENE	0.1072E-08	0.2273E-08	0.3665E-08	0.5230E-08	0.7047E-08
26	TOLUENE	0.8588E-09	0.1821E-08	0.2937E-08	0.4191E-08	0.5648E-08
27	XYLENES	0.0	0.0	0.0	0.0	0.0
28	TETRALIN	0.6281E-10	0.1482E-09	0.2644E-09	0.4058E-09	0.5638E-09
29	NAPHTHALENE	0.3140E-10	0.7411E-10	0.1321E-09	0.2084E-09	0.2874E-09
30	METHYLNAPHTHALENES	0.6531E-10	0.1358E-09	0.2149E-09	0.3063E-09	0.3984E-09
31	DIMETHYLNAPHTHALENES	0.0	0.0	0.0	0.0	0.0
32	BIPHENYL	0.8710E-09	0.1802E-08	0.2748E-08	0.3724E-08	0.4716E-08
33	PHENANTHRENE	0.6043E-09	0.1360E-08	0.2266E-08	0.3362E-08	0.4570E-08

TABLE XVI

MOLAR YIELDS OF PRODUCTS AT 150 DEG C

PARTICLE SIZE : -53+38 MICRONS
REACTOR TEMP. : 150 - 155
INLET GAS COMPOSITION: 100.% HYDROGEN + 0.% HELIUM

REACTED HOURS-> / COMPONENTS		1	2	3	4	5
1	ETHANE	0.1960E-08	0.4239E-08	0.8456E-08	0.5069E-07	0.6013E-07
2	PROPANE	0.1604E-07	0.3506E-07	0.5861E-07	0.8676E-07	0.1982E-06
3	ISO-BUTANE	0.2842E-08	0.7724E-08	0.1374E-07	0.2559E-07	0.3007E-07
4	N-BUTANE	0.4645E-08	0.1043E-07	0.2302E-07	0.4154E-07	0.1093E-06
5	NEO-PENTANE	0.2594E-09	0.5386E-09	0.9705E-09	0.1538E-08	0.1647E-08
6	ISO-PENTANE	0.5218E-08	0.1259E-07	0.2037E-07	0.3006E-07	0.6658E-07
7	N-PENTANE	0.3086E-08	0.8707E-08	0.1775E-07	0.4491E-07	0.1751E-06
8	CYCLOPENTANE	0.4968E-09	0.1328E-08	0.2464E-08	0.3640E-08	0.5398E-08
9	2-METHYLPENTANE	0.7916E-09	0.2322E-08	0.6145E-08	0.1103E-07	0.2690E-07
10	3-METHYLPENTANE	0.7916E-09	0.2150E-08	0.5973E-08	0.1071E-07	0.2366E-07
11	N-HEXANE	0.1237E-08	0.1080E-07	0.2269E-07	0.3881E-07	0.9953E-07
12	METHYLCYCLOPENTANE	0.5143E-08	0.1455E-07	0.4593E-07	0.5153E-07	0.7026E-07
13	CYCLOHEXANE	0.4803E-08	0.1322E-07	0.3518E-07	0.1310E-06	0.4705E-06
14	2-METHYLHEXANE	0.0	0.0	0.0	0.5819E-09	0.1970E-08
15	3-METHYLHEXANE	0.0	0.0	0.0	0.1164E-08	0.4269E-08
16	N-HEPTANE	0.1164E-08	0.2814E-08	0.2926E-07	0.5794E-07	0.1573E-06
17	DIMETHYLCYCLOPENTANE	0.1227E-08	0.5475E-08	0.1040E-07	0.1614E-07	0.4014E-07
18	METHYLCYCLOHEXANE	0.4761E-08	0.1153E-07	0.1983E-07	0.1050E-06	0.1289E-06
19	CYCLICOLEFINS	0.2645E-08	0.7373E-08	0.1471E-07	0.2560E-07	0.5135E-07
20	DIMETHYLCYCLOHEXANE	0.6645E-07	0.1545E-06	0.3451E-06	0.5663E-06	0.1183E-05
21	C8+	0.0	0.0	0.0	0.1142E-08	0.1139E-07
22	PROPYLENE	0.2906E-08	0.5217E-08	0.2248E-07	0.2415E-07	0.0
23	BUTENES	0.6495E-09	0.2228E-08	0.4209E-08	0.4824E-08	0.0
24	PENTENES	0.4096E-08	0.1409E-07	0.1577E-07	0.1628E-07	0.0
25	BENZENE	0.8681E-07	0.1929E-06	0.3022E-06	0.4252E-06	0.5896E-06
26	TOLUENE	0.2834E-07	0.6183E-07	0.9790E-07	0.1398E-06	0.6505E-06
27	XYLENES	0.5176E-07	0.1087E-06	0.1708E-06	0.2371E-06	0.3050E-06
28	TETRALIN	0.0	0.0	0.0	0.0	0.0
29	NAPHTHALENE	0.3533E-09	0.7655E-09	0.1295E-08	0.1867E-08	0.2472E-08
30	METHYLNAPHTHALENES	0.3674E-09	0.8588E-09	0.1476E-08	0.2341E-08	0.3328E-08
31	DIMETHYLNAPHTHALENES	0.1829E-09	0.4210E-09	0.7064E-09	0.1063E-08	0.1476E-08
32	BIPHENYL	0.5632E-10	0.2253E-09	0.5024E-09	0.8725E-09	0.1331E-08
33	PHENANTHRENE	0.1832E-08	0.3503E-08	0.5078E-08	0.6467E-08	0.7388E-08

TABLE XVII

MOLAR YIELDS OF PRODUCTS AT 200 DEG C

PARTICLE SIZE : -53+38 MICRONS
REACTOR TEMP. : 200 - 206
INLET GAS COMPOSITION: 100.% HYDROGEN + 0.% HELIUM

REACTED HOURS->		1	3	4	7	20
COMPONENTS| V					
1	ETHANE	0.2137E-07	0.1776E-06	0.4501E-06	0.8674E-06	0.2205E-05
2	PROPANE	0.7800E-07	0.2153E-06	0.5209E-06	0.8048E-06	0.2287E-05
3	ISO-BUTANE	0.1498E-07	0.1420E-06	0.1367E-05	0.1602E-05	0.3594E-05
4	N-BUTANE	0.2963E-07	0.2801E-06	0.7302E-06	0.1052E-05	0.2867E-05
5	NEO-PENTANE	0.4222E-08	0.4203E-07	0.7950E-07	0.4454E-06	0.1094E-05
6	ISO-PENTANE	0.1831E-07	0.2445E-06	0.4346E-06	0.5686E-06	0.1786E-05
7	N-PENTANE	0.3430E-07	0.4427E-06	0.7519E-06	0.1045E-05	0.2875E-05
8	CYCLOPENTANE	0.8922E-07	0.5668E-06	0.1705E-05	0.2231E-05	0.5011E-05
9	2-METHYLPENTANE	0.1387E-07	0.1037E-06	0.1699E-06	0.2059E-06	0.6057E-06
10	3-METHYLPENTANE	0.2086E-08	0.9466E-07	0.1527E-06	0.1838E-06	0.5494E-06
11	N-HEXANE	0.5473E-07	0.3569E-06	0.5714E-06	0.6806E-06	0.1933E-05
12	METHYLCYCLOPENTANE	0.2624E-06	0.2294E-05	0.3521E-05	0.5597E-05	0.1244E-04
13	CYCLOHEXANE	0.1546E-06	0.9080E-06	0.1407E-05	0.1632E-05	0.3962E-05
14	2-METHYLHEXANE	0.1864E-08	0.9939E-08	0.1753E-07	0.3335E-07	0.8911E-07
15	3-METHYLHEXANE	0.1536E-07	0.6377E-07	0.1040E-06	0.1434E-06	0.3171E-06
16	N-HEPTANE	0.2190E-07	0.9343E-07	0.1507E-06	0.1993E-06	0.4820E-06
17	DIMETHYLCYCLOPENTANE	0.1895E-06	0.8692E-06	0.1350E-05	0.1516E-05	0.3351E-05
18	METHYLCYCLOHEXANE	0.2422E-06	0.1059E-05	0.1666E-05	0.1982E-05	0.4977E-05
19	CYCLICOLEFINS	0.1698E-06	0.3886E-06	0.6219E-06	0.7569E-06	0.2830E-05
20	DIMETHYLCYCLOHEXANE	0.1806E-07	0.3452E-06	0.6062E-06	0.7213E-06	0.1671E-05
21	C8+	0.6814E-07	0.1873E-06	0.3540E-06	0.4381E-06	0.1038E-05
22	PROPYLENE	0.0	0.0	0.0	0.0	0.0
23	BUTENES	0.0	0.0	0.0	0.0	0.0
24	PENTENES	0.0	0.0	0.0	0.0	0.0
25	BENZENE	0.4428E-07	0.1278E-06	0.1762E-06	0.2460E-06	0.7946E-06
26	TOLUENE	0.7515E-08	0.3192E-07	0.3958E-07	0.5108E-07	0.1684E-06
27	XYLENES	0.1510E-07	0.6305E-07	0.7869E-07	0.1028E-06	0.3267E-06
28	TETRALIN	0.4907E-09	0.1501E-08	0.2038E-08	0.2858E-08	0.9196E-08
29	NAPHTHALENE	0.2699E-09	0.8938E-09	0.1236E-08	0.1914E-08	0.6245E-08
30	METHYLNAPHTHALENES	0.2041E-09	0.7867E-09	0.1015E-08	0.1057E-08	0.3460E-08
31	DIMETHYLNAPHTHALENES	0.7441E-10	0.3877E-09	0.4670E-09	0.5800E-09	0.1950E-08
32	BIPHENYL	0.9386E-10	0.3903E-09	0.5120E-09	0.7084E-09	0.2390E-08
33	PHENANTHRENE	0.5902E-08	0.1876E-07	0.2626E-07	0.2748E-07	0.9042E-07
34	PYRENE	0.0	0.0	0.0	0.0	0.0
35	FLUORANTHENE	0.5312E-09	0.1729E-08	0.2340E-08	0.3442E-08	0.1091E-07
36	BANZANTHRACENE	0.1298E-08	0.3386E-08	0.4146E-08	0.5087E-08	0.1843E-07
37	BENZOPYRENE	0.5312E-09	0.1277E-08	0.1679E-08	0.2237E-08	0.7377E-08

fluoranthene, benzanthracene, benzopyrene etc were totally absent at 100 deg C and 150 deg C runs.

The mole ratio of phenanthrene to biphenyl in the liquid product was found to be a strong function of temperature. This point is clearly emphasized in Table XVIII in which the data given in Tables XV through XVII have been reconstructed. As the temperature is increased, the mole ratio also increases. Furthermore, it is observed that at the highest temperature investigated, the phenanthrene to biphenyl mole ratio is significantly very high. In addition, the mole ratio decreases with time in the case of 150 deg C and 200 deg C runs, whereas the opposite is true at 100 deg C.

These results lead one to believe that the product distribution, yield and percent conversion are probably controlled by a rate limiting step in which phenanthrene type precursors are cracked off the coal surface which is then followed by secondary H atom reactions to produce smaller hydrocarbons.

In fact, phenanthrene is usually present in larger abundance in coal derived liquids . This can be attributed to the thermodynamic stability associated with the staggered phenanthrene-like compounds compared to the linear anthracene-like isomers (101). Hydrogenation of phenanthrene has been studied by several workers (102, 103 and 104) and most recently by Cowan (105). Hydrocracking of phenanthrene

TABLE XVIII

MOLE RATIO OF PHENANTHRENE TO BIPHENYL

Temp. °C	Hours 1	2	3	4	5	7
100	0.69	0.75	0.83	0.90	0.97	
150	32.2	15.5	10.1	7.4	5.5	
200	62.9		48.0	41.3		38.8

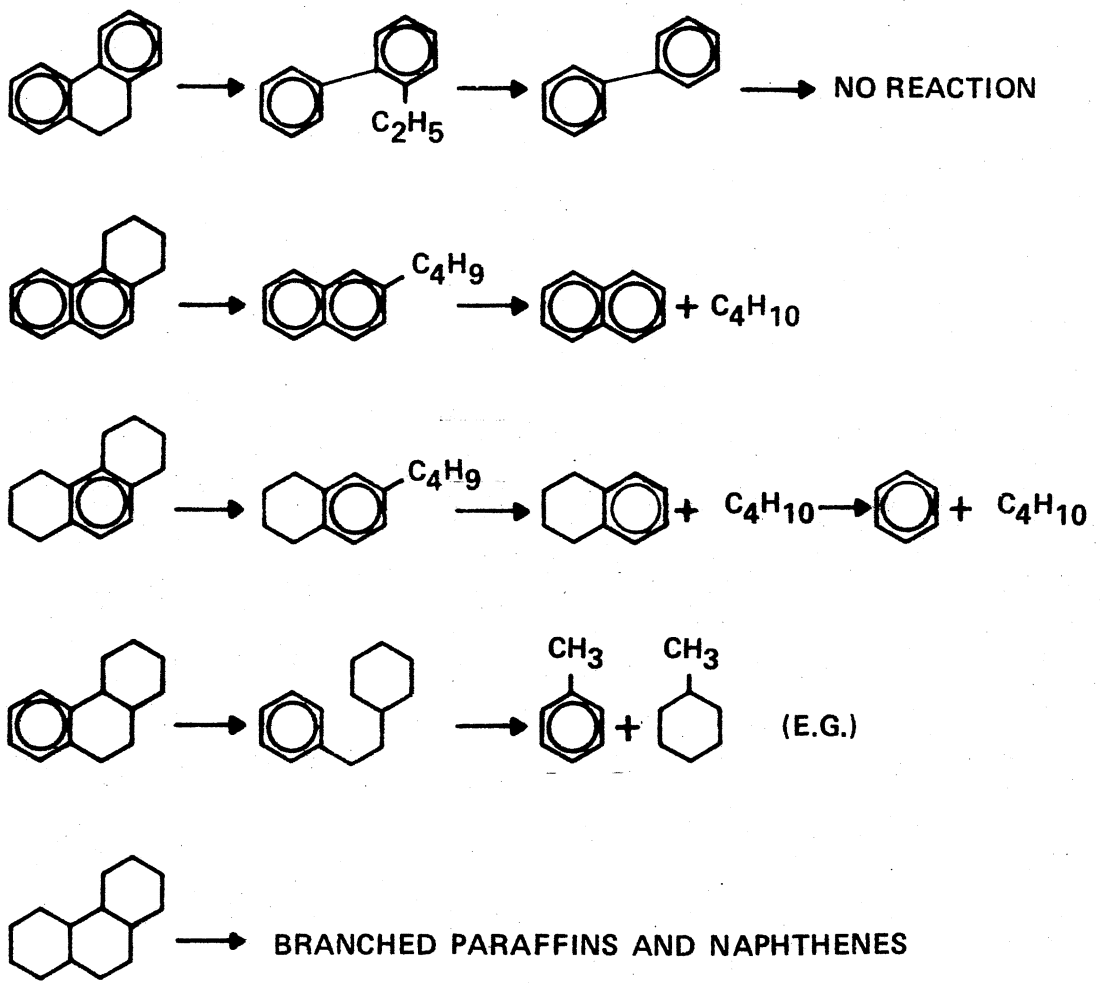

Figure 54. Hydrocracking Reactions of Phenanthrene

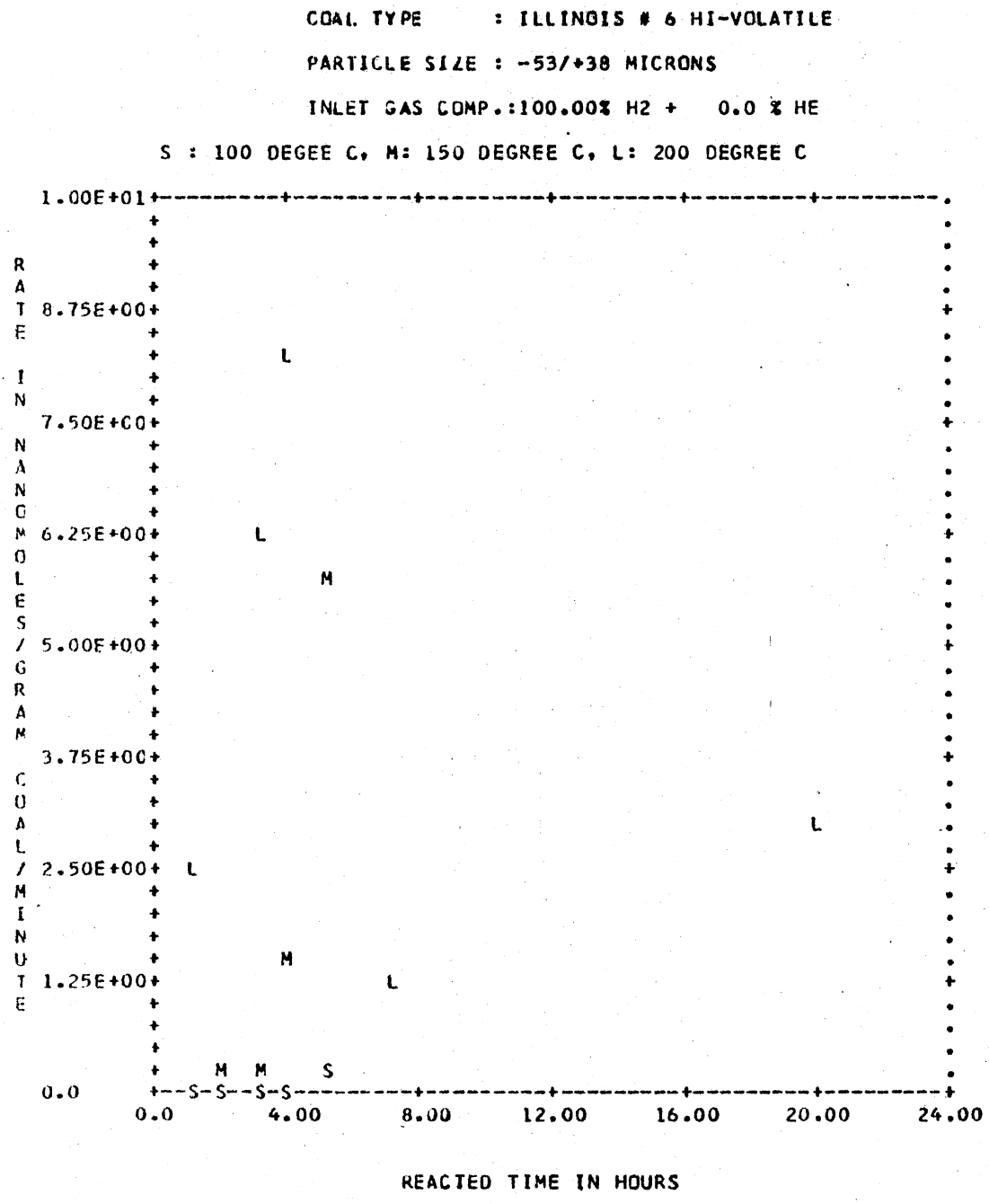

Figure 55. Effect of Temperature on the Rate of Formation of Cyclohexane

has been studied by Qader et al. (106) and Huang et al. (107). Cowan (105) studied the selectivity of different catalysts on the hydrogenation of several polynuclear aromatic hydrocarbons including phenanthrene, pyrene, benzanthracene and chrysene and concluded that Pt/C catalyst was selective to hydrogenation at the end rings whereas Pd/C and Rh/alumina catalysts were to inner rings. Haynes (108) has concluded that under hydrocracking conditions, at least, phenanthrene cracks almost exclusively by paths involving saturation, ring opening, possibly some isomerization, and cracking of terminal rings. Some hydrocracking reactions of phenanthrene are given in Figure 54. However, it should be noted that none of the studies mentioned above used direct H atoms as hydrogenating agents.

The available data from this investigation suggest that at low temperatures, hydrogenation of inner rings of condensed ring aromatics is predominant whereas as temperature is increased, the terminal ring hydrogenation becomes more pronounced. Hydrocracking of end rings of condensed ring aromatics can give rise to a variety of hydrocarbons as shown in Figure 54.

An analysis of Tables XIX, XX and XXI shows that the rates of formation of all saturated products follow one trend whereas those of aromatics another. In the case of saturated products, the rates of formation of each product follow the order 200 deg C>150 deg C>100 deg C. An example

of this is shown in Figure 55 in which the rates of formation of cyclohexane under various temperatures are plotted as function of time. One point to be noted from Figure 55 is the shifting of the maxima with decrease in the reaction temperature. The maximum for the rate of formation of cyclohexane at 200 deg C is found to occur at 3 hours whereas the slopes of the curves for 150 deg C and 100 deg C indicate a definite shifting of the maxima towards a longer time. This pattern is followed in all saturated hydrocarbons with exception of none.

The plots of rates of formation of benzene, toluene and xylene (Figures 56, 57 and 58) showed that at 200 deg C, the maximum for these compounds also occurred at 3 hours whereas for the lower temperature runs their slopes indicated the shifting of the maxima towards longer reaction periods. This indicates the possibility of production of saturated hydrocarbons from aromatic precursors.

A look at the plots 56, 57 and 58 indicates the order to be 150 deg C>200 deg C>100 deg C. The same was found to be true with naphthalenes too. This order may, first, seem to be inconsistent to our expectation. However, the answer for this unexpected behaviour lies in the following points: (i) with increase in temperature, ring saturation and ring opening processes also could increase and (ii) the smaller aromatic hydrocarbons, might, possibly, have been produced by cracking of large aromatic clusters cracked off the surface of coal.

TABLE XIX

RATE DATA AT 100 DEG C

PARTICLE SIZE : -53+38 MICRONS
REACTOR TEMP. : 100 - 106
INLET GAS COMPOSITION: 100.% HYDROGEN + 0.% HELIUM

REACTED HOURS->		1	2	3	4	5
COMPONENTS!						
1	ETHANE	0.4983E-11	0.1056E-10	0.3387E-10	0.3642E-10	0.1167E-09
2	PROPANE	0.1492E-09	0.2536E-09	0.3913E-09	0.4674E-09	0.1369E-08
3	ISO-BUTANE	0.9675E-11	0.1077E-10	0.3134E-10	0.3191E-10	0.9544E-10
4	N-BUTANE	0.2878E-10	0.3634E-10	0.7147E-10	0.1277E-09	0.3628E-09
5	NEO-PENTANE	0.0	0.0	0.0	0.0	0.0
6	ISO-PENTANE	0.1229E-10	0.1339E-10	0.2378E-10	0.3593E-10	0.1347E-09
7	N-PENTANE	0.2149E-10	0.2514E-10	0.2593E-10	0.2670E-10	0.9427E-10
8	CYCLOPENTANE	0.0	0.0	0.5382E-11	0.9833E-11	0.3464E-10
9	2-METHYLPENTANE	0.0	0.0	0.1132E-11	0.6683E-11	0.8273E-11
10	3-METHYLPENTANE	0.0	0.0	0.0	0.1132E-11	0.8290E-11
11	N-HEXANE	0.3537E-10	0.4112E-10	0.5358E-10	0.5946E-10	0.1972E-09
12	METHYLCYCLOPENTANE	0.0	0.0	0.2786E-11	0.1518E-10	0.4473E-10
13	CYCLOHEXANE	0.4725E-11	0.1821E-10	0.2229E-10	0.4278E-10	0.1582E-09
14	2-METHYLHEXANE	0.0	0.0	0.0	0.0	0.0
15	3-METHYLHEXANE	0.0	0.0	0.0	0.0	0.0
16	N-HEPTANE	0.2164E-10	0.3041E-10	0.4078E-10	0.4232E-10	0.1194E-09
17	DIMETHYLCYCLOPENTANE	0.1403E-10	0.1719E-10	0.1964E-10	0.2091E-10	0.5587E-10
18	METHYLCYCLOHEXANE	0.1482E-09	0.1755E-09	0.3428E-09	0.3793E-09	0.8480E-09
19	CYCLICOLEFINS	0.1513E-10	0.3708E-10	0.9399E-10	0.9894E-10	0.3032E-09
20	DIMETHYLCYCLOHEXANE	0.3010E-09	0.3587E-09	0.4755E-09	0.7992E-09	0.1948E-09
21	C8+	0.0	0.0	0.0	0.0	0.0
22	PROPYLENE	0.2053E-11	0.2937E-10	0.1367E-10	0.5001E-11	0.0
23	BUTENES	0.0	0.3396E-11	0.2396E-11	0.2411E-11	0.0
24	PENTENES	0.4437E-11	0.1208E-10	0.1074E-10	0.1081E-10	0.0
25	BENZENE	0.1786E-10	0.2002E-10	0.2321E-10	0.2608E-10	0.3029E-10
26	TOLUENE	0.1431E-10	0.1604E-10	0.1860E-10	0.2090E-10	0.2428E-10
27	XYLENES	0.0	0.0	0.0	0.0	0.0
28	TETRALIN	0.1047E-11	0.1424E-11	0.1936E-11	0.2357E-11	0.2633E-11
29	NAPHTHALENE	0.5234E-12	0.7118E-12	0.9657E-12	0.1272E-11	0.1317E-11
30	METHYLNAPHTHALENES	0.1088E-11	0.1176E-11	0.1317E-11	0.1524E-11	0.1535E-11
31	DIMETHYLNAPHTHALENES	0.0	0.0	0.0	0.0	0.0
32	BIPHENYL	0.1452E-10	0.1552E-10	0.1577E-10	0.1627E-10	0.1652E-10
33	PHENANTHRENE	0.1007E-10	0.1259E-10	0.1511E-10	0.1826E-10	0.2014E-10

TABLE XX

RATE DATA AT 150 DEG C

PARTICLE SIZE : -53+38 MICRONS
REACTOR TEMP. : 150 - 155
INLET GAS COMPOSITION: 100.% HYDROGEN + 0.% HELIUM

REACTED HOURS-> / COMPONENTS		1	2	3	4	5
1	ETHANE	0.3267E-10	0.3798E-10	0.7028E-10	0.7038E-09	0.1574E-09
2	PROPANE	0.2674E-09	0.3170E-09	0.3924E-09	0.4693E-09	0.1857E-08
3	ISO-BUTANE	0.4736E-10	0.8137E-10	0.1003E-09	0.1974E-09	0.7474E-10
4	N-BUTANE	0.7742E-10	0.9639E-10	0.2098E-09	0.3088E-09	0.1129E-08
5	NEO-PENTANE	0.4323E-11	0.4654E-11	0.7198E-11	0.9454E-11	0.1818E-11
6	ISO-PENTANE	0.8697E-10	0.1228E-09	0.1297E-09	0.1615E-09	0.6087E-09
7	N-PENTANE	0.5143E-10	0.9369E-10	0.1508E-09	0.4526E-09	0.2169E-08
8	CYCLOPENTANE	0.6280E-11	0.1385E-10	0.1893E-10	0.1960E-10	0.2930E-10
9	2-METHYLPENTANE	0.1319E-10	0.2551E-10	0.6371E-10	0.8142E-10	0.2644E-09
10	3-METHYLPENTANE	0.1319E-10	0.2264E-10	0.6372E-10	0.7887E-10	0.2159E-09
11	N-HEXANE	0.2061E-10	0.1594E-09	0.1981E-09	0.2688E-09	0.1012E-08
12	METHYLCYCLOPENTANE	0.8572E-10	0.1568E-09	0.5229E-09	0.9334E-10	0.3122E-09
13	CYCLOHEXANE	0.8005E-10	0.1402E-09	0.3661E-09	0.1597E-08	0.5658E-08
14	2-METHYLHEXANE	0.0	0.0	0.0	0.9698E-11	0.2313E-10
15	3-METHYLHEXANE	0.0	0.0	0.0	0.1940E-10	0.5176E-10
16	N-HEPTANE	0.1940E-10	0.2751E-10	0.4407E-09	0.4780E-09	0.1655E-08
17	DIMETHYLCYCLOPENTANE	0.2044E-10	0.7081E-10	0.8204E-10	0.9579E-10	0.3998E-09
18	METHYLCYCLOHEXANE	0.7935E-10	0.1128E-09	0.1384E-09	0.1420E-08	0.3976E-09
19	CYCLICOLEFINS	0.4408E-10	0.7880E-10	0.1223E-09	0.1816E-09	0.4291E-09
20	DIMETHYLCYCLOHEXANE	0.1107E-08	0.1468E-08	0.3177E-08	0.3685E-08	0.1028E-07
21	C8+	0.0	0.0	0.0	0.1903E-10	0.1709E-09
22	PROPYLENE	0.4843E-10	0.3851E-10	0.2877E-09	0.2791E-10	0.0
23	BUTENES	0.1083E-10	0.2630E-10	0.3302E-10	0.1025E-10	0.0
24	PENTENES	0.6827E-10	0.1665E-09	0.2800E-10	0.8618E-11	0.0
25	BENZENE	0.1447E-08	0.1768E-08	0.1822E-08	0.2050E-08	0.2740E-08
26	TOLUENE	0.4723E-09	0.5582E-09	0.6012E-09	0.6985E-09	0.8511E-08
27	XYLENES	0.8627E-09	0.9490E-09	0.1035E-08	0.1104E-08	0.1132E-08
28	TETRALIN	0.0	0.0	0.0	0.0	0.0
29	NAPHTHALENE	0.5888E-11	0.6870E-11	0.8832E-11	0.9530E-11	0.1008E-10
30	METHYLNAPHTHALENES	0.6123E-11	0.8191E-11	0.1029E-10	0.1441E-10	0.1645E-10
31	DIMETHYLNAPHTHALENES	0.3048E-11	0.3969E-11	0.4757E-11	0.5940E-11	0.6892E-11
32	BIPHENYL	0.9386E-12	0.2816E-11	0.4618E-11	0.6170E-11	0.7647E-11
33	PHENANTHRENE	0.3053E-10	0.2786E-10	0.2625E-10	0.2314E-10	0.1535E-10

TABLE XXI

RATE DATA FOR -53+38 MICRON COAL AT 200 DEG C FOR 100% H2

PARTICLE SIZE : -53+38 MICRONS
REACTOR TEMP. : 200 - 206
INLET GAS COMPOSITION: 100.% HYDROGEN + 0.% HELIUM

REACTED HOURS-> / COMPONENTS		1	3	4	7	20
1	ETHANE	0.3562E-09	0.1302E-08	0.4543E-08	0.2318E-08	0.1714E-08
2	PROPANE	0.1300E-08	0.1144E-08	0.5095E-08	0.1577E-08	0.1900E-08
3	ISO-BUTANE	0.2497E-09	0.1058E-08	0.2042E-07	0.1304E-08	0.2554E-08
4	N-BUTANE	0.4938E-09	0.2087E-08	0.7502E-08	0.1785E-08	0.2327E-08
5	NEO-PENTANE	0.7037E-10	0.3150E-09	0.6246E-09	0.2033E-08	0.8316E-09
6	ISO-PENTANE	0.3051E-09	0.1885E-08	0.3168E-08	0.7446E-09	0.1560E-08
7	N-PENTANE	0.5717E-09	0.3403E-08	0.5153E-08	0.1629E-08	0.2346E-08
8	CYCLOPENTANE	0.1487E-08	0.3980E-08	0.1897E-07	0.2923E-08	0.3564E-08
9	2-METHYLPENTANE	0.2311E-09	0.7485E-09	0.1103E-08	0.2003E-09	0.5125E-09
10	3-METHYLPENTANE	0.3476E-10	0.7715E-09	0.9680E-09	0.1726E-09	0.4687E-09
11	N-HEXANE	0.9122E-09	0.2518E-08	0.3576E-08	0.6068E-09	0.1605E-08
12	METHYLCYCLOPENTANE	0.4373E-08	0.1693E-07	0.2045E-07	0.1154E-07	0.8766E-08
13	CYCLOHEXANE	0.2577E-08	0.6278E-08	0.8321E-08	0.1249E-08	0.2986E-08
14	2-METHYLHEXANE	0.3107E-10	0.6729E-10	0.1265E-09	0.8791E-10	0.7148E-10
15	3-METHYLHEXANE	0.2560E-09	0.4034E-09	0.6712E-09	0.2184E-09	0.2227E-09
16	N-HEPTANE	0.3650E-09	0.5961E-09	0.9554E-09	0.2700E-09	0.3624E-09
17	DIMETHYLCYCLOPENTANE	0.3159E-08	0.5664E-08	0.8010E-08	0.9249E-09	0.2352E-08
18	METHYLCYCLOHEXANE	0.4037E-08	0.6810E-08	0.1011E-07	0.1753E-08	0.3840E-08
19	CYCLICOLEFINS	0.2831E-08	0.1823E-08	0.3888E-08	0.7501E-09	0.2658E-08
20	DIMETHYLCYCLOHEXANE	0.3011E-09	0.2726E-08	0.4350E-08	0.6394E-09	0.1217E-08
21	C8+	0.1136E-08	0.9932E-09	0.2778E-08	0.4673E-09	0.7685E-09
22	PROPYLENE	0.0	0.0	0.0	0.0	0.0
23	BUTENES	0.0	0.0	0.0	0.0	0.0
24	PENTENES	0.0	0.0	0.0	0.0	0.0
25	BENZENE	0.7381E-09	0.6957E-09	0.8075E-09	0.3875E-09	0.7034E-09
26	TOLUENE	0.1252E-09	0.2034E-09	0.1276E-09	0.6393E-10	0.1504E-09
27	XYLENES	0.2516E-09	0.3996E-09	0.2608E-09	0.1339E-09	0.2870E-09
28	TETRALIN	0.8178E-11	0.8416E-11	0.8963E-11	0.4551E-11	0.8127E-11
29	NAPHTHALENE	0.4498E-11	0.5200E-11	0.5703E-11	0.3766E-11	0.5553E-11
30	METHYLNAPHTHALENES	0.3402E-11	0.4855E-11	0.3811E-11	0.2325E-12	0.3080E-11
31	DIMETHYLNAPHTHALENES	0.1240E-11	0.2611E-11	0.1321E-11	0.6281E-12	0.1757E-11
32	BIPHENYL	0.1564E-11	0.2470E-11	0.2029E-11	0.1091E-11	0.2156E-11
33	PHENANTHRENE	0.9836E-10	0.1072E-09	0.1249E-09	0.6750E-11	0.8070E-10
34	PYRENE	0.0	0.0	0.0	0.0	0.0
35	FLUORANTHENE	0.8853E-11	0.9981E-11	0.1019E-10	0.6120E-11	0.9572E-11
36	BANZANTHRACENE	0.2164E-10	0.1739E-10	0.1267E-10	0.5228E-11	0.1710E-10
37	BENZOPYRENE	0.8853E-11	0.6212E-11	0.6703E-11	0.3099E-11	0.6590E-11

That the latter could be true is indicated by the rate of production of phenanthrene in the order 200 deg C>150 deg C>100 deg C and it should be remembered that the products of higher molecular weight such as pyrene, fluoranthene, benzanthracene and benzopyrene were not at all found among the liquid products at 100 and 150 deg C runs. Furthermore, the rate of formation of biphenyl was found to be larger at 100 deg C than either at 150 deg C or 200 deg C. This confirms the idea that at low temperature runs, phenanthrene, which was the highest molecular weight product found, undergoes hydrogenation at the middle ring the cracking of which will account for the formation of biphenyl.

In all these plots, the point at 20 hour run was not found to lie within the bounds of a smooth curve. Whether this is due to the minimal handling loss of products as a result of uninterrupted nature of the run or due to the actual change of nature of coal with conversion is not known.

Finally, mention has to be made of the presence of methylcyclohexene and olefins among the gaseous products. The survival of these products amidst the strong reducing environment is, indeed, surprising. It is possible that the olefins that are formed in the top of the reactor are swept away by the carrier gas before they could further react to produce saturated hydrocarbons.

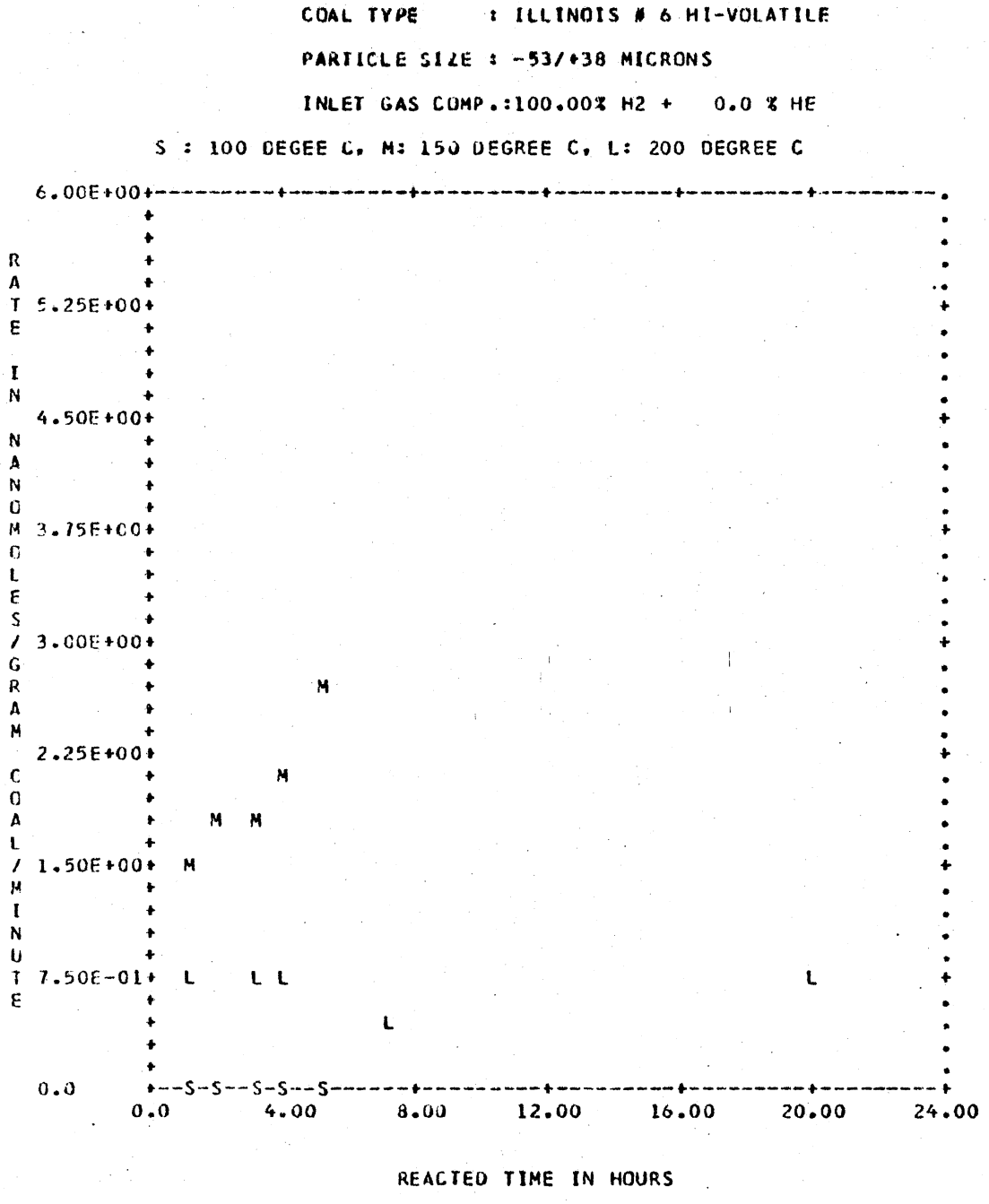

Figure 56. Effect of Temperature on the Rate of Formation of Benzene

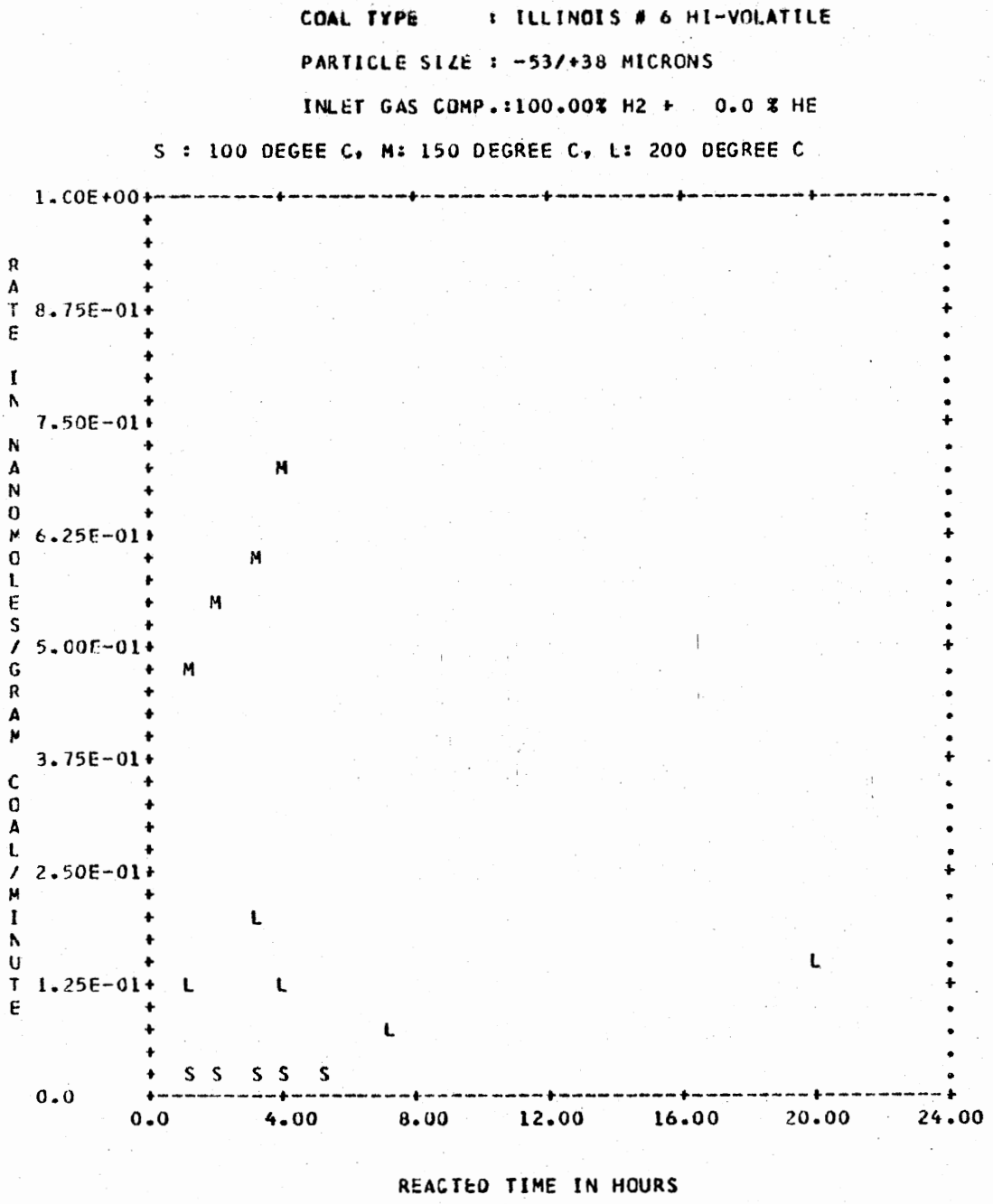

Figure 57. Effect of Temperature on the Rate of Formation of Toluene

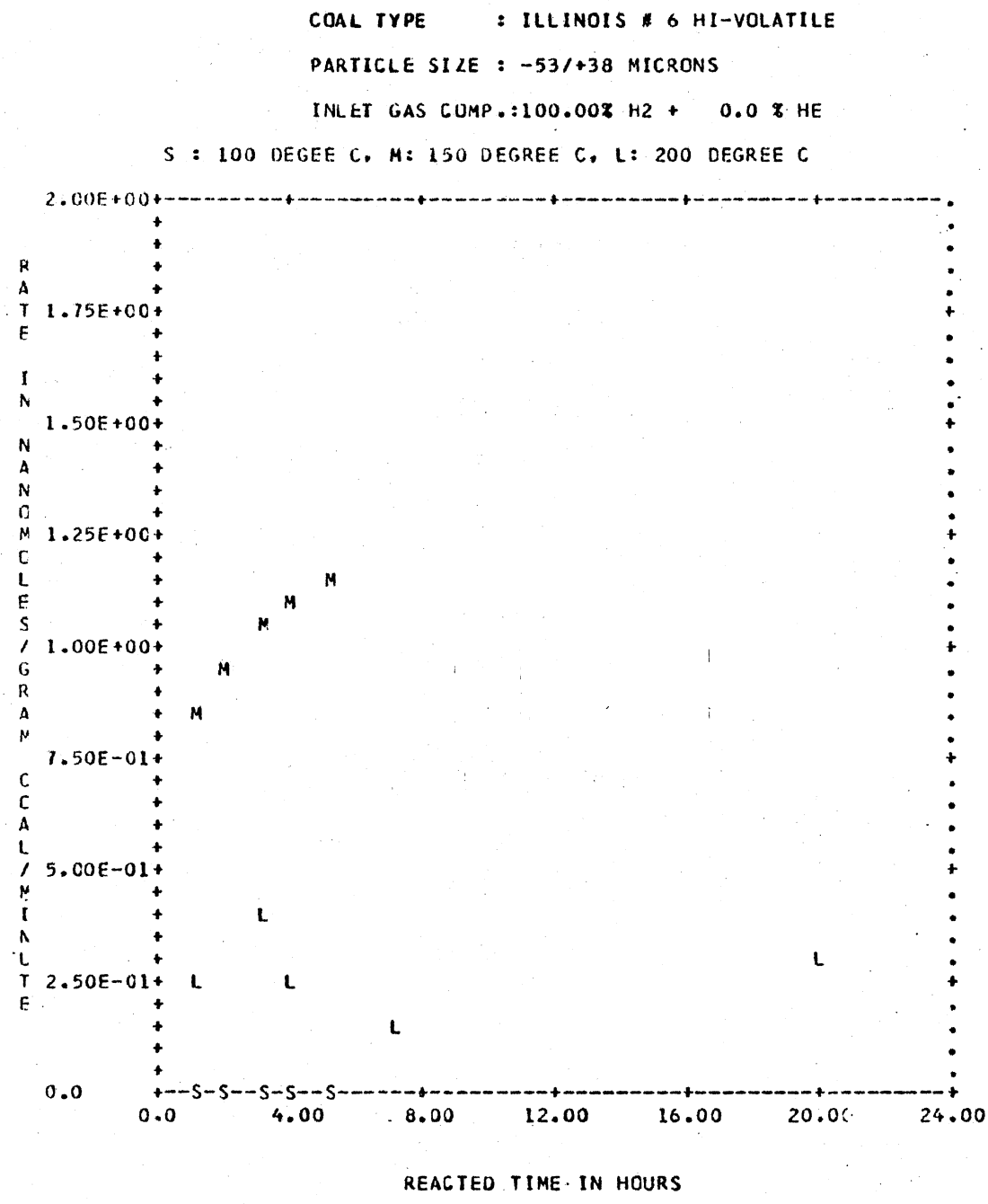

Figure 58. Effect of Temperature on the Rate of Formation of Xylenes

In principle, the effect of temperature on the overall rate of a photochemical reaction will be determined by the activation energies of all the important steps and the effect of temperature on I(a), light absorbed. However, the energy added to a molecule at a given wavelength by increasing the temperatures is small compared to the energy accompanying the absorption of a quantum of light. Hence, if the proper absorptivity is used, the temperature should not have a significant effect on the primary process. Furthermore, with respect to absorptivity variations, Noyes (109) noted that the integral

$$\int_{\lambda_1}^{\lambda_2} I(a)\, d\lambda$$

is nearly independent of temperature. i.e., the total absorption still remains same even though absorption band could broaden due to temperature changes; however, a decrease in absorption maximum can be expected. Hence, H atom concentration produced in a reactor via mercury photosensitization can be exptected to be independent of temperature.

Effect of Particle size

The percentage carbon conversion and the total yield would be independent of the particle size of coal used, if the reaction was chemically controlled. On the other hand, if the reaction was controlled by the available external surface area, then the conversion would be inversely proportional to the particle size. That the latter is true in the

photohydrogen atom cracking of coal dust is proved by the data presented in Table XXII. The particle sizes used were: (i) -90+53 micron, (ii) -53+38 micron and (iii) -38+25 micron. The -38+25 micron coal dust was obtained by sieving the -38 micron coal in an Alpine vacuum siever.

The data in Table XXII provide satisfactory evidence to show that a decrease in particle size is accompanied with an increase in the extent of conversion of coal to gaseous and liquid products. However, a serious problem of deposition of coal on the walls of the quartz reactor was noticed in the runs involving -38+25 micron coal dust. The tendency of agglomeration was restricted by maintaining separation between the coal particles by mixing coal with an equal amount of glass powder, of roughly the same size as coal. However, the separation between coal particles and the reactor walls was, evidently, not achieved in these runs. On the other hand, no coal was found to stick to the reactor wall even after 20 hours of irradiation in the case of a -53+38 micron coal. The deposition of coal on the reactor walls can produce two side effects: (i) attenuation of u.v. photons which, otherwise, would have entered the quartz reactor and (ii) pyrolysis of coal on the walls of the reactor. If, serious enough, the latter could lead to the formation of tars on the walls of the reactor which can drastically reduce the entry of u.v. photons inside the reactor.

TABLE XXII

EFFECT OF PARTICLE SIZE ON PROCESS EFFICIENCY

PARTICLE SIZE : -38+25 MICRONS
REACTOR TEMP. : 200 - 202
INLET GAS COMPOSITION: 100.% HYDROGEN + 0.% HELIUM

TIME	YIELD	CONVERSION	EFFICIENCY	H ATOMS
1	0.2731E-05	0.2021E-01	0.3807E-02	263.
2	0.8035E-05	0.6563E-01	0.5602E-02	179.
3	0.1232E-04	0.1063E+00	0.5725E-02	175.
4	0.1343E-04	0.1170E+00	0.4699E-02	213.
7	0.1502E-04	0.1317E+00	0.2992E-02	334.

PARTICLE SIZE : -53+38 MICRONS
REACTOR TEMP. : 200 - 206
INLET GAS COMPOSITION: 100.% HYDROGEN + 0.% HELIUM

TIME	YIELD	CONVERSION	EFFICIENCY	H ATOMS
1	0.1581E-05	0.1392E-01	0.2939E-02	341.
3	0.9137E-05	0.7802E-01	0.5662E-02	177.
4	0.1234E-04	0.9869E-01	0.5734E-02	176.
7	0.1655E-04	0.1337E+00	0.4394E-02	228.
20	0.2710E-04	0.2161E+00	0.2518E-02	397.

PARTICLE SIZE : -90+53 MICRONS
REACTOR TEMP. : 198 - 206
INLET GAS COMPOSITION: 100.% HYDROGEN + 0.% HELIUM

TIME	YIELD	CONVERSION	EFFICIENCY	H ATOMS
1	0.1269E-05	0.9547E-02	0.2359E-02	426.
2	0.3545E-05	0.2958E-01	0.3295E-02	308.
3	0.4955E-05	0.4237E-01	0.3071E-02	328.
4	0.6122E-05	0.5168E-01	0.2845E-02	351.
7	0.7364E-05	0.6181E-01	0.1955E-02	511.

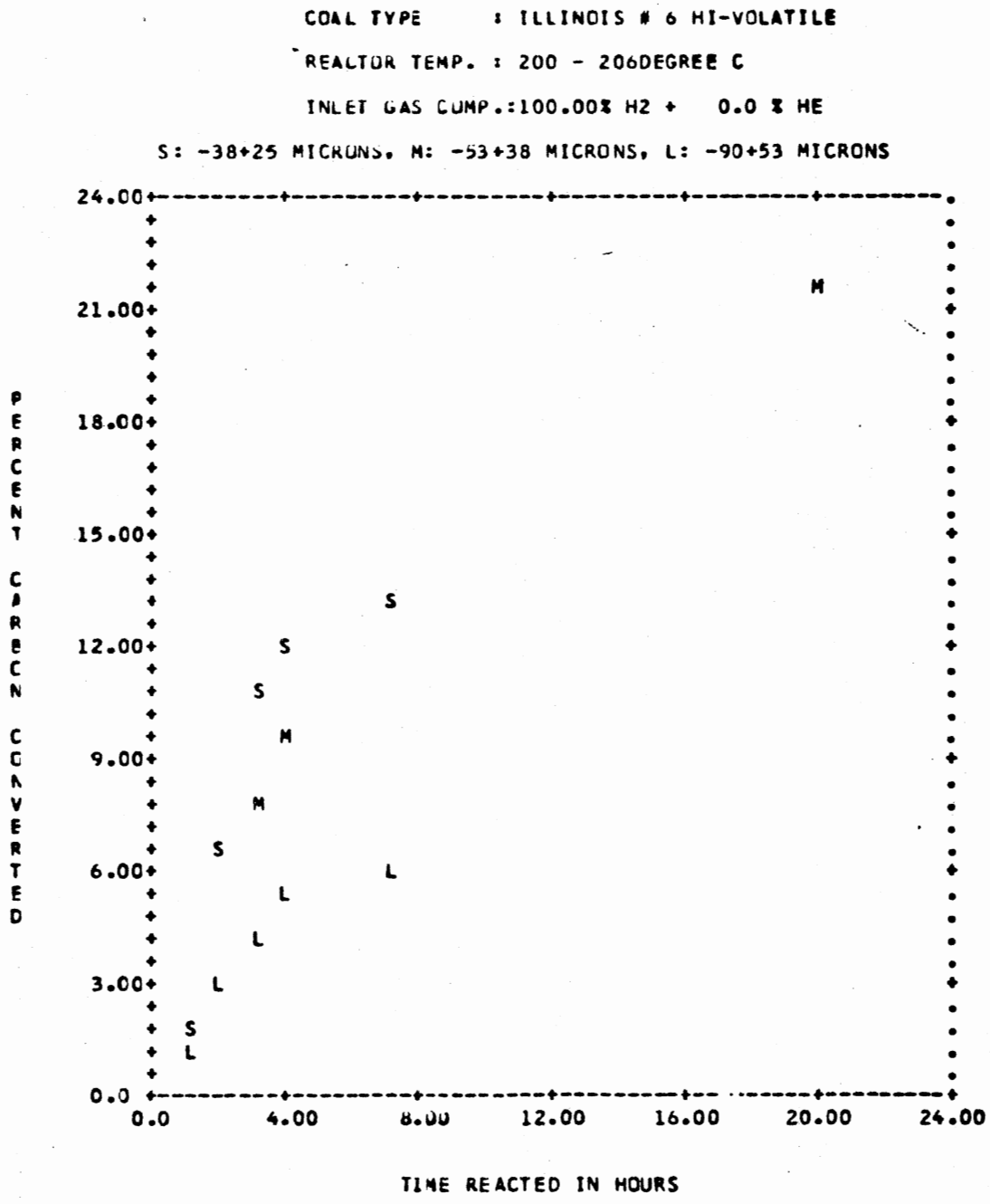

Figure 59. Effect of Particle Size on Percent Conversion

Listed in Table XXIII, XVII and XXIV are the yields of each product Due to the uncertainities arising out of the deposition of coal on the walls of the reactor the results must be considered only qualitative. In any case, there is no doubt that the reduction in particle size of coal results in increased conversion and also increased yield of aroamtics. A more quantitative statement, than this, unfortunately, can not be made at this time.

Despite the deposition of coal on the walls of the reactor, the plots for the rates of production of phenanthrene, pyrene and fluoranthene were (Figures 60, 61 and 62) were consistent. The rates were inversely proportional to the particle size of the coal dust. Furthermore, it could be seen from Figures 60 and 62 that the maxima for the smaller size coals occur at longer times than the others. This proves the increase in the conversion with increase in the surface area.

Effect of Inlet Gas Composition

A series of experiments were carried out with hydrogen composition in the inlet gas mixture varying from 2% to 100%. The gas mixture was made up with helium, an inert gas. The certified gases were purchased from Matheson Gas Company and they had a certified purity of 99.9% and our own analysis did not find any detectable hydrocarbon impurities. Due to the high costs of certified gas mixtures, the experi-

TABLE XXIII

MOLAR YIELD OF PRODUCTS FOR -38+25 MICRON COAL

PARTICLE SIZE : -38+25 MICRONS
REACTOR TEMP. : 200 - 202
INLET GAS COMPOSITION: 100.% HYDROGEN + 0.% HELIUM

REACTED HOURS->		1	2	3	4	7
COMPONENTS| V					
1	ETHANE	0.1087E-06	0.1937E-06	0.2845E-06	0.2852E-06	0.2860E-06
2	PROPANE	0.4888E-06	0.8072E-06	0.8182E-06	0.8194E-06	0.8209E-06
3	ISO-BUTANE	0.9880E-07	0.3061E-06	0.3887E-06	0.3944E-06	0.4026E-06
4	N-BUTANE	0.2190E-06	0.4160E-06	0.4479E-06	0.5045E-06	0.5685E-06
5	NEO-PENTANE	0.5028E-08	0.9132E-08	0.9132E-08	0.9132E-08	0.9132E-08
6	ISO-PENTANE	0.1583E-06	0.4533E-06	0.5755E-06	0.5996E-06	0.6353E-06
7	N-PENTANE	0.1212E-06	0.4499E-06	0.5580E-06	0.5931E-06	0.6126E-06
8	CYCLOPENTANE	0.1844E-07	0.2658E-06	0.2994E-06	0.3172E-06	0.3387E-06
9	2-METHYLPENTANE	0.2878E-07	0.1161E-06	0.1547E-06	0.1636E-06	0.1728E-06
10	3-METHYLPENTANE	0.5653E-07	0.5946E-07	0.7414E-07	0.8392E-07	0.1051E-06
11	N-HEXANE	0.5122E-07	0.1624E-06	0.2115E-06	0.2362E-06	0.2998E-06
12	METHYLCYCLOPENTANE	0.2188E-06	0.8610E-06	0.1101E-05	0.1247E-05	0.1470E-05
13	CYCLOHEXANE	0.1482E-06	0.4658E-06	0.9288E-06	0.1108E-05	0.1305E-05
14	2-METHYLHEXANE	0.5575E-08	0.2919E-07	0.3312E-07	0.3358E-07	0.3386E-07
15	3-METHYLHEXANE	0.5068E-08	0.2483E-07	0.2483E-07	0.2483E-07	0.2483E-07
16	N-HEPTANE	0.1521E-07	0.4578E-07	0.4578E-07	0.4578E-07	0.4578E-07
17	DIMETHYLCYCLOPENTANE	0.6410E-07	0.3166E-06	0.5523E-06	0.7007E-06	0.9211E-06
18	METHYLCYCLOHEXANE	0.5529E-07	0.4110E-06	0.1208E-05	0.1329E-05	0.1481E-05
19	CYCLICOLEFINS	0.2304E-07	0.8547E-07	0.1634E-06	0.1811E-06	0.1822E-06
20	DIMETHYLCYCLOHEXANE	0.0	0.4167E-06	0.7259E-06	0.7793E-06	0.8012E-06
21	C8+	0.0	0.2841E-06	0.6707E-06	0.7011E-06	0.7329E-06
22	ETHYLENE	0.4347E-08	0.1042E-07	0.2682E-07	0.3055E-07	0.3232E-07
23	PROPYLENE	0.9565E-07	0.1739E-06	0.2447E-06	0.2786E-06	0.3079E-06
24	BUTENES	0.3520E-07	0.1224E-06	0.1348E-06	0.1383E-06	0.1444E-06
25	BENZENE	0.1113E-06	0.2500E-06	0.4175E-06	0.5287E-06	0.7283E-06
26	TOLUENE	0.1706E-06	0.4222E-06	0.7335E-06	0.7589E-06	0.7883E-06
27	XYLENES	0.3284E-06	0.7965E-06	0.1358E-05	0.1404E-05	0.1471E-05
28	TETRALIN	0.8714E-09	0.2186E-08	0.3761E-08	0.5114E-08	0.7079E-08
29	NAPHTHALENE	0.3401E-08	0.9983E-08	0.1967E-07	0.3048E-07	0.3929E-07
30	METHYLNAPHTHALENES	0.8247E-09	0.2150E-08	0.4594E-08	0.7354E-08	0.1128E-07
31	DIMETHYLNAPHTHALENES	0.3017E-09	0.6649E-09	0.1394E-08	0.2033E-08	0.3307E-08
32	BIPHENYL	0.1285E-08	0.2649E-08	0.4179E-08	0.5224E-08	0.6686E-08
33	PHENANTHRENE	0.1825E-07	0.3943E-07	0.6656E-07	0.9679E-07	0.1717E-06
34	PYRENE	0.3150E-09	0.6912E-09	0.1150E-08	0.6238E-08	0.1454E-07
35	FLUORANTHENE	0.2834E-08	0.6454E-08	0.1120E-07	0.1687E-07	0.2808E-07
36	BANZANTHRACENE	0.3283E-08	0.6266E-08	0.7851E-08	0.8455E-08	0.1043E-07
37	BENZOPYRENE	0.3537E-08	0.6123E-08	0.7643E-08	0.8860E-08	0.1096E-07

TABLE XXIV

MOLAR YIELD OF PRODUCTS FOR -90+53 MICRON COAL

PARTICLE SIZE : -90+53 MICRONS
REACTOR TEMP. : 198 - 206
INLET GAS COMPOSITION: 100.% HYDROGEN + 0.% HELIUM

REACTED HOURS->		1	2	3	4	7
COMPONENTS↓						
1	ETHANE	0.3126E-07	0.1116E-06	0.1334E-06	0.2891E-06	0.3322E-06
2	PROPANE	0.1594E-06	0.2335E-06	0.2733E-06	0.5698E-06	0.5921E-06
3	ISO-BUTANE	0.1082E-06	0.1937E-06	0.2403E-06	0.6579E-06	0.8154E-06
4	N-BUTANE	0.2360E-06	0.3826E-06	0.5143E-06	0.1494E-05	0.1682E-05
5	NEO-PENTANE	0.1982E-07	0.7384E-07	0.7856E-07	0.1775E-06	0.1830E-06
6	ISO-PENTANE	0.5122E-07	0.1297E-06	0.1580E-06	0.4003E-06	0.4531E-06
7	N-PENTANE	0.7076E-07	0.1242E-06	0.1659E-06	0.3946E-06	0.4476E-06
8	CYCLOPENTANE	0.3835E-07	0.1014E-06	0.1394E-06	0.3344E-06	0.3754E-06
9	2-METHYLPENTANE	0.1906E-07	0.4413E-07	0.5923E-07	0.1204E-06	0.1305E-06
10	3-METHYLPENTANE	0.1867E-07	0.9892E-07	0.1142E-06	0.2385E-06	0.2401E-06
11	N-HEXANE	0.2827E-07	0.1296E-06	0.1722E-06	0.4138E-06	0.4653E-06
12	METHYLCYCLOPENTANE	0.9267E-07	0.3045E-06	0.4102E-06	0.9326E-06	0.9643E-06
13	CYCLOHEXANE	0.3096E-07	0.1248E-06	0.2007E-06	0.4954E-06	0.5043E-06
14	2-METHYLHEXANE	0.3185E-08	0.3623E-07	0.3986E-07	0.8109E-07	0.8586E-07
15	3-METHYLHEXANE	0.8602E-08	0.7339E-07	0.8695E-07	0.1753E-06	0.1800E-06
16	N-HEPTANE	0.8767E-08	0.1129E-06	0.1335E-06	0.2688E-06	0.2800E-06
17	DIMETHYLCYCLOPENTANE	0.4919E-07	0.1559E-06	0.2299E-06	0.4685E-06	0.5201E-06
18	METHYLCYCLOHEXANE	0.2513E-07	0.1187E-06	0.2540E-06	0.5309E-06	0.6421E-06
19	CYCLICOLEFINS	0.9210E-08	0.6010E-07	0.1245E-06	0.3275E-06	0.3573E-06
20	DIMETHYLCYCLOHEXANE	0.1642E-06	0.5954E-06	0.9682E-06	0.1986E-05	0.2150E-05
21	C8+	0.6515E-07	0.2702E-06	0.3373E-06	0.7368E-06	0.7454E-06
22	ETHYLENE	0.0	0.0	0.0	0.0	0.0
23	PROPYLENE	0.0	0.0	0.0	0.0	0.0
24	BUTENES	0.0	0.0	0.0	0.0	0.0
25	BENZENE	0.2603E-07	0.5727E-07	0.9789E-07	0.1547E-06	0.2359E-06
26	TOLUENE	0.9018E-08	0.2074E-07	0.3715E-07	0.6013E-07	0.9690E-07
27	XYLENES	0.1510E-07	0.6305E-07	0.7869E-07	0.1028E-06	0.3267E-06
28	TETRALIN	0.4907E-09	0.1501E-08	0.2038E-08	0.2858E-08	0.9196E-08
29	NAPHTHALENE	0.2699E-09	0.8938E-09	0.1236E-08	0.1914E-08	0.6245E-08
30	METHYLNAPHTHALENES	0.2041E-09	0.7867E-09	0.1015E-08	0.1057E-08	0.3460E-08
31	DIMETHYLNAPHTHALENES	0.7441E-10	0.3877E-09	0.4670E-09	0.5800E-09	0.1950E-08
32	BIPHENYL	0.9386E-10	0.3903E-09	0.5120E-09	0.7084E-09	0.2390E-08
33	PHENANTHRENE	0.5902E-08	0.1876E-07	0.2626E-07	0.2748E-07	0.9042E-07
34	PYRENE	0.0	0.0	0.0	0.0	0.0
35	FLUORANTHENE	0.5312E-09	0.1729E-08	0.2340E-08	0.3442E-08	0.1091E-07
36	BANZANTHRACENE	0.1298E-08	0.3386E-08	0.4146E-08	0.5087E-08	0.1843E-07
37	BENZOPYRENE	0.5312E-09	0.1277E-08	0.1679E-08	0.2237E-08	0.7377E-08

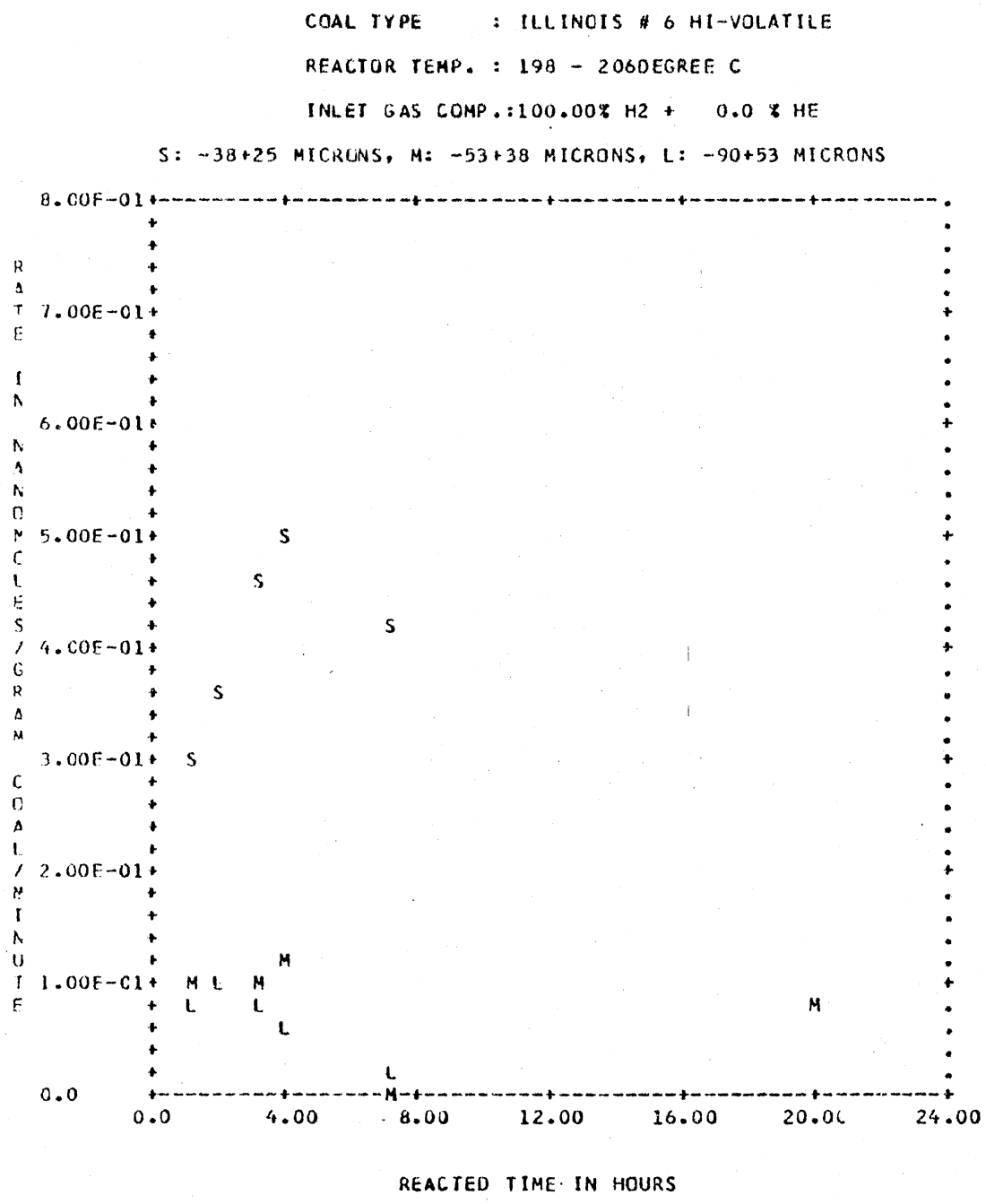

Figure 60. Effect of Particle Size on the Rate of Formation of Phenanthrene

ments with 2% and 10% hydrogen were carried out for a maximum of 4 hours only.

The effects of inlet gas composition on the total yield of products and, percent carbon conversion, product efficiency per H atom are shown in Table XXV. The percentage carbon conversion data for various inlet gas gas compositions are plotted as function of time in Figure 63.

Percentage carbon conversion was inversely proportional to the inlet gas composition. 90 to 98% reduction of hydrogen in the inlet gas mixture had a dramatic effect on the product yield and carbon conversion. For example, when the inlet gas mixture consisted of 2% hydrogen in it, the molar product yield was almost double compared to that at 100% hydrogen for an one-hour period. This is evident from Table XXV.

The increased yield at lower hydrogen input can be explained by assuming higher H atom concentration. Molecular hydrogen is a more effective third body for H atom recombination than helium. Since the rate of production of H atoms is same, and helium is less effective in the removal of H atoms, it follows that the steady state H atom concentration is higher in the presence of helium than in the presence of molecular hydrogen. At higher partial pressure of hydrogen, the recombination of H atoms seems to be favored over the hydrocarbon formation. Similar results have been reported in the literature before. In their study

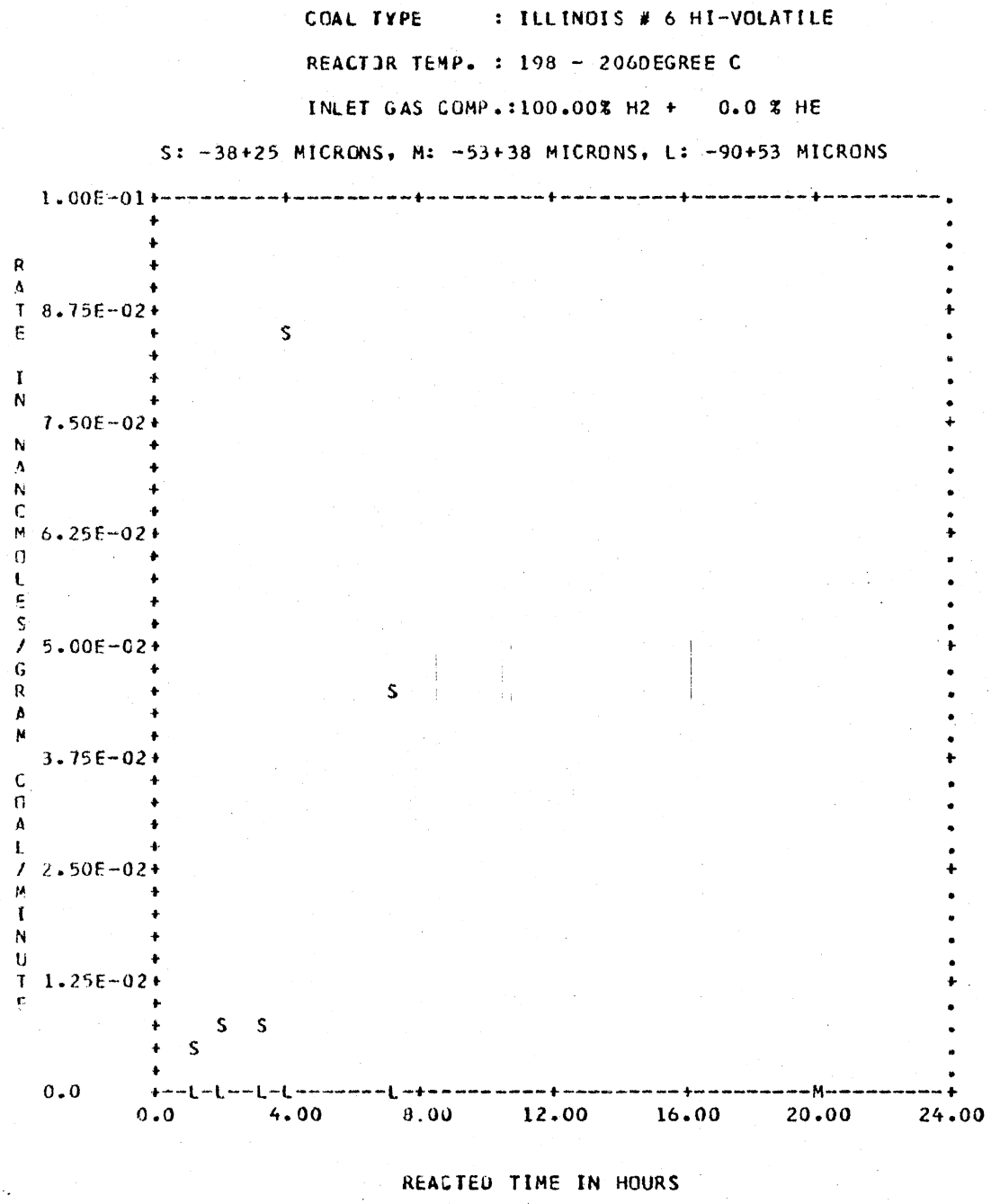

Figure 61. Effect of Particle Size on the Rate of Formation of Pyrene

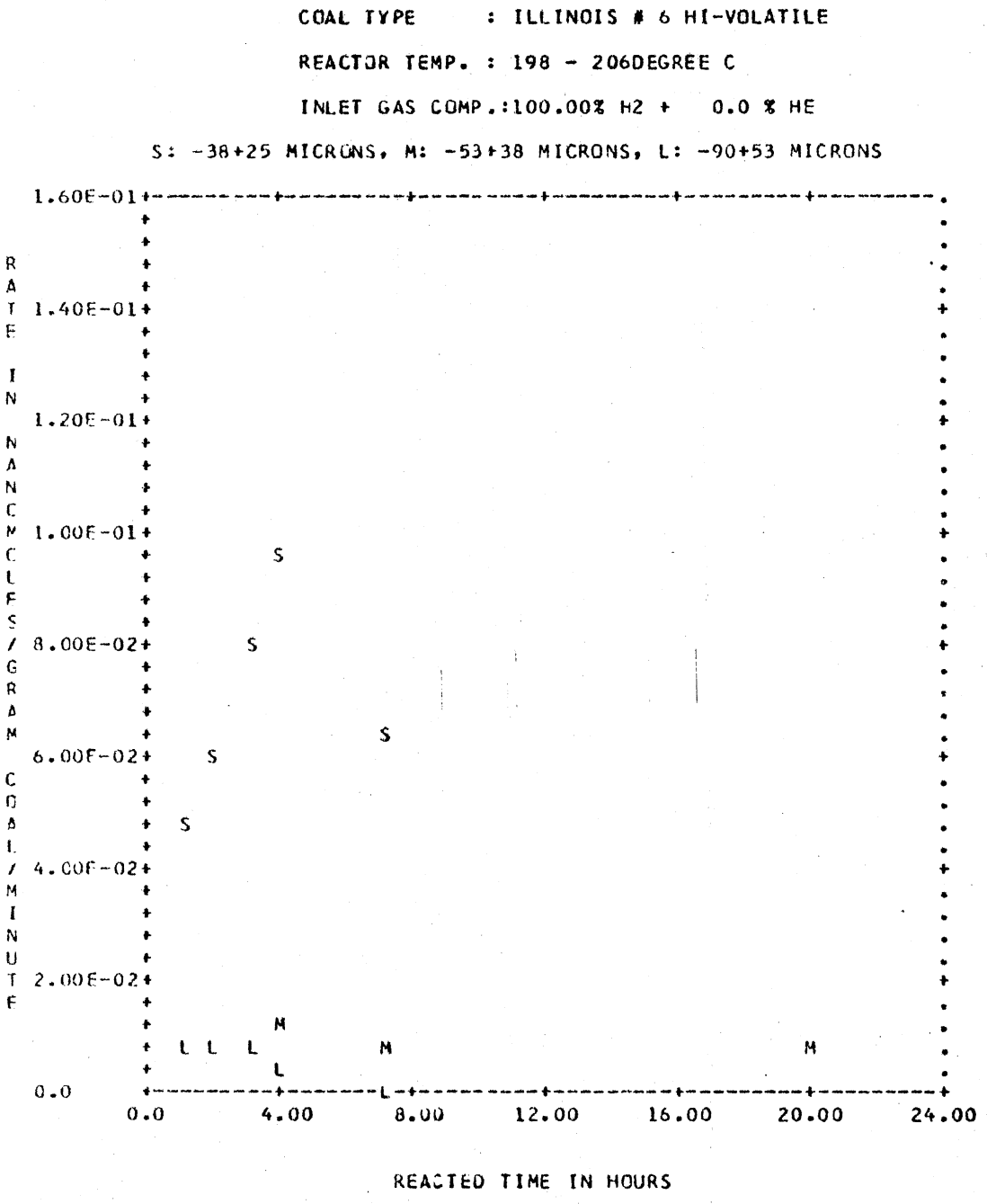

Figure 62. Effect of Particle Size on the Rate of Formation of Fluoranthene

of kinetics of carbon gasification by atomic hydrogen Coulon et al. (111, 112) found the rate to be independent of molecular hydrogen pressure upto 700 deg C and under 1 torr and above this pressure, the rate was strongly dependent on the molecular

hydrogen pressure. Snelson, (30) in his recent investigation of the reaction between discharge generated hydrogen atoms and coal (110) found that the molar yield of products was inversely proportional to the hydrogen feed rate. However, it must be noted that the conditions for their experiments were totally different from the ones under this investigation. Nonetheless, their observations are significant.

The rate data obtained as a function of percentage of hydrogen in the inlet gas mixture revealed several important points. The rates of formation of each product for reaction mixtures consisting of 2% , 10% and 100% hydrogen are given in Tables XXVIII, XXIX and XXI respectively. The rates of all saturated, normal and straight chain, aliphatics were inversely proportional to the percentage of hydrogen in the inlet gas mixture. Even though no discrete maxima were found in the plots of the rates of formation of these products within the reaction times studied, there are indications that the maxima occur sooner with decrease in the percentage of hydrogen in the inlet gas composition. An example of this is given in Figure 64 in which the rates of formation of iso-pentane are plotted against time for dif-

TABLE XXV

EFFECT OF INLET GAS COMPOSITION ON THE TOTAL YIELD AND PERCENT CONVERSION

PARTICLE SIZE : -53+38 MICRONS
REACTOR TEMP. : 196 - 203
INLET GAS COMPOSITION: 2.% HYDROGEN + 98.% HELIUM

TIME	YIELD	CONVERSION
1	0.2800E-05	0.2470E-01
2	0.7425E-05	0.6397E-01
3	0.1374E-04	0.1173E+00
4	0.2137E-04	0.1802E+00

PARTICLE SIZE : -53+38 MICRONS
REACTOR TEMP. : 198 - 203
INLET GAS COMPOSITION: 10.% HYDROGEN + 90.% HELIUM

TIME	YIELD	CONVERSION
1	0.2279E-05	0.1965E-01
2	0.5496E-05	0.4723E-01
3	0.1016E-04	0.8631E-01
4	0.1656E-04	0.1390E+00

PARTICLE SIZE : -53+38 MICRONS
REACTOR TEMP. : 200 - 206
INLET GAS COMPOSITION: 100.% HYDROGEN + 0.% HELIUM

TIME	YIELD	CONVERSION	EFFICIENCY	H ATOMS
1	0.1581E-05	0.1392E-01	0.2939E-02	341.
3	0.9137E-05	0.7802E-01	0.5662E-02	177.
4	0.1234E-04	0.9869E-01	0.5734E-02	176.
7	0.1655E-04	0.1337E+00	0.4394E-02	228.
20	0.2710E-04	0.2161E+00	0.2518E-02	397.

ferent initet gas compositions. The point at (0,0) in the plots involving inlet gas composition as a variable is an artifact of the plot-routine and does not represent a true datum.

On the other hand, the rates of formation of cyclic hydrocarbons were directly proportional to the percentage of hydrogen in the inlet gas mixture. Even though some scattering was found with respect to the order, which would not be unexpected in the case of a complicated reaction producing more than three dozen products, the change was definite as could be seen from Figures 65 through 69. This indicates that ring opening and ring cracking reactions become very pronounced, which, perforce, also involve consumption of more hydrogen atoms, with decrease in the hydrogen content of the reacting gas mixture. The implication of this is that the number of wasteful collisons of H atoms between themselves or with the walls of the reactor are less in the case of leaner mixtures.

If this is the case, then we can expect an increase in the rate of production of product presursors with decrease of hydrogen content in the inlet gas mixture. This was found to be absolutely true in the case of all aromatic precursors. The plots of rates of formation of all aromatic products as function of time are presented in Figures 70 through 82. In the cases where discrete maximum occurred, it was found to occur at 2 hours for mixtures consisting of

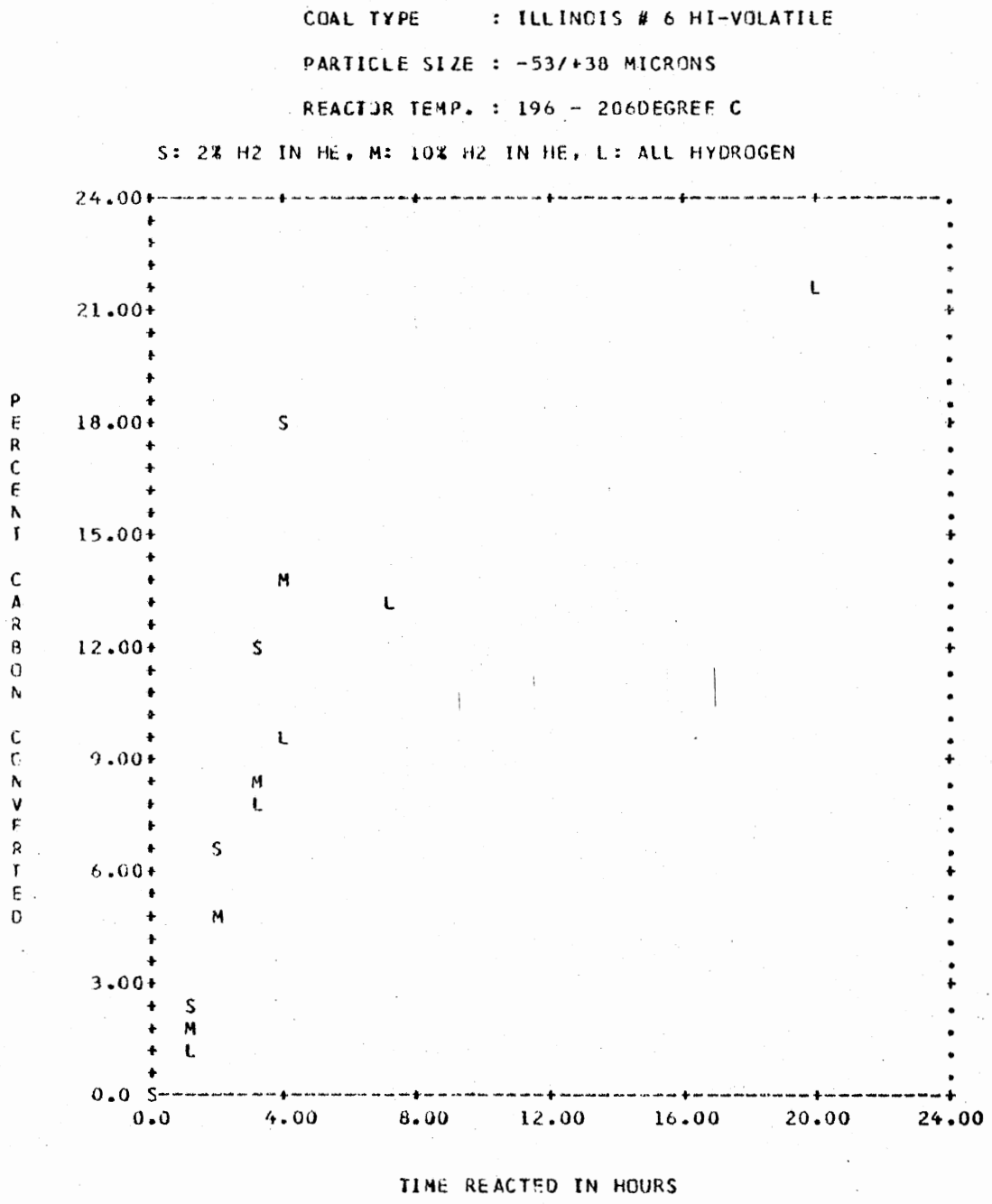

Figure 63. Effect of Inlet Gas Composition on the Percent Conversion X 100

TABLE XXVI

MOLAR YIELDS OF PRODUCTS WITH 2% H2 + 98% HE GAS MIXTURE

PARTICLE SIZE : -53+38 MICRONS
REACTOR TEMP. : 196 - 203
INLET GAS COMPOSITION: 2.% HYDROGEN + 98.% HELIUM

REACTED HOURS->		1	2	3	4
COMPONENTS! V					
1	ETHANE	0.6240E-07	0.3980E-06	0.9319E-06	0.1569E-05
2	PROPANE	0.1469E-06	0.3813E-06	0.7075E-06	0.1203E-05
3	ISO-BUTANE	0.1335E-06	0.2709E-06	0.4054E-06	0.5608E-06
4	N-BUTANE	0.1841E-06	0.4141E-06	0.7768E-06	0.1369E-05
5	NEO-PENTANE	0.2075E-07	0.6739E-07	0.1434E-06	0.2201E-06
6	ISO-PENTANE	0.1151E-06	0.2994E-06	0.6017E-06	0.1146E-05
7	N-PENTANE	0.2037E-06	0.4282E-06	0.7162E-06	0.1063E-05
8	CYCLOPENTANE	0.9490E-07	0.2425E-06	0.4769E-06	0.7530E-06
9	2-METHYLPENTANE	0.3058E-07	0.8643E-07	0.1706E-06	0.2858E-06
10	3-METHYLPENTANE	0.2198E-07	0.6602E-07	0.1349E-06	0.2112E-06
11	N-HEXANE	0.7286E-07	0.2950E-06	0.6240E-06	0.1055E-05
12	METHYLCYCLOPENTANE	0.1138E-06	0.2912E-06	0.5049E-06	0.7515E-06
13	CYCLOHEXANE	0.1330E-06	0.3185E-06	0.5490E-06	0.8004E-06
14	2-METHYLHEXANE	0.7305E-08	0.2247E-07	0.4043E-07	0.7064E-07
15	3-METHYLHEXANE	0.6743E-08	0.1938E-07	0.3434E-07	0.6240E-07
16	N-HEPTANE	0.1196E-06	0.4018E-06	0.7808E-06	0.1159E-05
17	DIMETHYLCYCLOPENTANE	0.1396E-06	0.3612E-06	0.5985E-06	0.8848E-06
18	METHYLCYCLOHEXANE	0.1838E-06	0.4427E-06	0.7624E-06	0.1234E-05
19	CYCLICOLEFINS	0.4598E-07	0.1412E-06	0.2561E-06	0.4131E-06
20	DIMETHYLCYCLOHEXANE	0.3038E-06	0.6581E-06	0.1478E-05	0.2443E-05
21	C8+	0.2450E-06	0.5503E-06	0.1115E-05	0.1778E-05
22	PROPYLENE	0.3466E-07	0.6851E-07	0.8669E-07	0.1045E-06
23	BUTENES	0.2504E-08	0.6216E-08	0.1920E-07	0.3167E-07
24	PENTENES	0.2807E-08	0.7800E-08	0.1861E-07	0.2820E-07
25	BENZENE	0.1257E-06	0.4973E-06	0.7830E-06	0.8688E-06
26	TOLUENE	0.1832E-07	0.5130E-07	0.7787E-07	0.9619E-07
27	XYLENES	0.1288E-06	0.4049E-06	0.5889E-06	0.7270E-06
28	TETRALIN	0.9421E-09	0.2826E-08	0.4240E-08	0.5286E-08
29	NAPHTHALENE	0.1178E-07	0.2617E-07	0.3873E-07	0.4920E-07
30	METHYLNAPHTHALENES	0.2123E-07	0.4735E-07	0.6966E-07	0.9143E-07
31	DIMETHYLNAPHTHALENES	0.6350E-08	0.1535E-07	0.2275E-07	0.2953E-07
32	BIPHENYL	0.4756E-08	0.1176E-07	0.1827E-07	0.2458E-07
33	PHENANTHRENE	0.2921E-07	0.6066E-07	0.9216E-07	0.1262E-06
34	PYRENE	0.8813E-09	0.2871E-08	0.4444E-08	0.5958E-08
35	FLUORANTHENE	0.1058E-07	0.3733E-07	0.6755E-07	0.9902E-07
36	BANZANTHRACENE	0.8813E-08	0.1549E-07	0.2140E-07	0.2720E-07
37	BENZOPYRENE	0.7177E-08	0.1385E-07	0.1977E-07	0.2556E-07

TABLE XXVII

MOLAR YIELD OF PRODUCTS WITH 10% H2 + 90% HE GAS MIXTURE

PARTICLE SIZE : -53+38 MICRONS
REACTOR TEMP. : 198 - 203
INLET GAS COMPOSITION: 10.% HYDROGEN + 90.% HELIUM

REACTED HOURS->		1	2	3	4
COMPONENTS! V					
1	ETHANE	0.5208E-07	0.1376E-06	0.3368E-06	0.7573E-06
2	PROPANE	0.1315E-06	0.3261E-06	0.5817E-06	0.1006E-05
3	ISO-BUTANE	0.9361E-07	0.1890E-06	0.3015E-06	0.4349E-06
4	N-BUTANE	0.1218E-06	0.3000E-06	0.5722E-06	0.1031E-05
5	NEO-PENTANE	0.1805E-07	0.5394E-07	0.1105E-06	0.1712E-06
6	ISO-PENTANE	0.7249E-07	0.1553E-06	0.2760E-06	0.4879E-06
7	N-PENTANE	0.1177E-06	0.2714E-06	0.5005E-06	0.8157E-06
8	CYCLOPENTANE	0.1765E-06	0.3987E-06	0.8329E-06	0.1374E-05
9	2-METHYLPENTANE	0.1500E-07	0.4204E-07	0.1161E-06	0.1991E-06
10	3-METHYLPENTANE	0.1931E-07	0.6085E-07	0.1149E-06	0.1785E-06
11	N-HEXANE	0.5271E-07	0.1665E-06	0.4166E-06	0.7094E-06
12	METHYLCYCLOPENTANE	0.1528E-06	0.4003E-06	0.6963E-06	0.1103E-05
13	CYCLOHEXANE	0.1625E-06	0.4282E-06	0.7417E-06	0.1107E-05
14	2-METHYLHEXANE	0.3700E-08	0.1175E-07	0.2024E-07	0.3083E-07
15	3-METHYLHEXANE	0.1549E-08	0.7172E-08	0.1377E-07	0.2348E-07
16	N-HEPTANE	0.6249E-07	0.1348E-06	0.2292E-06	0.3380E-06
17	DIMETHYLCYCLOPENTANE	0.1309E-06	0.2741E-06	0.4610E-06	0.6595E-06
18	METHYLCYCLOHEXANE	0.1973E-06	0.5258E-06	0.8687E-06	0.1331E-05
19	CYCLICOLEFINS	0.1593E-06	0.3550E-06	0.5962E-06	0.8554E-06
20	DIMETHYLCYCLOHEXANE	0.6997E-07	0.1722E-06	0.5024E-06	0.1202E-05
21	C8+	0.1055E-06	0.3030E-06	0.5130E-06	0.9940E-06
22	PROPYLENE	0.2529E-07	0.5031E-07	0.6864E-07	0.8614E-07
23	BUTENES	0.2279E-08	0.5848E-08	0.1021E-07	0.1454E-07
24	PENTENES	0.2562E-08	0.6857E-08	0.1365E-07	0.2323E-07
25	BENZENE	0.9877E-07	0.2145E-06	0.4568E-06	0.5345E-06
26	TOLUENE	0.1337E-07	0.3188E-07	0.6248E-07	0.9573E-07
27	XYLENES	0.1332E-06	0.2843E-06	0.4535E-06	0.6195E-06
28	TETRALIN	0.1177E-08	0.2441E-08	0.3890E-08	0.5008E-08
29	NAPHTHALENE	0.1202E-07	0.2443E-07	0.3729E-07	0.4801E-07
30	METHYLNAPHTHALENES	0.1489E-07	0.3596E-07	0.5804E-07	0.7841E-07
31	DIMETHYLNAPHTHALENES	0.5651E-08	0.1183E-07	0.1852E-07	0.2546E-07
32	BIPHENYL	0.5346E-08	0.1119E-07	0.1728E-07	0.2221E-07
33	PHENANTHRENE	0.2709E-07	0.5550E-07	0.8436E-07	0.1142E-06
34	PYRENE	0.5238E-09	0.1748E-08	0.2715E-08	0.3540E-08
35	FLUORANTHENE	0.9166E-08	0.2750E-07	0.4900E-07	0.5160E-07
36	BANZANTHRACENE	0.5016E-08	0.8879E-08	0.1196E-07	0.1371E-07
37	BENZOPYRENE	0.5288E-08	0.9403E-08	0.1247E-07	0.1467E-07

TABLE XXVIII

RATE DATA FOR 2% H2 + 98% HE GAS MIXTURE

PARTICLE SIZE : -53+38 MICRONS
REACTOR TEMP. : 198 - 203
INLET GAS COMPOSITION: 10.% HYDROGEN + 90.% HELIUM

REACTED HOURS->		1	2	3	4
COMPONENTS| V				
1	ETHANE	0.8679E-09	0.1426E-08	0.3320E-08	0.7007E-08
2	PROPANE	0.2191E-08	0.3244E-08	0.4260E-08	0.7069E-08
3	ISO-BUTANE	0.1560E-08	0.1590E-08	0.1875E-08	0.2224E-08
4	N-BUTANE	0.2031E-08	0.2969E-08	0.4536E-08	0.7653E-08
5	NEO-PENTANE	0.3009E-09	0.5981E-09	0.9418E-09	0.1013E-08
6	ISO-PENTANE	0.1208E-08	0.1380E-08	0.2012E-08	0.3531E-08
7	N-PENTANE	0.1962E-08	0.2562E-08	0.3817E-08	0.5254E-08
8	CYCLOPENTANE	0.2942E-08	0.3702E-08	0.7238E-08	0.9021E-08
9	2-METHYLPENTANE	0.2499E-09	0.4507E-09	0.1234E-08	0.1384E-08
10	3-METHYLPENTANE	0.3218E-09	0.6924E-09	0.9011E-09	0.1060E-08
11	N-HEXANE	0.6785E-09	0.1896E-08	0.4168E-08	0.4880E-08
12	METHYLCYCLOPENTANE	0.2547E-08	0.4123E-08	0.4934E-08	0.6774E-08
13	CYCLOHEXANE	0.2708E-08	0.4428E-08	0.5225E-08	0.6093E-08
14	2-METHYLHEXANE	0.6167E-10	0.1342E-09	0.1415E-09	0.1764E-09
15	3-METHYLHEXANE	0.2582E-10	0.9372E-10	0.1100E-09	0.1618E-09
16	N-HEPTANE	0.1042E-08	0.1206E-08	0.1572E-08	0.1813E-08
17	DIMETHYLCYCLOPENTANE	0.2182E-08	0.2387E-08	0.3115E-08	0.3308E-08
18	METHYLCYCLOHEXANE	0.3289E-08	0.5475E-08	0.5715E-08	0.7704E-08
19	CYCLICOLEFINS	0.2656E-08	0.3261E-08	0.4021E-08	0.4320E-08
20	DIMETHYLCYCLOHEXANE	0.1166E-08	0.1704E-08	0.5503E-08	0.1166E-07
21	C8+	0.1758E-08	0.3293E-08	0.3500E-08	0.8017E-08
22	PROPYLENE	0.4214E-09	0.4171E-09	0.3054E-09	0.2917E-09
23	BUTENES	0.3799E-10	0.5947E-10	0.7269E-10	0.7211E-10
24	PENTENES	0.4270E-10	0.7158E-10	0.1133E-09	0.1595E-09
25	BENZENE	0.1646E-08	0.1928E-08	0.4039E-08	0.1296E-08
26	TOLUENE	0.2229E-09	0.3084E-09	0.5099E-09	0.5542E-09
27	XYLENES	0.2221E-08	0.2518E-08	0.2819E-08	0.2767E-08
28	TETRALIN	0.1961E-10	0.2108E-10	0.2415E-10	0.1863E-10
29	NAPHTHALENE	0.2003E-09	0.2069E-09	0.2142E-09	0.1787E-09
30	METHYLNAPHTHALENES	0.2482E-09	0.3512E-09	0.3679E-09	0.3396E-09
31	DIMETHYLNAPHTHALENES	0.9419E-10	0.1030E-09	0.1115E-09	0.1157E-09
32	BIPHENYL	0.8911E-10	0.9745E-10	0.1015E-09	0.8210E-10
33	PHENANTHRENE	0.4516E-09	0.4734E-09	0.4810E-09	0.4969E-09
34	PYRENE	0.8729E-11	0.2040E-10	0.1612E-10	0.1377E-10
35	FLUORANTHENE	0.1528E-09	0.3055E-09	0.3584E-09	0.4331E-10
36	BANZANTHRACENE	0.8360E-10	0.6438E-10	0.5137E-10	0.2921E-10
37	BENZOPYRENE	0.8813E-10	0.6858E-10	0.5112E-10	0.3660E-10

TABLE XXIX

RATE DATA FOR 10% H2 + 90% HE GAS MIXTURE

PARTICLE SIZE : -53+38 MICRONS
REACTOR TEMP. : 196 - 203
INLET GAS COMPOSITION: 2.% HYDROGEN + 98.% HELIUM

REACTED HOURS->		1	2	3	4
COMPONENTS| V				
1	ETHANE	0.1040E-08	0.5594E-08	0.8898E-08	0.1062E-07
2	PROPANE	0.2448E-08	0.3908E-08	0.5435E-08	0.8263E-08
3	ISO-BUTANE	0.2226E-08	0.2289E-08	0.2241E-08	0.2590E-08
4	N-BUTANE	0.3068E-08	0.3834E-08	0.6044E-08	0.9878E-08
5	NEO-PENTANE	0.3458E-09	0.7774E-09	0.1266E-08	0.1278E-08
6	ISO-PENTANE	0.1919E-08	0.3071E-08	0.5038E-08	0.9073E-08
7	N-PENTANE	0.3394E-08	0.3742E-08	0.4801E-08	0.5783E-08
8	CYCLOPENTANE	0.1582E-08	0.2459E-08	0.3907E-08	0.4602E-08
9	2-METHYLPENTANE	0.5096E-09	0.9309E-09	0.1403E-08	0.1919E-08
10	3-METHYLPENTANE	0.3663E-09	0.7340E-09	0.1149E-08	0.1271E-08
11	N-HEXANE	0.1214E-08	0.3703E-08	0.5482E-08	0.7183E-08
12	METHYLCYCLOPENTANE	0.1897E-08	0.2956E-08	0.3563E-08	0.4110E-08
13	CYCLOHEXANE	0.2216E-08	0.3092E-08	0.3842E-08	0.4190E-08
14	2-METHYLHEXANE	0.1218E-09	0.2527E-09	0.2994E-09	0.5036E-09
15	3-METHYLHEXANE	0.1124E-09	0.2106E-09	0.2495E-09	0.4676E-09
16	N-HEPTANE	0.1994E-08	0.4702E-08	0.6317E-08	0.6295E-08
17	DIMETHYLCYCLOPENTANE	0.2327E-08	0.3693E-08	0.3955E-08	0.4771E-08
18	METHYLCYCLOHEXANE	0.3064E-08	0.4314E-08	0.5330E-08	0.7865E-08
19	CYCLICOLEFINS	0.7663E-09	0.1587E-08	0.1914E-08	0.2616E-08
20	DIMETHYLCYCLOHEXANE	0.5064E-08	0.5905E-08	0.1366E-07	0.1609E-07
21	C8+	0.4083E-08	0.5089E-08	0.9418E-08	0.1105E-07
22	PROPYLENE	0.5776E-09	0.5642E-09	0.3030E-09	0.2967E-09
23	BUTENES	0.4173E-10	0.6187E-10	0.2163E-09	0.2079E-09
24	PENTENES	0.4678E-10	0.8323E-10	0.1801E-09	0.1598E-09
25	BENZENE	0.2096E-08	0.6192E-08	0.4763E-08	0.1429E-08
26	TOLUENE	0.3054E-09	0.5496E-09	0.4428E-09	0.3054E-09
27	XYLENES	0.2147E-08	0.4601E-08	0.3067E-08	0.2300E-08
28	TETRALIN	0.1570E-10	0.3140E-10	0.2355E-10	0.1745E-10
29	NAPHTHALENE	0.1963E-09	0.2399E-09	0.2094E-09	0.1745E-09
30	METHYLNAPHTHALENES	0.3538E-09	0.4354E-09	0.3719E-09	0.3628E-09
31	DIMETHYLNAPHTHALENES	0.1058E-09	0.1499E-09	0.1235E-09	0.1129E-09
32	BIPHENYL	0.7926E-10	0.1168E-09	0.1085E-09	0.1051E-09
33	PHENANTHRENE	0.4868E-09	0.5141E-09	0.5351E-09	0.5666E-09
34	PYRENE	0.1469E-10	0.3315E-10	0.2623E-10	0.2522E-10
35	FLUORANTHENE	0.1763E-09	0.4459E-09	0.5036E-09	0.5246E-09
36	BANZANTHRACENE	0.1469E-09	0.1112E-09	0.9863E-10	0.9653E-10
37	BENZOPYRENE	0.1196E-09	0.1112E-09	0.9863E-10	0.9653E-10

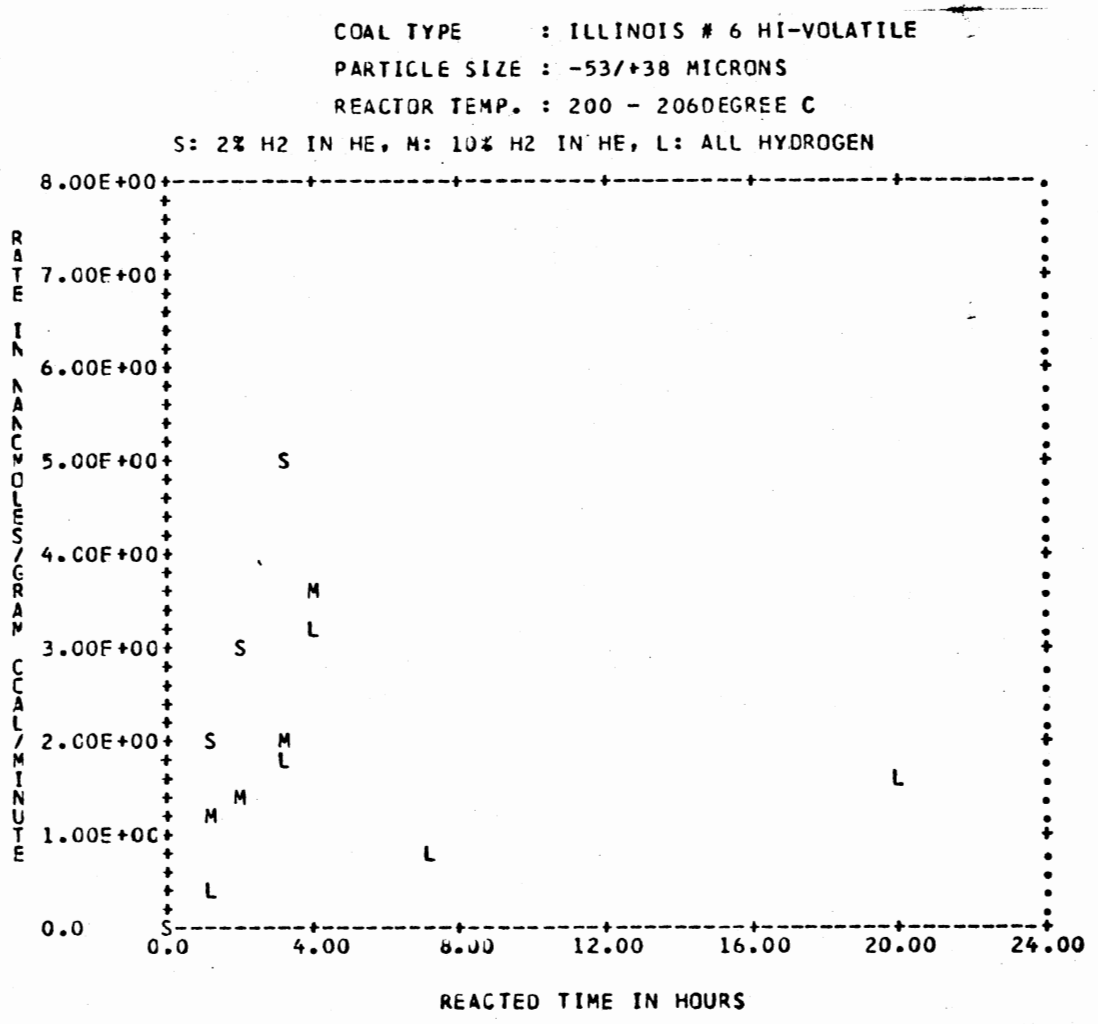

Figure 64. Effect of Inlet Gas on the Rate of Formation of iso-Pentane

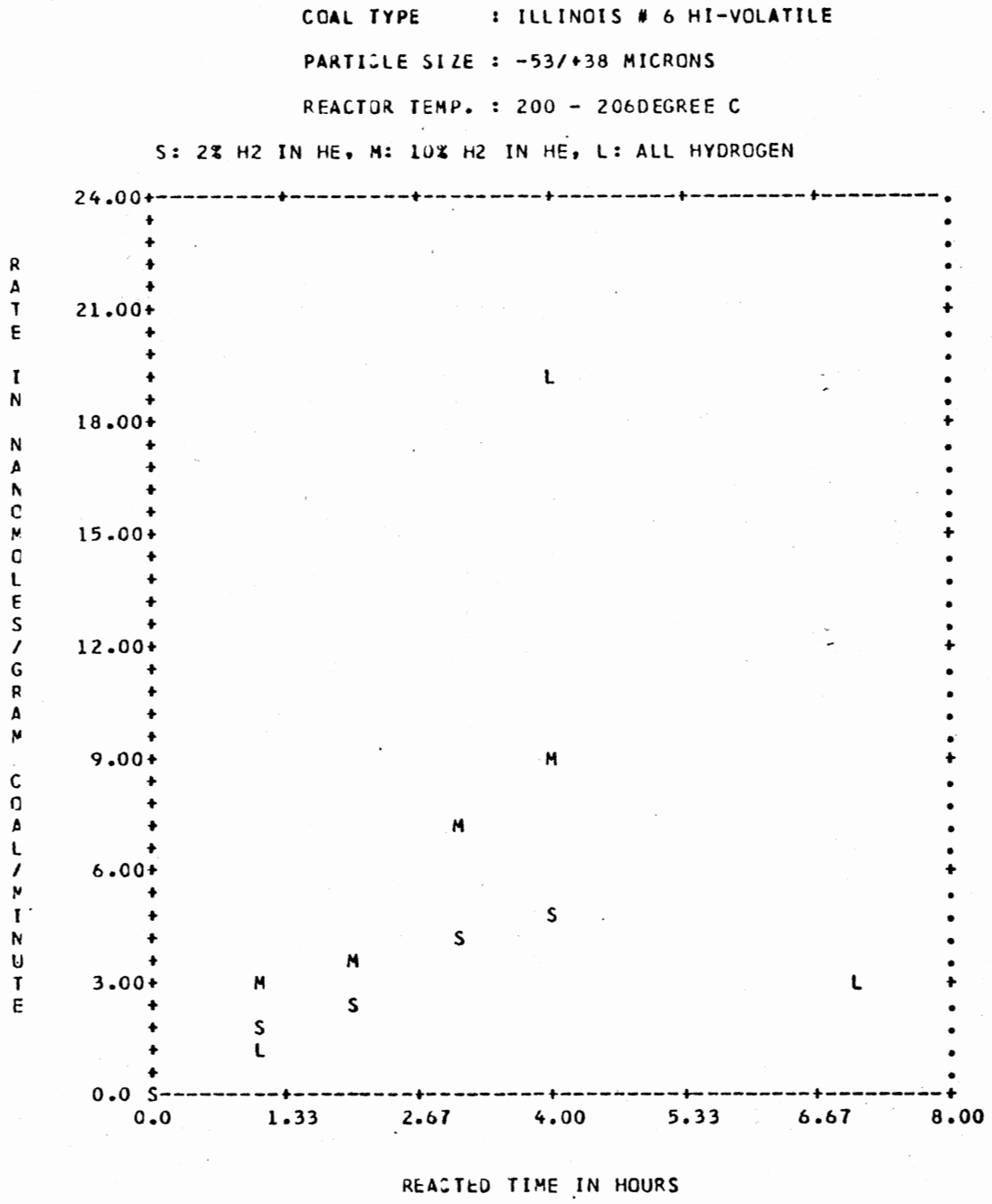

Figure 65. Effect of Inlet Gas on the Rate of Formation of Cyclopentane

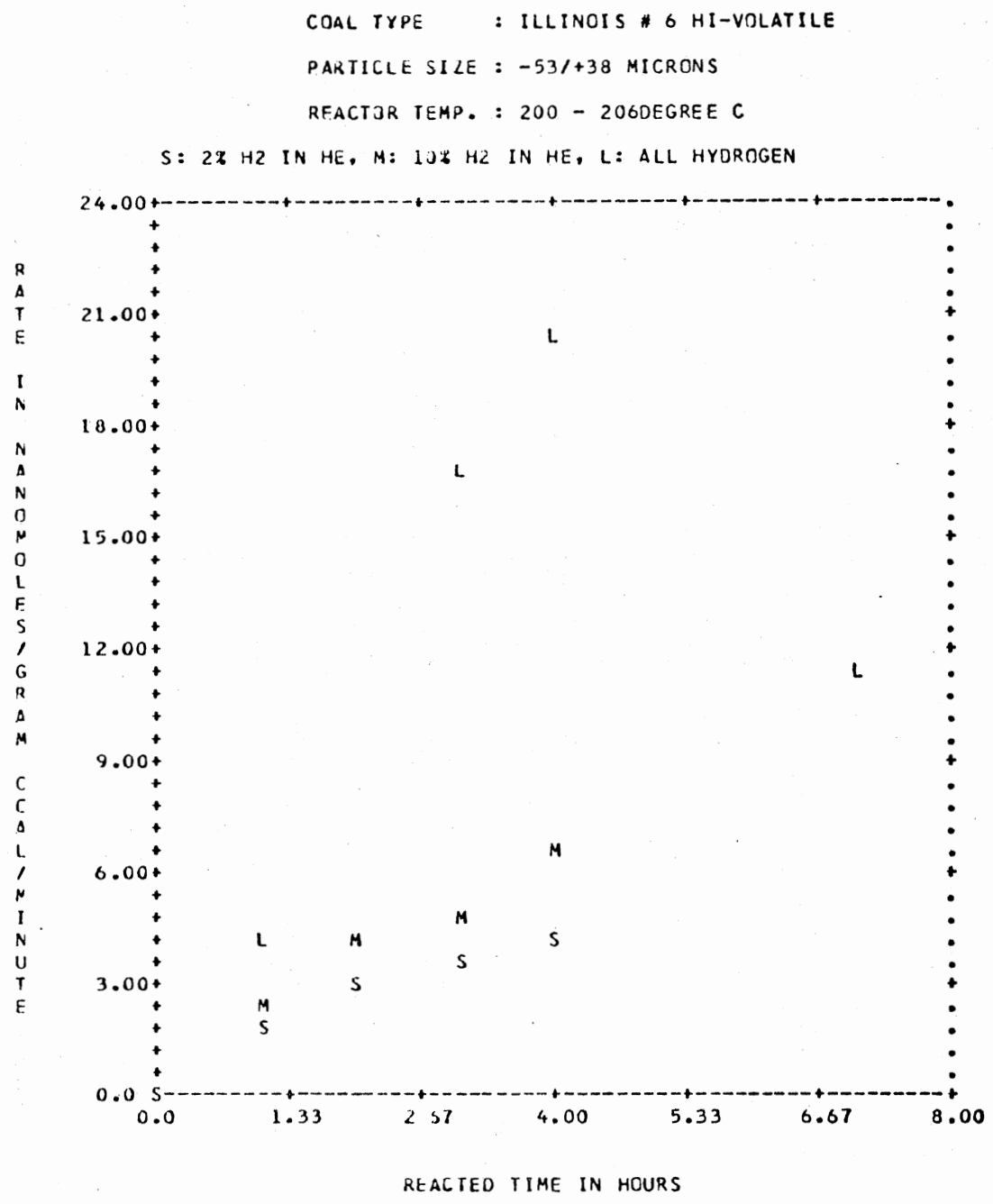

Figure 66. Effect of Inlet Gas on the Rate of Formation of Methylcyclopentane

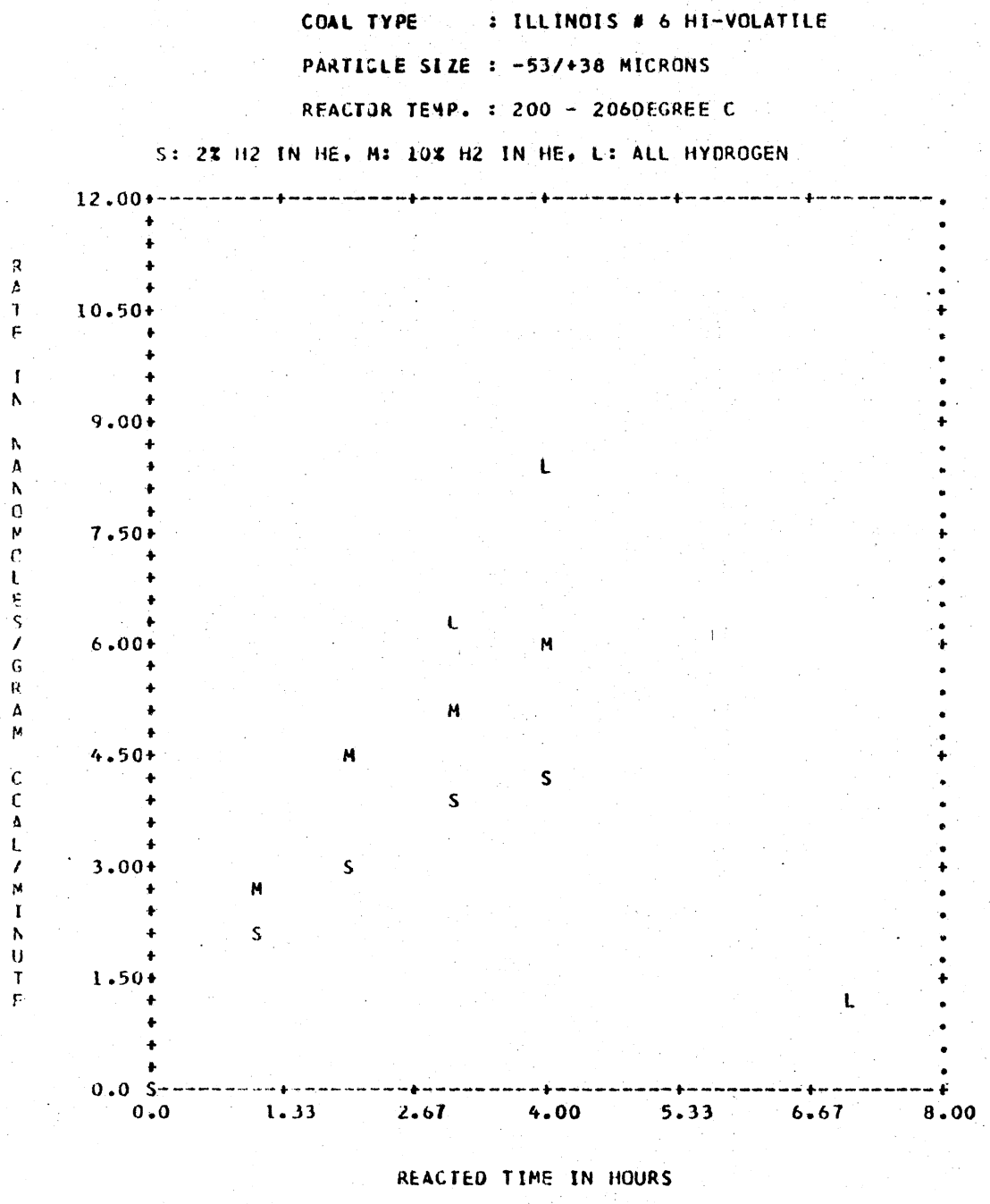

Figure 67. Effect of Inlet Gas on the Rate of Formation of Cyclohexane

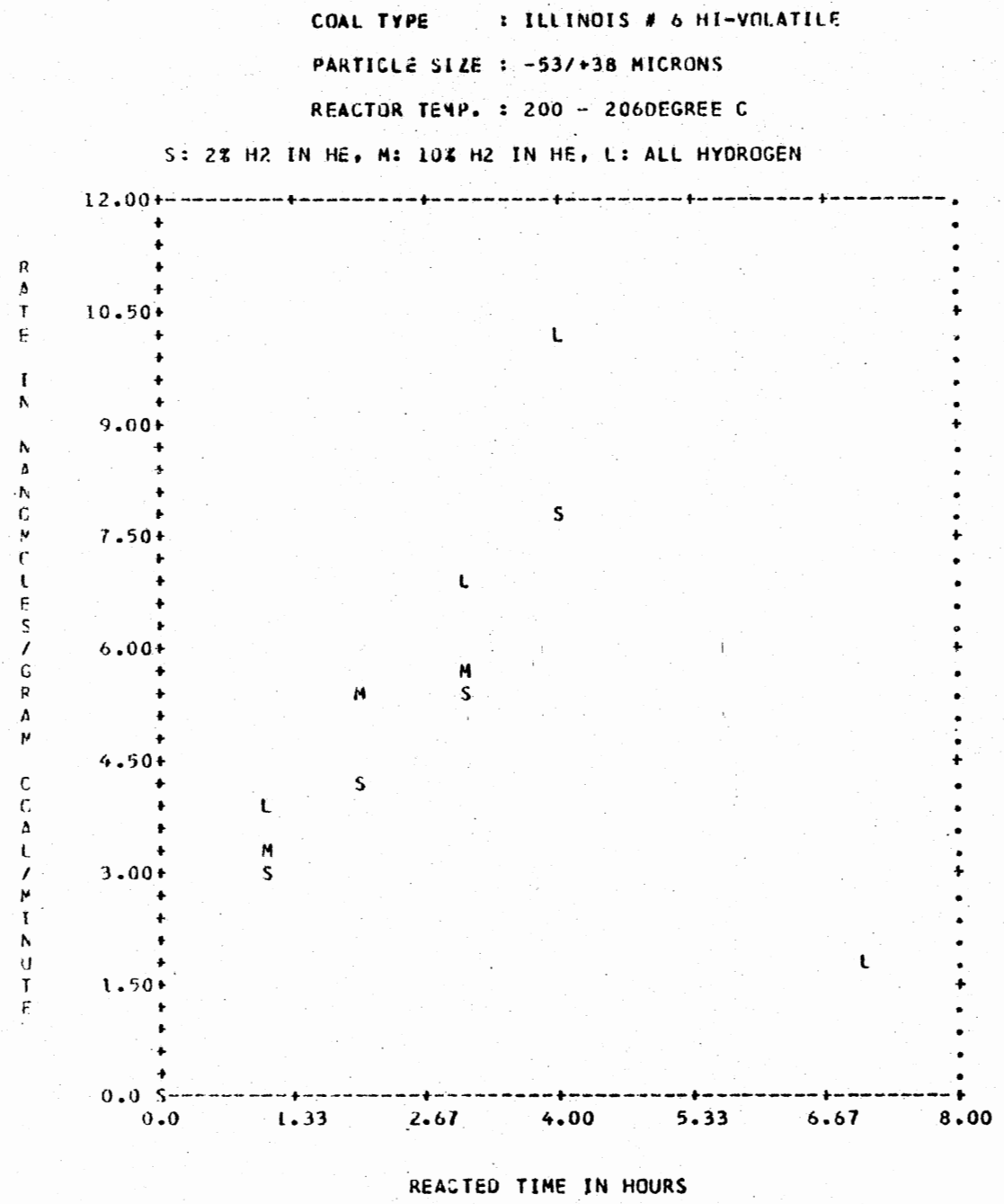

Figure 68. Effect of Inlet Gas on the Rate of Formation of Methylcyclohexane

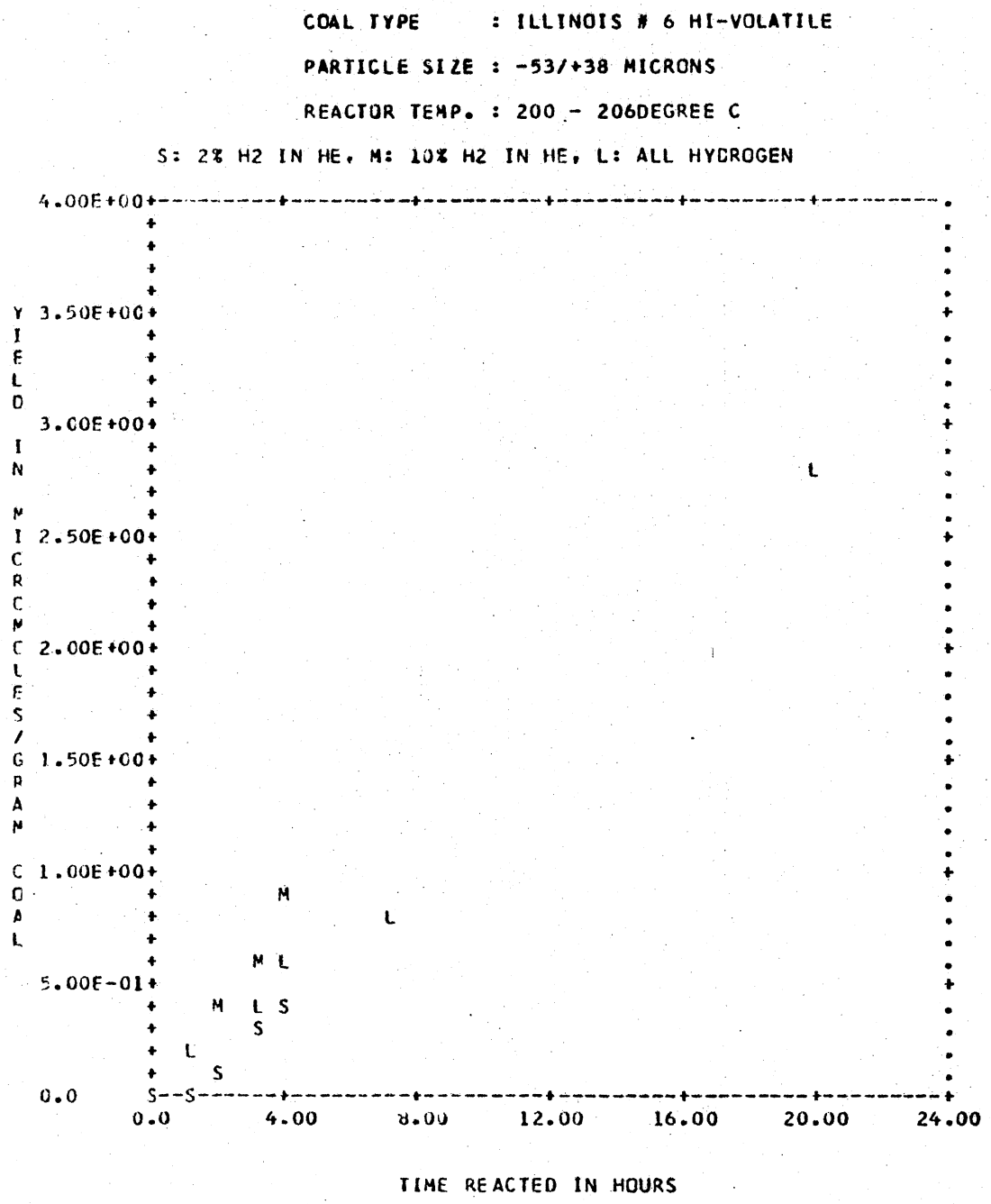

Figure 69. Effect of Inlet Gas on the Rate of Formation of Dimethylcyclohexane

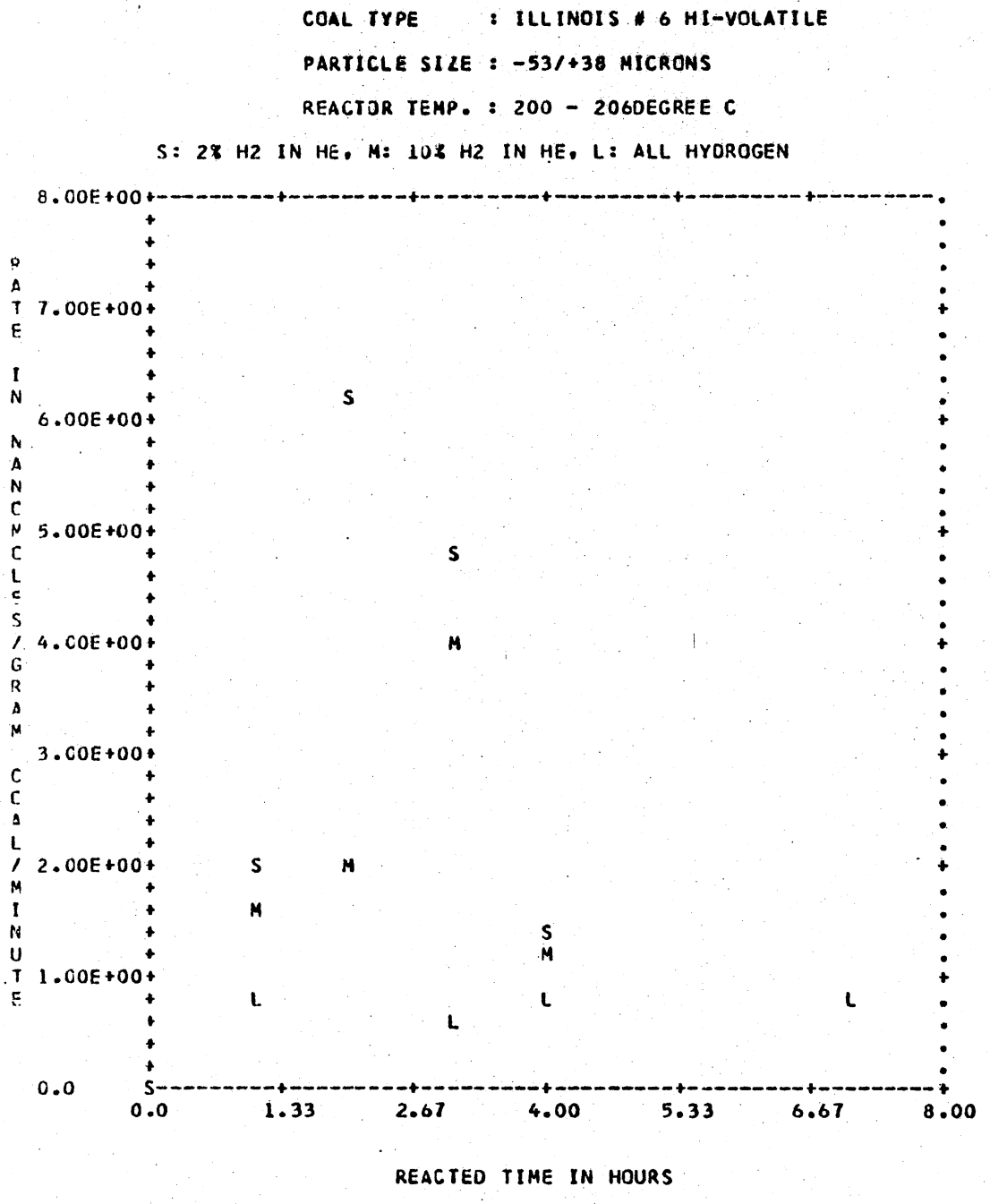

Figure 70. Effect of Inlet Gas on the Rate of Formation of Benzene

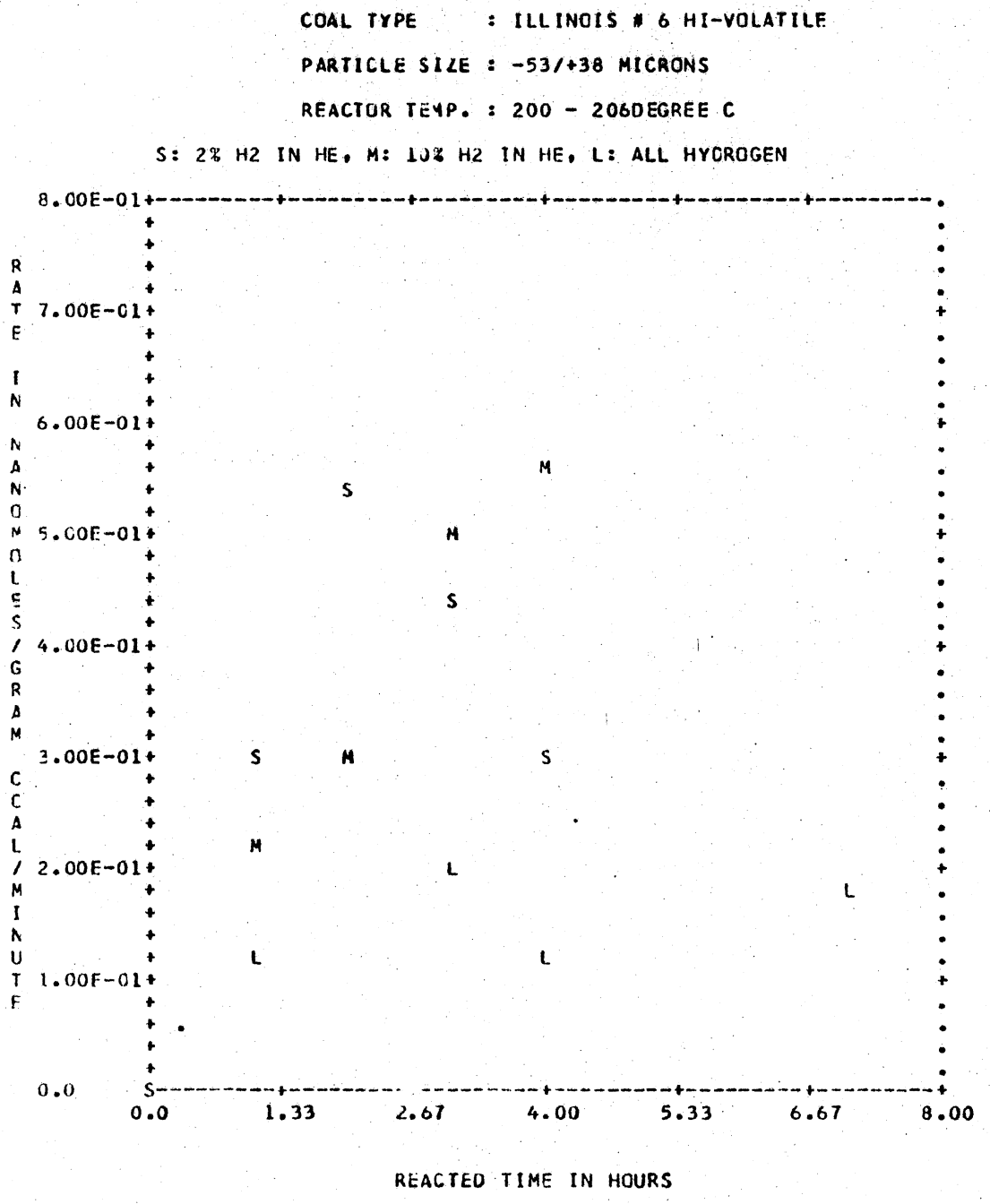

Fgiure 71. Effect of Inlet Gas on the Rate of Formation of Toluene

COAL TYPE : ILLINOIS # 6 HI-VOLATILE

PARTICLE SIZE : -53/+38 MICRONS

REACTOR TEMP. : 200 - 206DEGREE C

S: 2% H2 IN HE, M: 10% H2 IN HE, L: ALL HYDROGEN

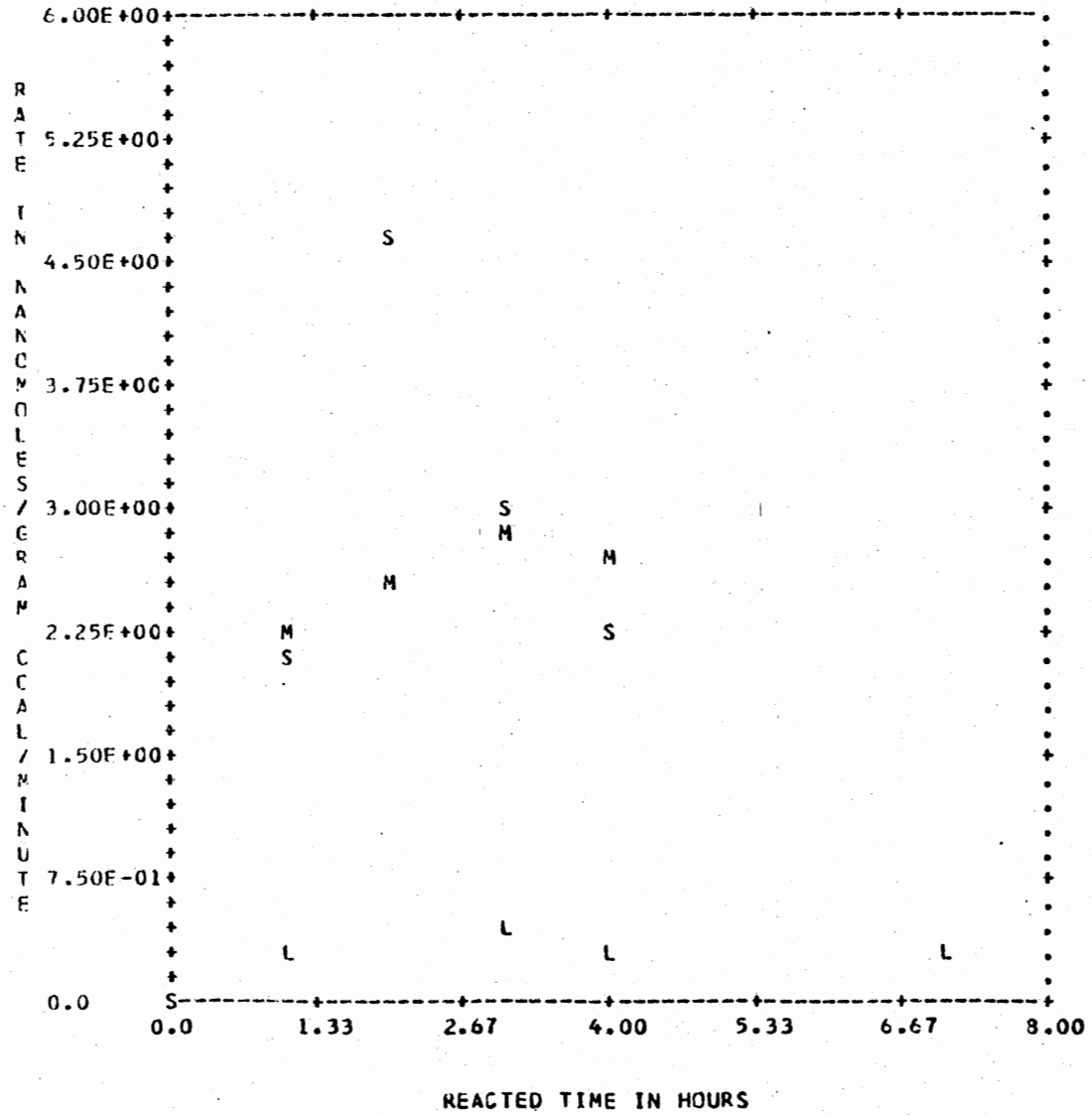

Figure 72. Effect of Inlet Gas on the Rate of Formation of Xylenes

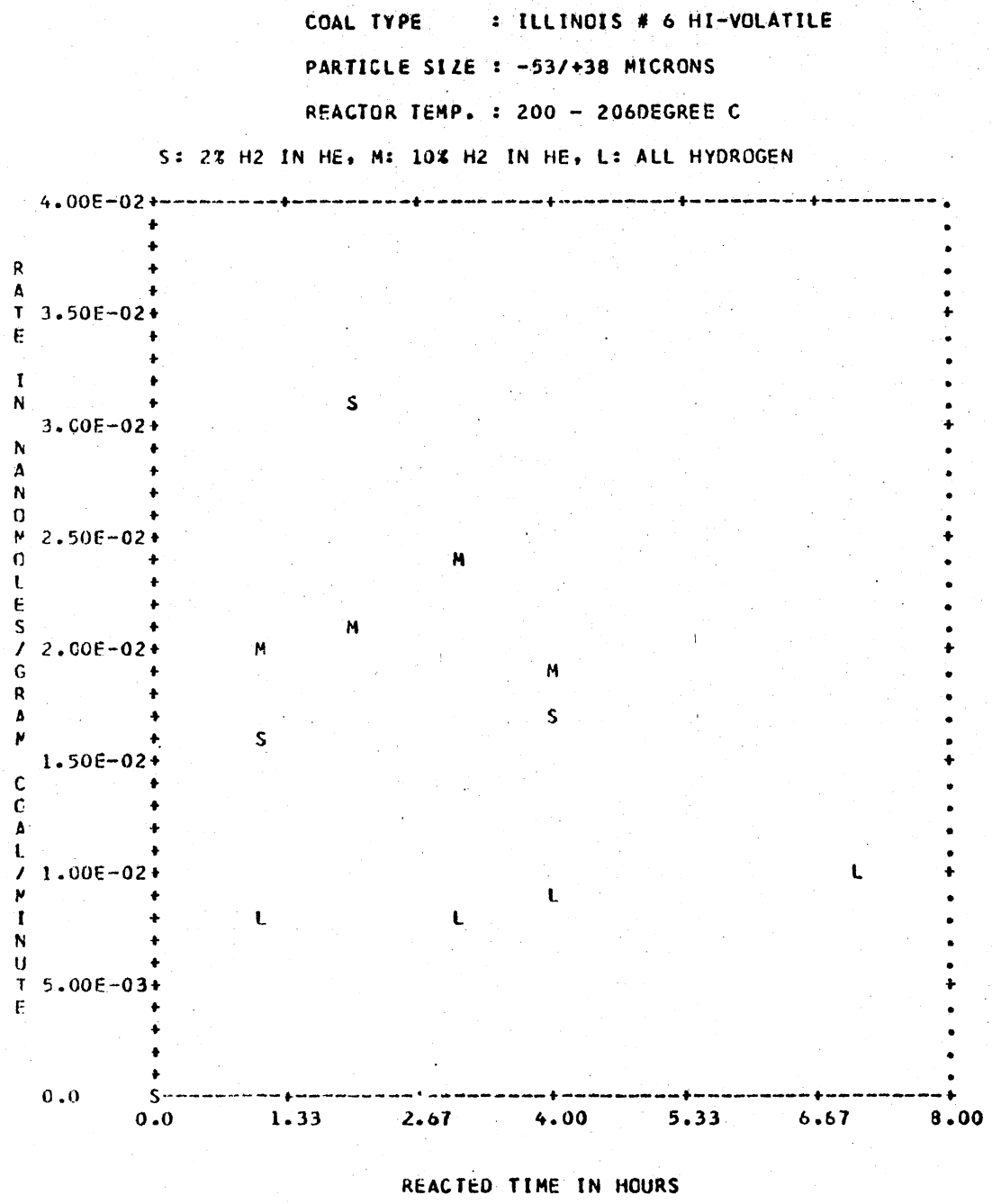

Figure 73. Effect of Inlet Gas on the Rate of Formation of Tetralin

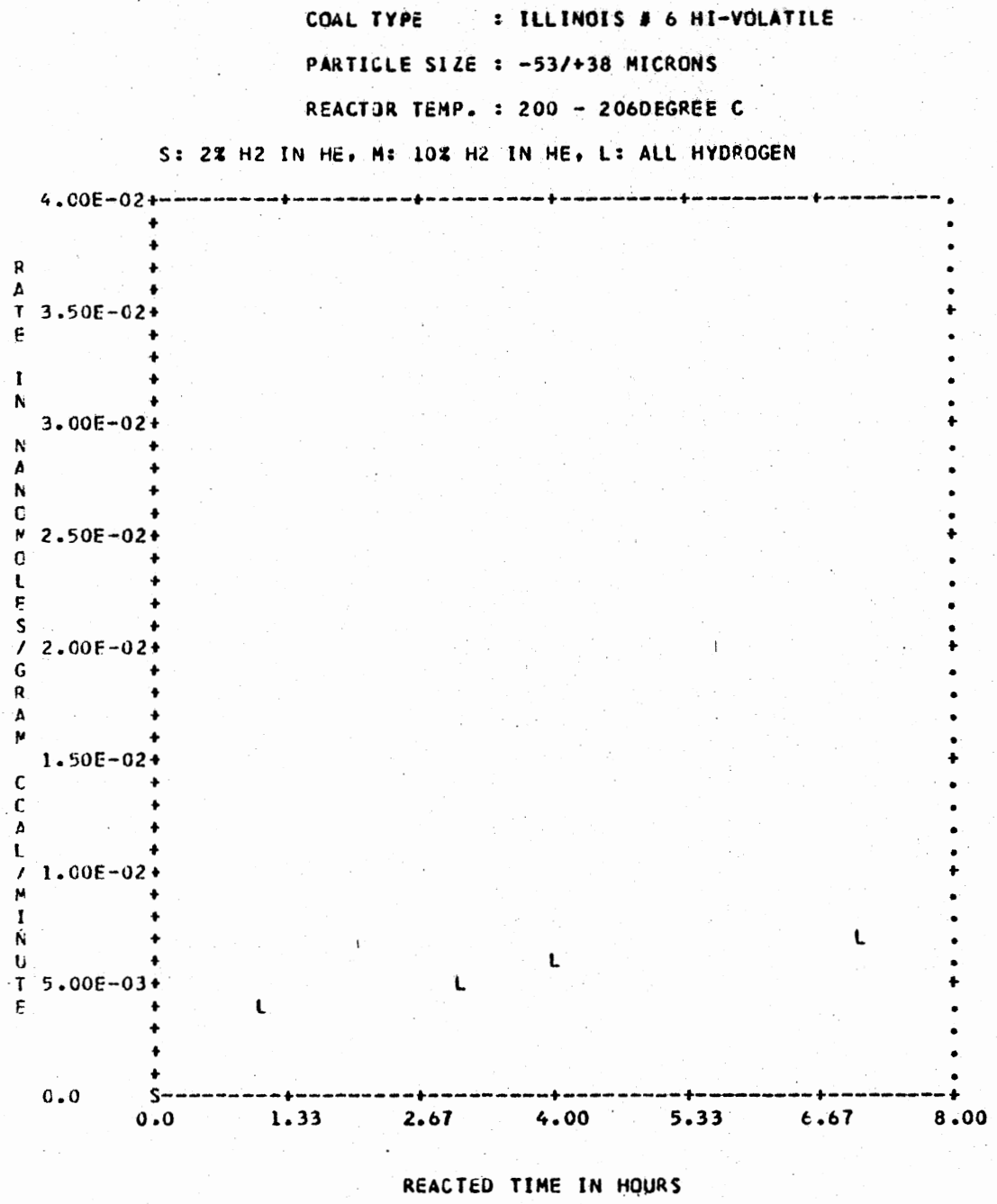

Figure 74. Effect of Inlet Gas on the Rate of Formation of Naphthalene

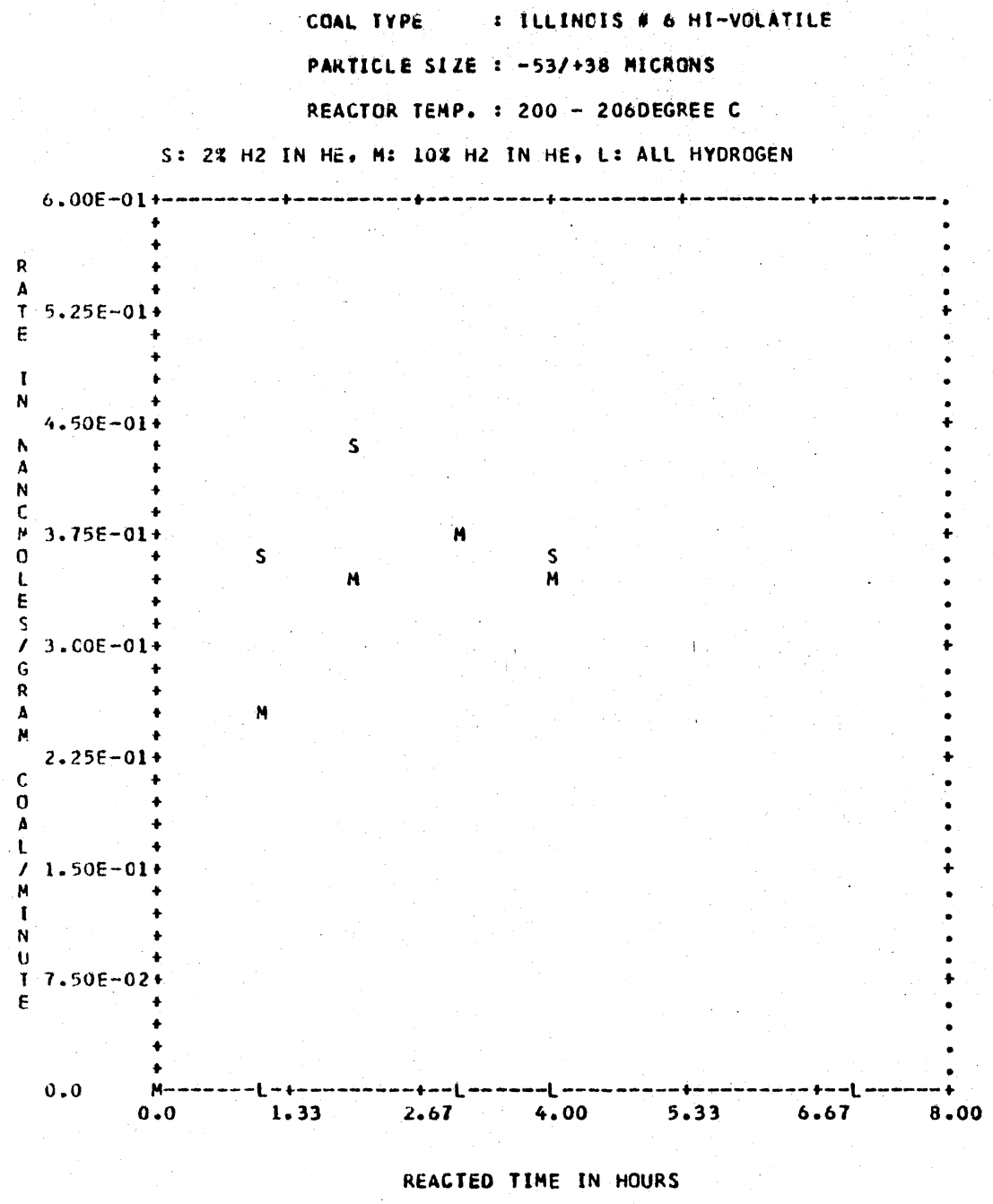

Figure 75. Effect of Inlet Gas on the Rate of Formation of Methylnaphthalenes

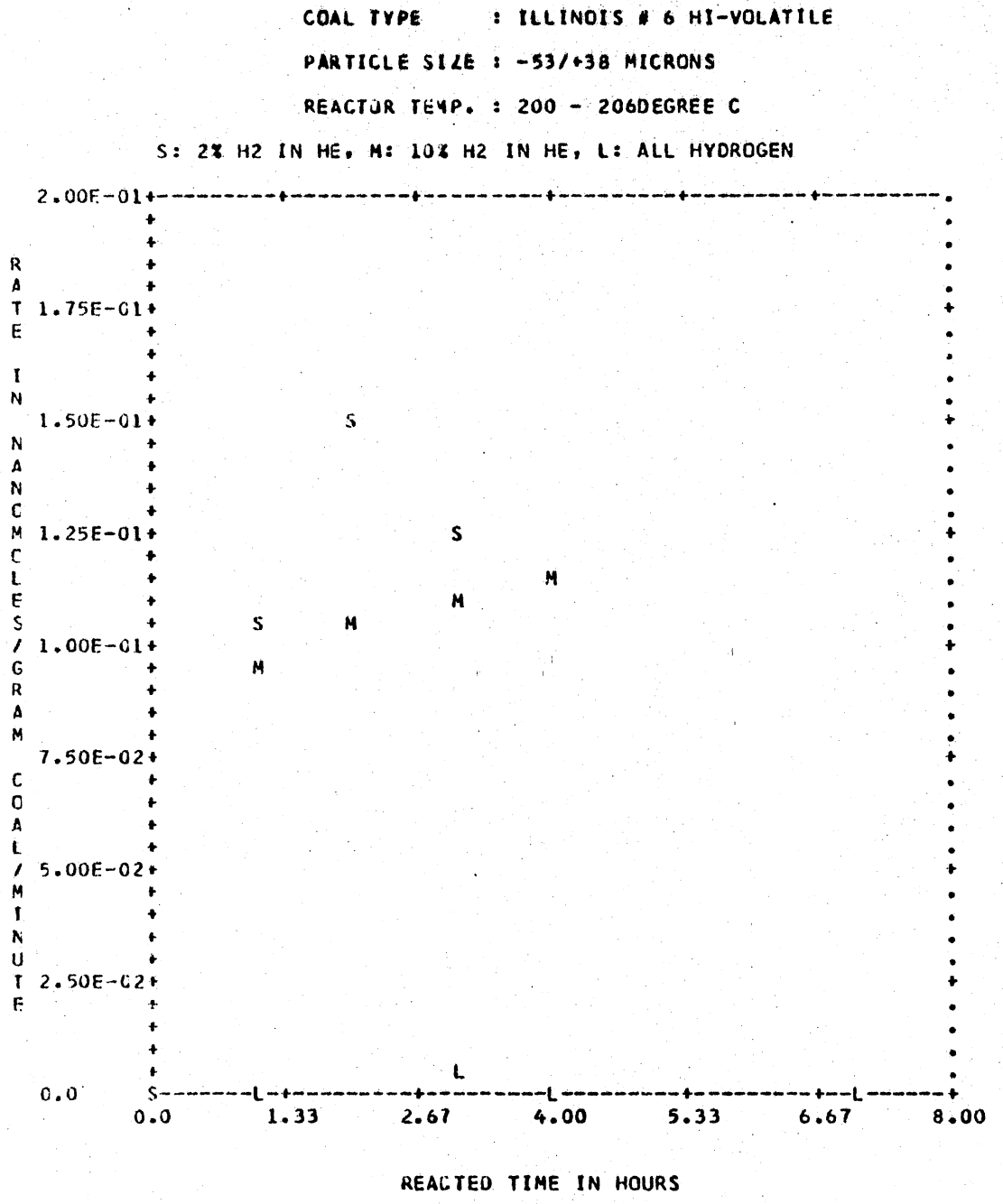

Figure 76. Effect of Inlet Gas on the Rate of Formation of Dimethylnaphthalenes

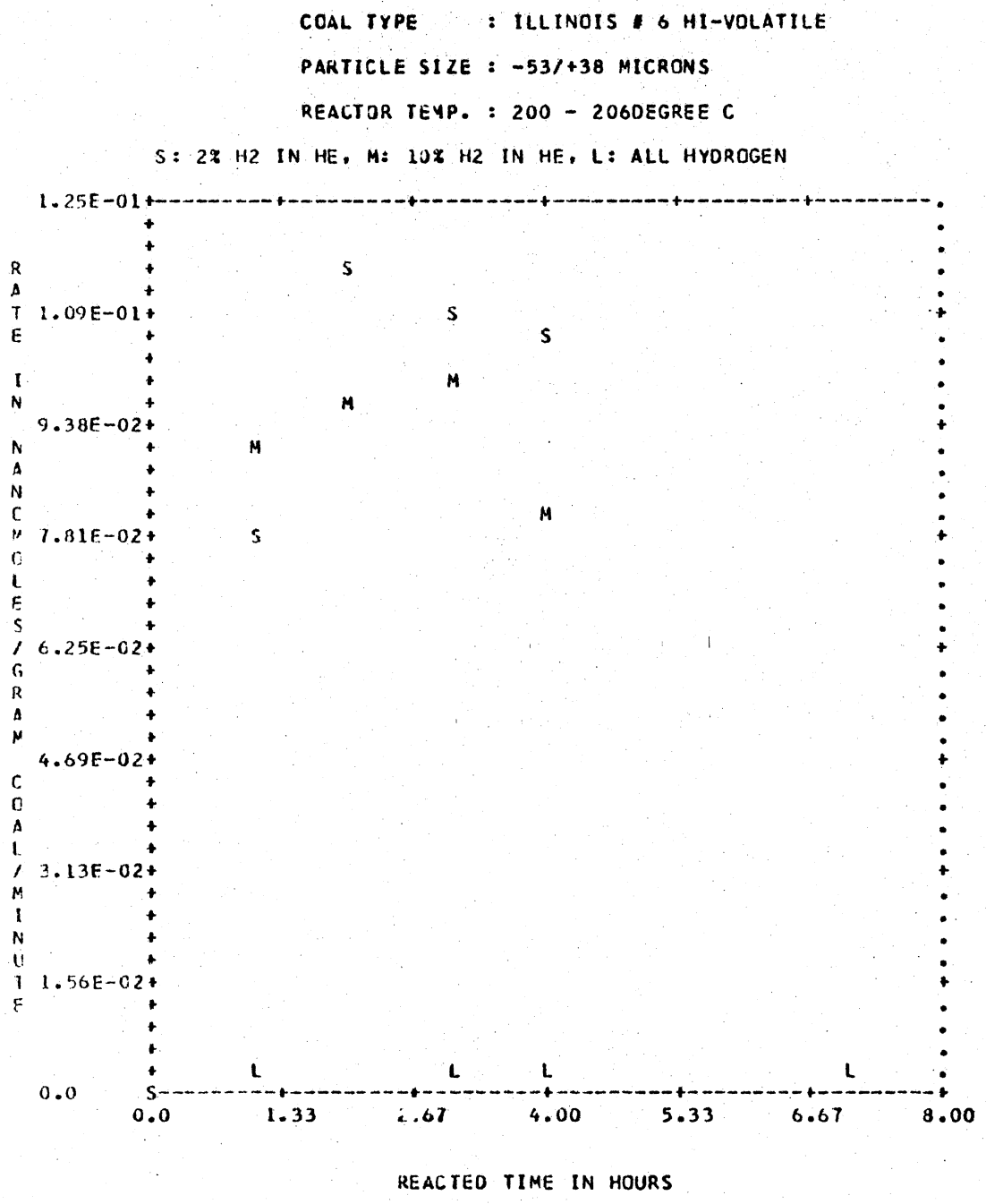

Figure 77. Effect of Inlet Gas on the Rate of Formation of Biphenyl

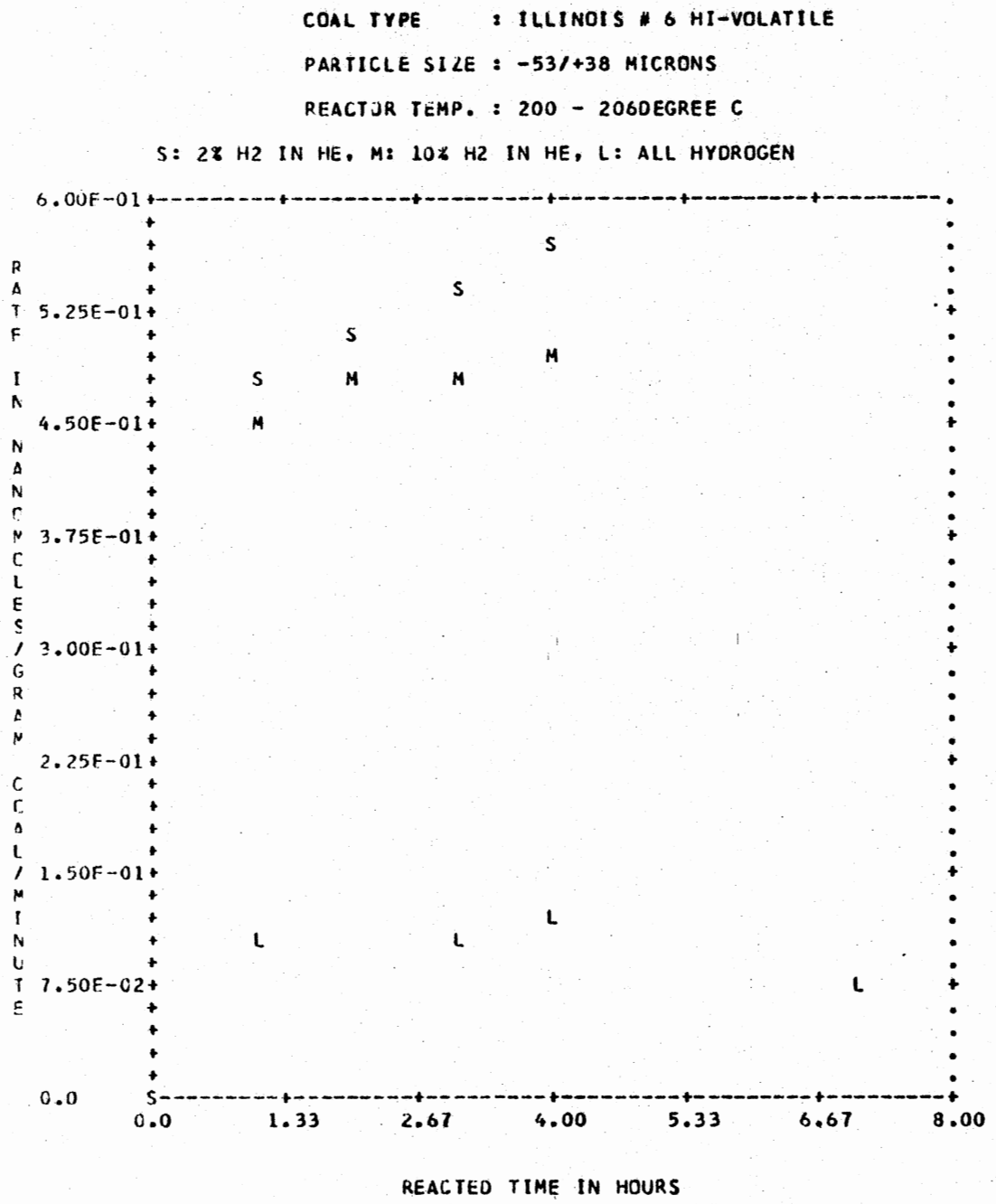

Figure 78. Effect of Inlet Gas on the Rate of Formation of Phenanthrene

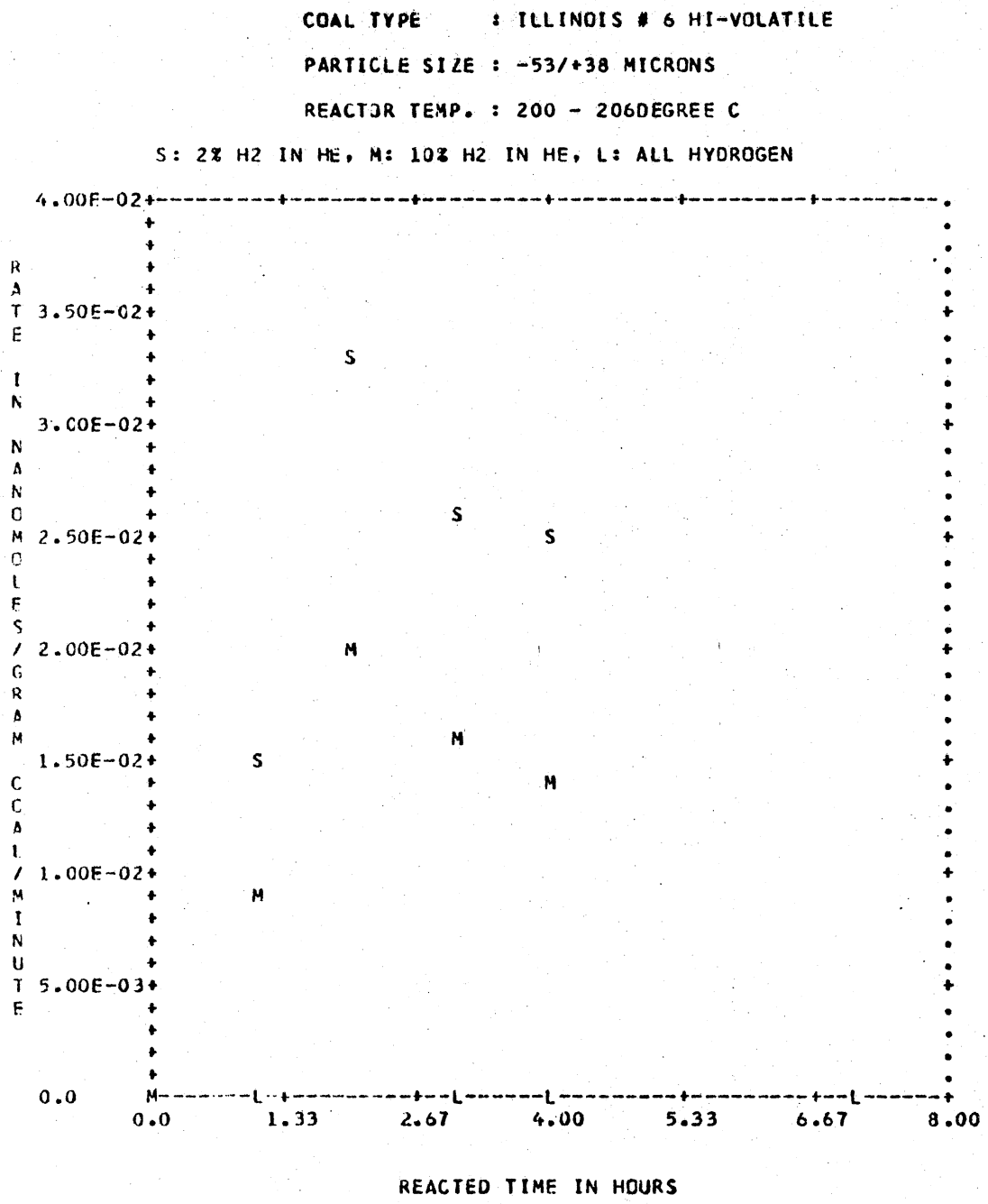

Figure 79. Effect of Inlet Gas on the Rate of Formation of Pyrene

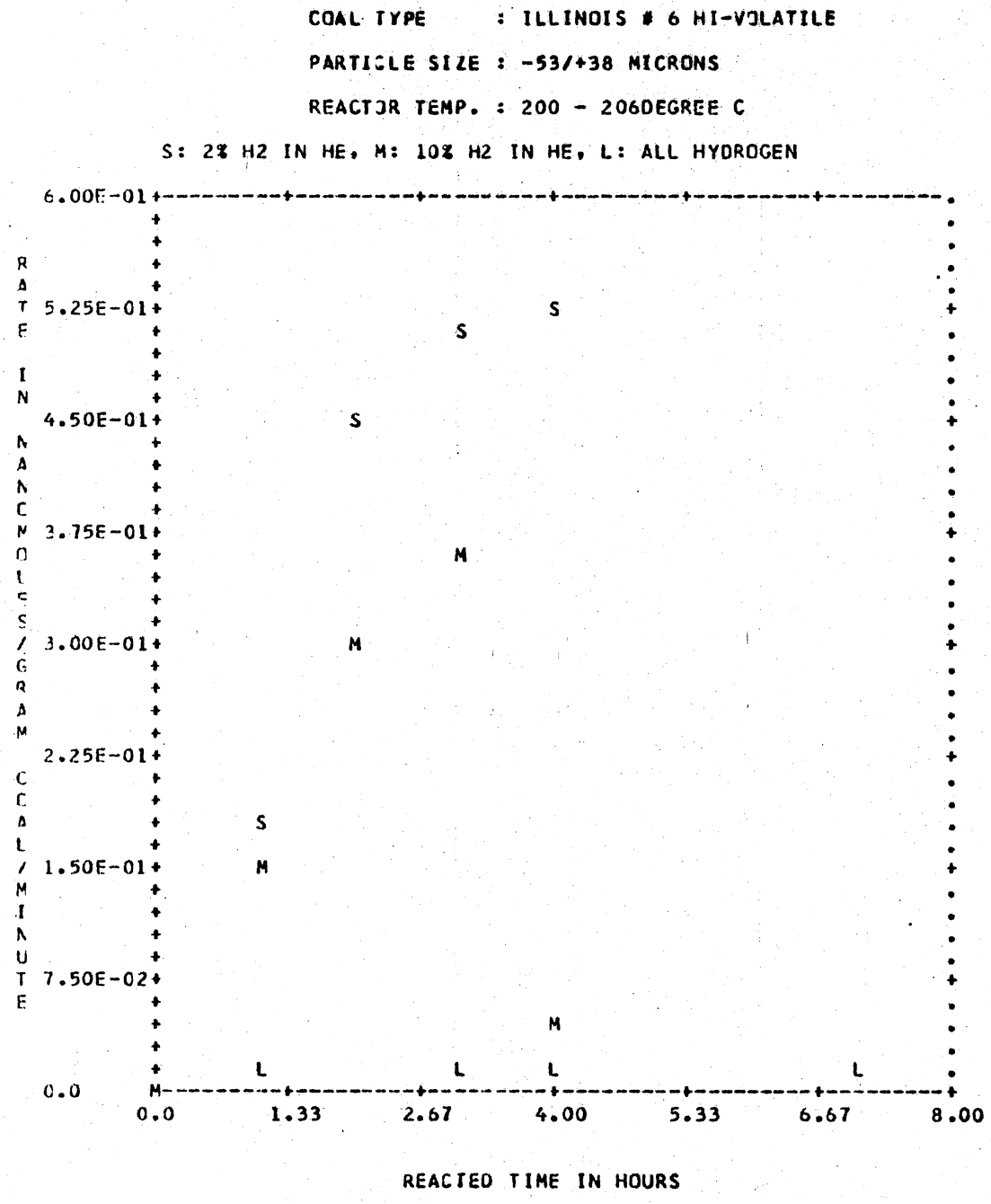

Figure 80. Effect of Inlet Gas on the Rate of Formation of Fluoranthene

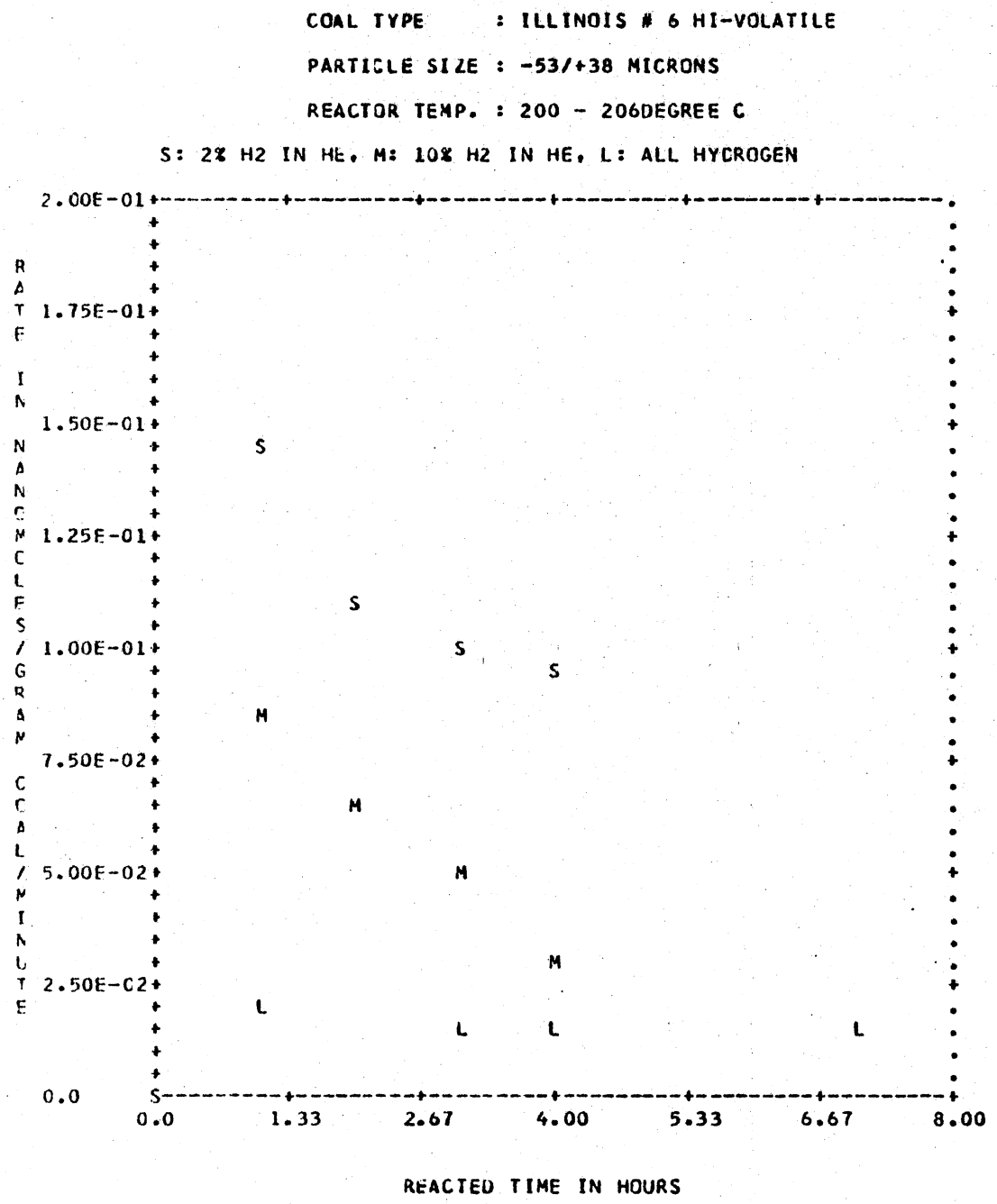

Figure 81. Effect of Inlet Gas on the Rate of Formation of Benzanthracene

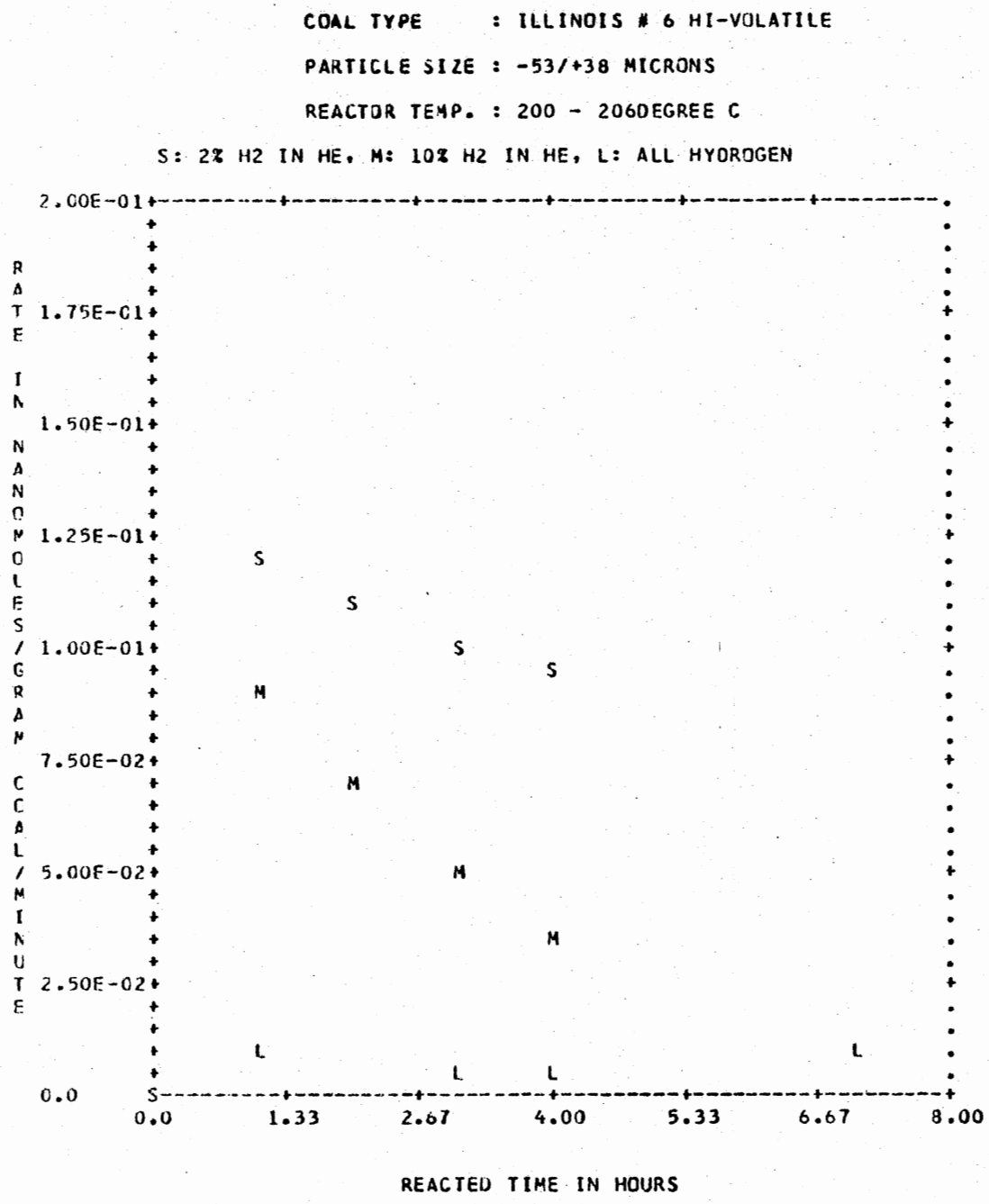

Figure 82. Effect of Inlet Gas on the Rate of Formation of Benzopyrene

2% hydrogen; 10% hydrogen followed the suit with few exceptions which, however, show the shifting of the maxima towards longer reaction times. i.e., The maxima in those cases were just not found within the range of reaction time studied. 100 % hydrogen shows, if at all, little variations in the rates.

On the other hand, phenanthrene and fluoranthene show continuous increase in their rates of formation whereas benzanthracene and benzopyrene show continued decrease. The point at 4th hour for fluoranthene in the case of a 10% hydrogen mixture causes concern because it does not follow the nominal course. Of the high molecular weight products pyrene is the only product that shows a definite maximum. In all cases, the rates of formation of these precursors are considerably higher with leaner mixtures than the one consisting of all hydrogen.

The decrease or increase in the rates of formation of these precursors may be related to the availability of such structures on the surface of coal and/or the ability of hydrogen atoms to crack them off the coal surface.

An attempt to correlate these data with the available models for coal would be in order. Models proposed by van Krevelen, Given and Sheer were already mentioned in Chapter II. Recently, Farcasiu of Mobil Research and Development (114) has reported the results of his studies on the short-time thermal liquefaction of coal (113) in an effort to

determine the chemical composition and structure of coal. He postulated that during the dissolution of coal in the presence of H-donor solvents, only a few bonds are broken in the absence of an added catalyst. Neither the hydrogenation of aromatic polycyclic hydrocabons nor the destruction or formation of polycyclic saturates were believed to take place under these conditions. On this basis, the structures in Figures 83 were assigned to two major fractions obtained from Illinois # 6 coal. These structures were believed to be present in coal, most probably, as such. However, it is hard to understand how the donor solvent could differentiate between these structures and the innumerable number of other bonds available from coal. It is the opinion of this author that the H-donor solvent entered the micropores of coal, reacted with the gases that had already been adsorbed (not merely trapped) on the walls of the micropores and then released them from the micropores. An objection to this would be the difficulty of releasing such a large cluster from the micropores of coal, the average size of which has been reported to be approximately 5-6 A in diameter (115). However, the 'bee-hive' walls could have been broken by continued bombardment of the solvent molecules on them does not seem to be unreasonable.

In any event, the formation of phenanthrene and fluoranthene, as well as other high molecular weight PNA hydrocabons from the present investigation can not be explained

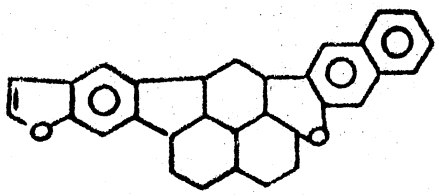

Fraction # 1

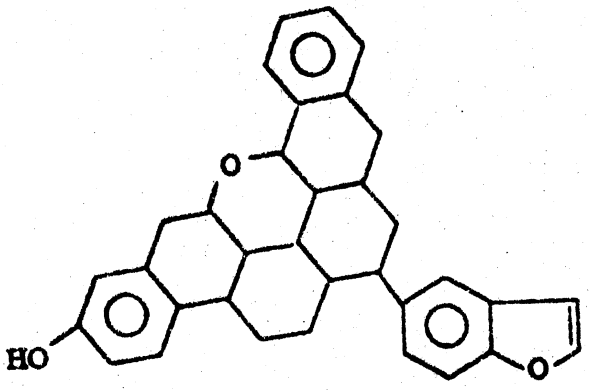

Fraction # 2

Figure 83. Most Probable Structural Units in Illinois # 6 Coal

on the basis of Farcasiu's structures. Rather, the heavily hydrogenated structures like the ones proposed by Farcasiu would have been more fitting under the conditions of this investigation. That this is not so, warrants a proposition of a different kind of structural unit that could be present, at least on the surface, in coal. An aromatic structural unit of fused phenanthrene and fluoranthene, that could be present, at least, on the surface of coal is presented in Figure 84. It needs to be emphasized that this may represent only a 'reactive' structural unit on the surface of coal which is different from other 'average' structures that were postulated from the studies involving diffusion controlled processes (at least initially).

It may appear unnecessary to propose a structural model for coal or its units from a single investigation only. Nonetheless, it is believed that questioning of all data arising out of such investigations may, eventually, lead to a more acceptable 'model' for coal in the near future.

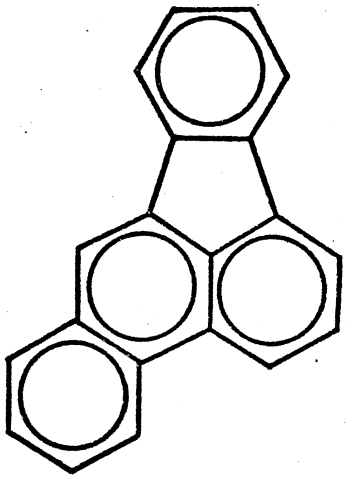

Figure 84. Probable Reactive Structural Unit on the Surface of Coal

CHAPTER XI

CONCLUSION

In view of the extreme complexity of the reaction products and the heterogeneous nature of the reaction, structural analysis of the reaction products from any coal conversion process is complicated and the results obtained are more often far from being satisfactory. The extent of conversion to gaseous or liquid products in the photochemical hydrogen atom cracking of coal was lower than anticipated. However, the data at 200 deg C do indicate that the product efficiency goes through a maximum. This shows the dependence of the reaction on the extent of convesion. It is possible that 'some' active sites on the surface of coal which were responsible for the intital stages of the reaction are depleted with conversion of coal to gaseous and liquid products and not renewed in sufficient numbers thereafter.

It is believed that the 'active' sites were initially created on the surface of coal by breaking of chemical bonds, generation of free radicals etc as a result of grinding and they were covered with layer(s) of atmospheric oxygen. From the rate data, it is concluded that the hydrogen atoms initially react with the adsorbed oxygen slowly expos-

ing the reactive surface. After the removal of the reactive surface, the hydrogen atoms are believed to encounter the surface of bulk coal which seems not to be as reactive as the grinding-induced reactive surface under the conditions of this research.

The rate data indicate that phenanthrene and fluoranthene structural types are cracked from the coal surface which undergo secondary H atom reaction to produce smaller hydrocarbons via a ring saturation, ring opening and ring cleavage sequence.

Nonetheless, hydrogen atom cracking of the coal surface has been achieved under the mildest hydrogenation conditions reported thusfar. The significance of this observation is that increasing the hydrogen atom concentration, for example by thermal dissociation of hydrogen at high temperatures, in commercial coal hydrogenation processes may lead to better conversion and cost versus value ratio.

BIBLIOGRAPHY

(1) Hendrikson, T. A., "Synthetic Fuels Data Handbook: U.S. Coal", Cameron Enginers Inc., Denver, Co., 1975, p.119.

(2) Larsen, J. W., Proc. NSF Worksh., 1975, p.8.

(3) Mains, G. J., Private Communication, Research Proposal to U. S. Department of Energy, 1976.

(4) Boddle, W. W., and Vyas, K. C., Clean Fuels from Coal Symposium II, Inst. Gas Tech., Chicago, 1975, PaperI.

(5) American Society for Testing and Materials, 1976 Annual Book of ASTM Standards, Designation: D-388-66, p.211.

(6) Weiss, A. J., Hydrocarbon Processing, June 1978, p.125-129.

(7) Fisher, C. H., Ind. Eng. Chem., 31, 1155 (1935).

(8) Bailey, M. E., J. Chem. Ed., 51, 446 (1974).

(9) van Krevelen, D. W., and Schuyer, J. J., Coal Science, Elsevier, 1957.

(10) Given, P. H., Fuel, 39, 147 (1960).

(11) Sheer, M., "Materials Problems and Research Opportunities in Coal Conversion", Vol. II, Corrosion Center, Ohio State U., Columbus, Ohio, 1974.

(12) Given, P. H., Proc. NSF Worksh., 1975, p. 42.

(13) Brooks, J. D., Durie, R. A., and Sternhell, S., J. Inst. Fuel., 29, 82(1956).

(14) Iyengar, M. S., Guha, S., and Beri, M.L., Fuel, 39, 235(1960).

(15) Hirsh, P. B., Proc. Roy. Soc. Lond., 2264, 143 (1954).

(16) Brown, J. K., Ladner, W. R., and Sheppard, N., Fuel, 39, 87 (1960).

(17) Richardson, F. W., 'Oil from Coal', Noyes Data Corporation, Park Ridge, N. J., 1975.

(18) Avramenko, V. J., J. Phys. Chem. (USSR), 20, 1229 (1946).

(19) Harris, G. M., and Tickner, A. W., Nature(Lond), 160, 871 (1947).

(20) Farkas, A., "Experimental Methods in Gas Reactions", McMillan, 1939, p.356.

(21) Blackwood, J. D., and McTaggart, F. K., Australian. J. Chem., 12, 533 (1959).

(22) Shahin, N. M., Nature(Lond.), 195, 992 (1962).

(23) Vastola, F. J., Walker, P. L., and Wightman, J. P., Carbon, 1, 11 (1963).

(24) King, A. B., and Wise., H. J., J. Phys. Chem., 67, 1163 (1963).

(25) Letort, M., Boyer, A. F., and Payen, P., Bull. Soc. Chim. Fr., 1589 (1963) vis Pinchin, F. J., Brit. Coal Util. Res. Asssoc., Monthly Bulletin, 29, 105 (1965).

(26) Gill, P. S., Toomy, R. E., and Moser, H. C., Carbon, 5, 43 (1967).

(27) Wood, B. J., and Wise, H., J. Phys. Chem., 73, 1348 (1969).

(28) Berkowitz, N., and Sanda, Y., Fuel, 48, 375 (1969).

(29) McCarroll, B., and McKee, D. W., Carbon, 9, 301 (1971).

(30) Snelson, A., A. C. S. Div. Fuel Chem. Proc., 18, 101 (1973).

(31) Weigert, F., Ann. der Phys., 24, 243(1907).

(32) Cario, G., and Frank, J., Z. Physiky., 17, 202(1923).

(33) Noyes, W. A., and Leighton, P. A., 'The Photochemistry of Gases', Reinhold (1941).

(34) Sodoski, T. T., and Roche, W. J., Annual IES Conf., July 13-17, San Franciso, Calif.

(35) Kimbeu, G. H., and Le Roy, D. J., Can. J. Chem., 38, 1714(1960).

(36) Mains, G. J., 'Mercury Photosensitization' - An unfolding story', Research Note # 138, Quantum Theoretical Group, Oklahoma State University, Stillwater (1973).

(37) Callear, A. B., and McGurk, J. C., J. Chem. Soc., Faraday II, 68, 289(1972).

(38) Callear, A. B., and Wood, P. M., J. Chem. Soc., Faraday II, 68, 302(1972).

(39) Mitchell, A.C.G., Proc. Nat. Acad. Sci., 11, 458(1925).

(40) Compton, K.T., and Turner, L. A., Phil. Mag., 48, 360(1924).

(41) Yang, K., and Hansel, C., J. Chem. Phys., 47, 3824(1967).

(42) Light, J. C., and Pechunkar, P., J. Chem. Phys., 42, 3821(1965).

(43) Hong, J. H., and Mains, G. J., J. Photochem., 1, 463(1973).

(44) Michael, J.V., and Yeh, C., J. Chem. Phys., 53, 59(1970).

(45) Burgess, H. J., and Wheeler, R. V., J. Chem. Soc., 105, 131(1914).

(46) (a) Melton, C. E., and Rudolph, P. S., Naturewissenchaften, 54, 297(1967). (b) Girling, G. W., J. Appl. chem., 13, 77(1963).

(47) Rahman, M., and Vahrman, M., Fuel, 50, 318(1971).

(48) Vahrman, M., and Watts, R. H., Fuel, 51, 236(1972).

(49) Radd, F. J., Carrel, A. B., and Hamming, W. C., 'Analytical Methods for Coal and Coal Products', ed. Karr, Jr., C., Academic Press, New York, NY - To be published.

(50) Melton, C. E., and Giardini, A. A., Fuel, 54, (1975).

(51) Solomon, J. A., and Mains, G. J., Fuel, 56, 302(1977).

(52) Micropulverizer, 6731431, Slick corporation, Summit, N. J.

(53) (a) Lowrison, G. C., 'Crushing and Grinding', Buttorworths, p. 33 (1974). (b) Nakanichi, E and Toyotate, K., Funsai (Micrometrics), 18, 94(1973) via Chemical Abstracts, 81, 171948. (c) Khrenekova, T., Lebedov, V., Goldenko, N., and glovina, G., Khim. Tverd. Topl., 11, 1975 via Chem. Abstr., 83, 13132.

(54) Field, M. A., Gill, D. W., Morgan, B. B., and Haksley, P. G. W., 'Combustion of Pulverised Coal', Brit. coal Res. Utl. Ass., Leatherhead, England, 1967, p.245.

(55) Allen, T., 'Particle size Measurement', 2nd Edn., John wiley & sons., N.Y., 1975.

(56) Solomon, J. A., and Enright, R. J., Proceedings of the 8th Biennial Conference of the international Briquetting Association, Denver, Co., 1963 , p.61.

(57) Pinchin, F. J., Brit. Coal Util. Res. Assoc., Monthly Bullettin, 29, 105(1963).

(58) Michael, J. V., and Ahumada, J., J. Phys. chem., 75, 465(1974).

(59) Kim, P., Lee, J., and Ahumada, R., and Timmons, R., J. Chem. Phys., 59, 4593(1973).

(60) Koller, L. R., 'Ultraviolet Radiation'. John wiley & sons, Inc., N.Y., 1965, p. 52.

(61) King, D.L., and Sester, D.W., Ann. Rev. Phy. Chem., 27, 407(1976).

(62) Roberts, R.E., Bunstein, R. B., and Curtis, R. F., J. Chem. Phys., 50, 5163(1969).

(63) Bennett, J. E., and Blackmore, D. R., Proc. Roy. Soc., A303, 53(1968).

(64) Baluch, D. L., Drysdale, D. D., Horne, D. G., and Lloyd, A. C., 'Evaluated Kinetic Data for High Temperature Reactions', Butterworths, London, 1973, Vol. 1.

(65) Trainer, D. W., Ham, D. D., and Kaufmann, F., J. Chem. Phys., 58, 4599(1973).

(66) Shuler, K. E., and Laidler, K. J., J. Chem. Phys., 17, 1212(1949).

(67) Sato, S., J. Chem. Soc. Japan, 76, 1308(1955).

(68) Wood, B. J., and Wise, H., J. Phys. Chem., 65, 1976(1961).

(69) Wood, B. J., and Wise, H., J. Phys. Chem., 65, 1976(1961).

(70) Gelb, A., and Kim, S. K., J. Chem. Phys., 55, 4935(1971).

(71) Oref, I., Rabinovitch, B. S., J. Phys. Chem., 72, 4488(1968).

(72) Whittle, E., 'Chemical Kinetics', Phys. Chem. Ser. One, Vol.9, Butteerworths, London, 1972, p.80.

(73) Cowfer, B. J., J. Phys. Chem., 65, 1976(1961).

(74) Bradley, J. N., Melville, H. W., and Rob, J. C., Proc. Roy. Soc.(London), A236, 339(1956).

(75) Smith, M. J., Beath, P. M., Pinder, J. A., and LeRoy, D. J., Can. J. Chem., 33, 821(1955).

(76) Melville, H. W., and Robb, J. C., Proc. Roy. Soc.(London), A196, 445(1949)., ibid, 46691949).

(77) Cvtanovic, R. J., 'Advances in Photochemistry', Ed. Noyes Jr., W. A., Hammond, G. S., and Pitts Jr., J. N., Vol. 1, Interscience, 1963, p. 151. Koller, L. R., 'Ultraviolet Radiation', John Wiley & Sons, Inc., N.Y., p.52, 1965.

(78) Mitchell, A., and Zemmansky, M., 'Resonance Radiation and Excited Atoms', Cambridge U. Press, 1961.

(79) Calvert, J., and Pitts, J., 'Photochemistry', John Wiley & Sons, Inc., N.Y., 1969, p. 689.

(80) Brown, R. A., Anal. Chem., 23, 430(1951).

(81) Swansiger, J. T., Dickso, F. E., and Best, H. T., Anal. Chem., 46, 730(1974).

(82) (a) Zweig, c., and Sherma, J., Anal. Chem., 46, 73R(1974). (b) Dark, W. A., Amer. Lab., August 1975, p. 50.

(83) Kirkland, J. J., J. Chromat., 125, 231(1976).

(84) Scott, R. P. W., Analyst, 103, 3791978).

(85) 'GLC and HPLC of Therapeutic Agents', Ed. Kiyoshi Tsuji, Marcel-Dekker, New York, N.Y., 1978, p.103.

(86) Waters Associates, 'Recycle Chromatography', Product Information Bulleettin.

(87) Friedel, R. A., and Orchin, M., 'Ultraviolet Spectra of Organic Compounds', John Wiley & Sons, Inc., NY, 1951.

(88) Linder, D. E., Abstract # 338, Pittsburgh Conference on Analytrical Chemistry, March 4-8, 1974.

(89) Campbell, B., CRC Crit. Rev. in Anal. Chem., October 1975.

(90) Penn, D., J. Electron Spectrosc., 9, 29(1976).

(91) Sieghban, K., 'Electron Spectroscopy', Ed. Shirley, D., North Holland Pub.Co., Amsterdam, 1972, p.24.

(92) Hutchital, D. A., and McKean, R. T., Appl. Phys. Lett., 20, 158(1972). Sieghban, K., 'Electron Spectroscopy', Ed. Shirley, D., North Holland Pub. Co., amsterdam, 1972, p. 24.

(93) Sieghban, K., J. Electron Spectrosc., 5, 13(1974).

(94) Frost, D. L., Leeds, N. R., and Tapping, R. L., Fuel, 53, 206(1974).

(95) Amano, A., Horie, O., and Hanh, W., Int. J. Chem. Kin., 8, 321(1976).

(96) Amano, A., Horie, O., and Hanh, N. H., Chem. Lett., Chem. Soc. Japan., 917(1972).

(97) Mulcahay, M. F. R., Harrisson, R. J., and Wilmhurst, J. R., Aust. J. Chem., 19, 1431(1966).

(98) Harrisson, T., J. Chem. Phys., 50, 4653(1969).

(99) ASTM Book of Standards, Designation 32597-3(1973).

(100) Vahrman, M., and Watts, R. H., Fuel, 51, 23591972).

(101) Pauling, L., 'The Nature of Chemical Bond', 3rd Ed., Cornell U. Press, Ithaca, N.Y., 1969, p. 199.

(102) Burges, A., and Mossettig, E., J. Amer. Chem. soc., 57, 2731(1935).

(103) Durland, J. R., and Adkins, H., J. Amer. Chem. Soc., 59, 135(1937).

(104) Durland, J. R., and Adkins, H., J. Amer. Chem. Soc., 60, 1501(1938).

(105) Kowan, K., Ph. D. Thesis, Oklahoma State University, Stillwater, Oklahoma, 1977.

(106) Qader, S. A., Chun Chen, L., andOmber, D. B., Div. Petr. Chem., ACS Meeting, Dallas, April 8-13 (1973), p. 60.

(107) Huang, C. s., Wang, K. C., and Hynes, H. W. Jr., 'Liquid fuels from Coal', Ed. Ellington, R. T., Academic Press, NY, 1977, p. 63.

(108) Hayness, H. W., Private Communication.

(109) Masson, G. R., Boekelheide, V., and Noyes, W. A., 'Photochemical Reactions' in 'Technique of Organic Chemistry', Vol. II, Interscience, New York, 1956.

(110) Snelson, A.,IIT Research Institute, Chicago, Private Communication.

(111) Coulon, M., and Bonnetain, L., J. Chemie. Physique., 71, 725(1974).

(112) Coulon, M., and Bonnetain, L., J. Chemie. Physique., 71, 717(1974).

(113) Whitehurst, D. D., and Mitchell, T. O., 'Liquid Fuels from Coal', Ed. Ellington, R. T., Academic Press, New York, N.Y., 1977, p.153-172.

(114) Farcasiu, M., A.C.S. Fuel Div., Pacific Conference, Honolulu, Hawaii, April 2-6, 1979, Preprints, 24(1), (1979).

(115) Walker, P., Jr., Fuel, 51, 207(1975).

APPENDIX A

COMPUTER PROGRAMS

```
C     THE INPUT DATA FOR THE PROGRAM ARE: (I) DETECTOR SENSITIVITY C  A
C     COMPOUND, (II) ITS MOLECULAR WEIGHT, (III) TOTAL  SIGNAL OUTPUT,
C     (IV) AMOUNT OF COAL LOADED, (V) H ATOM CONCENTRATION, (VI) %
C     CARBON IN THE COAL USED AND (VII) IRRADIATION TIME.  THE PROGR M
C     CAN BE USED TO COMPUTE THE FOLLOWING: (1) MOLAR YIELDS (ABSOLUTE)
C     (2) MOLE PERCENT, (3) WEIGHT PERCENT, (4)RATE PER  MINUTE,
C     (5) RATE PER H ATOM OF EACH COMPONENT, (6) PERCENTAGE OF CARBO
C     CONVERTED, (7) MOLES OF PRODUCT FORMED PER H ATOM (PRODUCT
C     EFFICIENCY), (8) % OF H ATOMS UTILIZED PER PRODUCT MOLECULE,
C     AND (9) GROUP YIELDS (MOLES, MOLE PERCENT AND WEIGHT PERCENT)  F
C     NORMAL, BRANCHED, CYCLIC HYDROCARBONS, OLEFINS, AROMATIC HYDRO
C     CARBONS, C2-C4, C5, C6, C7, C8, BTX HYDROCARBONS, 2-RING AROMATICS
C     3-RING AROMATICS ETC.  ALL THE ABOVE DATA COULD BE PLOTTED IN  DE
C     LINE PRINTER BY USING THE SUBROUTINE  SBSPLOT  WHICH IS INCLUDED
C     IN THE PROGRAM.
      DIMENSION RC(3,3,40,5), SUM(3,40,5), SUM1(3,40,5)
      DIMENSION XMOLE(3,3,40,5), GMCAR(3,3,40,5), WEIGHT(3,3,40,5),
     *          MMOLE(3,3,40,5), MPERT(3,3,40,5), RTIME(3,3,40,5),
     *          RTHATM(3,3,40,5), XLPCNT(3,3,40,5), WTPCNT(3,3,40,5)
      DIMENSION AVMOLE(3,40,5),AVRTHM(3,40,5),AVMTHM(3,40,5),
     *          AVMLPC(3,40,5),AV TPC(3,40,5)
      DIMENSION TAB1(40),TAB2(40),TAB3(40),TAB4(40),TAB5(40)
      DIMENSION SENS(40),CARBON(40),XMOLWT(40),
     $XLSUM(3,3,5),GCSUM(3,3,5),WTSUM(3,3,5),
     $TOTMOL(3,3,5), TOTCAR(3,3,5),TOTWT(3,3,5),
     $T(3,5), THATOM(3,3,5),
     $PCTCON(3,3,5),HATEFF(3,3,5),HATUTL(3,3,5)
      INTEGER TI(3,3,5) ,NORUNS(3,5)
      INTEGER T
      DIMENSION T2(3,3,5)
      REAL INTMOL(3,3,5), INTOCR (3,3,5),INPCON(3,3,5),PHATUT(3,3,5)
      DIMENSION C2C4ML(  3,5),CBIYML(  3,5),CSIXML(  3,5),CSYSML(  3,5)
     $          CBITML(  3,5),CAORML(  3,5),CBRRML(  3,5),CSAIML(  3,5)
     $          C2C4MP(  3,5),CBIYMP(  3,5),CSIXMP(  3,5),CSYSMP(  3,5)
     $          CBITMP(  3,5),CAORMP(  3,5),CBRRMP(  3,5),CSAIMP(  3,5)
      DIMENSION OLEFML(3,5),OLEFMP(3,5), AROMML(3,5),AROMMP(3,5),
     *          BTXML(3,5), BTXMP(3,5), C10HOL(3,5),C10HBP(3,5),
     *          RNG3ML(3,5),RNG3MP(3,5)
      DIMENSION ARO1ML(3,5),ARO1MP(3,5),ARO2ML(3,5),ARO2MP(3,5)
      DIMENSION RINGS(3,5),RINGP(3,5)
      DIMENSION AVTLML(3,5),AVPCCN(3,5),AVMEFF(3,5),AVHUTL(3,5)
      DIMENSION NAVRG(5),NPART1(5),NPART2(5),NTEMP1(5),NTEMP2(5)
      DIMENSION COALLD(5),MATOMS(5),P2(5),MG(5)
      WRITE (6, 1)
    1 FORMAT (////////////////, 40X, '*PHOTOCHEMICAL CONVERSION OF COAL
     $TO GASOLINE*', ////, 37X,'U.S. DEPARTMENT OF ENERGY CONTRACT [ EY
     $-76-S-05-5020',///,41X,'PRINCIPAL INVESTIGATOR: DR.GILBERT J. MAIN
     $ ', ////, 57X, ' PROGRAMMER:', ////, 55X, 'MURPU S. SUNDARAM', /
     $/, 52X, 'DEPARTMENT OF CHEMISTRY',   //, 51X, 'OKLAHOMA STATE  NI
     $VERSITY',   //, 50X, 'STILLWATER, OKLAHOMA 74074'  )
      READ(5,20) NPARM1,NPARM2
      DO 1000 MG= NPARM1,NPARM2
   11 FORMAT(1H1,////////////////////////////,45X,'PARAMETRIC VARIABLE',
     *'////,47X,'1. H ATOM CONCENTRATION')
   12 FORMAT(1H1,////////////////////////////,45X,'PARAMETRIC VARIABLE'
     *'////,47X,'2. TEMPERATURE')
   13 FORMAT(1H1,////////////////////////////,45X,'PARAMETRIC VARIABLE',
     *'////,43X,'3. COAL PARTICLE SIZE')
      GO TO (2,4,6), MG
    2 WRITE (6,11)
      GO TO 14
    4 WRITE (6,12)
      GO TO 14
    6 WRITE (6,13)
   14 CONTINUE
      READ (5,20) NV, M, N, NTRIAL
   20 FORMAT (10 I5)
      DO 17 L = 1, NV
   17 READ (5,20) (NORUNS(L,K), K = 1, NTRIAL)
      READ (5,20) (NAVRG(I), I = 1, NV)
      READ (5,10) MPEON, CPCNT
   10 FORMAT (F5.1,5X,F5.2)
      DO 15 I = 1, NV
   15 READ(5,20) NPART1(I),NPART2(I),NTEMP1(I),NTEMP2(I)
      DO 16 I = 1, NV
   16 READ (5,22) COALLD(I),MATOMS(I),P2(I),MG(I)
   22 FORMAT (F5.2,5X,E10.4,2(4X,F6.2))
      DO 25 K = 1, NV
      READ (5, 20) ( T(K,I), I = 1, M)
   25 CONTINUE
      DO 3 L = 1, NV
      DO 3 K = 1, NTRIAL
    3 READ (5,20) (TI(L,K,J), J = 1, M)
      DO 26 I = 1, N
      READ (5,51) TAB1(I), TAB2(I), TAB3(I), TAB4(I), TAB5(I)
   51 FORMAT (5A4)
   26 CONTINUE
      DO 50 I = 1, N
      READ (5, 40) SENS (I), CARBON (I), XMOLWT (I)
   40 FORMAT ( E 15. 8, 2 ( 4X, F6. 2))
   50 CONTINUE
      AVGNUM = 6. 023 E + 23
      DO 70 L = 1, NV
      DO  70 K = 1, NTRIAL
      DO 70 I = 1, N
      READ (5,60) (RC(L,K,I,J), J = 1, M)
   60 FORMAT (7 (E10. 4, 2X))
   70 CONTINUE
      DO 90 L = 1, NV
      COAL = COALLD(L)
      DO  90 K = 1, NTRIAL
      DO 90 I = 1, N
      DO 80 J = 1, M
      IF (SENS(I).EQ.0) GO TO 75
      IF (RC(L,K,I,J).EQ.0) XMOLE(L,K,I,J) = 0.
      IF (RC(L,K,I,J).NE.0) XMOLE(L,K,I,J) = (RC(L,K,I,J)*SENS(I))/COAL
      GO TO 76
   75 XMOLE(L,K,I,J) = 0.
   76 CONTINUE
      GMCAR(L,K,I,J) = XMOLE(L,K,I,J)*CARBON(I)
      WEIGHT(L,K,I,J) = XMOLE(L,K,I,J)*XMOLWT(I)
   80 CONTINUE
   90 CONTINUE
      DO 110 L = 1, NV
      DO 110 K = 1, NTRIAL
      DO 110 I = 1, N
```

```
      DO 100 J = 1, M
      XLSUM(L,K,J) = 0.
      GCSUM(L,K,J) = 0.
      WTSUM(L,K,J) = 0.
      TOTMOL(L,K,J) = 0.
      TOTCAR(L,K,J) = 0.
      TOTWT (L,K,J) = 0.
      HRMOLE(L,K,I,J) = 0.
      HRWEIT(L,K,I,J) = 0.
      TI(L,K,J) = FLOAT(TI(L,K,J))
  100 CONTINUE
  110 CONTINUE
      DO 130 L = 1, NV
      DO 130 K = 1, NTRIAL
      DO 130 J = 1, M
       DO 120 I   = 1, N
      XLSUM (L,K,J) = XLSUM (L,K,J) + XMOLE (L,K,I,J)
      GCSUM (L,K,J) = GCSUM (L,K,J) + GRMCAR(L,K,I,J)
      WTSUM (L,K,J) = WTSUM (L,K,J) + WEIGHT(L,K,I,J)
  120 CONTINUE
  130 CONTINUE
      DO 140 L = 1, NV
      DO 140 K = 1, NTRIAL
      DO 140 J = 1, M
      J1 = J - 1
      IF (J1.EQ.0) TOTMOL(L,K,J) = XLSUM(L,K,J)
      IF (J1.EQ.0) TOTCAR(L,K,J) = GCSUM(L,K,J)
      IF (J1.EQ.0) TOTWT (L,K,J) = WTSUM(L,K,J)
      IF (J1.NE.0) TOTMOL(L,K,J) = XLSUM(L,K,J) + TOTMOL(L,K,J1)
      IF (J1.NE.0) TOTCAR(L,K,J) = GCSUM(L,K,J) + TOTCAR(L,K,J1)
      IF (J1.NE.0) TOTWT (L,K,J) = WTSUM(L,K,J) + TOTWT (L,K,J1)
      IF(TOTMOL(L,K,J).NE.0) XNMOL(L,K,J)=TOTMOL(L,K,J)/TOTMOL(L,K,1)
  140 CONTINUE
      DO 160 L = 1, NV
      DO 160 K = 1, NTRIAL
      DO 160 I = 1, N
      DO 150 J = 1, M
      J1 = J - 1
      IF(XMOLE(L,K,I,J).EQ.0) HRMOLE(L,K,I,J) = 0.
      IF (J1.EQ.0) HRMOLE(L,K,I,J) = XMOLE(L,K,I,J)
      IF (J1.NE.0) HRMOLE(L,K,I,J) = XMOLE(L,K,I,J)+ HRMOLE(L,K,I,J1)
      IF (J1.EQ.0) HRWEIT(L,K,I,J) = WEIGHT(L,K,I,J)
      IF (J1.NE.0) HRWEIT(L,K,I,J) = WEIGHT(L,K,I,J)+HRWEIT(L,K,I,J1
  150 CONTINUE
  160 CONTINUE
      CALL SPSAVG(M,N,NV,NTRIAL,TI,HRMOLE,AVMOLE,RC,SUM)
      DO 190 L = 1, NV
      NATOM = NATOMS(L)
      DO 180 I = 1, N
      DO 180 J = 1, M
      J1 = J - 1
      IF(AVMOLE(L,I,J)) 175,175,176
  175 AVPTMX(L,I,J) = 0.
      AVPTMY(L,I,J) = 0.
      GO TO 180
  176 CONTINUE
      IF (J1.GT.0) GO TO 171
      AVPTMX (L,I,J) = AVMOLE(L,I,J) / (T(L,J)*60.)
       AVPTMY(L,I,J) = AVMOLE(L,I,J)/((T(L,J)*60.*NATOM*60.)/AVGNUM)
      GO TO 180
  171 IF (AVMOLE(L,I,J).EQ.0) AVPTMX(L,I,J) = 0.
      IF (AVMOLE(L,I,J).EQ.0) AVPTMY(L,I,J) = 0.
      IF(AVMOLE(L,I,J).EQ.0) GO TO 180
      AVPTMX(L,I,J) = (AVMOLE(L,I,J)-AVMOLE(L,I,J1))/
     *((T(L,J) - T(L,J1)) * 60.)
      AVPTMY (L,I,J) = (AVMOLE(L,I,J)-AVMOLE(L,I,J1))/((T(L,J)-T(L,J1)
     **60.*NATOM*60. / AVGNUM)
  180 CONTINUE
      DO 200 L = 1, NV
      DO 200 K = 1, NTRIAL
      DO 200 J = 1 , M
      DO 190 I = 1   , N
      IF (PC(L,K,I,J)) 185,185,186
  185 XLPCNT(L,K,I,J) = 0.
      WTPCNT(L,K,I,J) = 0.
      GO TO 190
  186 CONTINUE
      XLPCNT(L,K,I,J) = (HRMOLE(L,K,I,J)/TOTMOL(L,K,J)) * 100.
      WTPCNT(L,K,I,J) = (HRWEIT(L,K,I,J)/TOTWT (L,K,J)) * 100.
  190 CONTINUE
  200 CONTINUE
      DO 210 L = 1, NV
      COAL = COALLD(L)
      DO 210 K = 1, NTRIAL
      DO 210 J = 1 , M
       IF(TI(L,K,J).EQ.0) GO TO 210
      PCTCON(L,K,J) = (TOTCAR(L,K,J)/CPCNT) * 100.
      THATOM(L,K,J) = HATOMS(L)*60.*TI(L,K,J)*60.
      IAPCON(L,K,J) = PCTCON(L,K,J) / PCTCON(L,K,1)
      PHATUT(L,K,J) = THATOM(L,K,J) / (TOTMOL(L,K,J) * AVGNUM *COAL)
      PHATUT(L,K,J) = (HATUTL(L,K,J) /THATOM(L,K,J) * 100.)
      HATEFF(L,K,J) = 1. / HATUTL(L,K,J)
  210 CONTINUE
      CALL SPSAVC(M,N,NV,NTRIAL,TI,APCNT,AVWTPC,RC,SUM)
      CALL SPSAVG(M,N,NV,NTRIAL,TI,ALPCNT,AVWLPC,RC,SUM)
      NT = NTRIAL
      CALL SPSAVI (M,NV,NT,TI,TOTMOL,AVTLML,SUM1)
      CALL SPSAVI (M,NV,NT,TI,PCTCON,AVPCCN,SUM1)
      CALL SPSAVI (M,NV,NT,TI,HATEFF,AVHEFF,SUM1)
      CALL SPSAVI (M,NV,NT,TI,HATUTL,AVHUTL,SUM1)
      CALL SPSADD(N,HRMOLE,TOTMOL,C4,C4ML,C4C4MP, 1, 2, 3, 4, 0, 0, 0  0
     *              4,TI,NV,NT,M,SUM1)
      CALL SPSADD(N,HRMOLE,TOTMOL,CFIVML,CFIVMP, 5, 6, 7, 8, 0, 0, 0, 0
     *              4,TI,NV,NT,M,SUM1)
      CALL SPSADD(N,HRMOLE,TOTMOL,CSIXML,CSIXMP, 9,10,11,12,13, 0, 0,0,
     *              5,TI,NV,NT,M,SUM1)
      CALL SPSADD(N,HRMOLE,TOTMOL,CSVNML,CSVNMP,14,15,16,17,18,19, 0 0,
     *              6,TI,NV,NT,M,SUM1)
      CALL SPSADD(N,HRMOLE,TOTMOL,CSEIML,CSEIMP,20,21, 0, 0, 0, 0, 0,0,
     *              2,TI,NV,NT,M,SUM1)
      CALL SPSADD(N,HRMOLE,TOTMOL,CNORML,CNORMP, 1, 2, 4, 7,11,16, 0, 0
     *              6,TI,NV,NT,M,SUM1)
      CALL SPSADD(N,HRMOLE,TOTMOL,CPRNML,CPRNMP, 3, 5, 6, 9,10,14,15  0
     *              7,TI,NV,NT,M,SUM1)
      CALL SPSADD(N,HRMOLE,TOTMOL,CSATML,CSATMP, 8,12,13,17,19,20,21, 0
     *              7,TI,NV,NT,M,SUM1)

      CALL SPSADD(N,HRMOLE,TOTMOL,OLEFML,OLEFMP,22,23,24, 0, 0, 0, 0  0
     *              3,TI,NV,NT,M,SUM1)
      CALL SPSADD(N,HRMOLE,TOTMOL,ARO1ML,ARO1MP,25,26,27,28,29,30,31,32
     *              8,TI,NV,NT,M,SUM1)
      CALL SPSADD(N,HRMOLE,TOTMOL,ARO2ML,ARO2MP,33,34,35,36,37,38,39,40
     *              *,TI,NV,NT,M,SUM1)
      CALL SPSADD(N,HRMOLE,TOTMOL,BTXML ,BTXMP ,25,26,27, 0, 0, 0, 0  0
     *              3,TI,NV,NT,M,SUM1)
      CALL SPSADD(N,HRMOLE,TOTMOL,C10NML,C10NMP,28,29,30,31,32, 0, 0, 0
     *              5,TI,NV,NT,M,SUM1)
      CALL SPSADD(N,HRMOLE,TOTMOL,NNC3ML,NNC3MP,33,34, 0, 0, 0, 0, 0, 0
     *              2,TI,NV,NT,M,SUM1)
      CALL SPSADD(N,HRMOLE,TOTMOL,HIRNGL,HIRNGP,35,36,37,38,39,40, 0  0
     *              6,TI,NV,NT,M,SUM1)
  355 FORMAT(1PL, 42X,'PROCESS EFFICIENCY REPORT')
  365 FORMAT(//,14X,'TIME',11X,'YIELD',13X,'CONVERSION',10X,'EFFICIE CY
     *',6X,'H ATOMS',//)
  450 FORMAT (/,15X,I2,3(5X,E15.4),5X,F6.0)
      WRITE (6,355)
      DO 370 L = 1, NV
      CALL SPSASK (NV,NPART1,NPZ1,NPART2,NPZ2,NTEMP1,NTMP1,NTEMP2,NTMP2
     *MAXRG,MA,M2,M2C,ME,MEC,L,1)
      WRITE (6,365)
      DO 370 J = 1, M
       WRITE (6,450) T(L,J),AVTLML(L,J),AVPCCN(L,J),AVHEFF(L,J),AVHU L(
     *,J)
  370 CONTINUE
      WRITE (6,400)
  400 FORMAT (1H1,33X,'TOTAL YIELD BY GROUP SELECTIVITIES: ALIPHATICS')
      DO 452 L = 1, NV
      CALL SPSASM (NV,NPART1,NPZ1,NPART2,NPZ2,NTEMP1,NTMP1,NTEMP2,NTMP2
     *MAXRG,MA,M2,M2C,ME,MEC,L,1)
      WRITE (6,366)
  366 FORMAT(//,14X,'TIME',9X,'C2 - C4',18X,'C5',18X,'C6',17X,'C7',17X,
     **'C8',//)
  451 FORMAT (/,15X,I2,5(5X,E15.4))
```

```
      DO 452 J = 1, M
      WRITE (6,451) T(L,J),C2C4RL(L,J),CFIYRL(L,J),CSIXRL(L,J),CSVRRL(L
     *J),CEITRL(L,J)
452   CONTINUE
      WRITE (6,500)
500   FORMAT (1H1, 33X,'TOTAL YIELD BY GROUP SELECTIVITIES: AROMATICS')
      DO 502 L = 1, NV
      CALL SPSASN (NV,NPART1,NPZ1,NPART2,NPZ2,NTEMP1,NTMP1,NTEMP2,NTMP2
     *NAVRG,MA,M2,M2C,ME,MEC,L,1)
      WRITE (6,501)
501   FORMAT(//,14X,'TIME',11X,'BTX',18X,'2 RINGS',17X,'3 RINGS',15X,
     *'4+ RINGS')
      DO 502 J = 1, M
      WRITE (6,451) T(L,J),BTXRL(L,J),C10HRL(L,J),RNG3RL(L,J),RI*NGL(L,
     *)
502   CONTINUE
      WRITE (6,367)
367   FORMAT (1H1, 41X,'TOTAL YIELD BY COMPOUND TYPE')
      DO 369 L = 1, NV
      CALL SPSASN (NV,NPART1,NPZ1,NPART2,NPZ2,NTEMP1,NTMP1,NTEMP2,NTMP2
     *NAVRG,MA,M2,M2C,ME,MEC,L,1)
      WRITE (6,368)
368   FORMAT(//,14X,'TIME',11X,'NORMAL', 13X,'BRANCHED',13X,'CYCLIC'
     *13X,'OLEFINIC',13X,'AROMATIC')
      DO 369 J = 1, M
      AROMRL(L,J) = ARO1RL(L,J) + ARO2RL(L,J)
      WRITE (6,451) T(L,J),CNORRL(L,J),CBRNRL(L,J),CSATRL(L,J),OLEFRL(L
     *J), AROMRL(L,J)
369   CONTINUE
220   FORMAT (1H1)
      WRITE (6,378)
378   FORMAT(1H1,31X,'PERCENTAGE YIELD BY GROUP SELECTIVITIES: ALIPE TI
     *S')
      DO 371 L = 1, NV
      CALL SPSASN(NV,NPART1,NPZ1,NPART2,NPZ2,NTEMP1,NTMP1,NTEMP2,NTM 2,
     *NAVRG,MA,M2,M2C,ME,MEC,L,1)
      WRITE (6,366)
      DO 371 J = 1, M
      WRITE (6,451) T(L,J),C2C4RP(L,J),CFIYRP(L,J),CSIXRP(L,J),CSVRRP(L
     *J),CEITRP(L,J)
371   CONTINUE
      WRITE (6,510)
510   FORMAT (1H1,///,31X,'PERCENTAGE YIELD BY GROUP SELECTIVITIES: AROM
     *TICS')
      DO 512 L = 1, NV
      CALL SPSASN (NV,NPART1,NPZ1,NPART2,NPZ2,NTEMP1,NTMP1,NTEMP2,NTMP2
     *NAVRG,MA,M2,M2C,ME,MEC,L,1)
      WRITE (6,501)
      DO 512 J = 1, M
      WRITE (6,451) T(L,J),BTXRP(L,J),C10HRP(L,J),RNG3RP(L,J),RIRNGP(L,
     *)
512   CONTINUE
      WRITE (6,372)
372   FORMAT (1H1,///,39X,'PERCENTAGE YIELD BY COMPOUND TYPE')
      DO 373 L = 1, NV
      CALL SPSASN(NV,NPART1,NPZ1,NPART2,NPZ2,NTEMP1,NTMP1,NTEMP2,NTM 2,
     *NAVRG,MA,M2,M2C,ME,MEC,L,1)
      WRITE (6,368)
      DO 373 J = 1, M
      AROMRP(L,J) = ARO1RP(L,J) + ARO2RP(L,J)
      WRITE(6,451) T(L,J),CNORRP(L,J),CBRNRP(L,J),CSATRP(L,J),OLEFRP(L,
     *J),AROMRP(L,J)
373   CONTINUE
      WRITE (6,220)
      WRITE (6,239)
239   FORMAT(1HO,28X,'AVERAGE YIELD IN MOLES/GRAM COAL AS FUNCTION OF T
     *S*TIME')
      CALL SPSRIT(NV,M,N,T,AVMOLE,TAB1,TAB2,TAB3,TAB4,TAB5,NPART1,NP RT
     *,NTEMP1,NTEMP2,M2,ME)
      WRITE (6, 280)
280   FORMAT(1HO,24X,'AVERAGE RATE IN MOLES/GRAM COAL/MINUTE AS FUNC IO
     *S OF TIME')
      CALL SPSRIT(NV,M,N,T,AVRTMN,TAB1,TAB2,TAB3,TAB4,TAB5,NPART1,NPART
     *,NTEMP1,NTEMP2,M2,ME)
      WRITE (6, 300)
300   FORMAT(1HO,27X,'AVERAGE RATE IN MOLES/GRAM COAL/GRAM AROM S AS FU
     *SCTION OF TIME')
      CALL SPSRIT(NV,M,N,T,AVRTHY,TAB1,TAB2,TAB3,TAB4,TAB5,NPART1,NPART
     *,NTEMP1,NTEMP2,M2,ME)
      WRITE (6, 320)
320   FORMAT(1HO,32X,'AVERAGE WEIGHT PERCENT AS FUNCTION OF TIME')
      CALL SPSRIT(NV,M,N,T,AVWEPC,TAB1,TAB2,TAB3,TAB4,TAB5,NPART1,NPART
     *,NTEMP1,NTEMP2,M2,ME)
      WRITE (6, 340)
340   FORMAT(1HO,32X,'AVERAGE  MOLE  PERCENT AS FUNCTION OF TIME')
      CALL SPSRIT(NV,M,N,T,AVMEPC,TAB1,TAB2,TAB3,TAB4,TAB5,NPART1,NPART
     *,NTEMP1,NTEMP2,M2,ME)
      DO 177 L = 1, NV
      DO 177 J = 1, M
      AVTLML(L,J) = AVTLML(L,J) *1.0E+06
      AVPCCM(L,J) = AVPCCM(L,J) *1.0E+02
      AVHEFF(L,J) = AVHEFF(L,J) *1.0E+03
      C2C4ML(L,J) = C2C4ML(L,J) *1.0E+06
      CFIYML(L,J) = CFIYML(L,J) *1.0E+06
      CSIXML(L,J) = CSIXML(L,J) *1.0E+06
      CSVRML(L,J) = CSVRML(L,J) *1.0E+06
      CEITML(L,J) = CEITML(L,J) *1.0E+06
      CNORML(L,J) = CNORML(L,J) *1.0E+06
      CBRNML(L,J) = CBRNML(L,J) *1.0E+06
      CSATML(L,J) = CSATML(L,J) *1.0E+06
      OLEFML(L,J) = OLEFML(L,J) * 1.0E+06
      BTXML (L,J) = BTXML (L,J) * 1.0E+06
      C10HML(L,J) = C10HML(L,J) * 1.0E+06
      RNG3ML(L,J) = RNG3ML(L,J) * 1.0E+06
      AROMML(L,J) = AROMML(L,J) * 1.0E+06
177   CONTINUE
C        DO 141 L = 1, NV
      DO 141 I = 1, N
      DO 141 J = 1, M
      AVMOLE (L,I,J) = AVMOLE(L,I,J) * 1.0E+06
      AVRTMN (L,I,J) = AVRTMN(L,I,J) * 1.0E+09
      AVRTHY (L,I,J) = AVRTHY(L,I,J) * 1.0E+06
141   CONTINUE
      DO 142 L = 1, NV
      DO 142 K = 1, NTRIAL
      DO 142 J = 1, M
142   TOTMOL(L,K,J) = TOTMOL(L,K,J) * 1.0E+06
      CALL SPSCOM(NV,M,T,AVTLML,NPART1,NPART2,NTEMP1,NTEMP2,1,
     *M2,ME,M0,0)
      CALL SPSCOM(NV,M,T,AVPCCM,NPART1,NPART2,NTEMP1,NTEMP2,1,
     *M2,ME,M0,0)
      CALL SPSCOM(NV,M,T,AVHEFF,NPART1,NPART2,NTEMP1,NTEMP2,1,
     *M2,ME,M0,0)
      WRITE (6,220)
      CALL SPSYLD(NV,M,T,C2C4ML,CFIYML,CSIXML,CSVRML,CEITML,
     *NPART1,NPART2,NTEMP1,NTEMP2,NAVRG,
     *M2,ME,0,M0)
      CALL SPSYLD(NV,M,T,BTXML, C10HML,RNG3ML,RNG3ML,RNG3ML,
     *NPART1,NPART2,NTEMP1,NTEMP2,NAVRG,M2,ME,-2,M0)
      CALL SPSYLD(NV,M,T,CNORML,CBRNML,CSATML,OLEFML,AROMML,
     *NPART1,NPART2,NTEMP1,NTEMP2,NAVRG,
     *M2,ME,-1,M0)
      CALL SPSYLD(NV,M,T,C2C4RP,CFIYRP,CSIXRP,CSVRRP,CEITRP,
     *NPART1,NPART2,NTEMP1,NTEMP2,NAVRG,
     *M2,ME,0,M0)
      CALL SPSYLD(NV,M,T,BTXRP, C10HRP,RNG3RP,RNG3RP,RNG3RP,
     *NPART1,NPART2,NTEMP1,NTEMP2,NAVRG,M2,ME,-2,M0)
      CALL SPSYLD(NV,M,T,CNORRP,CBRNRP,CSATRP,OLEFRP,OLEFRP,
```

```
     *NPART1,NPART2,NTEMP1,NTEMP2,MAVRG,
     *M2,ME,-1,NO)
0316      WRITE (6,220)
0317      CALL SPSCOM(NV,M,T,C2C4ML,NPART1,NPART2,NTEMP1,NTEMP2,1,
     *M2,ME,NO,0)
0318      CALL SPSCOM(NV,M,T,CP1YML,NPART1,NPART2,NTEMP1,NTEMP2,1,
     *M2,ME,NO,0)
0319      CALL SPSCOM(NV,M,T,CSIXML,NPART1,NPART2,NTEMP1,NTEMP2,1,
     *M2,ME,NO,0)
0320      CALL SPSCOM(NV,M,T,CSVNML,NPART1,NPART2,NTEMP1,NTEMP2,1,
     *M2,ME,NO,0)
0321      CALL SPSCOM(NV,M,T,CEITML,NPART1,NPART2,NTEMP1,NTEMP2,1,
     *M2,ME,NO,0)
0322      CALL SPSCOM (NV,M,T,BIXML,NPART1,NPART2,NTEMP1,NTEMP2,1,
     *M2,ME,NO,0)
0323      CALL SPSCOM(NV,M,T,C10ML,NPART1,NPART2,NTEMP1,NTEMP2,1,
     *M2,ME,NO,0)
0324      CALL SPSCOM(NV,M,T,RNG3ML,NPART1,NPART2,NTEMP1,NTEMP2,1,
     *M2,ME,NO,0)
0325      WRITE (6,220)
0326      CALL SPSCOM(NV,M,T,CNORML,NPART1,NPART2,NTEMP1,NTEMP2,1,
     *M2,ME,NO,0)
0327      CALL SPSCOM(NV,M,T,CBRNML,NPART1,NPART2,NTEMP1,NTEMP2,1,
     *M2,ME,NO,0)
0328      CALL SPSCOM(NV,M,T,CSATML,NPART1,NPART2,NTEMP1,NTEMP2,1,
     *M2,ME,NO,0)
0329      CALL SPSCOM(NV,M,T,APOMML,NPART1,NPART2,NTEMP1,NTEMP2,1,
     *M2,ME,NO,0)
0330      CALL SPSCMP(NV,M,N,T,AVWOLE,NPART1,NPART2,NTEMP1,NTEMP2,1,
     *M2,ME,NO,0)
0331      CALL SPSCMP(NV,M,N,T,AVBTPM,NPART1,NPART2,NTEMP1,NTEMP2,1,
     *M2,ME,NO,0)
0332      WRITE (6,220)
0333      CALL SPSCMP(NV,M,N,T,AVWTPC,NPART1,NPART2,NTEMP1,NTEMP2,1,
     *M2,ME,NO,0)
0334      WRITE (6,220)
0335 1000 CONTINUE
0336      STOP
0337      END
```

```
0001      SUBROUTINE SPSAVG(M,NV,NT,NTIME,VALUE1,AVG1,RC,SUM1)
0002      DIMENSION RC(NV,NT,K,M),SUM1(NV,M,M),AVG1(NV,M,M),
     *VALUE1(NV,NT,M,M)
0003      DIMENSION NTIME(NV,NT,M)
0004      DO 10 L = 1, NV
0005      DO 10 I = 1,M
0006       DO 10 J = 1,M
0007      SUM1(L,I,J) = 0.
0008   10 CONTINUE
0009      DO 20 L  = 1, NV
0010      DO 20 I = 1, M
0011      DO 20 J = 1, M
0012      NUM = 0
0013      DO 20 K = 1, NT
0014      IF(RC(L,K,I,J).GT.0) NUM = NUM + 1
0015      SUM1 (L,I,J) = SUM1(L,I,J) + VALUE1(L,K,I,J)
0016      IF (K.LT.NT) GO TO 20
0017      IF (NUM) 15,15,16
0018   15 AVG1(L,I,J) = 0.
0019      GO TO 20
0020   16 CONTINUE
0021      IF (SUM1(L,I,J).GT.0.)AVG1 (L,I,J) = SUM1(L,I,J) / NUM
0022   20 CONTINUE
0023      RETURN
0024       END
```

```
0001      SUBROUTINE SPSAV1(M,NV,NT,NTIME,VALUE,AVG,SUM)
0002      DIMENSION NTIME(NV,NT,M),VALUE(NV,NT,M),AVG(NV,M),SUM(NV,M)
0003      DO 10 L = 1, NV
0004      DO 10 J = 1, M
0005   10 SUM(L,J) = 0.
0006      D O 20 L = 1, NV
0007      DO 20 J = 1, M
0008      J1 = J  - 1
0009      NUM = 0
0010      DO 20 K = 1, NT
0011      IF (NTIME(L,K,J).EQ.0) GO TO 20
0012      NUM = NUM + 1
0013      SUM (L,J) = SUM(L,J) + VALUE(L,K,J)
0014      IF (SUM(L,J).NE.0) AVG(L,J) = SUM(L,J) / NUM
0015   20 CONTINUE
0016       RETURN
0017       END
```

```
0001      SUBROUTINE SPSWIT(NV,M,N,T,COMPNT,A,B,C,D,E,NPART1,NPART2,NTE P1
     *NTEMP2,M2,ME)
0002      DIMENSION T(NV,M),COMPNT(NV,N,M),A(N),B(N),C(N),D(N),E(N)
0003      DIMENSION NPART1(NV),NPART2(NV),NTEMP1(NV),NTEMP2(NV)
0004      DIMENSION M2(NV),ME(NV)
0005      INTEGER T
0006    5 FORMAT(///,40X,'PARTICLE SIZE : ',I3,'**',I2,' MICRONS',/,  42X, 'TE
     *CTOR TEMP. : ',I3,' - ',I3,//,30X,'INLET GAS COMPOSITION:',F5.3,
     **% HYDROGEN +',F5.3,'% HELIUM',//)
0007      DO 70 K = 1, NV
0008      NPZ1 = NPART1(K)
0009      NPZ2 = NPART2(K)
0010      NTMP1 = NTEMP1(K)
0011      NTMP2 = NTEMP2(K)
0012      M2C = M2(K)
0013      MEC = ME(K)
0014       WRITE (6,5) NPZ1,NPZ2,NTMP1,NTMP2 ,M2C,MEC
0015      WRITE (6,10) (T(K,J),J=1,M)
0016   10 FORMAT(///,2X,'REACTED HOUES->',
     *11X,5(7X,I2,7X))
0017      WRITE (6,20)
0018   20 FORMAT (//,2X,'COMPONENTS(',//,12X,'V')
0019   30 FORMAT ('V',2X,I3)
0020   40 FORMAT ('+',28X,5(E15.4))
0021      DO 60 I = 1, N
0022      WRITE (6,30) I
0023      WRITE (6,50) (A(I),B(I),C(I),D(I),E(I))
0024   50 FORMAT ('+',4X,5E14)
0025      WRITE (6,40) (COMPNT(K,I,J),J=1,M)
0026   60 CONTINUE
0027      WRITE (6,65)
0028   65 FORMAT (1H1)
0029   70 CONTINUE
0030      RETURN
0031       END
```

```
0001      SUBROUTINE SPSASN(NV,NA,NA1,NB,NB1,NC,NC1,ND,ND1,NE,NE1,NF,NF ,
     *NG,NG1,L,NZ)
0002      DIMENSION NA(NV),NB(NV),NC(NV),ND(NV),NE(NV),NF(NV),NG(NV)
0003      NA1 = NA(L)
0004      NB1 = NB(L)
0005      NC1 = NC(L)
0006      ND1 = ND(L)
0007      NE1 = NE(L)
0008      NF1 = NF(L)
0009      NG1 = NG(L)
0010   10 FORMAT(//,40X,'PARTICLE SIZE : ',I3,'**',I2,' MICRONS',/,  42X,'TE
     *CTOR TEMP. : ',I3,' - ',I3,//,30X,'INLET GAS COMPOSITION:',F5.3,
     **% HYDROGEN +',F5.3,'% HELIUM',//)
0011      IF (NZ.GT.0) WRITE (6,10) NA1,NB1,NC1,ND1,NF1,NG1
0012       RETURN
0013      END
```

```
0001            SUBROUTINE SPSADD(M,L,TOT,GRTLAV,GRPCAV,N1,N2,N3,N4,N5,N6,N7,K ,N
               *,II,NV,NT,P,SUM1)
0002            DIMENSION GRUPTL(3,3,5),GRUPTP(3,3,5),TOT(3,3,5),A(3,3,N,5)
0003            DIMENSION GRTLAV(3,5),GRPCAV(3,5), TI(3,3,5),SUM1(NV,M)
0004            DO 130 L = 1, NV
0005            DO 100 K = 1, NT
0006            DO 100 J = 1, M
0007            GO TO (70,60,50,40,30,20,10,5), NF
0008          5 GRUPTL(L,K,J) = A(L,K,N1,J) + A(L,K,N2,J) + A(L,K,N3,J) +
                *                 A(L,K,N4,J) + A(L,K,N5,J) + A(L,K,N6,J) +
                *                 A(L,K,N7,J) + A(L,K,N8,J)
0009            GO TO 80
0010         10 GRUPTL(L,K,J) = A(L,K,N1,J) + A(L,K,N2,J) + A(L,K,N3,J) +
               $A(L,K,N4,J) + A(L,K,N5,J) + A(L,K,N6,J) + A(L,K,N7,J)
0011            GO TO 80
0012         20 GRUPTL(L,K,J) = A(L,K,N1,J) + A(L,K,N2,J) + A(L,K,N3,J) +
               $A(L,K,N4,J) + A(L,K,N5,J) + A(L,K,N6,J)
0013            GO TO 80
0014         30 GRUPTL(L,K,J) = A(L,K,N1,J) + A(L,K,N2,J) + A(L,K,N3,J) +
               $A(L,K,N4,J) + A(L,K,N5,J)
0015            GO TO 80
0016         40 GRUPTL(L,K,J) = A(L,K,N1,J) + A(L,K,N2,J) + A(L,K,N3,J) +
               $A(L,K,N4,J)
0017            GO TO 80
0018         50 GRUPTL(L,K,J) = A(L,K,N1,J) + A(L,K,N2,J) + A(L,K,N3,J)
0019            GO TO 80
0020         60 GRUPTL(L,K,J) = A(L,K,N1,J) + A(L,K,N2,J)
0021            GO TO 80
0022         70 GRUPTL(L,K,J) = A(L,K,N1,J)
0023         80 CONTINUE
0024            IF(TOT(L,K,J).NE.0)GRUPTP(L,K,J)=(GRUPTL(L,K,J)/TOT(L,K,J))*10
0025        100 CONTINUE
0026            CALL SPSAVI(M,NE,LT,T1,GRUPTL,GRTLAV,SUM1)
0027            CALL SPSAVI(M,NV,NT,T1,GRUPTP,GRPCAV,SUM1)
0028            RETURN
0029            END
```

```
0001            SUBROUTINE SPSPLT(X,LX,Y,LY,Z,LZ,NPT,NPLOT,NCOPY,NCD,NDIM,NAT
               *REAK,NA,NPA1,NPA2,NTAP1,NTAP2,N2C,NEC,NUM1,NUM2)
C             PURPOSE
C               THIS SUBROUTINE PLOTS UP TO TEN RELATIONSHIPS OF THE FORM Y =  (X
C               IT WILL ALSO PREPARE TOPOGRAPHIC MAPPINGS OF THREE DIMENSIONAL
C               SURFACES.
C             USAGE
C               CALL KSUPLT(X,LX,Y,LY,Z,LZ,NPT,NPLOT,NCOPY,NCD,NDIM,NATREM,NPAGE)
C               X, Y, Z - COORDINATES OF DATA POINTS
C               LX, LY, LZ - SCALING FACTORS.  THE SCALES ON EACH AXIS MAY BE  IN
C                    ONE CYCLE LOG, TWO CYCLE LOG, ...SIX CYCLE LOG
C               NPT - NUMBER OF POINTS TO BE PLOTTED
C               NPLOT  - NUMBER OF RELATIONSHIPS TO BE PLOTTED IN DIFFERENT
C                    SYMBOLS IF PLOTS ARE TWO DIMENSIONAL.  IF A TOPOGRAPHIC
C                    MAPPING IS CALLED FOR NPLOT IS NUMBER OF CONTOURS TO BE PLOT
C               NCOPY - NUMBER OF DUPLICATE PLOTS TO BE MADE
C               NCD - NUMBER OF INFORMATION CARDS TO BE READ.  IF NCD IS ZERO NO
C                    CARDS ARE READ.  OTHERWISE SEE WRITE UP.
C               NDIM - IF THE RELATIONSHIPS WHICH ARE TO BE PLOTTED ARE TWO
C                    DIMENSIONAL NDIM IS 2, AND IF A TOPOGRAPHICH MAPPING IS DESI
C                    NDIM IS 3.
C               NATREM - IF NATREM IS 1, A CARD WITH THE LIMITING VALUES OF
C                    THE X, Y, AND Z SCALES IS READ.  OTHERWISE THEY ARE
C                    CALCULATED WITHIN THE SUBROUTINE SO THAT ALL DATA POINTS WIL
C                    APPEAR ON THE PLOT.
C               NPAGE - NUMBER OF PAGES THE PLOT IS TO COVER.  IF NPAGE IS 1 THE
C                    IS 50 LINES HIGH.  EACH INCREASE OF 1 IN NPAGE CAUSES THE
C                    PLOT TO EXTEND ACROSS AN ADDITIONAL 64 LINES.
C             SUBROUTINES REQUIRED
C               THE FORTRAN IV SUBROUTINE PDT IS INCLUDED AS PART OF IPS
C               PLOTTING PACKAGE.
C
0002            REAL M
0003            DIMENSION X(1),Y(1),Z(1),SX(7),TITLE(20),L(134),NCH(41),NH(41)
               *,NOP(42),FM1(6),FM2(6),FM3(6),FM4(8),FM5(8),FM6(8),FM7(6),FRT(9)
               1,SCL(3)
0004            DATA FM1/24H(1H ,A1,F9.2,12A1)          /

0005            DATA FM2/24H(1H ,A1,F9.4,12A1)          /

0006            DATA FM3/24H(1H ,A1,1PE9.2,12A1)        /

0007            DATA FM4/30H(1X,1PE16.2,5E20.2,E15.2)           /

0008            DATA FM6/30H(5X,F9.2,5(11X,F9.2),9X,F9.2)       /

0009            DATA FM5/30H(5X,F9.4,5(11X,F9.4),9X,F9.4)       /

0010            DATA NCH/1H0,1H1,1H2,1H3,1H4,1H5,1H6,1H7,1H8,1H9,1HA,1HB,1HC,1 ),
               *1HE,1HF,1HG,1HH,1HI,1HJ,1HK,1HL,1HM,1HN,1HO,1HP,1HQ,1HR,1HS,1HT,
               *HU,1HV,1HW,1HX,1HY,1HZ,1H*,1H$,1H=,1H-,1H+,1H(,1H)/
0011            DATA N0,N1,N2,N3,N4/1H ,1H+,1H-,1H /

0012            DATA SCL/1HX,1HY,1HZ/
0013         1  FORMAT(20A4)
0014           2 FORMAT (42A1,10A1,7A4)
0015         201 FORMAT (/,27X,'EFFECT OF PARTICLE SIZE ON')
0016         202 FORMAT (/,29X,'EFFECT OF TEMPERATURE ON')
0017         203 FORMAT (/,25X,'EFFECT OF INLET GAS COMPOSITION ON')
0018         204 FORMAT (1H ,///,20A4,///,23X,'COAL TYPE      : ILLINOIS # 6 HI-VC AT
               *LE',/)
0019         205 FORMAT (23X,'PARTICLE SIZE : ',13,'/',12,' MICRONS',/)
0020         206 FORMAT (23X,'REACTOR TEMP. : ',13,' - ',13,'DEGREE C',/)
0021         207 FORMAT (23X,'INLET GAS COMP.:',F6.2,'% H2 + ',F6.2,'% N2',/)
0022         208 FORMAT (27X,'# OF RUNS/POINT:',I1,/)
0023         209 FORMAT(12X,'S: -38+25 MICRONS, M: -53+38 MICRONS, L: -90+53 MI RO
               *S',/)
0024         210 FORMAT(12X,'S : 100 DEGREE C, M: 150 DEGREE C, L: 200 DEGREE C',/)
0025         211 FORMAT(12X,'S: 2% H2 IN N2, M: 10% H2 IN N2, L: ALL HYDROGEN',  )
0026         212 FORMAT(12X,'4: C2-C4, 5: C5, 6: C6, 7: C7, 8: C8 HYDROCARBONS',/)
0027         213 FORMAT (12X,'N: NORMAL,B: BRANCHED,C: CYCLIC(SATURATED),O: OLEFIN
               *',/)
```

```
      214 FORMAT (12X,'1 : BTX, 2: 2-RINGS, 3 : 3-RINGS,4: >3RINGS AROMATIC
     *,/)
        5 FORMAT(132A1)
        6 FORMAT(5H ALL ,A1,57H VALUES ARE NEGATIVE.  LOG SCALE MAY NOT BE .
     *PECIFIED.                                                          )
        7 FORMAT(1PE17.2,E115.2)
        8 FORMAT(1PE17.2,E61.2,E54.2)
        9 FORMAT(1PE17.2,2E40.2,F35.2)
       10 FORMAT(1PE17.2,3E30.2,E25.2)
       11 FORMAT(1PE17.2,4E24.2,E19.2)
       12 FORMAT (///,1HK,29X,7A4)
       74 FORMAT(6E12.2)
       76 FORMAT(1H1)
       80 FORMAT(70H NPT(NO. OF PTS.) MUST BE EVENLY DIVISIBLE BY NPLOT(NO.
     *OF CURVES.)                                                       )
       84 FORMAT(1X,36HNONE DIMENSIONAL PLOT NOT ALLOWED.      )
       94 FORMAT(42A1,10X,7A4)
          DO95I=1,41
       95 NB(I)=NCH(I)
          N = 40 + 66 * (NPAGE - 1)
          LLX=LX+1
          NDD=NC0+1
            GOTO(15,13,14,13),NDD
       13  READ(5,1)(TITLE(I),I=1,20)
       14 IF(NDD.LT.3)GOTO15
          IF(NDIM.NE.3)GOTO93
          READ(5,94)(POP(I),I=1,42),TAB1,TAB2,TAB3,TAB4,TAB5,TAB6,TAB7
          GO TO 91
       93 READ(5,2)( POP(I),I=1,42),( NH(I),I=1,10),TAB1,TAB2,TAB3,TAB4,TAB5
         1TAB6,TAB7
          GOTO91
       15 DO92I=1,42
       92 POP(I)=NB
       91 NCH(41)=NB
          IF(FLOAT(NPT/NPLOT)-FLOAT(NPT)/FLOAT(NPLOT))101,85,101
       85 IF(NXTPEN.EQ.1)GOTO72
          YMIN=1.00E 75
          XMIN=YMIN
          ZMIN=YMIN

          YMAX=1.00E-78
          XMAX=YMAX
          ZMAX=YMAX
          DO51I=1,NPT
          GOTO(103,52,53),NDIM
       53 IF(Z(I).GE.ZMAX)ZMAX=Z(I)
          IF(Z(I).LE.ZMIN)ZMIN=Z(I)
       52 IF(Y(I).GE.YMAX)YMAX=Y(I)
          IF(Y(I).LE.YMIN)YMIN=Y(I)
          IF(X(I).GE.XMAX)XMAX=X(I)
          IF(X(I).LE.XMIN)XMIN=X(I)
       51 CONTINUE
          IF(LX.GT.0)GOTO900
          XMIN=XMIN-(XMAX-XMIN)/75.0
          XMAX=XMAX+(XMAX-XMIN)/75.0
      900 IF(LY.GT.0)GOTO73
          YMIN=YMIN-(YMAX-YMIN)/30.0
          YMAX=YMAX+(YMAX-YMIN)/30.0
          GOTO73
       72 READ(5,74)XMIN,XMAX,YMIN,YMAX,ZMIN,ZMAX
       73 IF(YMAX.GT.10000.0.OR.YMIN.LT.(-10000.0))GOTO60
          IF (YMAX-YMIN.LT.5.0)GOTO60
          IF(YMAX.GT.10.0.OR.YMIN.LT.(-10.0))GOTO62
          IF(YMAX.LT.0.01.OR.ABS(YMAX).LT.0.01)GOTO60
          DO59I=1,6
       59 FMT(I)=FM2(I)
          GOTO65
       60 DO61I=1,6
       61 FMT(I)=FMJ(I)
          GOTO65
       62 DO63I=1,6
       63 FMT(I)=FM1(I)
       65 IF(XMAX.GT.10000.0.OR.XMIN.LT.(-10000.0))GOTO67
          IF(XMAX-XMIN.LT.5.0)GOTO67
          IF(XMAX.GT.10.0.OR.XMIN.LT.(-10.0))GOTO69
          IF(XMAX.LT.0.01.OR.ABS(XMIN).LT.0.01)GOTO67
          DO66I=1,8
       66 FMT(I)=FM5(I)
          GOTO70
       67 DO68I=1,8
       68 FMT(I)=FM4(I)
          GOTO70
       69 DO71I=1,8
       71 FMT(I)=FM6(I)
       70 IF(LX.GT.0)GOTO17
          CX= 60./(XMAX-XMIN)
          SX(1) = XMIN
          SX(7) = XMAX
          M=XMIN
          DO 16 K = 2, 6
          U = (XMAX - XMIN)/6. +0
       16 SX(K)=U
          GOTO19
       17 XLX=LX
          MS=1
          IF(XMAX.LE.0.0)GOTO100
          XMIN=10.0**(ALOG10(XMAX*9.999999)-FLOAT(LX))
          CX = 60. / XLX

          MX=ALOG10(XMIN)
          IF(XMIN.LT.1.0)MX=ALOG10(XMIN)-0.9999999
          XMIN=10.0**MX
          DO18K=1,LLX
       18 SX(K)=10.**(MX+K-1)
       19 CALLPOT(X,XMIN,LX,NPT,0, 60.,CX)
          IF(LY.GT.0)GOTO20
          CY=A/(YMAX-YMIN)
          GOTO21
       20 YLY=LY
          MS=2
          IF(YMAX.LE.0.0)GOTO100
          YMIN=10.0**(ALOG10(YMAX*9.999999)-FLOAT(LY))
          CY=M/YLY
          KY=CY
          MY=ALOG10(YMIN)
          IF(YMIN.LT.1.0)MY=ALOG10(YMIN)-0.9999999
          YMIN=10.0**MY
       21 CALLPOT(Y,YMIN,LY,NPT,1,M,CY)
          IF(NDIM.LT.3)GOTO24
          FPLOT=NPLOT
          IF(LZ.GT.0)GOTO22
          CZ=FPLOT/(ZMAX-ZMIN)
          GOTO23
       22 ZLZ=LZ
          MS=3
          IF(ZMAX.LE.0.0)GOTO100
          ZMIN=10.0**(ALOG10(ZMAX*9.999999)-ZLZ)
          CZ=FPLOT/ZLZ
          IF(ZMIN.GE.1.0)GO TO 23
          IA=ALOG10(ZMIN)-.9999999
          ZMIN=10.0**IA
       23 CALL POT(Z,ZMIN,LZ,NPT,0,FPLOT,CZ)
          DO77I=1,NPT
          IZ=Z(I)+1.0
          Z(I)=NCH(IZ)
       77 CONTINUE
          GOTO99
       24 NPN=NPT/NPLOT
          DO 78I=1,NPLOT
          JJ=(I-1)*NPN+1
          JK=I*NPN
          DO78J=JJ,JK
          Z(J)=NH(I)
       78 CONTINUE
       99 DO102I=1,NPT
          DO102J=1,NPT
          IF(X(I).GE.Y(J))GOTO102
          A=Y(I)
          B=X(I)
          Y(I)=Y(J)
          X(I)=X(J)
          Y(J)=A
          X(J)=B
          C=Z(I)
          Z(I)=Z(J)
          Z(J)=C
      102 CONTINUE
```

```
      DO56NO=1,NCOPY
      M1=1
      M2=1
      LL=0
      LYY=LY
      TT=H
      WRITE(6,76)
      IF(NOD.EQ.1.OR.NOD.EQ.3)GO TO 97
      IF(NUM1.LE.0) GO TO 107
      GO TO (104,105,104), NUM1
104   WRITE (6,201)
      WRITE (6,204) (TITLE(I),I = 1,20)
      WRITE (6,206) NTMP1,NTMP2
      WRITE (6,207) M2C,MEC
      WRITE (6,209)
      GO TO 112
105   WRITE (6,202)
      WRITE (6,204) (TITLE(I),I = 1,20)
      WRITE (6,205) MPZ1,MPZ2
      WRITE (6,207) M2C,MEC
      WRITE (6,210)
      GO TO 112
106   WRITE (6,203)
      WRITE (6,204) (TITLE(I),I = 1,20)
      WRITE (6,205) MPZ1,MPZ2
      WRITE (6,206) NTMP1,NTMP2
      WRITE (6,211)
      GO TO 112
107   GO TO (108,109,110), NUM2
108   CONTINUE
      WRITE (6,204) (TITLE(I),I = 1,20)
      WRITE (6,205) MPZ1,MPZ2
      WRITE (6,206) NTMP1,NTMP2
      WRITE (6,207) M2C,MEC
      IF(NUM1.EQ.0) WRITE (6,212)
      IF (NUM1.EQ.-1) WRITE (6,213)
      IF (NUM1.EQ.-2) WRITE (6,214)
      GO TO 112
109   CONTINUE
      WRITE (6,204) (TITLE(I),I = 1,20)
      WRITE (6,205) MPZ1,MPZ2
      WRITE (6,206) NTMP1,NTMP2
      WRITE (6,207) M2C,MEC
      IF(NUM1.EQ.0) WRITE (6,212)
      IF (NUM1.EQ.-1) WRITE (6,213)
      IF (NUM1.EQ.-2) WRITE (6,214)
      GO TO 112
110   CONTINUE
      WRITE (6,204) (TITLE(I),I = 1,20)
      WRITE (6,205) MPZ1,MPZ2
      WRITE (6,206) NTMP1,NTMP2
      WRITE (6,207) M2C,MEC
      IF(NUM1.EQ.0) WRITE (6,212)
      IF (NUM1.EQ.-1) WRITE (6,213)
      IF (NUM1.EQ.-2) WRITE (6,214)
112   CONTINUE
      IF (M1.GT.1) WRITE (6,208) M1
 97   NN=N+1.0

      DO43KK=1,NN
      M=1
      NNN=NPN
      JLO=1
      T=INT(N)-KK+1
      DO 25 J =  1,73
 25   L (J) = NB
      L (73) = A0
      IF(LY.GT.0)GOTO26
      L(13)=MP
      IF(T.GT.TT)GOTO30
      SCALE=T/CY+YMIN
      L (73) = MP
      M=0
      TT=TT-5.
      IF(T.LE.0.)SCALE=YMIN
      GOTO30
26    GOTO(27,27,28,28,27,28),LY
27    SS=KY*LYY
      GOTO29
28    SS=KY*LYY+1
29    L(13)=MD
      IF(T.GT.SS)GOTO30
      SCALE=10.**(MY+LYY)
      M=0
      LYY=LYY-1
      L(13)=MP
      L (73) = MP
30    IF(M.EQ.T)GOTO31
      IF(J..NE.T)GOTO37
31    DO 32 J = 14, 73
32    L(J)=MM
      IF(LX.GT.0)GOTO34
      DO 33 J = 13, 73, 10
33    L(J)=MP
      GOTO36
34    KX = 60 / LX
      DO 35 J = 13, 73, KX
35    L(J)=MP
36    IF(M.EQ.T)L( 73)=MD
37    LL=LL+1
      IF(LL.GT.NPI)GOTO79
      IF(Y(LL)-T)79,92,37
92    J=X(LL)
      L(J+13)=Z(LL)
      GOTO37
79    LL=LL-1
      IF(M1.GT.4+( INT(N)-50)/2  .AND.M1.LT.47+( INT(N)-50)/2  )GOTO54
      L(2)=MB
      GOTO55
54    L(7)=MOP(M2)
      M2=M2+1
55    M1=M1+1
41    IF(M.EQ.1)GOTO42
      WRITE(6,FAT)L(2),SCALE,(L(J),J=13,73 )
      GOTO43
42    WRITE(6,5)(L(J),J=1,11),(L(J),J=13,73)
43    CONTINUE

      GOTO(44,45,46,47,48,49,44),LLX
44    WRITE (6,111) (SX (K), K = 1, 7 )
111   FORMAT (4X, 7 (5X,F 5.2))
      GOTO50
45    WRITE(6,7)(SX(K),K=1,LLX)
      GOTO50
46    WRITE(6,8)(SX(K),K=1,LLX)
      GOTO50
47    WRITE(6,9)(SX(K),K=1,LLX)
      GOTO50
48    WRITE(6,10)(SX(K),K=1,LLX)
      GOTO50
49    WRITE(6,11)(SX(K),K=1,LLX)
50    IF(NOD.LT.3)GOTO56
      WRITE(6,12)TAB1,TAB2,TAB3,TAB4,TAB5,TAB6,TAB7
56    CONTINUE
83    RETURN
100   WRITE(6,6)SCL(MS)
      RETURN
101   WRITE(6,80)
      RETURN
103   WRITE(6,84)
      RETURN
      END
```

```
      SUBROUTINE SPOT(Y,YMIN,LY,NP,J,YC,C)
      DIMENSION Y(1)
      IF(LY.GT.0)GOTO2
      DO1I=1,NP
    1 Y(I)=FLOAT( INT(C*(Y(I)-YMIN)+.5))
      GOTO4
    2 YMIN=10.0**( INT(ALOG10(YMIN)))
      DO3I=1,NP
      IF(Y(I).LE.0.0)GOTO3
      Y(I)=FLOAT( INT(C*(ALOG(Y(I)/YMIN)/2.302585)+.5))
      YT=Y(I)
    3 CONTINUE
    4 DO5I=1,NP
      IF(Y(I).LT.0.)GOTO5
      IF(Y(I).LE.YC)GOTO6
    5 Y(I)=YC+1.
    6 CONTINUE
      RETURN
      END
```

```
      SUBROUTINE SPSKTN(NV,M,N,T,VALUE,NI,NF,NPART1,NPART2,NTEMP1,I EN
     *2,DUMMY,NAVAG,H2,HE,NUM1,NUM2)
      DIMENSION  TIME(50),COMPNT(50),SMTING(50),VALUE(NV,N,M)
      DIMENSION  DUMMY(NV,N,M),NPART1(NV),NPART2(NV),NTEMP1(NV),NTE P2
     *(NV),NAVAG(NV),H2(NV),HE(NV)
      INTEGER T(NV,M)
      NPTS = M * ((NF-NI) +1)
      NPLOT = NPTS/M
      DO 20 K = 1, NV
      CALL SPSASK (NV,NPART1,NPZ1,NPART2,NPZ2,NTEMP1,NTEP1,NTEMP2,NT P2
     *NAVAG,NA,H2,H2C,HE,HEC,K,0)
      L = 0
      DO 10 I = NI, NF
      DO 10 J = 1, M
      L = L + 1
      TIME(L) = FLOAT(T(I,J))
      COMPNT(L) = VALUE(K,I,J)
      IF  (DUMMY(K,I,J).EQ.0.) TIME(L) = 0.
      IF  (DUMMY(K,I,J).EQ.0.) COMPNT(L) = 0.
      SMTING (L) = TIME(L)
   10 CONTINUE
      CALL SPSPLT(TIME,0,COMPNT,0,SMTING,0,NPTS,NPLOT,1,3,2,1,1,NA,
     *NPZ1,NPZ2,NTMP1,NTMP2,H2C,HEC,NUM1,NUM2)
   20 CONTINUE
      RETURN
      END
```

```
      SUBROUTINE SPSCO(NV,M,N,T,VALUE,NPZ1,NPZ2,NTMP1,NTMP2,NA,H2,HE
     *NUM1,NUM2)
      DIMENSION T(NV,M),VALUE(NV,N,M),NPZ1(NV),NPZ2(NV),NTMP1(NV),NTMP2
     *(NV),NA(NV),H2(NV),HE(NV)
      CALL SPSPTN(NV,M,N,T,VALUE, 1, 4,NPZ1,NPZ2,NTMP1,NTMP2,VALUE,NA,
     *H2,HE,NUM1,NUM2)
      CALL SPSPTN(NV,M,N,T,VALUE, 5, 8,NPZ1,NPZ2,NTMP1,NTMP2,VALUE,N ,
     *H2,HE,NUM1,NUM2)
      CALL SPSPTN(NV,M,N,T,VALUE, 9,13,NPZ1,NPZ2,NTMP1,NTMP2,VALUE,NA,
     *H2,HE,NUM1,NUM2)
      CALL SPSPTN(NV,M,N,T,VALUE,14,19,NPZ1,NPZ2,NTMP1,NTMP2,VALUE,NA,
     *H2,HE,NUM1,NUM2)
      CALL SPSPTN(NV,M,N,T,VALUE,20,21,NPZ1,NPZ2,NTMP1,NTMP2,VALUE,N ,
     *H2,HE,NUM1,NUM2)
      CALL SPSPTN(NV,M,N,T,VALUE,22,24,NPZ1,NPZ2,NTMP1,NTMP2,VALUE,NA,
     *H2,HE,NUM1,NUM2)
      CALL SPSPTN (NV,M,N,T,VALUE,25,27,NPZ1,NPZ2,NTMP1,NTMP2,VALUE,NA,
     *H2,HE, NUM1,NUM2)
      CALL SPSPTN (NV,M,N,T,VALUE,28,30,NPZ1,NPZ2,NTMP1,NTMP2,VALUE, N,
     *H2,HE, NUM1,NUM2)
      CALL SPSPTN (NV,M,N,T,VALUE,32,32,NPZ1,NPZ2,NTMP1,NTMP2,VALUE,NA,
     *H2,HE, NUM1,NUM2)
      RETURN
      END
```

```
      SUBROUTINE  SPSYLD(NV,M,T,VALUE1,VALUE2,VALUE3,VALUE4,VALUE5,
     *NPART1,NPART2,NTEMP1,NTEMP2,NAV,H2,HE,NUM1,NUM2)
      DIMENSION TIME(50),COMPNT(50),SMTING(50),VALUE1(NV,M),VALUE2(NV,
     *M),VALUE3(NV,M),VALUE4(NV,M),VALUE5(NV,M)
      DIMENSION NPART1(NV),NPART2(NV),NTEMP1(NV),NTEMP2(NV),NAV(NV)
      DIMENSION H2(NV),HE(NV)
      INTEGER T(NV,M)
      NPTS = 5 * M
      NPLOT = NPTS/M
      DO 60 I = 1, NV
      NPZ1 = NPART1(I)
      NPZ2 = NPART2(I)
      NTMP1 = NTEMP1(I)
      NTMP2 = NTEMP2(I)
      NA = NAV(I)
      H2C = H2(I)
      HEC = HE(I)
      L = 0
      DO 10 J = 1, M
      L = L + 1
      TIME(L) = FLOAT(T(I,J))
      COMPNT(L) = VALUE1(I,J)
      SMTING(L) = TIME(L)
   10 CONTINUE
      DO 20 J = 1, M
      L = L + 1
      TIME(L) = FLOAT(T(I,J))
      COMPNT(L) = VALUE2(I,J)
      SMTING(L) = TIME(L)
   20 CONTINUE
      DO 30 J = 1, M
      L = L + 1
      TIME(L) = FLOAT(T(I,J))
      COMPNT(L) = VALUE3(I,J)
      SMTING(L) = TIME(L)
   30 CONTINUE
      DO 40 J = 1, M
      L = L + 1
      TIME(L) = FLOAT(T(I,J))
      COMPNT(L) = VALUE4(I,J)
      SMTING(L) = TIME(L)
   40 CONTINUE
      DO 50 J = 1, M
      L = L + 1
      TIME(L) = FLOAT(T(I,J))
      COMPNT(L) = VALUE5(I,J)
      SMTING(L) = TIME(L)
   50 CONTINUE
      CALL SPSPLT(TIME,0,COMPNT,0,SMTING,0,NPTS,NPLOT,1,3,2,1,1,NA,
     *NPZ1,NPZ2,NTMP1,NTMP2,H2C,HEC,NUM1,NUM2)
   60 CONTINUE
      RETURN
      END
```

```
0001                SUBROUTINE SPSCOM(NV,M,T,VALUE,NPART1,NPART2,NTEMP1,NTEMP2,NA, 2,
                   *ME,NUM1,NUM2)
0002                DIMENSION TIME(50),COMPNT(50),SMTING(50),VALUE(NV,M)
0003                DIMENSION NPART1(NV),NPART2(NV),NTEMP1(NV),NTEMP2(NV)
0004                DIMENSION M2(NV),ME(NV)
0005                INTEGER T(NV,M)
0006                MPTS = M*NV
0007                NPLOT=MPTS/M
0008                L = 0
0009                DO 10 I = 1, M
0010                DO 10 J = 1, N
0011                L = L + 1
0012                TIME(L) = FLOAT(T(I,J))
0013                COMPNT(L) = VALUE(I,J)
0014                SMTING(L) = TIME(L)
0015              10 CONTINUE
0016                IF(NUM1.EQ.0) GO TO 14
0017                IF(NUM1) 15,20,20
0018              14 IF(NUM2) 15,20,20
0019              15 CONTINUE
0020                 NPZ1 = NPART1(1)
0021                 NPZ2 = NPART2(3)
0022                 NTMP1 = NTEMP1(1)
0023                 NTMP2 = NTEMP2(3)
0024                 M2C = M2(1)
0025                 MEC = ME(1)
0026                 GO TO 25
0027              20 CONTINUE
0028                 NPZ1 = NPART1(2)
0029                 NPZ2 = NPART2(2)
0030                 NTMP1 = NTEMP1(1)
0031                 NTMP2 = NTEMP2(3)
0032                 M2C = M2(1)
0033                 MEC = ME(1)
0034              25 CONTINUE
0035                 CALL SPSPLT(TIME,0,COMPNT,0,SMTING,0,MPTS,MPLOT,1,3,2,1,1,NA,
                    *NPZ1,NPZ2,NTMP1,NTMP2,M2C,MEC,NUM1,NUM2)
0036                 RETURN
0037                 END



0001                SUBROUTINE SPSCMP(NV,M,N,T,VALUE,NPART1,NPART2,NTEMP1,NTEMP2,K ,
                   *M2,ME,NUM1,NUM2)
0002                DIMENSION TIME(50),COMPNT(50),SMTING(50),VALUE(NV,N,M)
0003                DIMENSION NPART1(NV),NPART2(NV),NTEMP1(NV),NTEMP2(NV)
0004                DIMENSION  M2(NV),ME(NV)
0005                 INTEGER T(NV,M)
0006                MPTS = M *NV
0007                NPLOT = MPTS/M
0008                DO 20 K = 1, N
0009                L = 0
0010                DO 10 I = 1, NV
0011                NPZ1 = NPART1(I)
0012                NPZ2 = NPART2(I)
0013                NTMP1 = NTEMP1(I)
0014                NTMP2 = NTEMP2(I)
0015                M2C = M2(I)
0016                MEC = ME(I)
0017                DO 10 J = 1, M
0018                L = L + 1
0019                 TIME(L) = FLOAT(T(I,J))
0020                COMPNT(L) = VALUE(I,K,J)
0021                SMTING(L) = TIME(L)
0022              10 CONTINUE
0023                 CALL SPSPLT(TIME,0,COMPNT,0,SMTING,0,MPTS,MPLOT,1,3,2,1,1,NA,NPZ1
                    *NPZ2,NTMP1,NTMP2,M2C,MEC,NUM1,NUM2)
0024              20 CONTINUE
0025                 RETURN
0026                 END
```

APPENDIX B

MASS SPECTRAL DATA

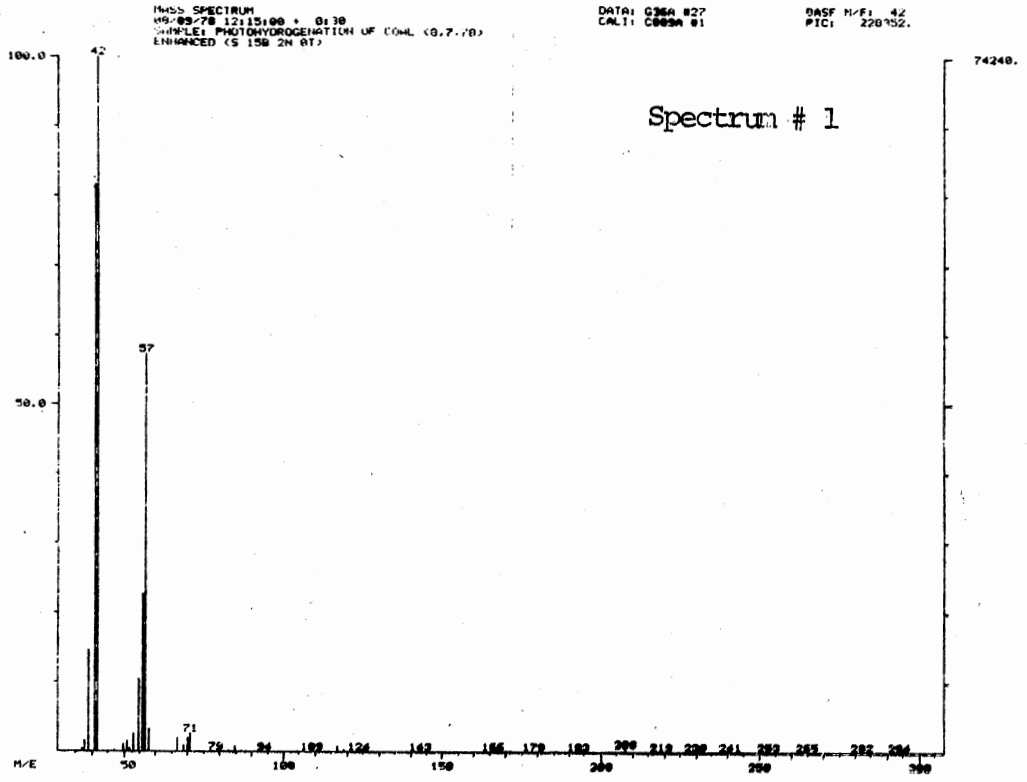
MASS SPECTRUM
SAMPLE: PHOTOHYDROGENATION OF COAL (8,7,78)
ENHANCED (S 150 2N 0T)
DATA: G36A #27
CAL1: C003A 01
BASE M/E: 42
RIC: 220352.
74240.
100.0
50.0
M/E
Spectrum # 1

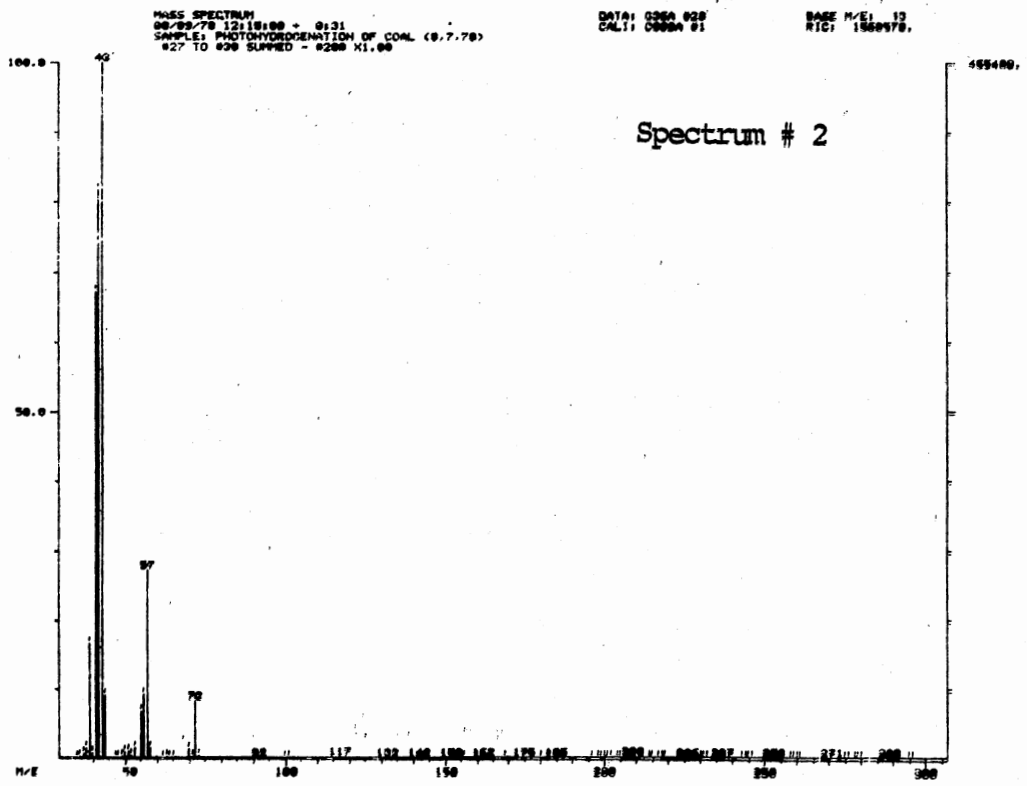
MASS SPECTRUM
SAMPLE: PHOTOHYDROGENATION OF COAL (8,7,78)
#27 TO #30 SUMMED - #200 X1.00
DATA: G36A #28
CAL1: C003A 01
BASE M/E: 43
RIC: 1566578.
465480.
100.0
50.0
M/E
Spectrum # 2

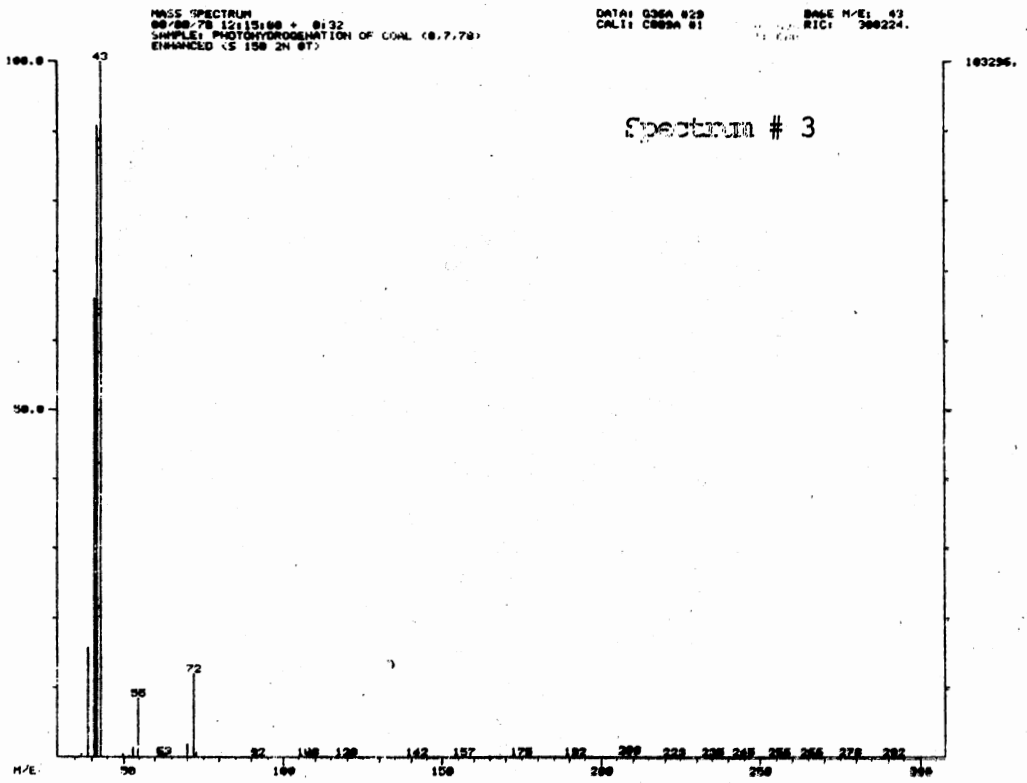
MASS SPECTRUM
SAMPLE: PHOTOHYDROGENATION OF COAL (8,7,78)
ENHANCED (S 150 2N 8T)
DATA: 036A 029
CALI: C009A 01
BASE M/E: 43
RIC: 300224.
100.0
50.0
43
72
55
M/E
103296.
Spectrum # 3

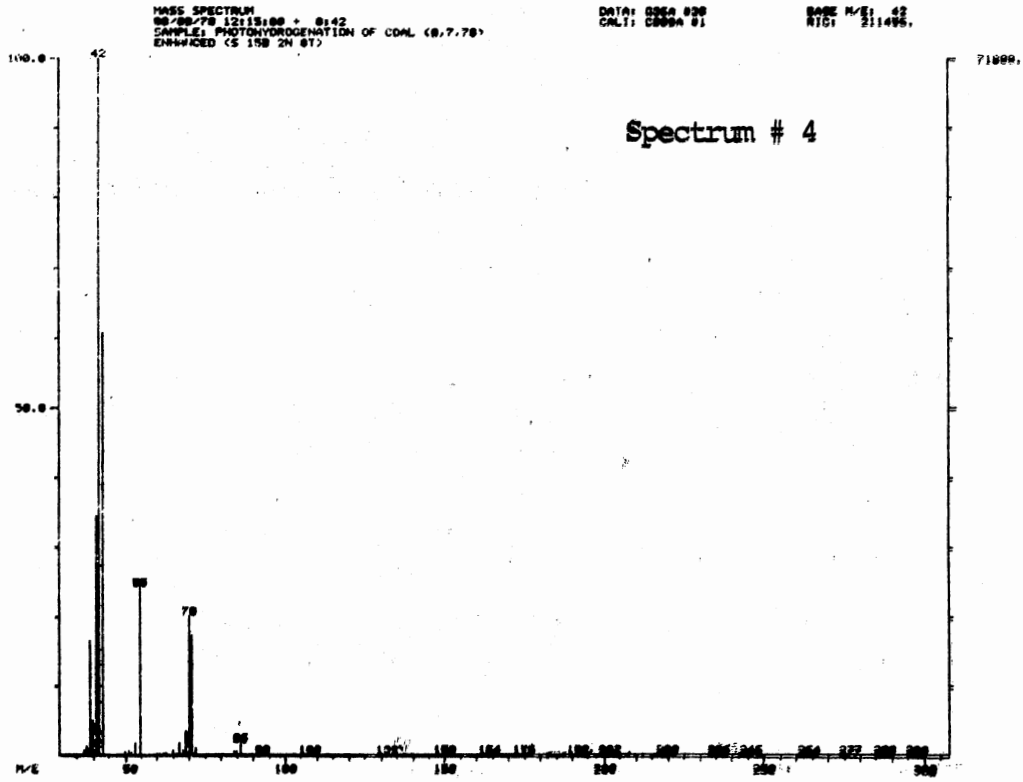
MASS SPECTRUM
SAMPLE: PHOTOHYDROGENATION OF COAL (8,7,78)
ENHANCED (S 150 2N 8T)
DATA: 036A 030
CALI: C009A 01
BASE M/E: 42
RIC: 211495.
100.0
50.0
42
55
79
M/E
71889.
Spectrum # 4

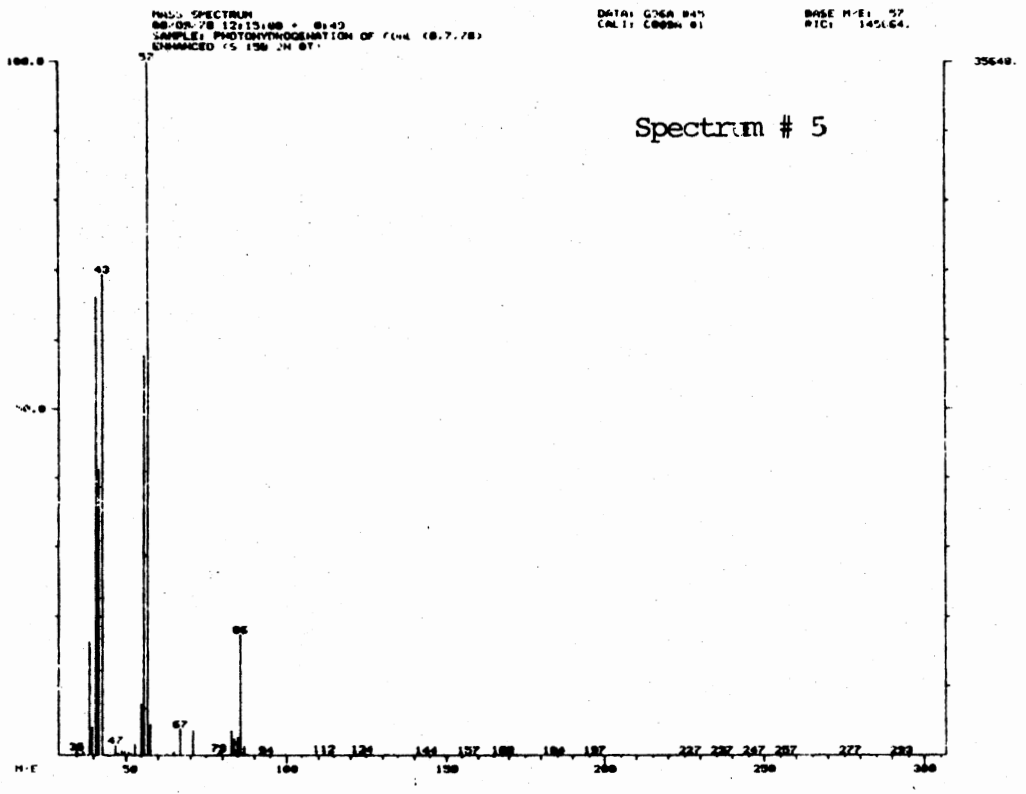
Spectrum # 5

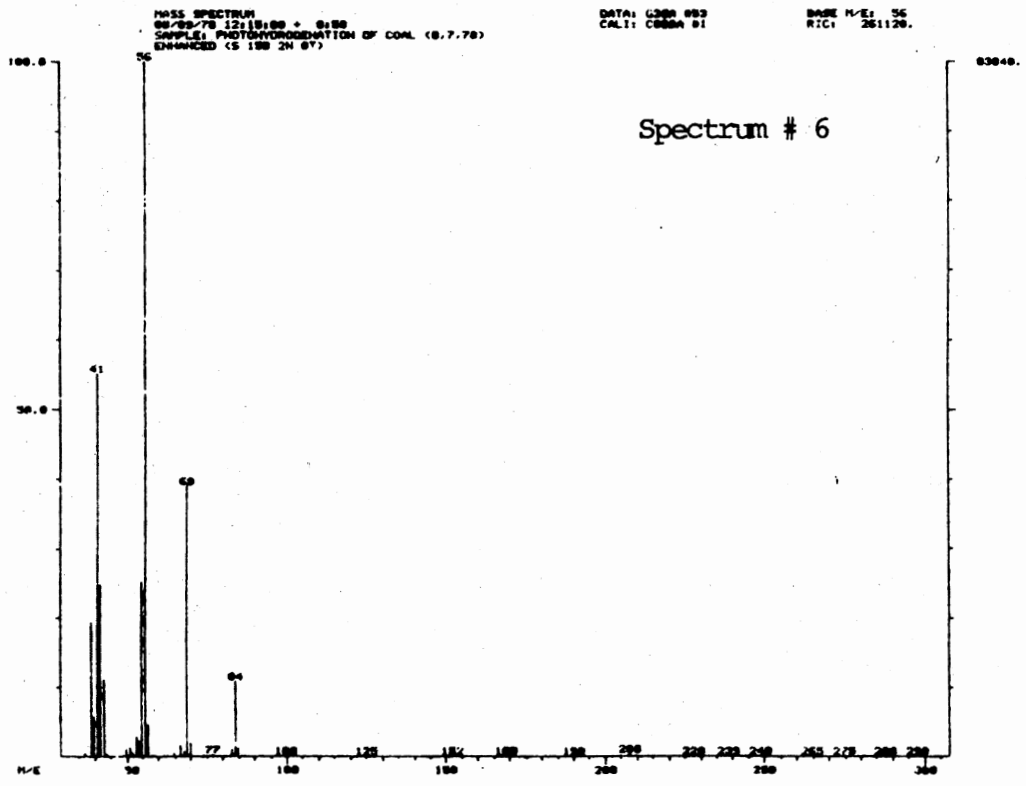
Spectrum # 6

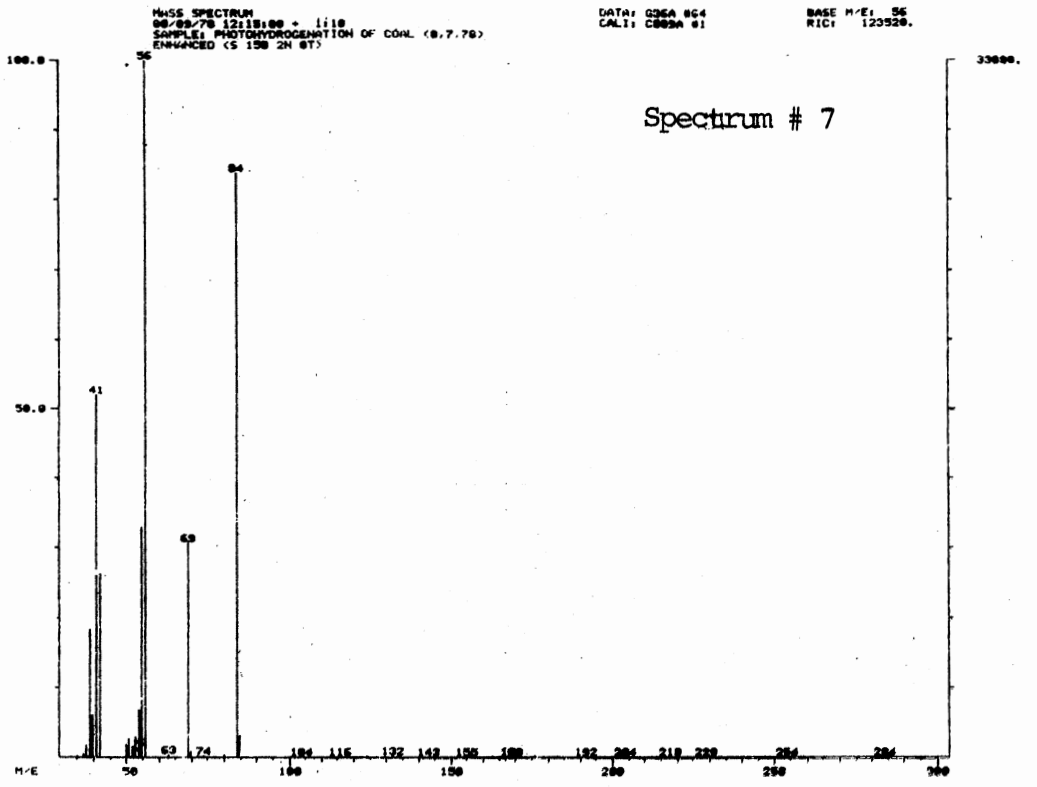
MASS SPECTRUM
SAMPLE: PHOTOHYDROGENATION OF COAL (8.7.78)
ENHANCED (S 150 2N 8T)
DATA: G36A 864
CAL1: C000A 01
BASE M/E: 56
RIC: 123520.
Spectrum # 7
M/E

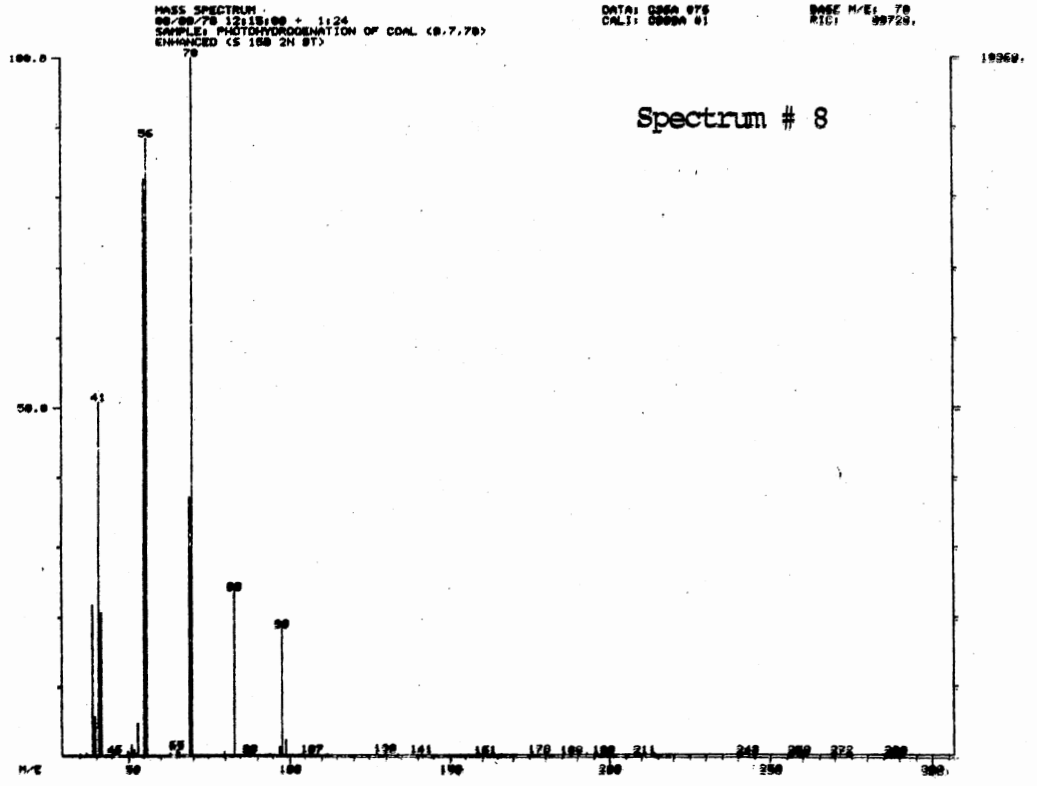
MASS SPECTRUM
SAMPLE: PHOTOHYDROGENATION OF COAL (8.7.78)
ENHANCED (S 150 2N 8T)
DATA: G36A 876
CAL1: C000A 01
BASE M/E: 70
RIC: 99720.
Spectrum # 8
M/E

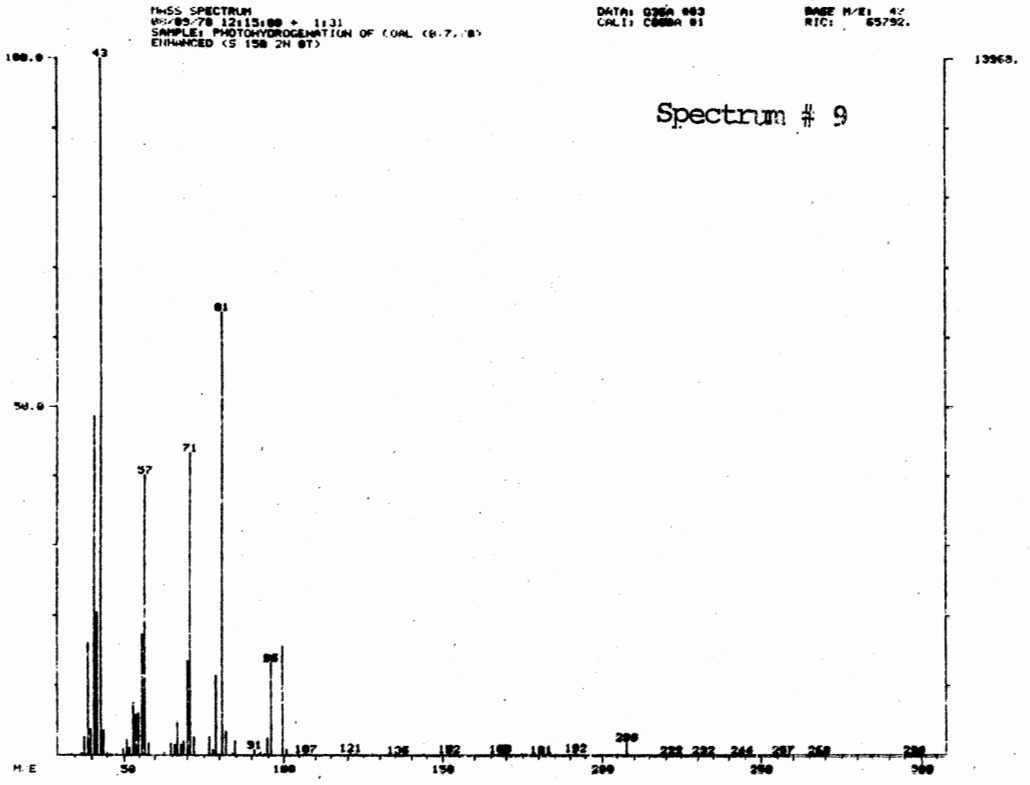
MASS SPECTRUM
SAMPLE: PHOTOHYDROGENATION OF COAL (8,7,78)
ENHANCED (S 150 2H 8T)
DATA: 0000A 003
CAL1: C000A 01
BASE M/E: 43
RIC: 65792.
100.0
50.0
M/E
13968.
Spectrum # 9

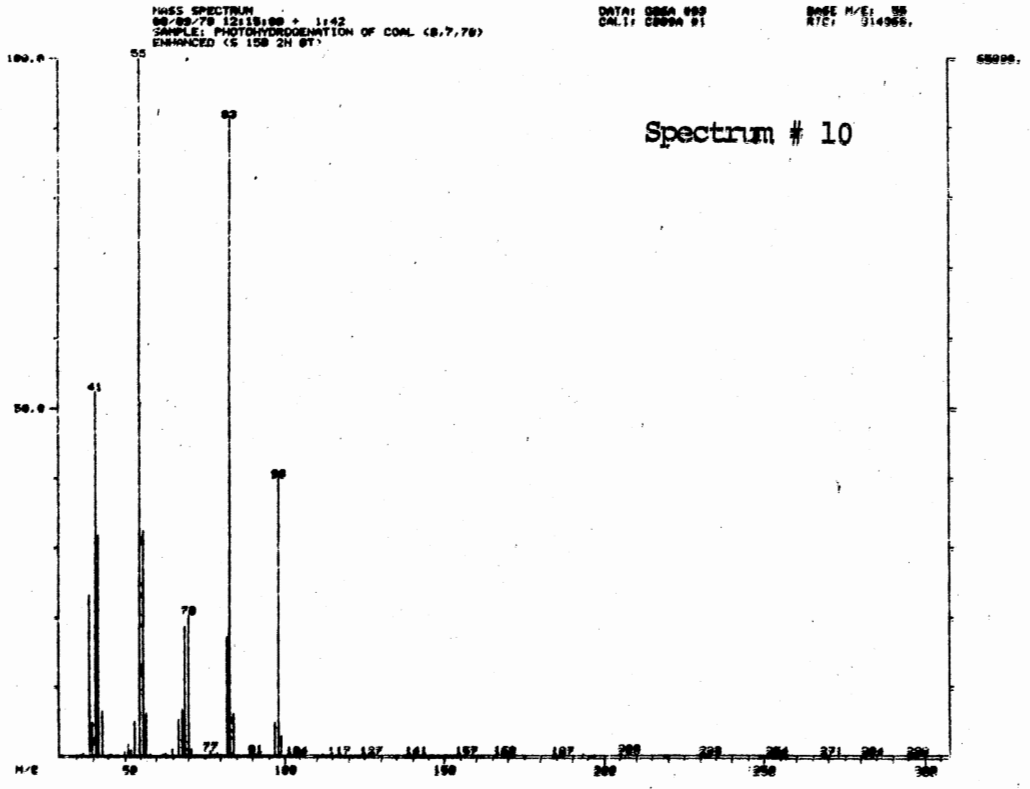
MASS SPECTRUM
SAMPLE: PHOTOHYDROGENATION OF COAL (8,7,78)
ENHANCED (S 150 2H 8T)
DATA: 0000A 009
CAL1: C000A 01
BASE M/E: 55
RIC: 514968.
100.0
50.0
M/E
65000.
Spectrum # 10

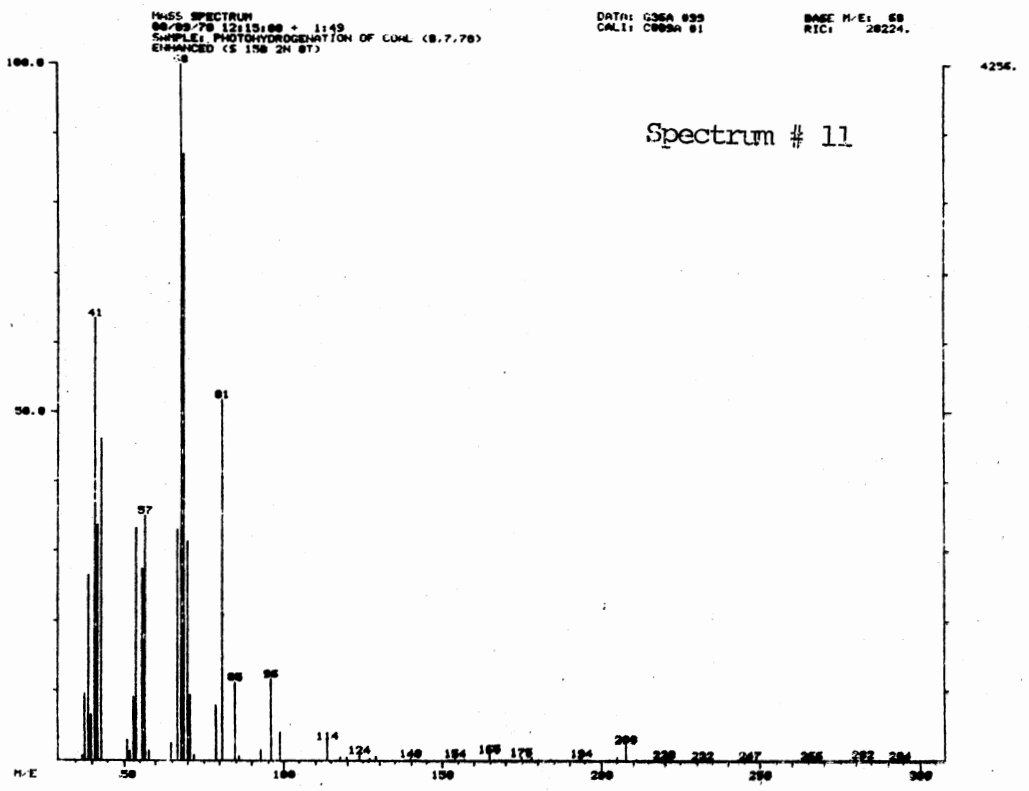
MASS SPECTRUM
08/09/78 12:15:00 + 1:49
SAMPLE: PHOTOHYDROGENATION OF COAL (8,7,78)
ENHANCED (S 150 2N 8T)
DATA: G36A 039
CALI: C060A 01
BASE M/E: 68
RIC: 20224.
4256.
100.0
50.0
M/E
Spectrum # 11

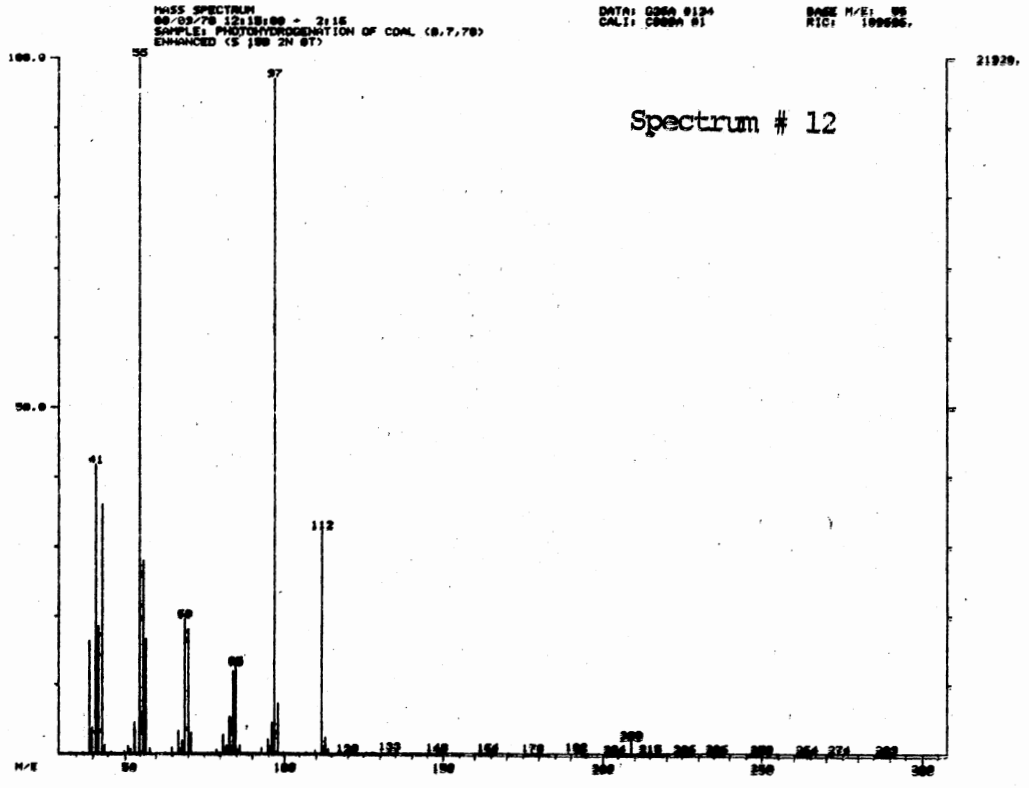
MASS SPECTRUM
08/09/78 12:18:00 + 2:16
SAMPLE: PHOTOHYDROGENATION OF COAL (8,7,78)
ENHANCED (S 180 2N 8T)
DATA: G36A 0134
CALI: C060A 01
BASE M/E: 55
RIC: 199686.
21920.
100.0
50.0
M/E
Spectrum # 12

G36A # 133

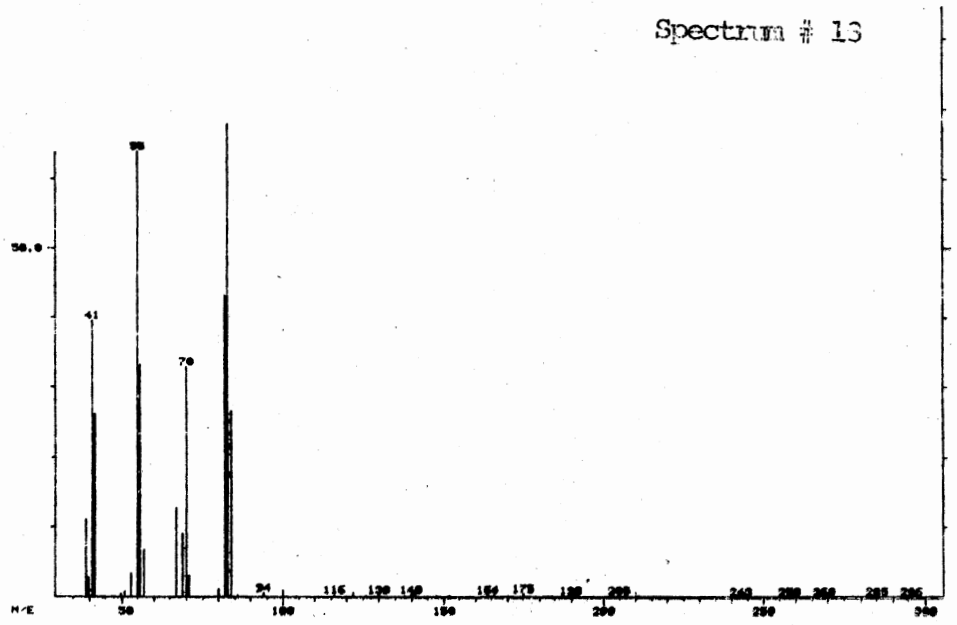
Spectrum # 13
50.0
41
70
95
M/E
50
100
150
200
250
300

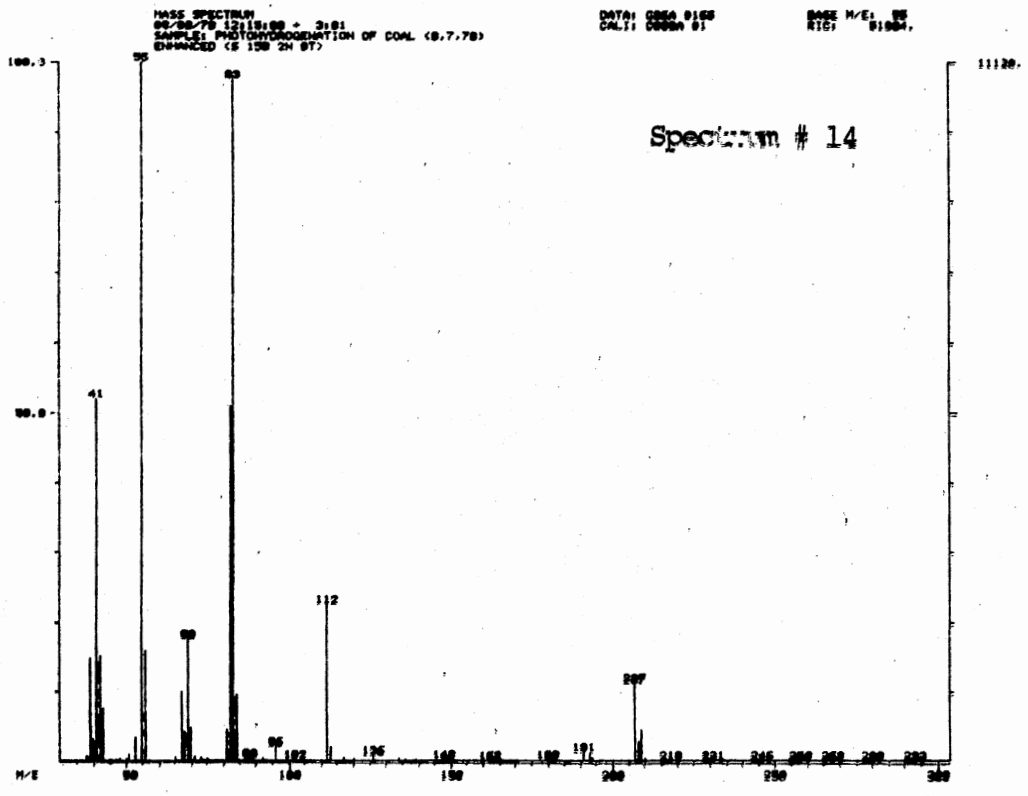
MASS SPECTRUM
SAMPLE: PHOTOHYDROGENATION OF COAL (8,7,78)
ENHANCED (F 150 2M 8T)
DATA: G36A 0165
CALI: G36A 01
BASE M/E: 95
RIC: 81984.
100.0
11120.
Spectrum # 14
41
55
69
83
97
112
191
M/E
50
100
150
200
250
300

G36A # 183

Spectrum # 15

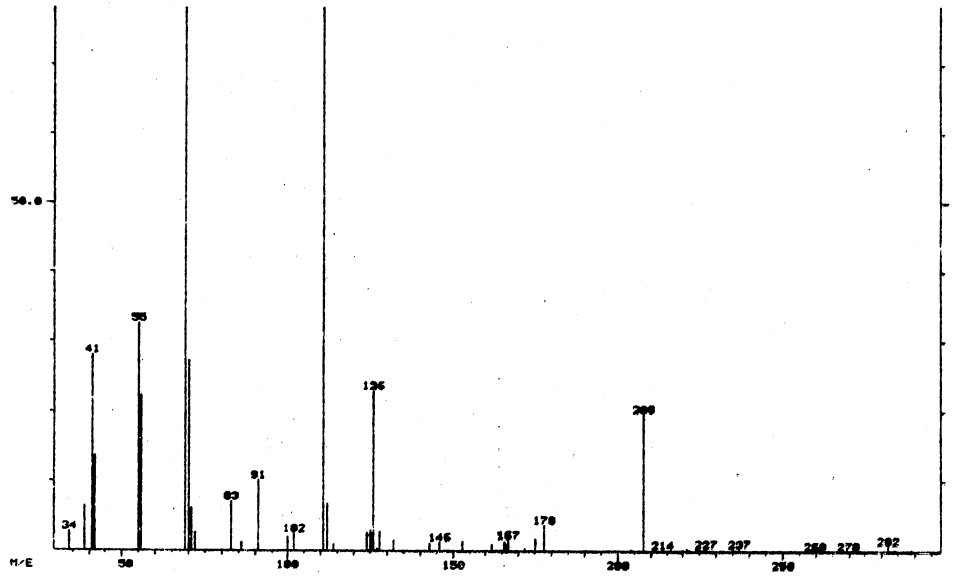

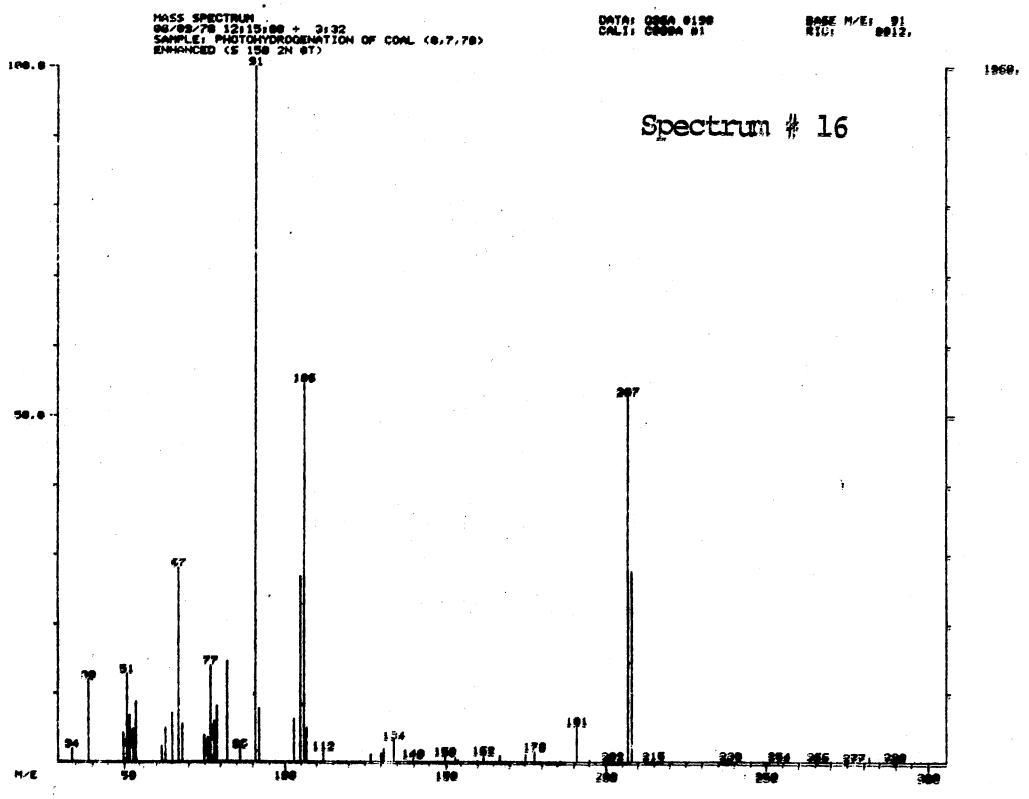

Spectrum # 16

G36A # 211

Spectrum # 17

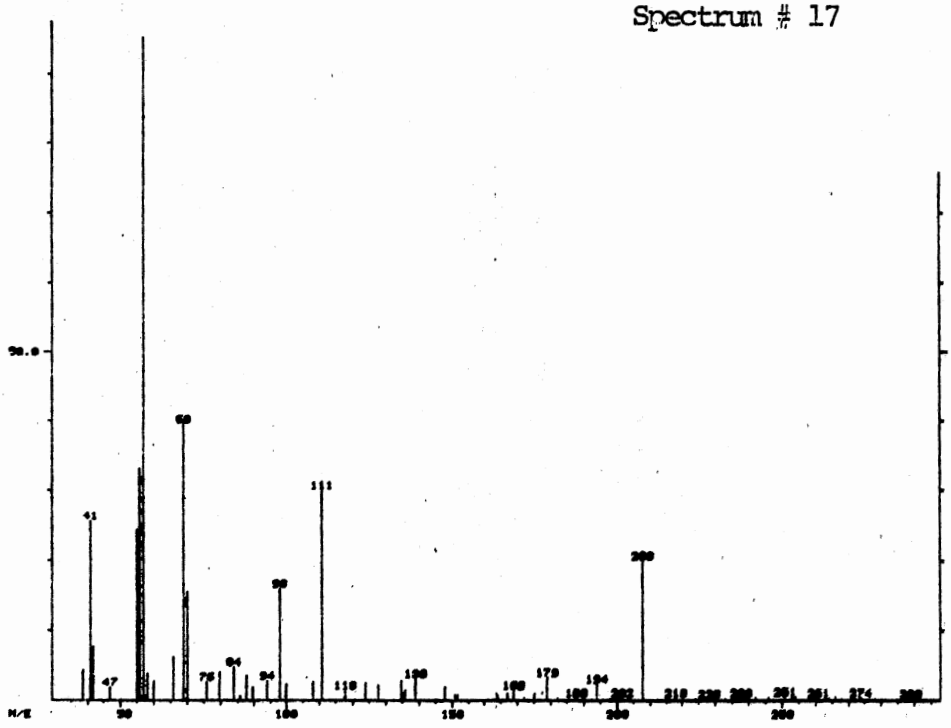

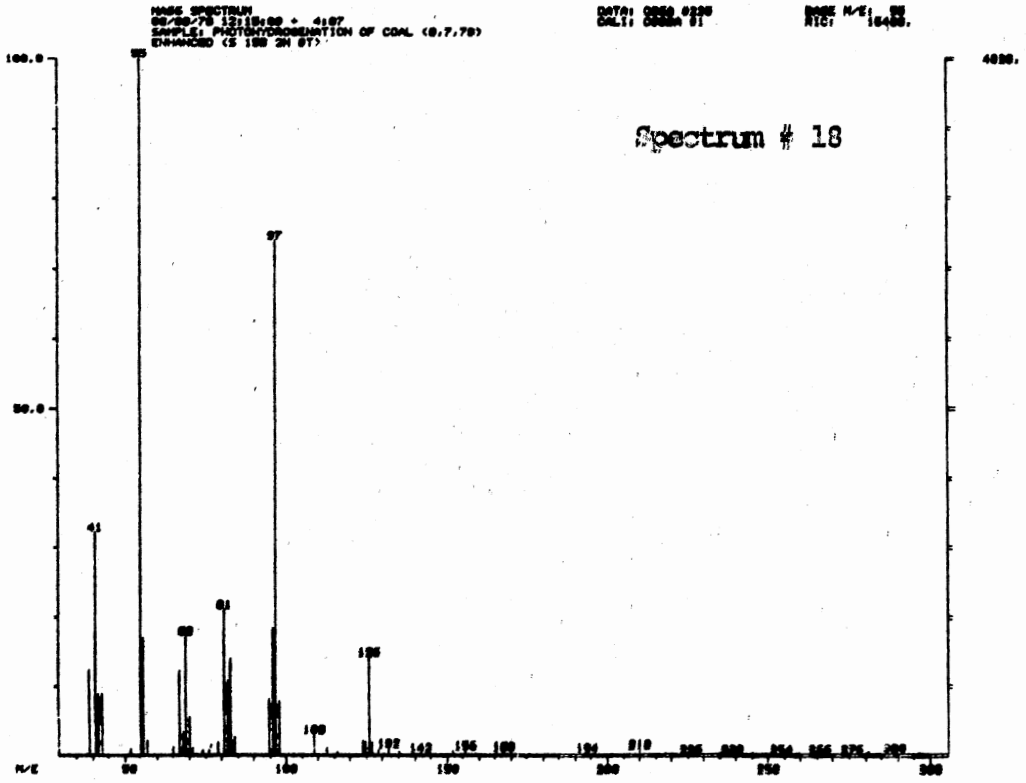

Spectrum # 18

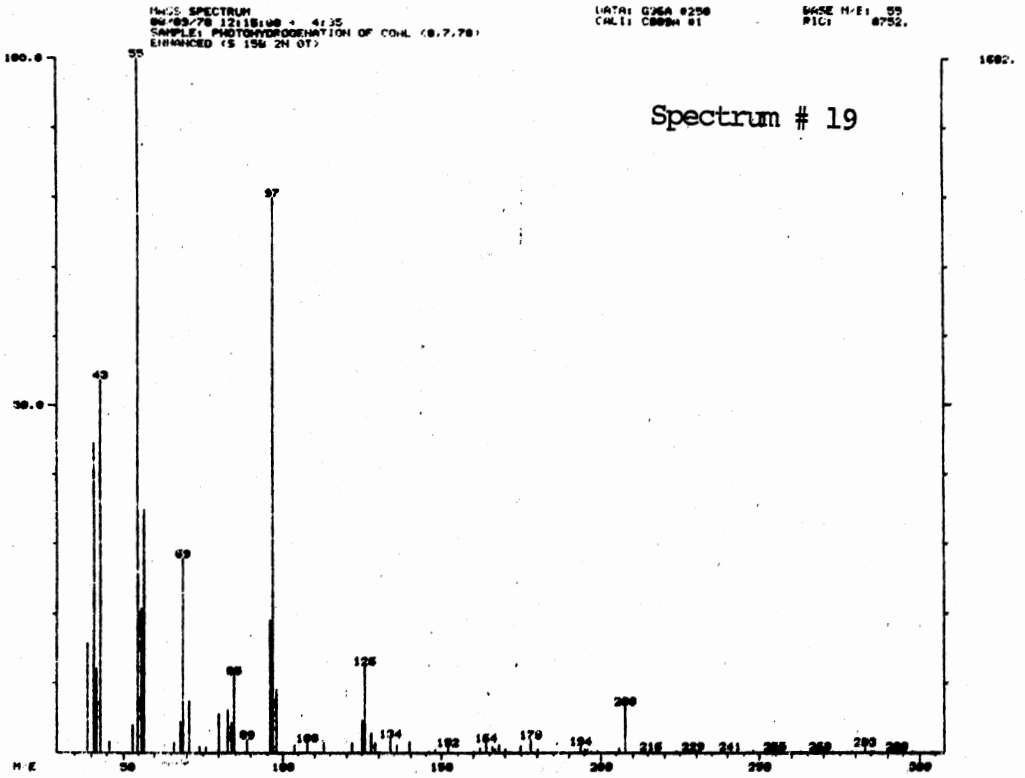
Spectrum # 19

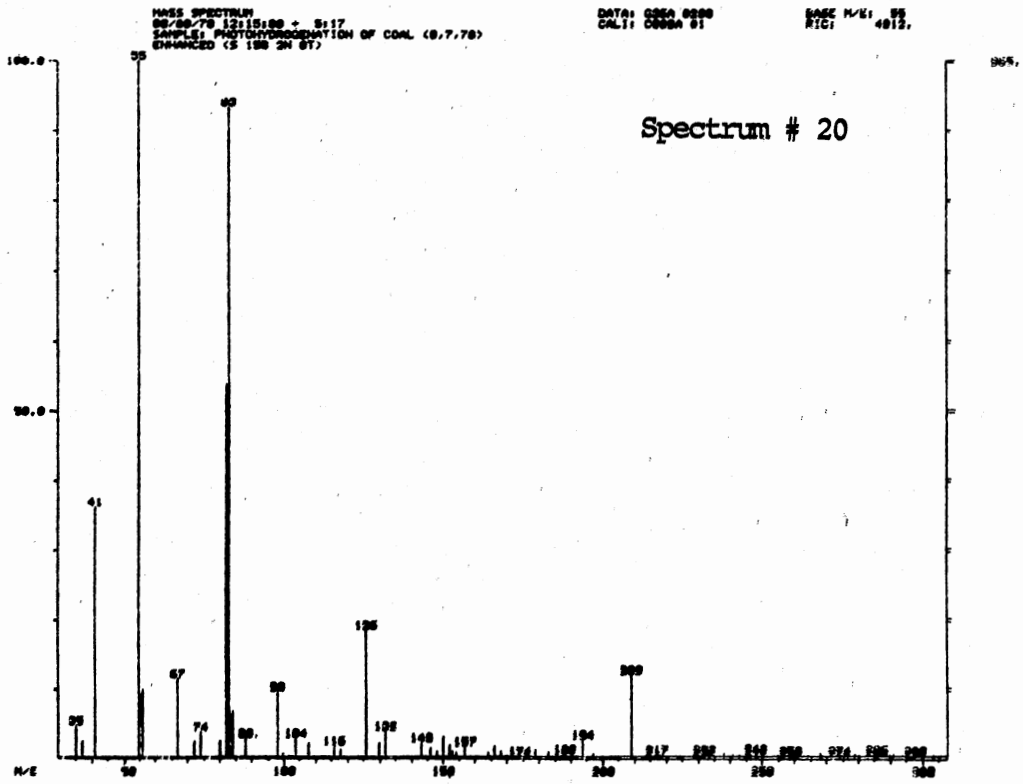
Spectrum # 20

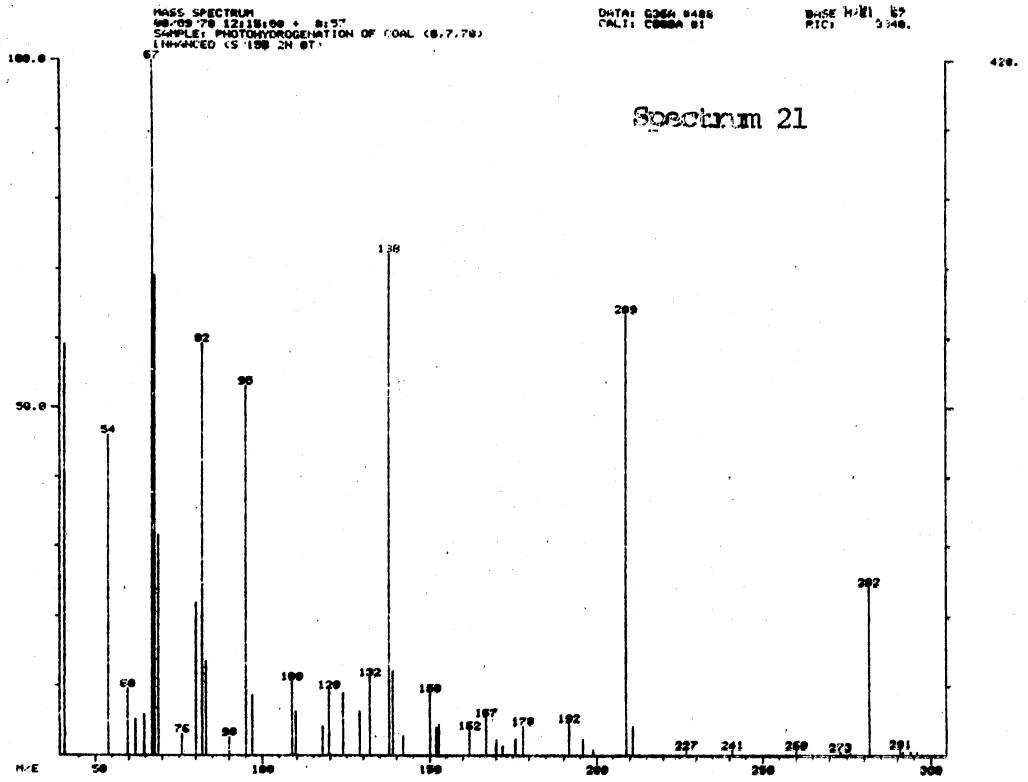
MASS SPECTRUM
SAMPLE: PHOTOHYDROGENATION OF COAL (8.7.78)
ENHANCED (S 100 2N 0T)
Spectrum 21
M/E

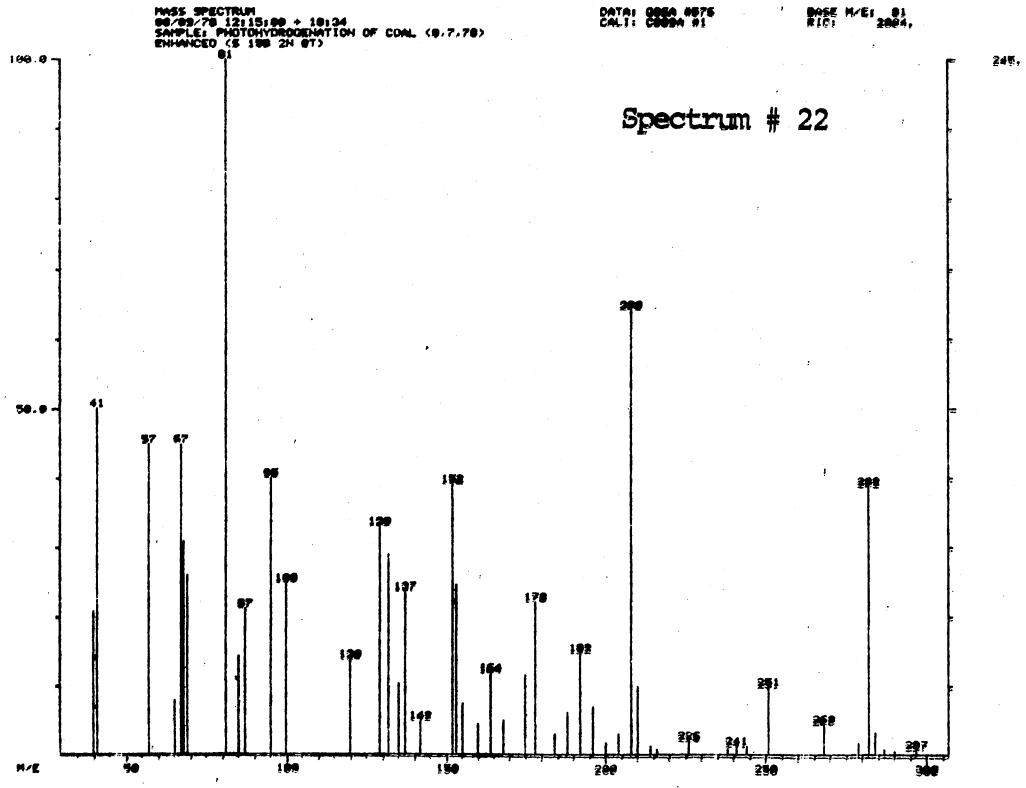
MASS SPECTRUM
SAMPLE: PHOTOHYDROGENATION OF COAL (8.7.78)
ENHANCED (S 100 2N 0T)
Spectrum # 22
M/E

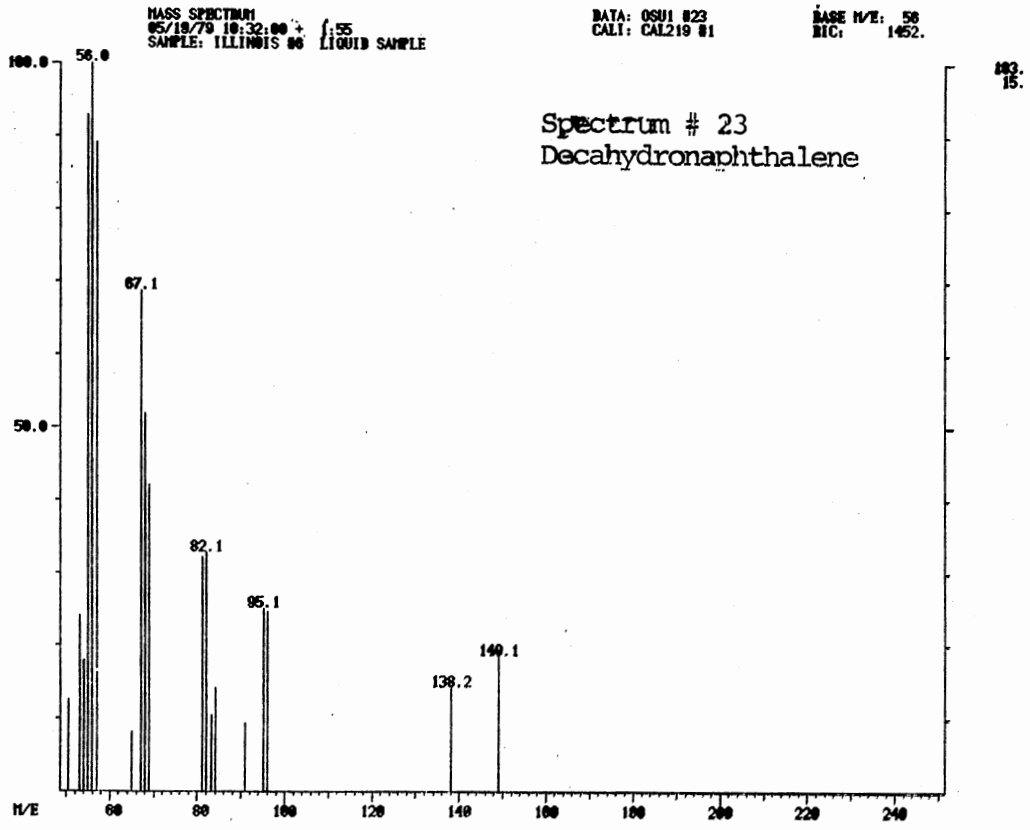
MASS SPECTRUM
05/19/79 10:32:00 + 1:55
SAMPLE: ILLINOIS 86 LIQUID SAMPLE
DATA: OSU1 823
CALI: CAL219 81
BASE M/E: 56
TIC: 1452.
Spectrum # 23
Decahydronaphthalene
56.0
67.1
82.1
95.1
138.2
140.1
M/E

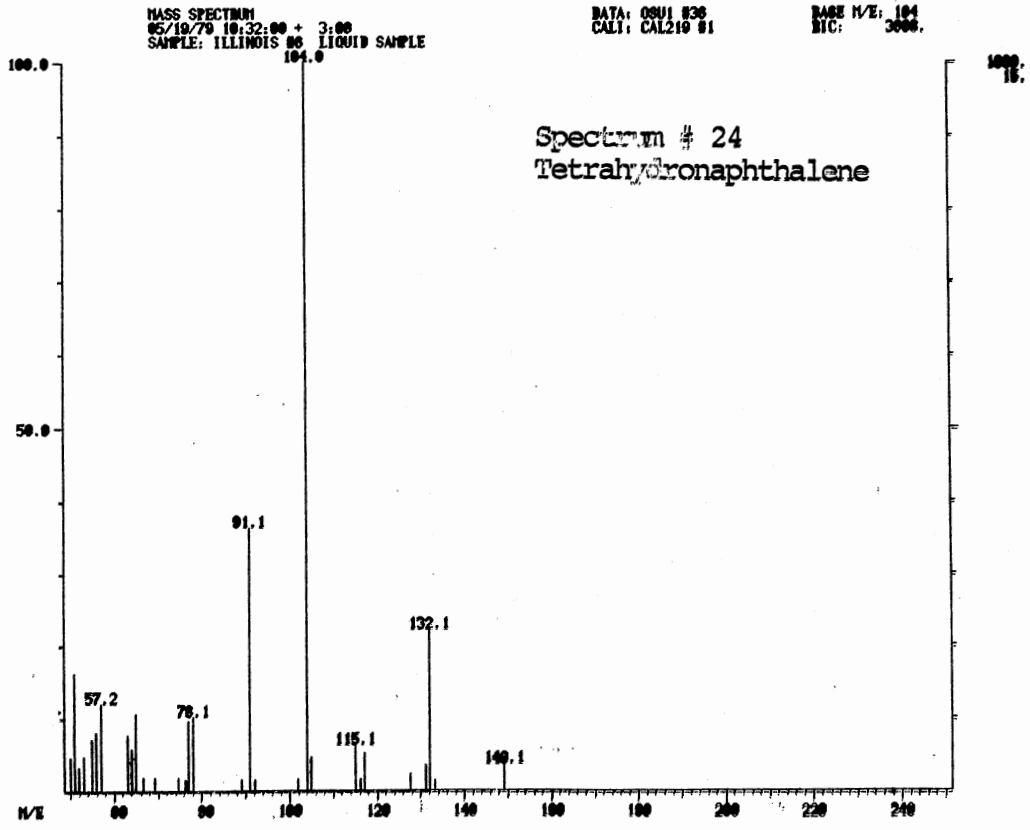
MASS SPECTRUM
05/19/79 10:32:00 + 3:00
SAMPLE: ILLINOIS 86 LIQUID SAMPLE
DATA: OSU1 836
CALI: CAL219 81
BASE M/E: 104
TIC: 3000.
Spectrum # 24
Tetrahydronaphthalene
104.0
91.1
132.1
57.2
78.1
115.1
140.1
M/E

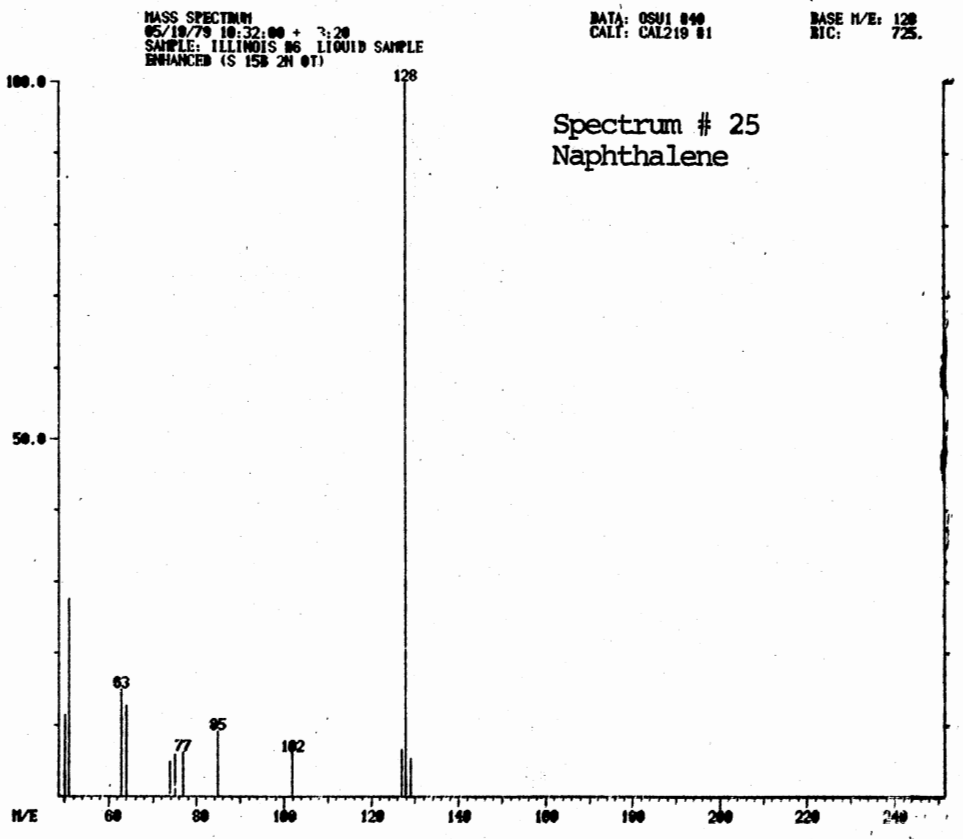

Spectrum # 25
Naphthalene

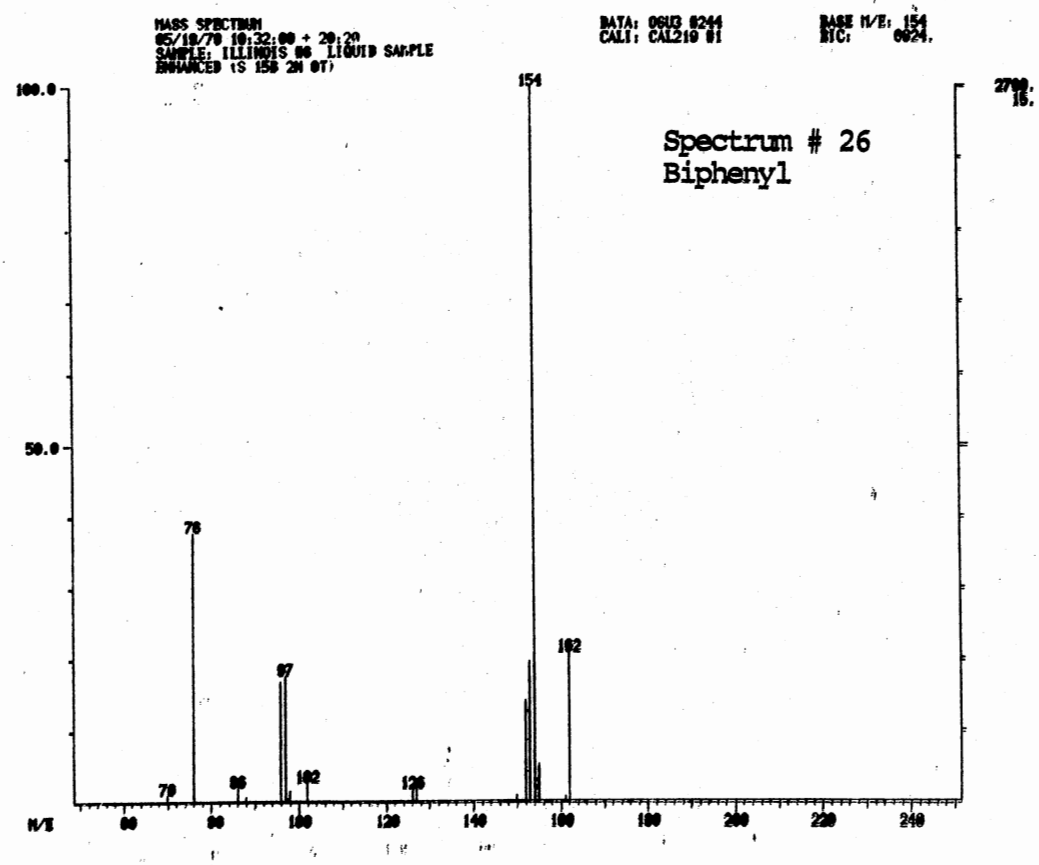

Spectrum # 26
Biphenyl

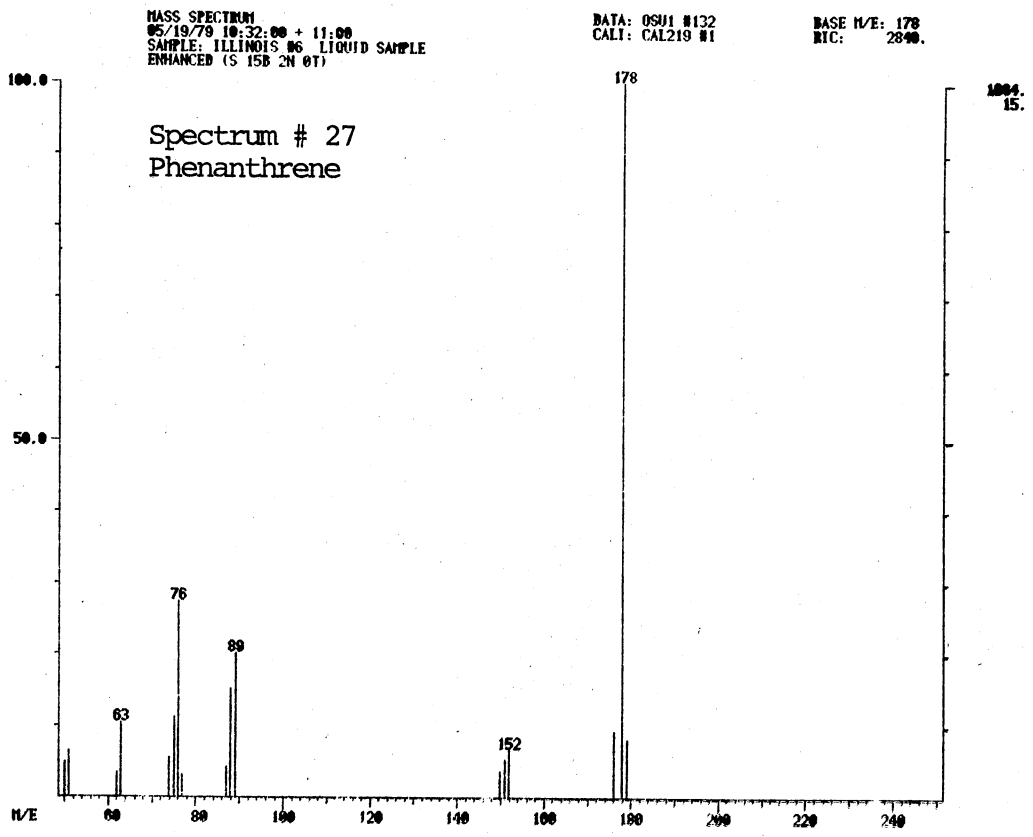
MASS SPECTRUM
05/19/79 10:32:00 + 11:00
SAMPLE: ILLINOIS #6 LIQUID SAMPLE
ENHANCED (S 15B 2N 0T)
DATA: OSU1 #132
CALI: CAL219 #1
BASE M/E: 178
RIC: 2840.
Spectrum # 27
Phenanthrene
178
76
89
63
152
M/E

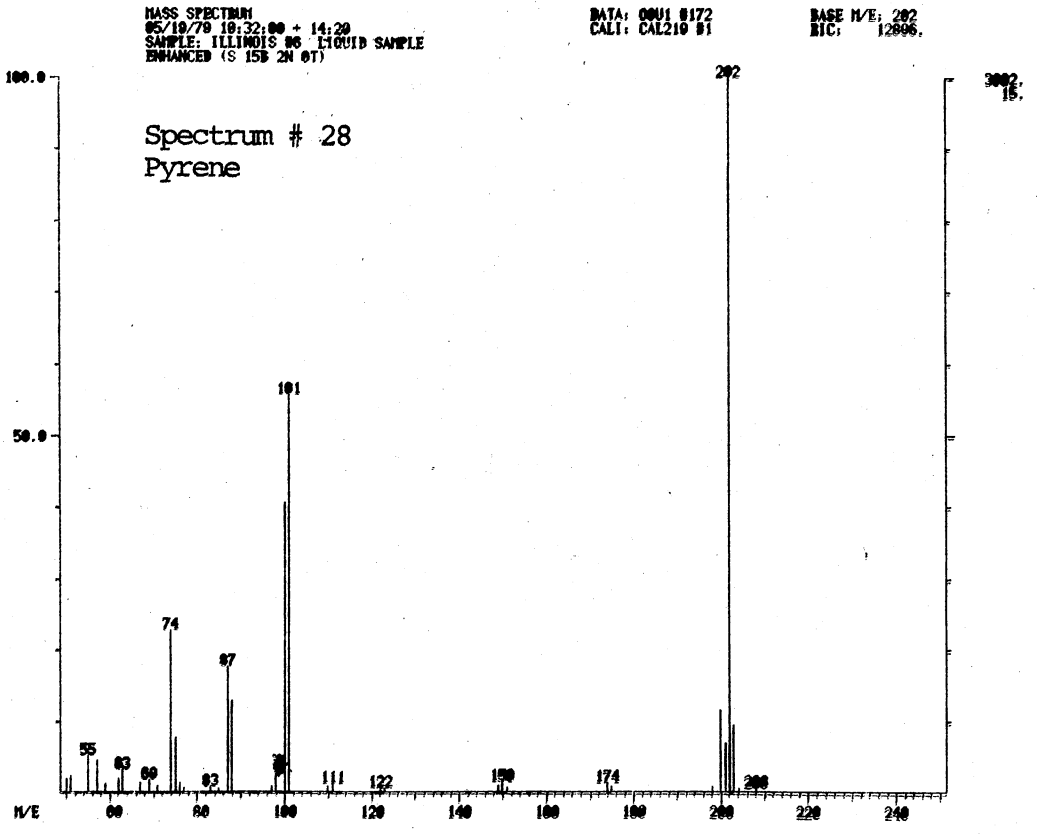
MASS SPECTRUM
05/19/79 10:32:00 + 14:20
SAMPLE: ILLINOIS #6 LIQUID SAMPLE
ENHANCED (S 15B 2N 0T)
DATA: OSU1 #172
CALI: CAL219 #1
BASE M/E: 202
RIC: 12896.
Spectrum # 28
Pyrene
202
101
74
87
55
63
111
122
150
174
M/E

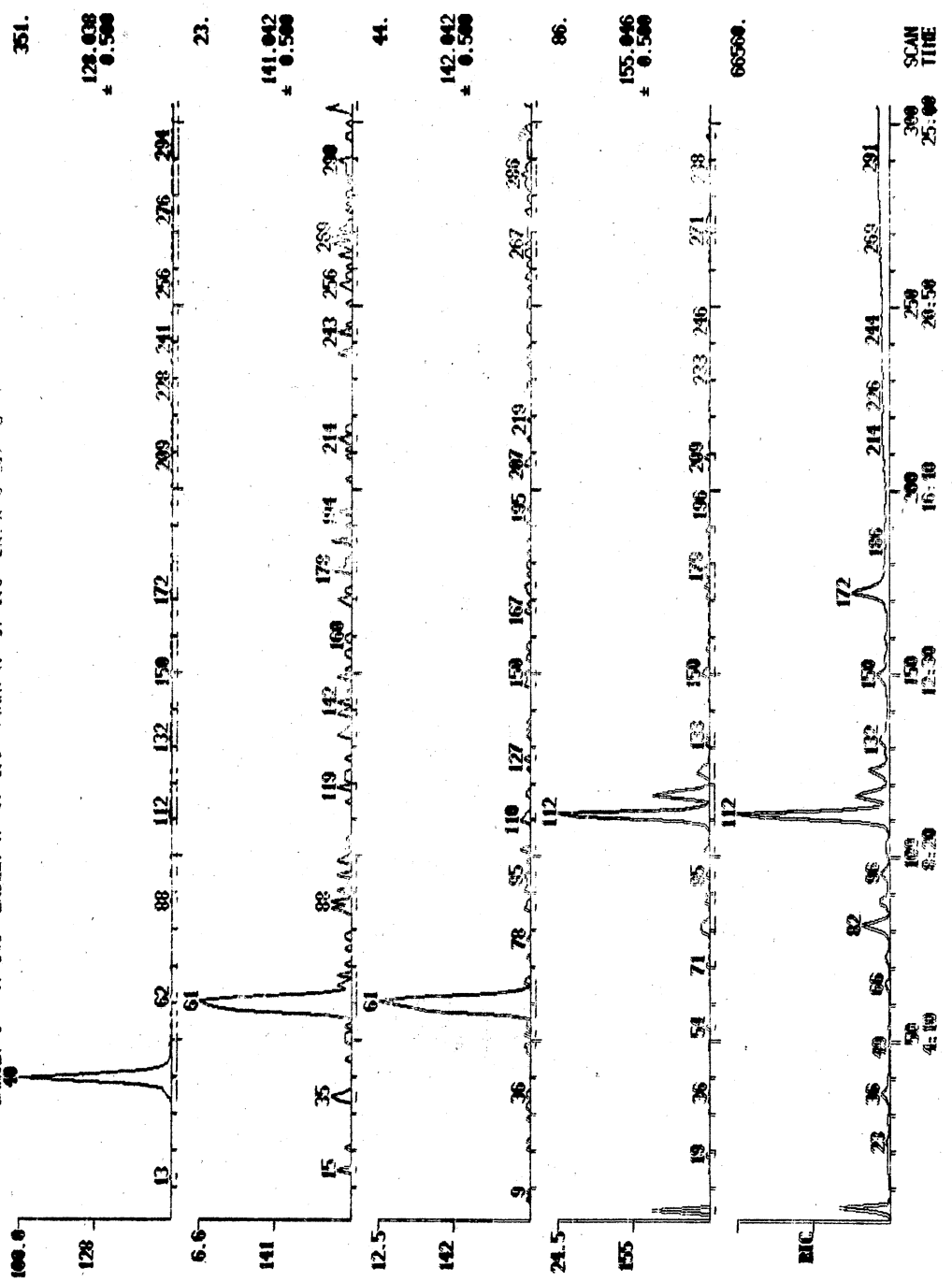

Characteristic Ion Maps for Naphthalenes

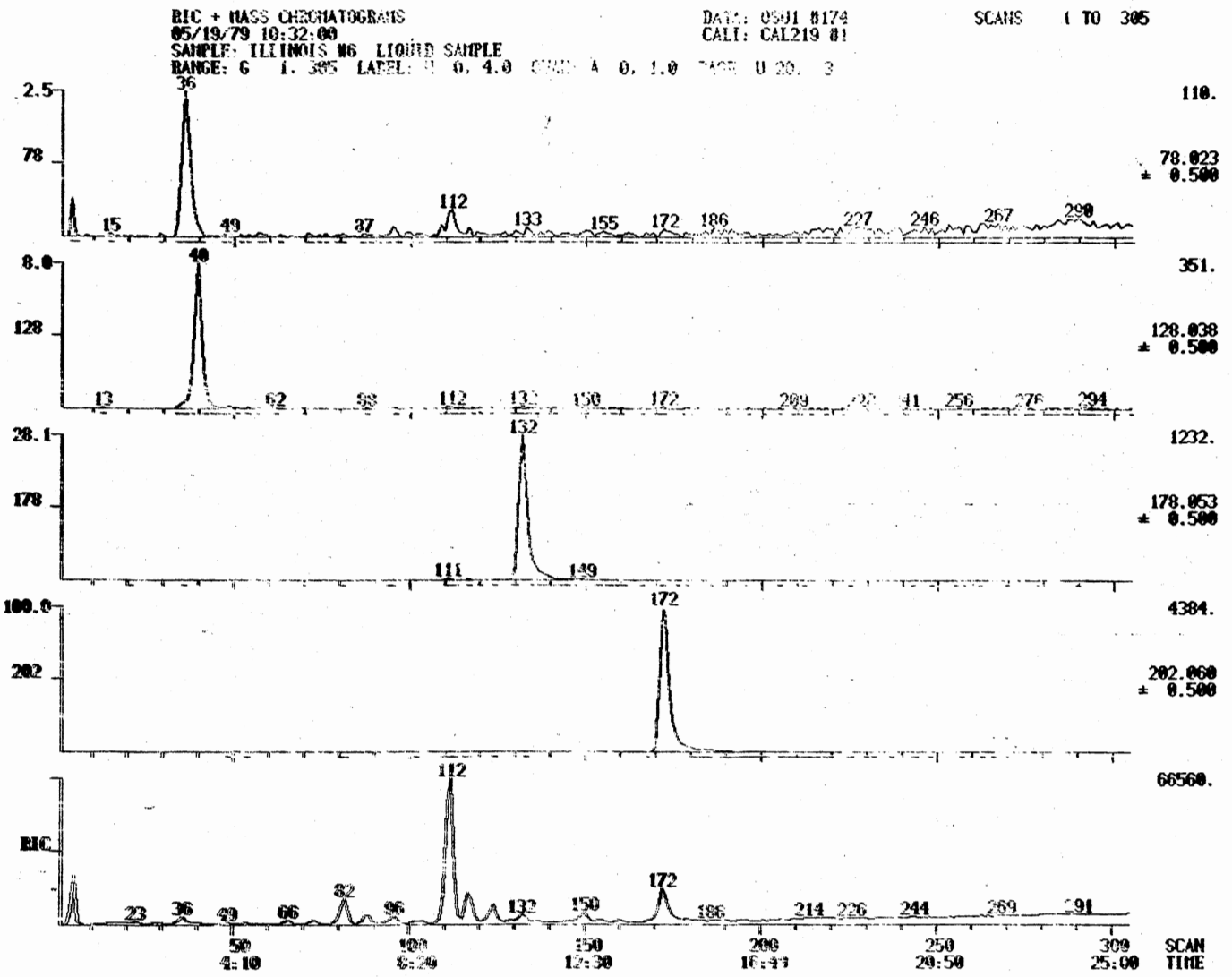

Characteristic Ion Maps for Benzene, Naphthalene and Pyrene

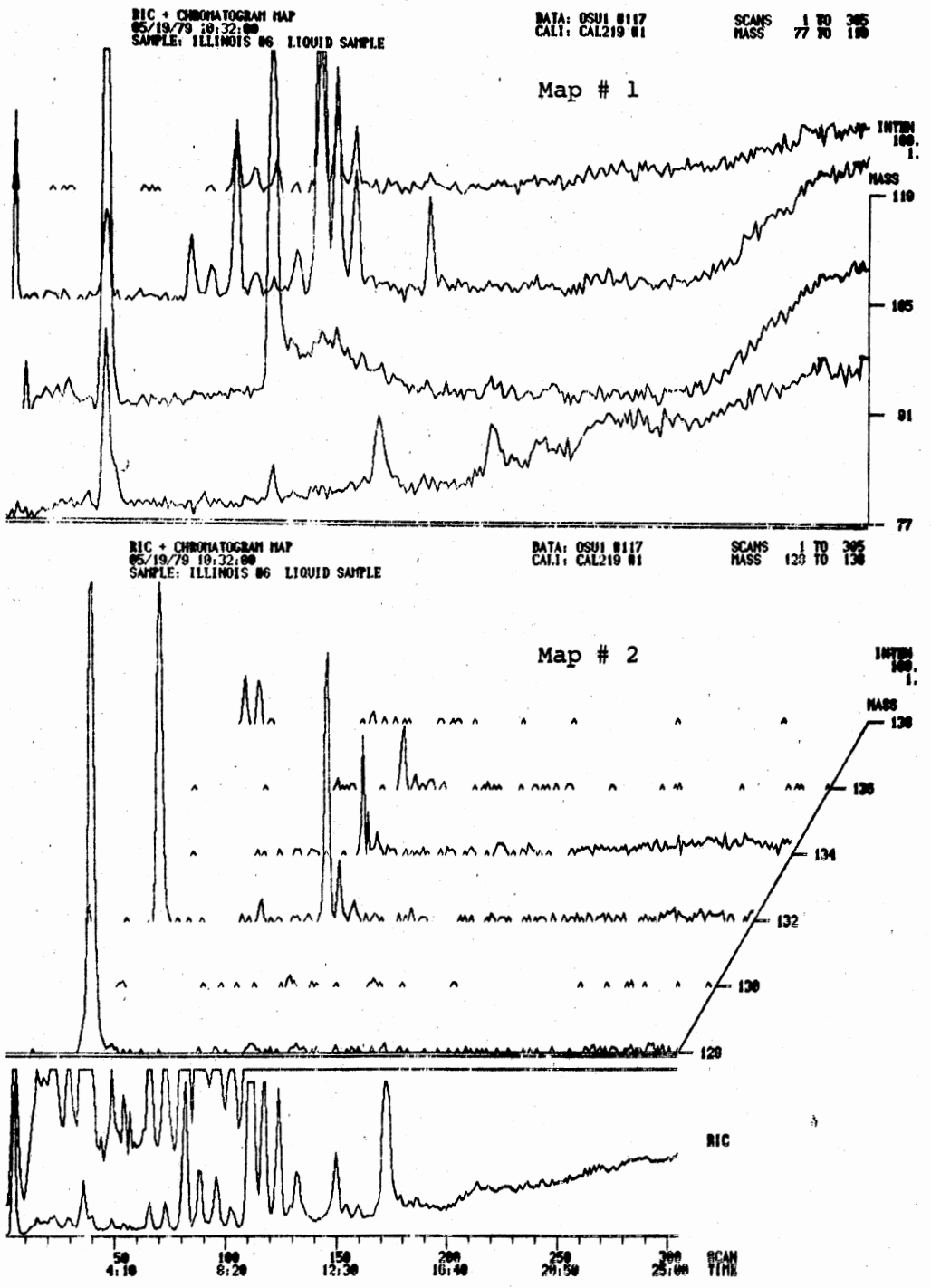

TIC Mapping of Benzenes and Hydrogenated Naphthalenes

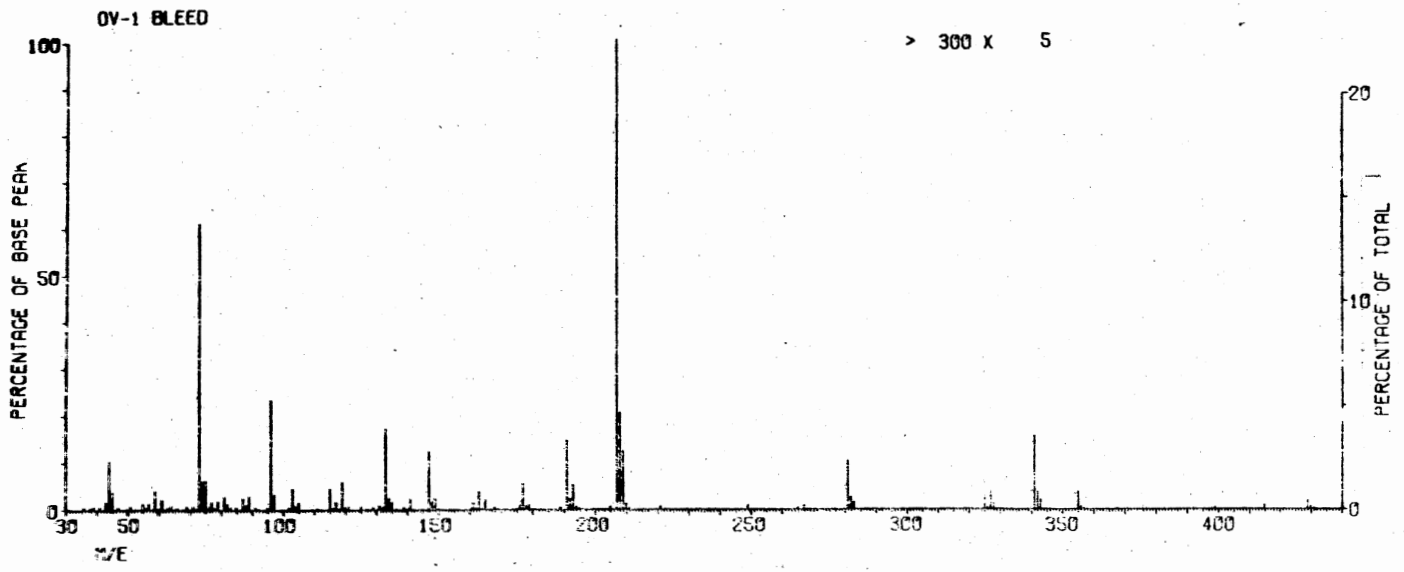

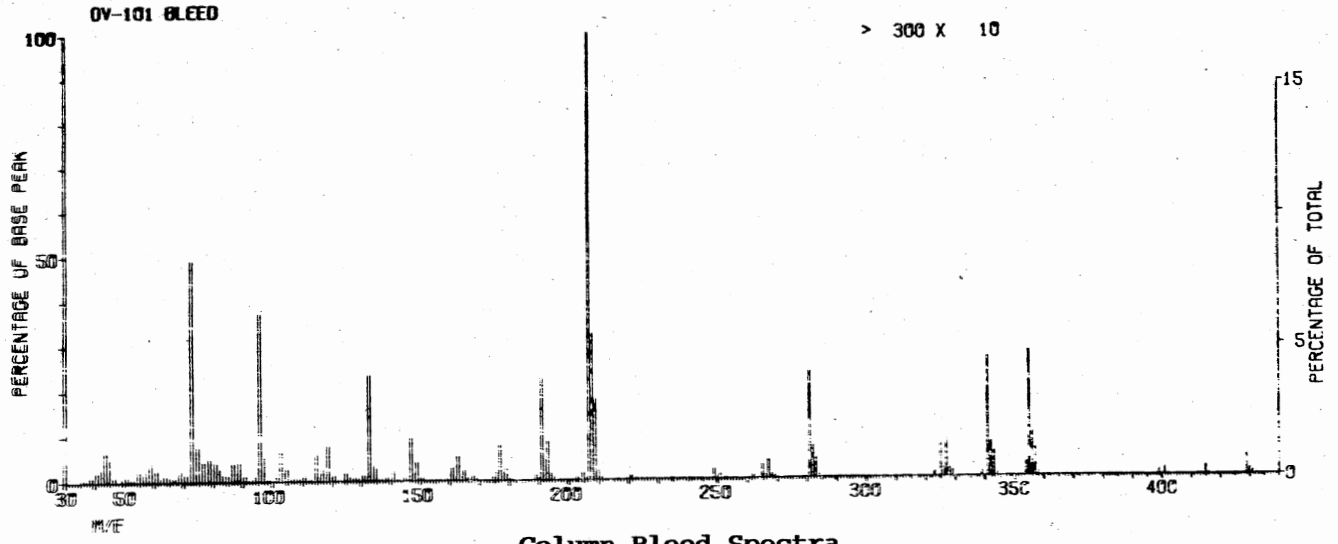

Column Bleed Spectra

VITA

Subramanian Sundaram

Candidate for the Degree of

Doctor of Philosophy

Thesis: PHOTOCHEMICAL CONVERSION OF COAL TO GASOLINE IN AN ENTRAINED BED REACTOR

Major Field: Chemistry

Biographical:

Personal data: Born in Nattarasankottai, India, on June 2, 1948, to Mr. M. Subramanian Chettiar and Mrs. M. Sp. Kannammai Achi. Married to Kannathal on January 25, 1967; two children: Shanthi, born on November 16, 1967 and Karpagavalli, born on April 20, 1972.

Education: Graduated from Subramaniam Chettiar Gurukulam Residential High School, Amaravathipudur, India, in March 1964; received Bachelor of Science degree in Chemistry at Alagappa College, University of Madras, Karaikudi, India, in June 1969; received Master of Science degree in Chemistry from Annamalai University, Annamalainagar, India, in July 1971; completed the requirements for the Degree of Doctor of Philosophy at Oklahoma State University, Stillwater, Oklahoma, in July 1979.

Professional Experience: Instructor at Government Arts College, Cheyyar, India, in 1971; Assistant Professor , Government Arts College, Karur, from January 1972 through June 1974; Assistant Professor at Government Arts College, Mannargudi, India, July 1975; Graduate Teaching Assistant at Oklahoma State University from August 1975 through May 1976; U. S. Department of Energy Research Associate from June 1976 through June 1979.